A. Zanardi
2010

N-heterocyclic-carbene based Ditopic and Hemicleaveable ligands for the design of improved catalysts

Escola Superior de Tecnologia i Ciències Experimentals.
Departament de Química Inorgànica i Orgànica.

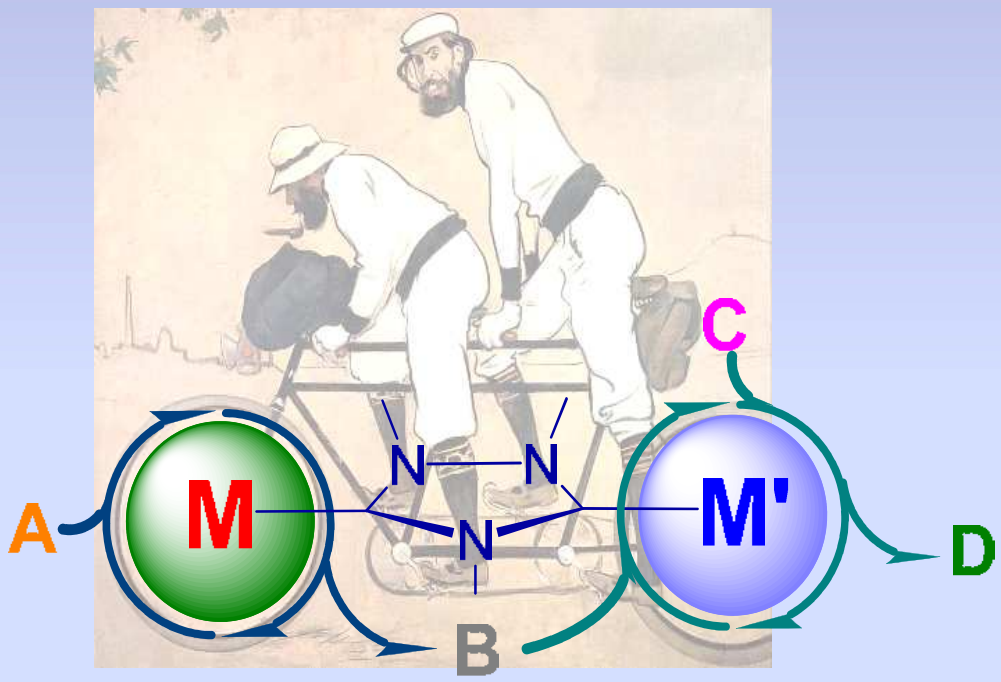

N-heterocyclic-carbene based Ditopic and Hemicleaveable ligands for the design of improved catalysts

Alessandro Zanardi
Castellón, November 2010

UNIVERSITAT JAUME I
Departamento de Química Inorgánica y Orgánica
Área de Química Inorgánica

N-heterocyclic-carbene-based Ditopic and Hemicleaveable ligands for the design of improved catalysts

Alessandro Zanardi
Castellón, November 2010

D. EDUARDO PERIS FAJARNÉS, PROFESOR DE QUÍMICA INORGÁNICA DE LA UNIVERSIDAD JAUME I Y D. JOSÉ A. MATA MARTINEZ, PROFESOR DE QUÍMICA INORGÁNICA DE LA UNIVERSIDAD JAUME I,

CERTIFICAN: Que la Tesis Doctoral con Titulo "*N-heterocyclic-carbene-based Ditopic and Hemicleaveable ligands for the design of improved catalysts*" ha sido desarrollado bajo su dirección, en el área de Química Inorgánica de la Universidad Jaime I, por Alessandro Zanardi.

Castellón de la Plana, a 30 de Septiembre de 2010.

Fdo. Dr. Eduardo Peris Fajarnés Fdo. Dr. José A. Mata Martinez

Contents

Abstract
Acknowledgements
List of abbreviations

Chapter 1 – Introduction

1.1 **Introduction:** N-heterocyclic carbene (Pag. 3)
1.2 **General properties of NHCs** (Pag. 4)
1.3 **Reactivity of NHCs** (Pag. 6)
1.3 **NHCs as ligands** (Pag. 7)
1.4 **Metallation (**Pag**.** 10)
1.5 **NHCs in our Group** (Pag. 15)
References (Pag. 17)

Chapter 2 – NHC-Based compounds for Tandem Catalysis

2.1 **Introduction to Tandem Catalysis** (Pag. 23)
2.2 **Ditopic catalysts for Tandem Processes** (Pag. 26)
2.3 **Ditz-based homometallic complexes and their catalytic properties** (Pag. 31)
2.3.1 Synthesis of homometallic complexes (Pag. 31)
2.3.2 Catalytic Behaviour of complexes **4L** and **5L** (Pag. 38)
2.3.3 Synthesis and characterization of new bimetallic and monometallic NHC-Palladium and Platinum pyridine stabilized complexes (Pag. 42)
2.3.4 Tandem Catalysis with Pd complexes (Pag. 46)
2.4 **Heterometallic complexes (Pag. 54)**

2.4.1 Synthesis and characterization of heterobimetallic Ir^{III}/Ir^{I} and Ir^{III}/Rh^{I} complexes using triazolyl-di-ylidene ligand (Pag. 54)

2.4.2 Catalytic evaluation of the heterobimetallic species **12L** and **13L**: initial attempts to build tandem process up (Pag. 63)

2.4.3 Synthesis and characterization of heterobimetallic Ir^{III}/M (M = Pd, Pt) complexes using *ditz* (Pag. 71)

2.5 **Tandem catalysis using Ir-Pd complexes** (Pag. 77)

2.5.1 Dehalogenation/transfer hydrogenation of halo-acetophenones (Pag. 77)

2.5.2 Reduction of nitroarenes to anilines/coupling with primary alcohols to afford imines (Pag. 85)

2.6 **Tandem Catalysis with the Ir-Pt complex 16L** (Pag. 94)

References (Pag. 100)

Chapter 3 – Synthesis, Reactivity and Catalytic Properties of Iridium Complexes with Alkenyl-NHC ligands

3.1 **Introduction: Hydrosilylation of terminal alkynes** (Pag. 109)

3.2 **Synthesis and characterization of Iridium complexes with alkenyl-imidazolyl-ylidene** (Pag. 112)

3.3 **Synthesis and characterization of bisalkenyl-imidazolyl-ylidene ligands** (Pag. 113)

3.4 **Synthesis of mono-coordinated, chelate and pincer alkenyl-NHC Iridium complexes** (Pag. 116)

3.5 **Catalytic Hydosilylation** (Pag.128)

References (Pag. 133)

SUMMARY (Pag. 137)

Chapter 4 – Experimental Section

4.1 **Analytical Techniques** (Pag. 143)

4.2 **Working Techniques and Reagents** (Pag. 144)

4.3 **Synthesis and characterization** (Pag. 147)

4.4 **Crystallographic data collection** (Pag. 165)

4.5 **Mass Spectrometry** (Pag. 180)

References (Pag. 181)

Chapter 5 – Diseño de Catalizadores con Ligandos Ditópicos y Hemiactivables de Tipo Carbeno N-Heterocíclico

5.1 **Introducción: Carbenos N-heterocíclico** (Pag. 185)

5.2 **Objetivos de la investigación** (Pag. 187)

5.3 **Discusión y Resultados** (Pag. 189)

5.3.1 Uso de triazolil-di-ilidenos en la síntesis de catalizadores ditópicos (Pag. 189)

5.3.2 Reactividad y propiedades cataliticas de compuestos de Pd^{II} y Pt^{II} con ligandos de tipo triazolil-di-ilideno (Pag. 193)

5.3.3 Estudio de procesos catalíticos tipo *tándem* con compuestos heterobimetálicos de Ir^{III}/Ir^{I} y Ir^{III}/Rh^{I} con el ligando triazolil-di-ilideno (Pag. 195)

5.3.4 Estudio de procesos catalíticos tipo *tándem* con compuestos heterobimetálicos de Ir^{III}/Pd^{II}: transformación de 4-halobenzofenonas (Pag. 198)

5.3.5 Estudio de procesos catalíticos tipo *tándem* con compuestos heterobimetálicos de Ir^{III}/Pd^{II}: formación de iminas por reducción de nitro-arenos/acoplamiento con alcoholes (Pag. 201)

5.3.6 Estudio de procesos catalíticos tipo *tándem* con compuestos heterobimetálicos de Ir^{III}/Pt^{II} con ligandos triazolil-di-ilideno (Pag. 204)

5.3.7 Síntesis y caracterización de catalizadores de Ir^{I} con ligandos alquenil-imidazolil-ilideno (Pag. 207)

5.4 **CONCLUSIONES** (Pag. 210)

Referencias (Pag. 212)

ABSTRACT

"N-heterocyclic-carbene-based Ditopic and Hemicleaveable ligands for the design of improved catalysts"

Alessandro Zanardi

Castellón 2010

The work presented in this manuscript was realized in the department of Inorganic and Organic Chemistry of the University Jaume I. The dissertation concerns the synthesis and properties of NHC (N-heterocyclic carbene) ligands and their derived transition metal complexes.

Chapter two describes the synthesis and the catalytic activity of new bimetalic complexes using a trizolyl-di-ylidene ligand. With this ligand, we obtained a series of homobimetallic complexes of Ir, Pd, and Pt and also heterobimetallic compounds of Rh^{I}/Ir^{III}, Pd^{II}/Ir^{III}, Pt^{I}/Ir^{III} and mixed valence complex of Ir^{III}/Ir^{I}. All these compounds were tested in the research of new tandem catalytic processes. For example homobimetallic complexes of Pd were successfully applied in a tandem process that comprises a Sonogashira coupling followed by a cyclic hydroalkoxylation to afford benzufurans. Otherwise, in the heterobimetallic complex such as the Ir-Pd species, the presence of the two different metals allows tandem processes designed by combining reactions that are typically catalyzed by Ir and Pd. The use of halo-acetophenones, as starting substrates, for example, allow us to combine transformations for which the Pd and the Ir fragment can afford distinct catalytic reactions.

Although we did not perform any detailed studies on the electronic communication of these species, we observed that the coordination of the ligand to the bimetallic species provided activities that were enhanced compared to those shown by the monometallic analogues.

Chapter three details the synthesis of a family of alkenyl-functionalized NHC–Iridium(I) complexes, providing a series of mono-coordinated, chelate and pincer alkenyl-NHC species.

Olefin coordination is highly influenced by the nature of the substituents on the NHC ring, and on the length of the alkenyl branch. A fluxional process involving

coordination/decoordination of the olefin in bis-allyl-NHC complexes has been studied. The mono-coordinated complexes are highly active in the hydrosilylation of terminal alkynes, showing high selectivity for the Z-isomers, with no α-isomers or dehydrogenative silylation processes being observed.

Chapter four details the experimental section about synthesis, characterization and catalytic processes used while Chapter five represents a resume of this manuscript in Spanish language.

Acknowledgements-Agradecimientos-Agraïments-Ringraziamenti

…..finally the Acknowledgements. Without any doubts my first “Thanks to..” is going directly to my thesis directors, Prof. Eduardo Peris and Prof. José Mata. Thank you for accepting me in this group and for the opportunity that you gave to me to work with all that beautiful chemistry that we developed. Thank you also for the continuing support. I especially appreciate the enormous patience that they demonstrated during the first year when the chemistry was not so productive.

Muchas gracias por todos esos consejos y nuevos conocimientos de la síntesis organometálica y de la catálisis, que en aquella época eran para mi desconocidos. Y gracias por la oportunidad de haberme dejado meter también en el mundo del “borrowing-hydrogen”. El BUTANOLO no sería nada sin mi…(es broma). Gracias por todas las ayudas que me habéis dado a nivel personal cuando no tenia todavía beca y por cuando vino a “visitarnos” Andrea.….I’m also glad for the opportunity that they later gave to me to develop my ideas or better said, to develop my “chemical instinct”…..Thank you once again.

I have also to say a BIG THANK YOU to all the past and present members of the NHC-QIO-UJI-LAB. En orden cronológico: Juan de la Cierva Codorniu-Dra E(plus), cuando llegué i oí esos gritos me querría volver a Italia…mítica; Dra CorberanS, la rouse-grande POZZANGHERA, gracias por aquellas ayudas en aquel primer pionero *ditz-based-domino approach* per la sintesis de indoles; Dra MonicS, y watccctxx….!!!, y todo aquel fabuloso mundo del Rutenio-NHC. Y menos mal que estaba también tu padre que me ayudaba con el cotxe….Y a tu madre, a ver si le traigo un cd de Raffaella (la Carrá, claro….). To next-Dr. André Pontes, “el portu”, because with him I started my phd, with the doctorate courses, and later we also spent a lot of time together, in the lab, playing “foot-basketball” in the corridor, making dinners with mixed-typical dishes, “Tascas –Time” and especially drinking a lot of, in very large scale,“café-solo”. I hope to visit you early in Lisboa or in London, why not!?!. A la Ramon y Cajal-Dra MacarenS, por ser así muy paciente y preocuparse para los demás; a Ampawers, ya veras que dentro de poco serás la numero uno en el *“borrowing-hydrogen”* de todos los tiempos, no te preocupes por nada que tienes una tesis wapa wapa; a la Dra BeniteS, por haber compartido comentarios y discusiones siempre muy interesantes en el labo y por llevarme muchas veces a la estación cuando

estaba a punto de perder el tren y/o autobús; a Candels, por ser así de simple y querer aprender el Italiano, ANDIAMO E VILAVELLA CAPITALE!!!!; A Arthurit le querria decir: “mesa que más aplauda, mesa que más aplauda…le mando la niña….y SA SA SA, SACUSA SACUSA…”. Ya veras como la química te irá de maravilla…Al Dr. Sanz, el valenciá parlante, gracias por haberme animado en apuntarme a los exámenes de valenciano pero no ha sido posible. Probaré seguro en Catalunya y verás….Y a la última new entry Sergio. A ver si sale algo con esta química del fluor tan interesante, muchas suerte….

I would like to thank all the people of the 0^{th} and 4^{th} floor, Santi, Cesar, Antonio, Ira, Javi, Jorge, “los José”, Bea, Marta, Hector, Puri, Eloisa, Maria Agustina and all the QIO members. In particular, I have to spend few words to the members of the Carda’s group: thanks a lot for lending me all those important reagents.

I wish to acknowledge Cristian for the Mass spectrometry (“GRANDE”…..y los Lakers???), Gabriel for acquiring X-ray data and Laura for the Elemental Analysis.

I have to thank Sylviane Sabo-Etienne to accept my incorporation in her group for my stage in Toulouse at the LCC. For the good time during the coffee breaks and for the many conversations about Ru-exahydride. I have to thank also Gilles, Marie, Yann, Yang, Hellen and Rebecca to help me with the glove box and for the many NMR spectra that they have done for me. Thank you for the chemistry that I learned in your labs. Unfortunately I didn’t learn French due to the big Spanish community. Really sorry!

Thank you to the FIGIPAS, Vienna 2007. In that congress I had the opportunity to won a poster-prize. A great periodic table with a Diploma, not too bad…..

Aixi mateix, vull fer arribar el meu agraïment a la GENERALITAT VALENCIANA per la concessió d’una beca FPI que m’ha permés realitzar aquest treball d’alt nivell scientific, així com viatjar a l’estranger per a complimentar la meva formació i l’asistencia a congresos. MOLTES GRACIES!!!

Gracias a Rubén y Juanma por esos partiditos de baloncesto finalizados con ese torneo a Burriana, fantástico!!!

A todos mis compañeros de pisos y en particular a Virgilio por todas esas discusiones y por haber pasados siempre muy buenos momentos y haberme ayudado mucho. Y ahora a ganar el maratón de New York…..

Ai miei genitori, che per quattro anni consecutivi mi hanno chiamato sempre ogni due giorni. Per aver sempre creduto in me e per darmi quella sensazione di non mollare mai anche quando le cose sono complicatei. Sempre grazie. E grazie anche per tutti i vostri aiuti da 1000 km di distanza. Grazie anche a mia sorella e alla sua famiglia per tutti quei buoni consigli.....

Gracias a la familia de la Eu, sus padres y en particular a Vanesa y su familia, para habernos ayudado MUCHISIMO durante todo este ultimo año y medio. GRACIAS!!!

Alla mia Eu e al nostro piccolo Andrea. La mia famiglia. Questo lavoro é frutto di tutti i vostri sforzi per aver saputo aspettarmi e starmi sempre vicino, anche se la maggior parte delle volte non ero li con voi. Adesso peró abbiamo tutto il tempo per recuperare.....

List of Abbreviations

Δ	Refluxing temperature
η	Ligand hapticity
μ	Bridge ligand
AcOH	Acetic Acid
$acac^-$	acethylacetonate
ad. Ox	Oxidant Addition
B	Base
Bz	Benzyl
Bu	Butyl
Cat	Catalyst
COD	1,5-cyclooctadiene
COSY	Correlation Spectroscopy
Cp*	Pentamethyl cyclopentadienyl
Cy	Cyclohexyl
DCE	1,2-dichloroethane
DFT	Density Functional Theory
DMSO	Dimethylsulfoxide
EA	Elemental Analysis
ESI-MS	Electrospray ionization mass spectrometry
ESI-TOF-MS	Electrospray ionization-time of flight-mass spectrometry
Et	Ethyl
EtOH	Ethanol
h	hour
HETCOR	Heteronuclear Correlation
i-	*iso-*
IR	Infrarred spectroscopy
Imid	Imidazol
Me	Methyl
Mes	Mesityl

M-NHC		Metal complex with N-heterocyclic carbene
NaOAc		Sodium acetate
NEt_3		Triethylamine
NHC		N-heterocyclic carbene
NMR		Nuclear Magnetic Resonance
	br	broad
	d	doublet
	dt	doublet of triplets
	J	coupling constant
	m	multiplet
	ppm	parts per million
	s	singlet
	t	triplet
	δ	chemical shift
OAc		Acetate anion
OMe		Methoxide group
ORTEP		Oak Ridge Thermal Ellipsoid Plot
OTf		Triflate anion
Pag.		Page
Ph		Phenyl
pk_a		Acid dissociation constant at logarithmic scale
PR_3		Trialkylphosphine
Py		Pyridine
rt		room temperature
t		time
T		Temperature
TBABr		tetrabuthylammonium bromide
*t*Bu		*tert*-Butyl
*t*BuOK		potassium *tert*-buthoxide
THF		Tetrahydrofurane
TOCSY		Total Correlation Spectroscopy

Alla Eu e Andrea
Ai miei genitori

Chapter 1

Introduction

1.1 INTRODUCTION: N-Heterocyclic Carbenes

For the late transition metal catalysis, supporting ligands built around one or more phosphorus donor atoms are the most widely used, although nitrogen, oxygen, sulphur and other donor atoms are increasingly employed nowadays. One type of ligand that has attracted increasing interest implies a neutral divalent carbon atom with six electrons on its valence shell (**Scheme 1.1**). The ligand binds through a sp^2-hybridized lone pair on the carbon atom, and can be described as a carbene.

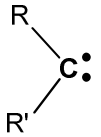

Scheme 1.1. Schematic representation of a carbene.

Since the pioneering work by Doering in 1954,[1] carbenes have been recognised as a unique type of intermediates with distinct characteristics from those shown by radicals already known in the organic chemistry community.[2] Since then, research on carbenes has rapidly expanded, but almost no attempts were made to stabilize free carbenes until the 1980s, when Tomioka started to study persistent triplet diarylcarbenes.[3a]

The first isolable carbenes were reported in 1988 by Bertrand[3b] (**1.1**) and in 1991 by Arduengo (**1.2**).[4] The phosphinocarbene **1.1** can be distilled at 80-85°C/10^{-2} Torr and *N*-heterocyclic carbene (NHC) **1.2** is a solid that melts at above 240-241°C and its crystal structure was solved by X-ray diffraction (**Scheme 1.2**).

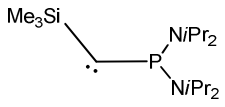

1.1

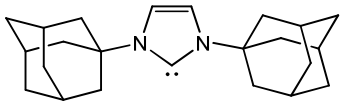

1.2

Scheme 1.2. The first isolated carbenes.

Wanzlick observed the dimerisation of NHCs to form N-tetraamines,[5] and trapped them to form mercury-carbene complexes,[6, 32] although the first free NHC carbene was isolated in 1991.[4] The particular stability of the NHCs made them very popular, and during the following years further analogues were synthesized (**Scheme 1.3**).

In 1995, Arduengo proved,[7] using NHC **1.3**, that aromaticity was not needed for the stabilization, and in 1996 Alder isolated the acyclic NHC **1.4**.[8] Other cyclic and acyclic N-containing carbenes were later isolated, as the four-membered carbene **1.5** by Grubbs[9], and the alkyl carbene **1.6** by Bertrand[10] in 2004.

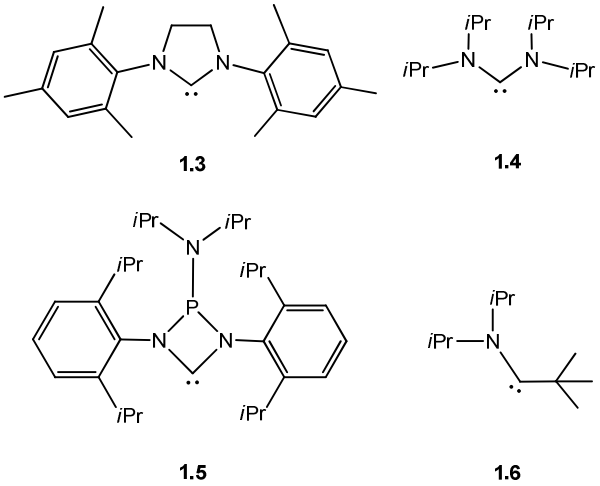

Scheme1.3 . Cyclic and acyclic stable carbenes.

1.2 General Properties of N-Heterocyclic Carbenes

The two nitrogen substituents next to the $C_{carbene}$ atom in NHCs, are known to stabilise their singlet state (two paired electrons in the σ orbital) by a push-pull effect (**Scheme 1.4**).[12] Firstly, the σ-electronwithdrawing nitrogens inductively stabilize the σ-nonbonding orbital by increasing its σ-character. Secondly, the energy of the vacant p_π-orbital at the carbon is increased by the interaction with the symmetric combination of the nitrogen lone pairs. The combination of the two effects increases the σ-p_π gap at the carbene-carbon and therefore stabilizes the singlet state. Additionally, the sp^2 hybridisation adopted by the $C_{carbene}$ atom in its singlet state matches the flat geometry of the NHC five-membered ring.

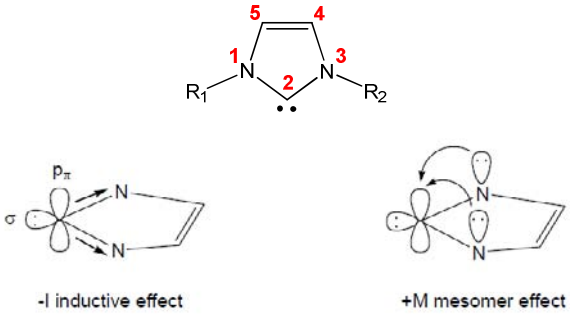

Scheme 1.4. Electronic Stabilization of NHCs.

The interaction of the nitrogen lone pair with the p_π-orbital of the carbene is reflected by a N-$C_{carbene}$ bond length of 1.365 Å, which is consistent with a double bond character. An accurate assessment of the π-backbonding was found by analysing the dynamic ^{1}H-NMR behaviour of the acyclic bis(diisopropylamine)carbene **1.4** (**Scheme 1.3**).[8] As the major part of this process involves rotation about the N-$C_{carbene}$ bonds, the measured rotation barrier of 53 kJ/mol was mostly attributed to the substantial π-component of these bonds. The major limitation of the design of stable saturated diaminocarbenes is their dimerization into tetraazafulvalene (or enetetramines).[12, 13]

This reaction has likely prevented the isolation of the 1,3-diphenylimidazolidinylidene by the Wanzlick group more in the early 60s.[14] The dimerization involves the attack of the occupied σ lone pair of one carbene center on the vacant p_π orbital of a second carbene.[15] Imidazolidinylidenes require sterically demanding ligands to prevent their dimerization to tetraazafulvalenes,[16] on the contrary this process is thermodynamically unfavourable for imidazolylidenes even for small ligands such as methyl groups (**Scheme 1.5**).

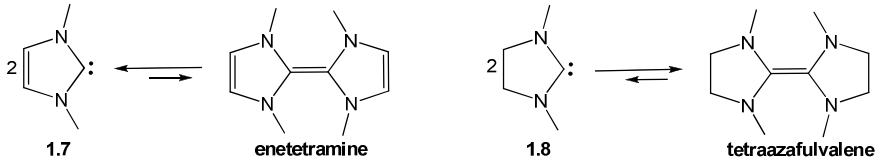

Scheme 1.5. Dimerization of NHC.

The strength of the C=C bond in enetetramines can be approximated by the strength of the gap (sp^2-sp^2)σ and the (p-p)π bonds in ethylene (172 Kcal/mol),[17] minus the sum of the singlet-triplet energy gap for both dissociated carbenes.[18] The energy gap between the singlet and triplet state is higher for imidazolidinylidenes (85 kcal mol^{-1}) than for imidazolinylidenes (70 kcal mol^{-1}) due to an extra-stabilization provided by the partial aromatic character of the imidazole ring.[14, 19]

Consequently imidazolylidenes (**1.7**, **Scheme 1.5**) do not form enetetramines easily as the C-C bond would be very weak or even energetically disfavored. In contrast, imidazolidinylidenes (**1.8**, **Scheme 1.5**) readily form tetraazafulvalenes, which are difficult to dissociate. The dimerization reaction has to be kinetically hampered by steric protection. The ^{13}C-NMR chemical shifts range from 210-220 ppm for unsaturated NHCs (**1.7**), and 235-245 ppm for saturated NHCs (**1.8**).[20]

1.3 Reactivity of NHCs

NHCs do not react with dioxygen for kinetic reasons (**Scheme 1.6**), but can be oxidized to the corresponding ureas **1.10** in the presence of catalytic amounts of CuCl or with NO (**Scheme 1.7**). [12, 21, 22]

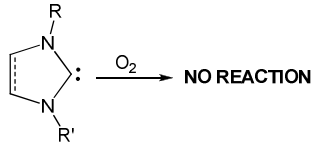

1.9

Scheme 1.6

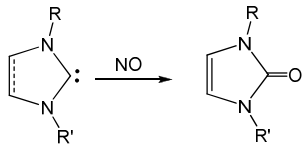

1.9 **1.10**

Scheme 1.7

NHCs slowly react with dihydrogen to form aminals (**1.11**) by 1,1-addition in the presence of a catalytic amount of palladium or platinum (**Scheme 1.8**).[21]

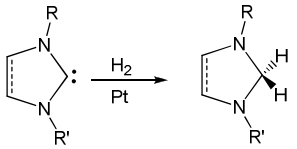

1.9 **1.11**

Scheme 1.8

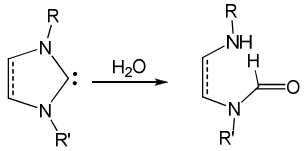

1.9 **1.12**

Scheme 1.9

The 'air sensitivity' of NHCs is mostly due to the attack of water, which leads to ring opening to give the formamides type **1.12** (**Scheme 1.9**).

While saturated NHCs are instantly hydrolyzed by moist THF or by brief exposure to air, hydrolysis of the unsaturated NHCs requires days to become noticeable and months to be completed.[22] As a result of this difference in reactivity, unsaturated NHCs can be handled in air for brief periods of time, while saturated NHCs require the usual inert gas techniques. The hydrolysis of NHCs can, in principle, proceed through a polar, stepwise mechanism (attack of H^+ or OH^- as initial step) or as insertion of the carbene into H_2O (**Scheme 1.10**).[12]

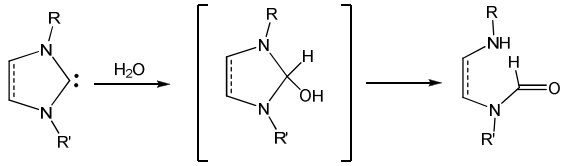

1.9 **1.12**

Scheme 1.10

NHCs react with acids and form imidazolium salts quantitatively due to their high p*K*a values, ranging from 20 to 30 (in water).[12, 23] Given the tendency to consider carbenes as potential replacements for phosphine ligands in many catalytic reactions, Yates and Cavell compared the relative basicities of the two types of ligands through theoretical calculations. **Table 1.1** shows some of the reported results by the authors. [23b]

Table 1.1. Basicity of carbene **1.7** and **1.8** and common phosphines in aqueous solution.[23b]

Compound	pK_a (H_2O)[1]
1.7	27.4 ± 0.4
1.8	28.5 ± 0.4
PPh_3	2.73[a]
PMe_3	3.84[a]
PEt_3	8.69[a]
PCy_3	9.70[a]
P(*t*-Bu)$_3$	11.40[a]

[1] **pK_a** values are referred to the conjugated acids of the carbenes (the imidazolium salts); due to the importance of basicity concept in organometallic and catalytic chemistry (particularly in relation to phosphines) it is a common practice to refer to a pK_a of a base;[23b] in this table more high is the value of pK_a and more basic is the carbene. [a] Reference 24

It is evident that even the most basic phosphine (P(*t*Bu)$_3$) is still ~ 16 pK_a units less basic than carbene **1.7**. In addition, they are among the most powerful neutral organic bases and their strength is comparable to DBU (DBU=1,5-Diazabicyclo[4.3.0]non-5-ene) and pentacyclic vinamidines.[12, 25]

1.4 NHC as ligands

Although the metal carbene bond in Schrock and Fischer carbene complexes are both described as double bonds, they differ in the distribution of the electron density along the bond. This difference arises from the difference in relative energy between the d_π orbital of the metal and the p_π orbital of the carbene (**Scheme 1.11**). If the d_π orbital is lower in energy than the p_π orbital, the metal carbon bond is polarised δ^- on the metal and δ^+ on the carbene (Fischer carbene complex).

Contrary, if the d_π orbital is higher in energy than the p_π orbital, the metal carbon bond is polarised δ^+ on the metal and δ^- on the carbene (Schrock carbene complex). NHCs are extreme examples of Fisher carbenes in which the p_π orbital has a very high energy due to the bonding between the carbene-carbon atom and the two nitrogens. As a result, the p_π orbital of the carbene-carbon does not interact well with the d_π metal orbital, thus preventing almost any

π-backbonding from the metal to the carbene. This implies that, in general, in NHC-complexes, the metal carbon bond is best represented by a single bond.

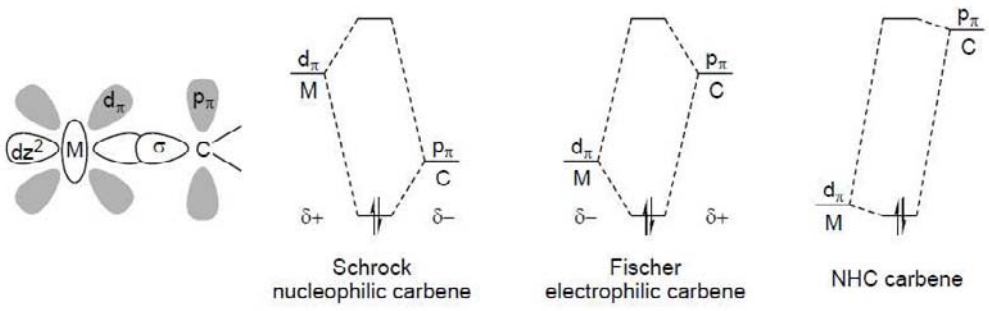

Scheme 1.11. Partial molecular diagram for Schrock, Fischer and NHC carbene complexes.

The fundamental difference between a typical Schrock alkylidene and an NHC is exemplified in the crystal structure of $[RuCl_2(NHC)_2(=CHC_6H_4Cl)]$ (NHC = 1,3-diisopropylimidazolin-2-ylidene) where the two types of carbenes are linked to the same metal centre.[23] The ruthenium-carbon bond of the Schrock carbene, generally written as a double bond, has a bond length of 1.821(3) Å, whereas the Ru-C bond length to the NHC (2.107(3) Å and 2.115 (3)Å) justifies its representation as a single bond (σ-donor and virtually no π-acceptor).

NHCs are often considered as analogs of tertiary phopshine ligands, but they display many different properties, such as increased electron donor power. This electron-richness of has an impact on many elementary steps of catalytic cycles, for example, facilitating the oxidative addition step. Furthermore, as a consequence of their strong electron donor property, NHCs are considered to be higher field as well as higher *trans* influence ligands than phosphines.[30]

IR spectroscopy proved to be a particularly useful technique for the evaluation of ligand donor properties via CO stretching frequencies of metal carbonyls. A number of recent experimental and computational studies have employed $Ni(CO)_3(NHC)$, $Rh(CO)_2X(NHC)$, and $Ir(CO)_2X(NHC)$ (X = halide) complexes.[26, 27] For example, Nolan et al, in order to achieve a deeper understanding of the fundamental steric and electronic factors characterizing the NHC ligands, reported a detailed study on the substitution reaction involving $Ni(CO)_4$ and NHC ligands, proposing the first dissociation energies of decarbonylation.[28]

In order to place all representative NHC ligands on the same stereoelectronic scale, in a way similar to the seminal work of Chadwick Tolman,[26, 29] Gusev carried out a study covering a large group of $Ni(CO)_3(NHC)$ complexes. In this work the author showed that good estimations of IR data can be obtained with the help of DFT calculations.[26] The results found, included also a better steric descriptor, named **r** ("repulsiveness"), which correlates with the ease of CO loss from the $Ni(CO)_3(NHC)$ complexes; in other words, the direct repulsive

interactions between the NHCs and COs ligands.[26] According to Gusev's calculations, the reaction enthalpies for the decarbonylation of $Ni(CO)_3(NHC)$ and formation of the corresponding 16 electron $Ni(CO)_2(NHC)$ species, are governed by steric control since the most stable tricarbonyl complex possesses the smallest ligand.[26] Gusev concluded that a increase of wing-tip size promotes a decrease of the TEP (cm^{-1}) (Tolman electronic parameter), and an increase of the NHC ring size from 5 to 6 members makes them a better σ-donor ligands.

Also, substitution on the C-4, 5 of the imidazole ring has a major effect on TEP (cm^{-1}); for example, the donor power increases significantly in the order NO_2 < CN < CF_3 < F≈Cl < CO_2Me < H < OMe < Me. **Figure 1.1** shows a plot of TEP vs average C-O bond distances in the $Ni(CO)_3(NHC)$ complexes, with added points for typical phosphines. In this picture Gusev tried to visualize differences between the different ligands.[26] The author named the ligands using the following format: [parent heterocycle](substituents)$_n$*N*(substituents)$_m$. For example, Im*N*Me_2 and Im*N*Me^{t}Bu are derivatives of imidazole and have two *N*Me groups and one *N*Me and one *N*^{t}Bu group, respectively. Saturated derivatives of the heterocycles are named accordingly, e.g., sIm*N*Me_2 or sImPh_2*N*Me_2.[26]

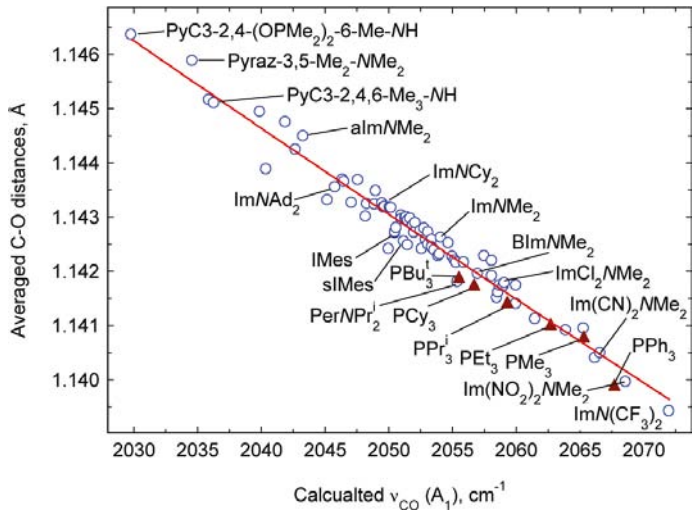

Figure 1.1. Plot of calculated TEP vs *d*(CO) values for a series of $Ni(CO)_3L$ complexes.[26]

N-heterocyclic carbenes have very similar levels of electron-donating ability, whereas phosphines span a much wider electronic range going from alkyl to aryl phosphines. The reason for this marked difference is that for NHC*s* only substituents on the periphery of the

ligand are exchanged, whereas for phosphines the different substituents are directly attached to the donor atom itself.[30]

The structural differences for free NHCs and metal complexed NHCs are very small. In the ^{13}C-NMR spectra, the signals for the free carbene carbon are usually shifted upfield by about 20-30 ppm upon complexation of the NHC to a transition metal.

1.5 Metallation

Without forgetting Lappert's[31] and Wanzlick's[32] pioneering works on the preparation of NHC-metal complexes, several easy synthetic methodologies have been most commonly applied in the literature for the preparation of NHC metal complexes: [33]

I) Use of isolated free carbene:

The preparation of the first free stable NHCs by Arduengo,[4] broke with the idea that these compounds were very unstable to be used as ligands in the preparation of transition metal complexes. Although in the beginning it was thought that the stability of free NHCs is mainly due to steric effects, it is now assumed that electronic effects play a more important role.[41] Arduengo was the first to propose that the nitrogen lone pairs and the C=C (in unsaturated NHCs) provide enough kinetic stability to allow the isolation of this type of carbenes,[42] and this, in fact, may justify why most of the NHCs obtained from the 'free NHC route' are of the unsaturated form. The use of preformed N-heterocyclic carbenes has the advantage that they can be directly used to replace labile ligands on a suitable complex precursor. The most widely used method for the preparation of NHCs is the deprotonation of an azolium salt with NaH or KO^{t}Bu.[20, 34, 36] Once obtained the carbene, this may directly react with the metal precursor (**Scheme 1.12**)

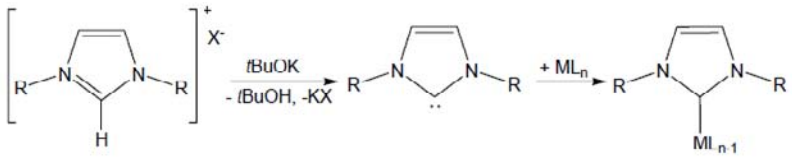

Scheme 1.12. Metalation of a previously isolated free NHC.

II) Use of enetetramines (or tetraazafulvalene), "Lappert's method":

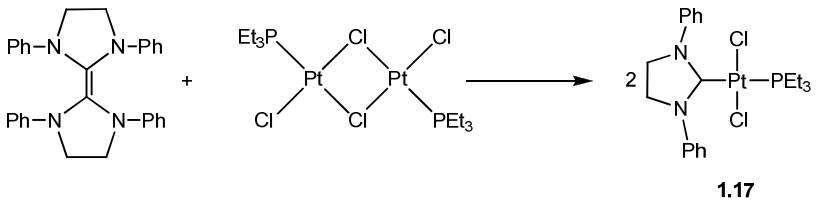

1.17

Scheme 1.13. Metal-NHC complex from enetetramine.

The reaction of electron-rich olefins with the corresponding metal complexes can provide mono-, bis-, tris- and even tetrakiscarbene complexes. A review about this type of reaction was published by Lappert in 1988.[31] All the NHC complexes obtained by this method are saturated NHCs. The first carbene complex, **1.17**, prepared by this method is shown in **Scheme 1.13**.[37]

III) Use of a metal complex with basic ligands:

The coordination of NHC-precursors (mainly imidazoliums) can be achieved using basic ligands on the metal complexes. Commercially available or easy-to-prepare metal complexes with acetate, alkoxide, hydride or acetylacetonate ligands are frequently used. Wanzlick[32] and Öfele[38] used this method to synthesize the first imidazolylidene complexes starting from $Hg(OAc)_2$ and $[CrH(CO)_5]^-$, respectively. More than 25 years later the use of metal(II) diacetates became a method which was often used to prepare imidazolylidene, triazolylidene and benzimidazlylidene complexes of Pd and Ni, providing monodentate-, bidentate and tridentate NHC complexes. [39-45]**Scheme 1.14** shows the preparation of a bis-NHC complex of Pd^{II} by this method.[34] In these reactions the acetate is eliminated as acetic acid.

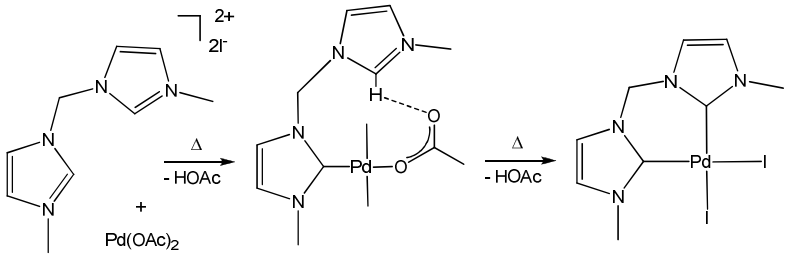

Scheme 1.14

IV) Deprotonation with an external base:

Several strong bases have been used in the deprotonation of azolium salts prior to the addition of the metal precursor to provide the desired NHC-complex. The election of the base is sometimes crucial in order to achieve the desired results. Changes in basicity and nucleophility can produce variations in the reaction products, or undesired activations of the ligand and metal complex. In this sense, bases such as NaH,[45] *n*BuLi,[46, 47] *t*BuLi,[48] *t*BuOLi or *t*BuOK,[49-51] and $KN(SiMe_3)_2$ are among the most widely used ones, and can be applied to imidazolium, triazolium and benzimidazolium salts for their complexation to a large variety of metals.[52, 53] The use of strong bases requires that dry solvents must be used for the reaction, and in many occasions low temperatures are needed during the deprotonation process, in order to avoid undesired activations of the ligand precursor. The method is useful for the preparation of simple monocarbene complexes, but it can also be used in the preparation of chelate bis-, and even one tris-carbene.[46]

Methylene-bridged bisimidazolium salts can be deprotonated by *n*BuLi at low temperature (-70ºC) generating a biscarbene that can coordinate to a metal complex. In the case of reaction with PdI_2, an homoleptic complex containing two bidentate biscarbenes can be obtained (**Scheme 1.15**).[45]

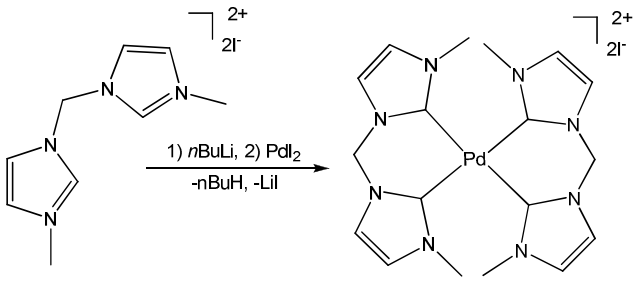

Scheme 1.15

The use of a strong base is very convenient in the sense that it warranties complete deprotonation of the azolium precursor, and can be used for a wide variety of azolium salts and metal precursors. However, for those metal- or carbene-precursors with acidic or electrophilic centers other than the C2-H position in the azolium ring, undesired activations can be produced leading to decomposition products.

As an alternative, a weak base can also be used in a number of occasions. For the election of the weak base, a clear knowledge of the acidity/basicity of the azolium/NHC has to be accounted. The basicity of NHCs has been studied from the experimental[54] and theoretical points of view, as previously stated in *section 1.3* at pag. 8.[23b] The most basic carbene shows

pKa values (in MeCN scale) of 39.1, while the less basic one is 25.6 (pKa values referred to the acidity values of the azolium salts).[23b] This in turn means that the less basic NHC is more basic than the most basic phosphine [$P(But)_3$, pKa ~ 10], thus implying a high proton affinity. From this point of view it is not easy to justify why weak bases such as NEt_3, NaOAc, Cs_2CO_3, provide very good results in the preparation of NHC-M complexes starting from azolium salts. Although detailed studies have not been made, it is difficult to believe that high concentrations of free carbenes are generated from mixtures of azolium salts and weak bases. A possible explanation for the high yields in the preparation of NHC compounds by this method may come from the stabilization provided by the NHC-complex, thus making the overall reaction favourable (**Scheme 1.16**).[55]

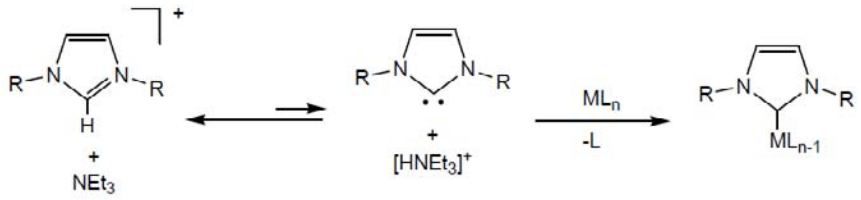

Scheme 1.16. Deprotonation of the imidazolium salt with a weak base and coordination to the metal.

V) Transmetallation via pre-formed silverNHC- complexes:

A method for preparing NHC metal compounds via silver NHC-complexes was first developed by Wang and co-workers.[56] Silver NHC complexes are readily prepared upon mixing the corresponding imidazolium salt with Ag_2O in CH_2Cl_2 (or many other solvents) at room temperature. Subsequent reaction with a transition metal source gives the desired NHC metal complex that can be easily separated from AgCl (**Scheme1.17**).

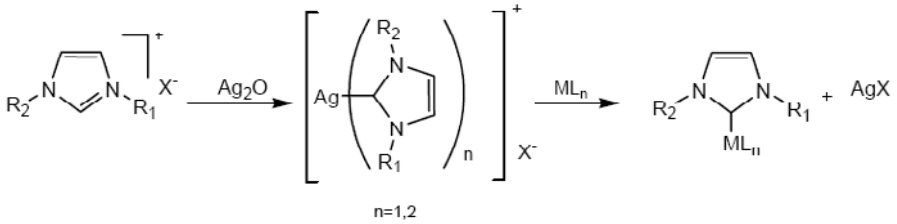

Scheme 1.17. Transmetalation reaction starting from a silver (I) carbene.

VI) *Use of carbene-adduct or protected NHC species:*

The use of protected carbenes represents a valuable procedure for the preparation of NHC complexes. N-heterocyclic rings containing alcoxo or chloromethyl groups, as shown in **Scheme 1.18** can be considered NHC-adducts because the elimination of alcohol or chloroform generate the free carbene that can be further coordinated to the metal. [57]

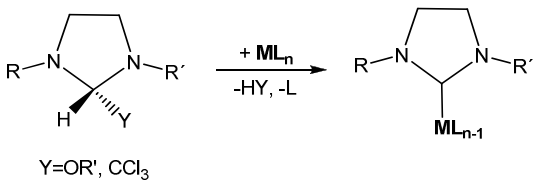

Scheme 1.18. Metalation from a carbene-adduct.

VII) Oxidative addition via activation of the C2-X bond (X= Me, halogen, H) of an imidazolium cation:

Direct oxidative addition of C2-X bonds (X = Me, halogen, H) of imidazolium cations to low-valent transition metal compounds constitute a facile access to NHC-M complexes under certain circumstances (**Scheme 1.19**).

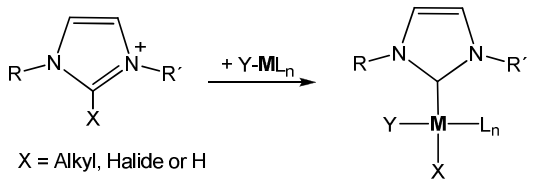

Scheme 1.19. Direct oxidative addition of C2-X bonds of imidazolium salts.

The oxidative addition of C-Cl bonds in azolium salts to generate carbene complexes is known since 1974.[58] In that case, 2- chloro-methylthiazolium salts were used as carbene precursors. In 2001, Cavell and coworkers extended the method to 2-iodo-imidazolium salts, and studied the oxidative addition process to group 10 M(0) complexes (Ni, Pd, Pt), both by an experimental and theoretical points of view.[59-61] The C2-H oxidative addition of imidazolium salts to metal complexes was recently proved in our group to account to other metals than low valent group 10.[62]

1.6 N-heterocyclic carbenes in our group

During the last ten years, our group has developed a research line based on the synthesis and applications of "stable NHC-based complexes" and their use as improved homogeneous catalysts.[63] For the preparation of such stable metal complexes, two basic principles were applied: i) the strength of the M-$C_{carbene}$ bond, and ii) the stabilizing chelating effect provided by bis- or tris chelating ligands.

After the synthesis of a palladium *pincer* NHC complex in 2001 (**Scheme 1.20**), which was obtained in collaboration with the Crabtree group,[64] the coordination of such pincer NHC ligands was extended to other metals such as Rh, Ir and Ru.[65, 66]

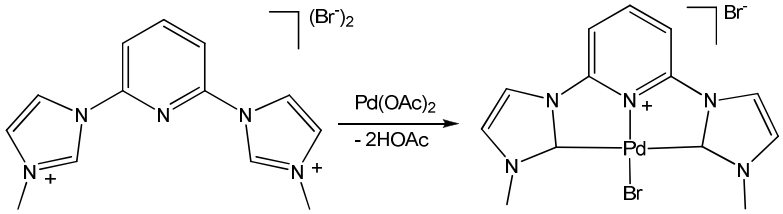

Scheme 1.20

The work was then extended to the preparation of transition metal complexes with bis-chelating-NHCs, in which the properties of the ligands were modulated by introducing modifications in the wingtips, linker and backbones, as depicted in **Scheme 1.21.** A series of metal complexes were obtained based on the ligands used, so that the geometry of the resulting species could be modulated according to the reaction conditions used. As shown in **Scheme 1.21**, many complexes with pincer (**1.13** and **1.14**),[65, 66] bridging (**1.15** and **1.16**),[65, 67] bis-chelating (**1.17**),[67] and tripod coordintation forms (**1.18** and **1.19**)[68, 69] of the NHC ligands were prepared and fully characterized.

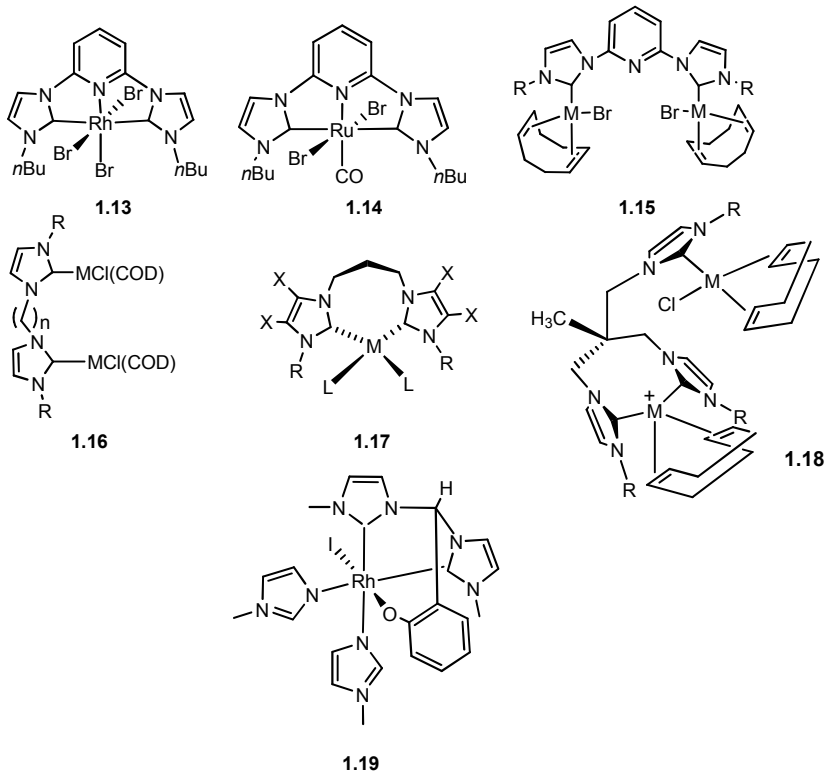

Scheme 1.21

In general, the introduction of chelating NHCs not only yielded more stable metal complexes, but they also provided interesting features that can fine tune topological properties such as steric hindrance, bite angles, chirality and fluxional behaviour. The complexes so obtained were tested in a wide variety of catalytic transformations, such as hydrosilylation, hydroformylation, oxidation of olefnins, Pd-catalyzed C-C coupling reactions, hydro- and diboration, selective deuteration, and most processes included under the term 'borrowing-hydrogen', among many others. The work developed in the last few years has been recently accounted in a review article.[70]

References

(1) W. v. E. Doering, A. K. Hoffmann, *J. Am. Chem. Soc.*, **1954**, *76*, 6162.

(2) W. A. Pryor (Ed.), Organic Free Radicals, American Chemical Society, Washington, D.C., 1977; W. Kimse, Carbene Chemistry, Academic Press, New York &London, 1964, p. 5.

(3) (a) H. Tomioka, *Acc. Chem. Res.* **1997**, *30*, 315; (b) A. Igau, H. Grutzmacher, A. Baceiredo, G. Bertrand, *J. Am. Chem. Soc.*, **1988**, *110*, 6463.

(4) A. J. Arduengo, III, R. L. Harlow, M. Kline, *J. Am. Cem. Soc.*, **1991**, *113*, 361.

(5) H. W. Wanzlick, E. Schikora, *Angew. Chem.* **1960**, *72*, 494.

(6) H. J. Schoenherr, H. W. Wanzlick, *Chem. Ber.* **1970**, *103*, 1037;

(7) A. J. Arduengo, III, J. R. Goerlich, W. J. Marshall, *J. AM. CHEM. SOC* **1995**, *117*, 11027.

(8) R. W. Alder, P. R. Allen, M. Murray, A. G. Orpen, *Angew. Chem., Int. Ed.* **1996**, *35*, 1121.

(9) E. Despagnet-Ayoub, R. H. Grubbs, *J. Am. Chem. Soc.*, **2004**, *126*, 10198.

(10) V. Lavallo, J. Mafhouz, Y. Canac, B. Donnadieu, W. Schoeller Wolfgand, G. Bertrand, *J. Am. Chem. Soc.*, **2004**, *126*, 8670.

(11) L. Pauling, *Chem. Commun.* **1980**, 688.

(12) P. de Frémont, N. Marion, S. P. Nolan, *Coord. Chem Rev.*, **2009**, *253*, 862.

(13) (a) A. J. Arduengo III, *Acc. Chem. Res.*, **1999**, *32*, 913; (b) R. W. Alder, M. E. Blake, L. Chaker, J. N. Harvey, F. Paolini, J. Schuetz, *Angew. Chem., Int. Ed.* **2004**, *43*, 5896.

(14) E. Fjedor, K. H. Jerg, H. W. Wanzlick, *Chem. Ber.*, **1963**, *96*, 1208.

(15) (a) E. A. Carter, W. A. Goddard, *J. Phys. Chem.*, **1986**, *90*, 998; G. Trinquier, J. P. Malrieu, *J. Am. Chem. Soc.*, **1989**, *111*, 5916; T. Ziegler, H. Jacobsen, *J. Am.. Chem. Soc.*, **1994**, *116*, 3667.

(16) F. L. Zheng, A. Hezharkani, M. K. Denk, *Eur. J. Inorg. Chem.*, **2007**, 3527 and reference therein.

(17) S. I. Miller, *J.Chem. Educ.*, **1978**, *55*, 778.

(18) H. Grutzmacher, M. Driess, *Angew. Chem. Int. Ed. Engl.*, **1996**, *35*, 828; P. Chen, *Adv. Carbene Chem.*, **1998**, *2*, 45.

(19) (a) W. Thiel, C. Heinemann, *Chem. Phys. Lett.*, **1994**, *217*, 11; (b) C. H. Hu, M.J. Cheng *Chem. Phys. Lett.*, **2001**, *349*, 477.

(20) D. Bourissou, O. Guerret, F. P. Gabbaie, G. Bertrand, *Chem. Rev.*, **2000**, *100*, 39.

(21) J. P. Donahue, R. H. Hola, *Polyhedron*, **1993**, *12*, 571.

(22) M. K. Denk, J. M. Rodezno, S. Gupta, A., *J. Lough, J. Organomet. Chem.*, **2001**, *617/618*, 242.

(23) (a) R. W. Alder, P. R. Allen, S. J. Williams, *J. Chem. Soc., Chem. Comm.*, **1995**, 1267; (b) A. M. Magill, K. J. Cavell, B. F. Yates, *J. Am. Chem. Soc.*, **2004**, *126*, 8717.

(24) M. M. Rahman, H.-Y. Liu, K. Eriks, A. Prock, W. P. Giering, *Organometallics*, **1989**, *8*, 1.

(25) I. Kaljurand, T. Rodina, I. Leito, I. A. Koppel, R. Schwesinger, *J. Org. Chem.*, **2000**, *65*, 6202.

(26) D. Gusev, *Organometallics*, **2009**, *28*, 6458.

(27) (a) G. Altenhoff, R. Goddard, C. W. Lehmann, F. Glorius, *J. Am. Chem. Soc*, **2004**, *126*, 15195; (b) W. A. Herrmann, J. Schütz, G. D. Frey, E. Herdtweck,. *Organometallics*, **2006**, *25*, 2437; (c) H. Türkmen, B. J. Cetinkaya, *J. Organomet. Chem.*, **2006**, *691*, 3749; (d) S. Leuthäusser, D. Schwarz, H. Plenio, *Chem.;Eur. J.*, **2007**, 13, 7195; (e) A. Bittermann, P. Härter, E. Herdtweck, S. D. Hoffmann, W. A. Herrmann, *J. Organomet. Chem.*, **2008**, *693*, 2079. (f) R. A. III Kelly, H. Clavier, S. Giudice, N. M. Scott, E. D. Stevens, J. Bordner, I. Samardjiev, C. D. Hoff, L. Cavallo, S. P. Nolan, *Organometallics*, **2008**, *27*, 202; (g) D. M. Khramov, E. L. Rosen, J. A. V. Er, P. D. Vu, V. M Lynch, C. W. Bielawski, *Tetrahedron*, **2008**, *64*, 6853; (h) G. Song, Y. Zhang, X. Li, *Organometallics*, **2008**, *27*, 1936; (h) K. Hirano, S. Urban, C. Wang, F. Glorius, *Org. Lett.*, **2009**, *11*, 1019; (i) R. Tonner, G. Frenking, *Organometallics*, **2009**, *28*, 3901.

(28) R. Dorta,E. D. Stevens, N. M. Scott, C. Costabile, L. Cavallo, C. D. Hoff, S. P. Nolan, *J. Am. Chem. Soc*, **2005**, *127*, 2485.

(29) C. A. Tolman, *Chem. Rev.*, **1977**, *77*, 313.

(30) F. Glorius, *Top. Organomet. Chem.*, **2007**, *21*, 5.

(31) D. J. Cardin, B. Cetinkay, M. F. Lappert, *Chem. Rev.*, **1972**, *72*, 545; D. J. Cardin, B. Cetinkay, M. J. Doyle, M. F. Lappert, *Chem. Soc. Rev.*, **1973**, *2*, 99; M. F. Lappert, *J. Organom. Chem.*, **1988**, *358*, 185; M. F. Lappert, *J. Organom. Chem.*, **2005**, *690*, 5467.

(32) H. –W. Wanzlick, H.-J. Schönherr, *Angew. Int. Ed. Engl.*, **1968**, *7*, 141.

(33) E. Peris, *Top. Organomet. Chem.*, **2007**, *21*, 83.

(34) Weskamp, T.; Bohm, V. P. W.; Herrmann, W. A. *J. Organomet. Chem.*, **2000**, *600*, 12.

(35) A. J. Arduengo, H. Bock, H. Chen, M Denk, D. A. Dixon, J. C. Green, W. A. Herrmann, N. L. Jones, M. Wagner, R. West, *J. Am. Chem. Soc.*, **1994**, *116*, 6641; A. J. Arduengo, H. V. Dias, D. A. Dixon, R. L. Harlow, W. T. Klooster, T. F. Koetzle, *J. Am. Chem. Soc.*, **1994**, *116*, 6812; A. J. Arduengo, D. A. Dixon,K. K. Kumashiro, C. Lee, W. P. Power, K. W. Zilm, *J. Am. Chem. Soc.*, **1994**, *116*, 6361.

(36) W. A. Herrmann, *Angew. Chem. Int. Edit.*, **2002**, *41*, 1291.

(37) D. J. Cardin, B. Cetinkay, M. F. Lappert, L. Manojlov; K. W. Muir, *J. Chem. Soc., Chem. Comm.*, **1971**, 400.

(38) K. Oefele, *J. Organomet. Chem.*, **1968**, *12*, 42.

(39) Herrmann, W. A.; Elison, M.; Fischer, J.; Kocher, C.; Artus, G. R. J. *Angew.Chem. Int. Edit. Engl.*, **1995**, *34*, 2371.

(40) Herrmann, W. A.; Elison, M.; Fischer, J.; Kocher, C.; Artus, G. R. J. *Chem.-Eur.J.*, **1996**, *2*, 772.

(41) W. A. Herrmann, J. Schwarz, M. G. Gardiner, M. Spiegler, *J. Organomet. Chem*., **1999**, *575*, 80.

(42) W. A. Herrmann, G. Gerstberger, M. Spiegler, *Organometallics*, **1997**, *16*, 2209.

(43) J. Schwarz, V. P. W. Bohm, M. G. Gardiner, M. Grosche, W. A. Herrmann, W. Hieringer, G. Raudaschl-Sieber, *Chem.-Eur. J.*, **2000**, *6*, 1773; W. A. Herrmann, C. P. Reisinger, M. Spiegler, *Organomet. Chem.*, **1998**, *557*, 93; M. G. Gardiner, W. A. Herrmann, C. P. Reisinger, J. Schwarz, M. Spiegler, M., *J. Organomet. Chem.*, **1999**, *572*, 239; W. A. Herrmann, V. P. W. Bohm, V. P. W.; C. P. Reisinger, *J. Organomet. Chem.*, **1999**, *576*, 23; G. Bertrand, E. Diez-Barra, J. Fernandez-Baeza, H. Gornitzka, A. Moreno, A. Otero, R. I. Rodriguez-Curiel, J. Tejeda, *Eur. J. Inorg. Chem.*, **1999**, 1965; D. S. McGuinness, W. Mueller, P. Wasserscheid, K. J. Cavell, B. W. Skelton, A. H. White, U. Englert, U. *Organometallics* **2002**, *21*, 175.

(44) J. A. Loch, M. Albrecht, E. Peris, J. Mata, J. W. Faller, R. H. Crabtree, *Organometallics* **2002**, *21*, 700; E. Peris, J. A. Loch, J. Mata, R. H. Crabtree, *Chem. Commun.*, **2001**, 201.

(45) R. E. Douthwaite, J. Houghton, B. M. Kariuki, *Chem. Commun.*, **2004**, 698; M. Alcarazo, M.; S. J. Roseblade, A. R. Cowley, R. Fernandez, J. M. Brown, J. Lassaletta, *J. Am. Chem. Soc.*, **2005**, *127*, 3290.

(46) R. E. Douthwaite, J. Houghton, B. M. Kariuki, *Chem. Commun.*, **2004**, 698; M. Alcarazo, M.; S. J. Roseblade, A. R. Cowley, R. Fernandez, J. M. Brown, J. Lassaletta, *J. Am. Chem. Soc.*, **2005**, *127*, 3290.

(47) U. Kernbach, M. Ramm, P. Luger, W. P. Fehlhammer, *Angew. Chem. Int. Edit. Engl.*, **1996**, *35*, 310.

(48) W. A. Herrmann, L. J. Goossen, M. Spiegler, *J. Organomet. Chem.*, **1997**, *547*, 357.

(49) M. V. Baker, S. K. Brayshaw, B. W. Skelton, A. H. White, C. C. Williams, *J. Organomet. Chem.*, **2005**, *690*, 2312; W. A. Herrmann, L. J. Goossen, M. Spiegler, *Organometallics*, **1998**, *17*, 2162.

(50) D. Enders, H. Gielen, G. Raabe, J. Runsink, J. H. Teles, *Chem. Ber.-Recl.*, **1996**, *129*, 1483.

(51) Clyne, D. S.; Jin, J.; Genest, E.; Gallucci, J. C.; RajanBabu, T. V. *Org. Lett.*, **2000**, *2*, 1125.

(52) Danopoulos, A. A.; Winston, S.; Motherwell, W. B. *Chem. Commun.*, **2002**, 1376.

(53) Coleman, K. S.; Turberville, S.; Pascu, S. I.; Green, M. L. H. *J. Organomet. Chem.*, **2005**, *690*, 653.

(54) Y. J. Kim, A. Streitwieser, *J. Am. Chem. Soc*, **2002**, *124*, 5757; R. W. Alder, P. R. Allen, S. J. Williams, *J. Chem. Soc.-Chem. Commun.*, **1995**, 1267.

(55) M. Poyatos, M. Sanau, E. Peris, *Inorg. Chem.*, **2003**, *42*, 2572.
(56) H. M. J. Wang, I. J. B. Lin, *Organometallics*, **1998**, *17*, 972.
(57) D. Enders, H. Gielen, G. Raabe, J. Runsink, J.H. Teles, *Chem. Ber*., **1996**, 129, 1483.
(58) P. J. Fraser, W. R. Roper, F. G. A. Stone, *J. Chem. Soc.-Dalton Trans.*, **1974**, 760; P. J. Fraser, W. R. Roper, F. G. A. Stone, *J. Chem. Soc.-Dalton Trans.*, **1974**, 102.
(59) D. S. McGuinness, K. J. Cavell, B. F. Yates, B. W. Skelton, A. H. White, *J. Am. Chem. Soc.*, **2001**, *123*, 8317.
(60) D. S. McGuinness, K. J. Cavell, B. F. Yates, *Chem. Commun.*, **2001**, 355.
(61) K. J. Cavell, D. S. McGuinness, *Coord. Chem. Rev.*, **2004**, *248*, 671.
(62) M. Viciano, E. Mas-Marza, M. Poyatos, M. Sanau, R. H. Crabtree, E. Peris, *Angew. Chem. Int. Ed*., **2005**, *44*, 444.
(63) T. Myers, *Inorg. Chem*., **1978**, *17*, 952.
(64) E. Peris, J. A. Loch, J. Mata, R. H. Crabtree, *Chem. Comm*., **2001**, 201.
(65) M. Poyatos, E. Mas-Marza, J. A. Mata, M. Sanau, E. Peris, *Eur. J. Inorg. Chem.*, **2003**, 1215.
(66) M. Poyatos, J. A. Mata, E. Falomir, R. H. Crabtree, E. Peris, *Organometallics*, **2003**, *22*, 1110.
(67) M. Viciano, E. Mas-Marza, M. Sanau, E. Peris, *Organometallics*, **2006**, *25*, 3063.
(68) E. Mas-Marza, M. Poyatos, M. Sanau, E. Peris, *Inorg. Chem.*, **2004**, *43*, 2213.
(69) E. Mas-Marza, M. Poyatos, M. Sanau, E. Peris, *Organometallics*, **2004**, *23*, 323.
(70) R. Corberan, E. Mas-Marza, E. Peris, *Eur. J. Inorg. Chem.*, **2009**, *13*, 1700.

Chapter 2

NHC-Based compounds for Tandem Catalysis

2.1 Introduction to Tandem Catalysis

The integration of several steps in a one-pot has gained considerable interest in the past decades. The objectives for this are clear: not only can a reduction in effort, waste and energy consumption be achieved, but also the synthesis of complex products that are otherwise difficult to obtain comes within reach.

Perhaps the best examples of the concept of cooperating catalytic systems can be found in the human body; in wich many enzymes involves the cooperation of two or more reactive centres (e.g. the multi-step glycolysis pathway which comprises the digestive conversion of glucose into energy and pyruvate).[1, 2, 3] It is considered that by imitating nature, the principle of multifunctional catalysis could offer many advantages over existing strategies.[4, 5]

The nomenclature used in literature associated with performing multiple catalytic mechanisms in one pot is confusing and frequently inconsistent. The terms *domino catalysis*, *tandem catalysis* and *cascade catalysis* are only applicable if multiple catalytic actions on a single molecule are performed in one pot and if all (pre)catalysts (masked or apparent) are present from the outset. If this is not the case, one can only speak of a *multicomponent reaction (MCR)*.[6] A *multicomponent reaction (MCR)* is a chemical process in which three or more reactants successively react in one reactor to give a product that incorporates substantial portions of all the substrates.[7] MCRs possess several inherent advantages over the usual combination of reactions used to create individual covalent bonds, including time and cost savings, atom economy, environmental friendliness, and applications in diversity-oriented synthesis and combinatorial chemistry.

The term *domino catalysis* has been used to describe a process of two or more chemical transformations occurring under identical conditions, in which the subsequent transformation takes place at the functionalities obtained in the former transformation.[8] **Scheme 2.1** shows a typical example of catalytic *domino reaction*.[9]

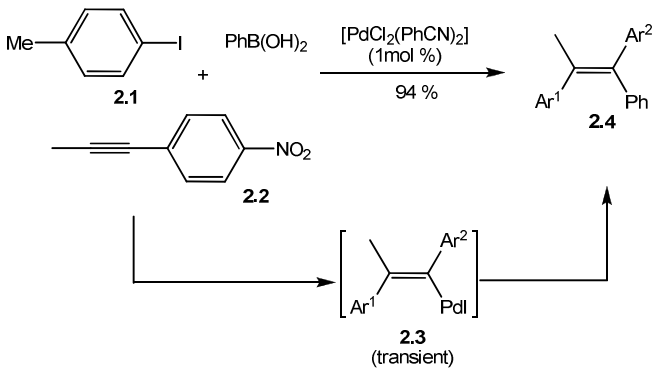

Scheme 2.1. An example of *domino catalysis*: synthesis of tetrasubstituted olefins catalyzed by a Pd catalyst (Ar^1 = *p*-MeC_6H_4, Ar^2 = *p*-$NO_2C_6H_4$).[9]

In the reaction sequence, the first event is a regioselective carbopalladation of **2.2** with aryl palladium generated by the oxidative addition of Pd^0 with aryl halide **2.1**. Further transmetalatation of resulting vinyl palladium **2.3** with phenyl boronic acid followed by reductive elimination gives product **2.4** and regenerates Pd^0. During the reaction course, the catalytic activation event occurs only once and intermediate **2.3** cannot be isolated as a stable species.

Furthermore, *Cascade catalysis* is a subcategory of domino catalysis, applying to systems with more than two transformations.[6] *Tandem catalysis* is applied to systems where multiple catalytic mechanisms are exploited in one pot. Because *tandem catalysis* involves more than two catalyst-controlled chemical reactions, highly diverse transformations are possible with a single synthetic operation, as compared with the catalytic *domino reaction*. In the early literature, the concept of tandem catalysis was sometimes confused and misused.[6] To avoid the confusion, Baker and Bazan et al. proposed the term *concurrent tandem catalysis (CTC)*, which involves the cooperative action of two or more catalytic cycles in a single reactor.[10]

Fogg and dos Santos proposed a classification of tandem catalysis into three subcategories: *orthogonal-*, *assisted-*, and *auto*-tandem catalysis. Their classification is based on the efficiency of the catalyst(s).[11]

Orthogonal tandem catalysis consists of two or more noninterfering catalysts or precatalysts, each of which catalyzes an independent chemical transformation (**Scheme 2.2**).

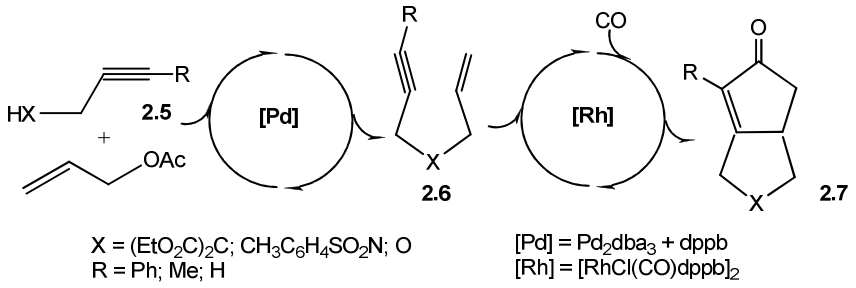

Scheme 2.2. An example of orthogonal-tandem catalysis: synthesis of substitued bicyclopentenones catalyzed by using Pd and Ru catalysts.[12]

In the process shown in **Scheme 2.2**, described by Shin[12], in the first step, the palladium catalyzes the allylation of the activated alkyne **2.5** generating an enyne intermediate, **2.6**, which then undergoes a rhodium-catalyzed Pauson-Khand reaction forming the bicyclopentenone **2.7** product in the presence of carbon monoxide.[12]

Assisted-tandem catalysis employs only one catalyst; after the first catalytic cycle is completed, chemical triggers are added to change the species of the catalyst and start the second cycle (**Scheme 2.3**).[6]

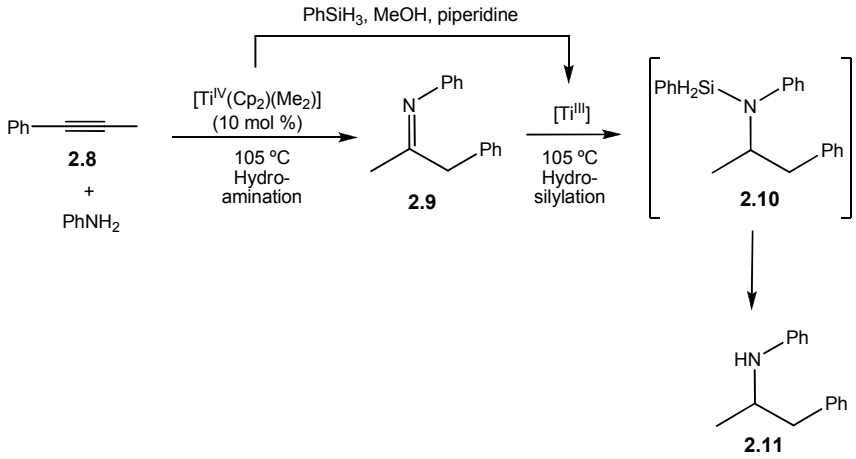

Scheme 2.3. An example of assisted-tandem catalysis: Ti^{IV}-catalyzed hydro-amination and subsequent hydrosilylation catalyzed by in situ generated Ti^{III}.[6]

In the reaction shown, the Ti^{IV} complex first initiates the hydroamination of acetylene **2.8** with aniline to give imine **2.9**, and then the Ti^{III} species, which is generated by using $PhSiH_3$ as a chemical trigger, promotes hydrosilylation. As a result, secondary amine **2.11** is produced after N-Si bond cleavage of **2.10** during the basic work-up.[6]

However, the operational simplicity is lower than the other reactions because the monitoring of the completion of the first transformation and interventional addition of chemical triggers are required.

The third class is *auto-tandem catalysis*. In the reaction sequence, one catalyst promotes more than two chemical transformations, the reaction mechanisms are different to each other, and no additional trigger reagent is required (**Scheme 2.4**).[6]

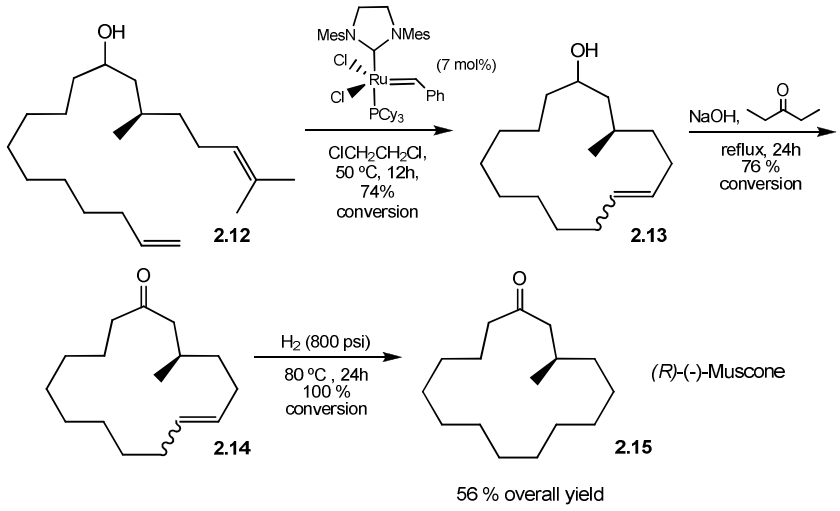

Scheme 2.4. One pot three-step procedure of olefin metathesis, transfer dehydrogenation, and hydrogenation with a single-component Ru complex.[6]

Grubbs *et al.* elegantly demonstrated that a *N*-heterocyclic ruthenium benzylidene is highly useful in performing one-pot three tandem catalytic reactions including ringclosing olefin metathesis (RCM) of dienes **2.12**, transfer dehydrogenative oxidation of alcohols **2.13**, and hydrogenation of olefins **2.14** (**Scheme 2.4**).[13] The strategy was applied to a one-pot three-step synthesis of (*R*)-(2)-muscone **2.15**, a natural product with a desirable fragrance. In this case, after the ring-closing metathesis (RCM) of a diolefinic alcohol **2.12**, the transfer dehydrogenation of the resulting cycloalkenyl alcohol **2.13** was carried out in the presence of 3-pentanone and NaOH. Subsequent hydrogenation of the olefinic ketone intermediate **2.14** was presumed to proceed by *in situ* generated ruthenium hydride catalyst in excellent yield under mild conditions. The ruthenium catalyst in this protocol exhibits compatibility with many functional groups under the reduction conditions, which is not the case for many hydrogenation procedures.[13]

The illustrations where two catalysts perform sequential organic transformations in a single vessel are significantly increasing in recent years. In many aspects, this approach of one-pot tandem catalysis demonstrates that it makes the processes more economical and time saving compared to the traditional one-catalyst one-reaction routes. When multiple catalysts are used, they should be mutually compatible with respect to the required reaction conditions.

This requires fine-tuning of the catalytic systems and conditions to allow for the right concerted cooperation. In addition, the catalytic action should be sufficiently selective and high-yielding. Since intermediate purification is left out in a one-pot reaction, imperfection in selectivity and yield is amplified when multiple processes are coupled. Side-products from one reaction step might have a detrimental effect on the activity of the other catalyst in the system. For developing tandem catalytic processes, in-depth knowledge is required of the mechanistic characteristics of both catalytic processes, and of the interplay of the catalysts. Important questions are whether the catalysts, substrates and/or reagents affect each other, which side-reactions might play a role and whether the reaction conditions can be matched.

2.2 Ditopic catalysts for tandem processes

The design of an effective (or active) *tandem* catalyst in more than one catalytic process is a hard challenge in homogeneous catalysis. Basically, two different types of catalytic systems can be used in a tandem reaction: i) a single catalyst performs the mechanistically distinct reactions of the tandem process, or ii) two (or more) different catalysts are added to the reaction medium to afford the two (or more) different transformations (**Scheme 2.5**).

Each of these two possibilities has a series of advantages and disadvantages. If we use a single catalyst, in the construction of the tandem sequence, we can only combine transformations for which this catalyst is active. Alternatively, we can use two different catalysts to increase the number of possible combinations, especially if we pretend to combine reactions that are fundamentally different in nature. However, this alternative obviously reduces the atomic economy of the reaction, especially if we take into account that the

preparation of the two different catalysts requires double amount of time, solvents, reagents and purification and characterization procedures.

Alternatively, we can design a ditopic catalyst, a complex with two different metallic fragments where each fragment can catalyze one of the reactions comprised in the tandem sequence. For the preparation of the ditopic catalyst the choice of the proper ligands capable to bridge the two (probably very) different metallic fragments represents the major challenge.

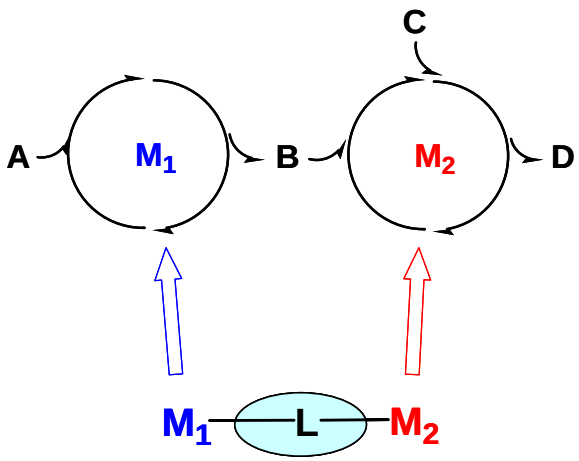

Scheme 2.5. One-complex-two-metals tandem catalyst.

It is well known that N-heterocyclic carbenes (NHCs) have appeared as a versatile class of ligands in the preparation of new homogeneous catalysts.[14] Their chemical versatility not only allows a wide structural diversity and coordination modes, but also a high capability to form stable complexes with a large number of transition metals with different oxidation states. Another interesting feature of NHCs is that they can show two types of coordination, depending on which carbon atom is bound to the metal center, and are thus classifed as normal (C2-bound, **A** in **Scheme 2.6**) and abnormal (C4-bound, **B** in **Scheme 2.6**) carbenes as a consequence of the studies first reported by Crabtree and co-workers.[15]

Under these circumstances, it is not difficult to imagine a situation with simultaneous coordination of two metal fragments at the C2 and C4 positions of the azole ring, resulting in a new ditopic form of coordination of the NHC (**C**, **Scheme 2.6**). This latter situation would represent a very interestig starting point for the preparation of NHC-briged heterometallic catalysts. Prelimminary studies carried out in our lab in order to get such dual coordination form of NHCs did not get any satisfactory results.

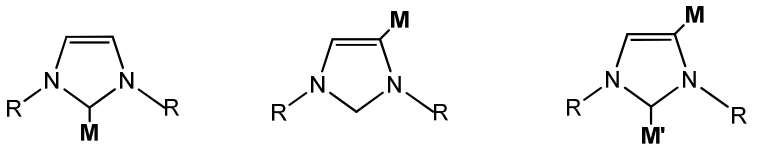

Scheme 2.6. Coordination mode of NHCs ligands.

A very interesting situation was recently reported by Bielawski and co-workers,[16] who described a series of benzobis(imidazolylidene)s. These compounds show facially opposed coordination abilities (*Janus-head* type) thus forming homo-binuclear complexes of rhodium, palladium, platinum, and silver (**Scheme 2.7**). The denomination Janus-Head is attributed to its analogy to the representation to the Roman God *Janus*, who had two faces looking at opposite directions.

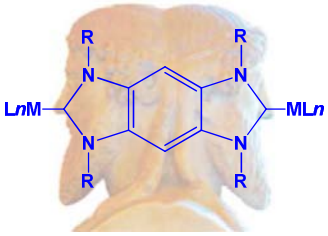

Scheme 2.7. Schematic analogy into the complexes using the NHC-based bridge described for Bielawski and the Roman God *Janus.*

A much simpler NHC-based bridge can be obtained using the dicationic 1,2,4-trialkylated triazolium salts described by Curphey in 1972 (**Scheme 2.8**).[17]

Scheme 2.8. Synthesis of *ditz*H_2.

The possibility of obtaining dicationic triazolium biscarbene precursors[17] to potentially bind two metal centers was suggested early on by Bertrand and co-workers,[18, 19] who described a polymeric silver biscarbene compound using a trizolyl-di-ylidene ligand (**Scheme 2.9**).[19]

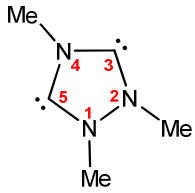

"ditz"

Scheme 2.9. "ditz" ligand.

The potential of this ligand is extraordinary, and also its high versatility for the coordination of a wide range of metals opens the possibility for the preparation of new homo- and hetero-bimetallic species.

In addition, the connection of two metal fragments through an aromatic linker may also have interesting implications for their catalytic cooperativity. This property makes the triazolediylidene ligand ("***ditz***", **Scheme 2.10**) the simplest building block for the preparation of NHC-based tandem catalysts.

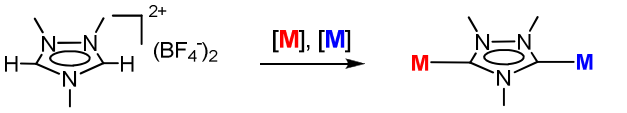

Scheme 2.10.

Ditz,[20, 21, 22] was recently used in our research group for the preparation of homobimetallic compounds of Ru^{II},[21] Ir^{I} and Rh^{I},[20] and also a heterobimetallic complex of Ir^{I}/Rh^{I} (**1L**, **Scheme 2.11**).[20]

The synthesis of the heterobimetallic compound **1L**[20] was carried out using a sequential strategy as shown in **Scheme 2.11**. In the first step, the reaction of dicationic triazolium salt (*ditz*) with the $[IrCl(cod)]_2$ in the presence of 1 equivalent of *t*BuOK produced the formation of a monometalated cationic species of Ir^{I}. This reaction was performed at - 40ºC to avoid the generation of a homobimetallic Ir^{I} complex. The subsequent addition of one equivalent of base and $[RhCl(cod)]_2$ allowed the formation of the heterobimetallic compound, in wich the 1,2,4-trimethyltriazolyl-di-ylidene (*ditz*) is bridging the two metallic fragments.[20] In the reaction conditions used, the corresponding monometalated cationic Ir^{I} species was not isolated.

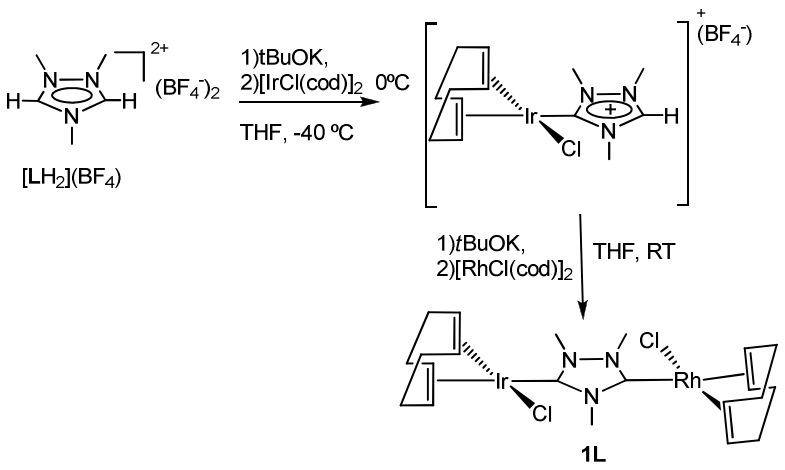

Scheme 2.11. Coordination of "*ditz*" to Rh^{I} and Ir^{I}.

The preparation of this new molecule allows novel strategies for the design of new homo- and hetero-binuclear species with potentially improved catalytic properties. In fact, the effective preparation of the Ir–Rh species **1L** opens the possibility for a wide range of bimetallic combinations, especially if we take into account the high coordination versatility of NHCs. This property makes the triazolediylidene ligand (***"ditz"***) a unique building block for the preparation of tandem catalysts.

2.3 Ditz-based homometallic complexes and their catalytic properties

2.3.1 Synthesis of homometallic complexes

The synthesis of the 1,2,4-trimethyltriazolium tetrafluoroborate is described in literature[17] and implies a double quaternization of the 1-methyltriazole with a strong alkylating agent such as trimethyloxonium tetrafluoroborate ("Meerwein reagent"). The reaction was performed refluxing the mixture in dichloroethane (DCE) for 45 minutes (**Scheme 2.12**). The solid obtained is then filtered and crystallized from hot CH_3CN.

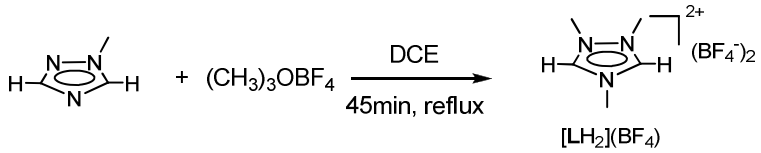

Scheme 2.12. Synthesis of "LH_2" salt.

Taking into account the results obtained in our group on the coordination of **L** to Rh^{I} and Ir^{I},[20] we decided to extend its coordination to Ir^{III}, Pd^{II} and Pt^{II}. For the preparation of the bis-Ir^{III} complex, we decided to use $[Cp^*IrCl_2]_2$ as metal source, because studies carried out in our group showed the high catalytic applicabilities of Cp*IrNHC species.[23] The synthetic procedure to the Ir^{III} homobimetallic complex is shown in **Scheme 2.13**.

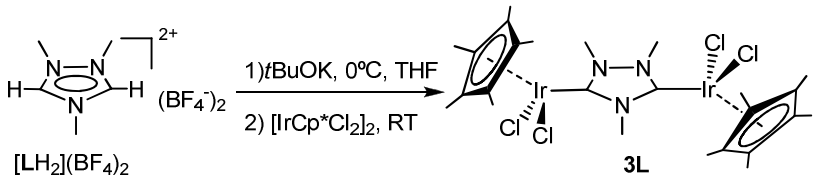

Scheme 2.13. Synthesis of complex **3L**.

The triazolium salt $[\mathbf{L}H_2](BF_4)_2$ was deprotonated with *t*BuOK at 0 ºC. The corresponding dicarbene reacted *in situ* with $[Cp^*IrCl_2]_2$ at room temperature (**Scheme 2.13**). The mixture was then evaporated at reduced pressure, redissolved in dichloromethane and filtered through Celite in order to eliminate the potassium salts formed during the reaction. The crude was purified by column cromatography. The pure compound **3L** was eluted with dichloromethane/acetone (8:2) and precipitated from a mixture of dichloromethane/diethyl ether to give an orange solid, in a 60% yield.

Compound **3L** was characterized by NMR spectroscopy (^1H and ^{13}C) and mass spectrometry and gave satisfactory elemental analysis.

*^{1}H NMR spectrum of complex **3L***

The ^{1}H NMR spectrum of **3L** shows that the signal due to the two acidic HC*H*N protons has disappeared, thus providing the first evidence that the coordination of the di-NHC ligand had taken placed. The resonances due to the methyl groups at δ 4.32 (**a**, **b**), suggest that the compound has a two-fold symmetry. The corresponding protons of the methyls of the Cp* ring appear as a singlet at 1.6 ppm (**c**) (**Figure 2.1**).

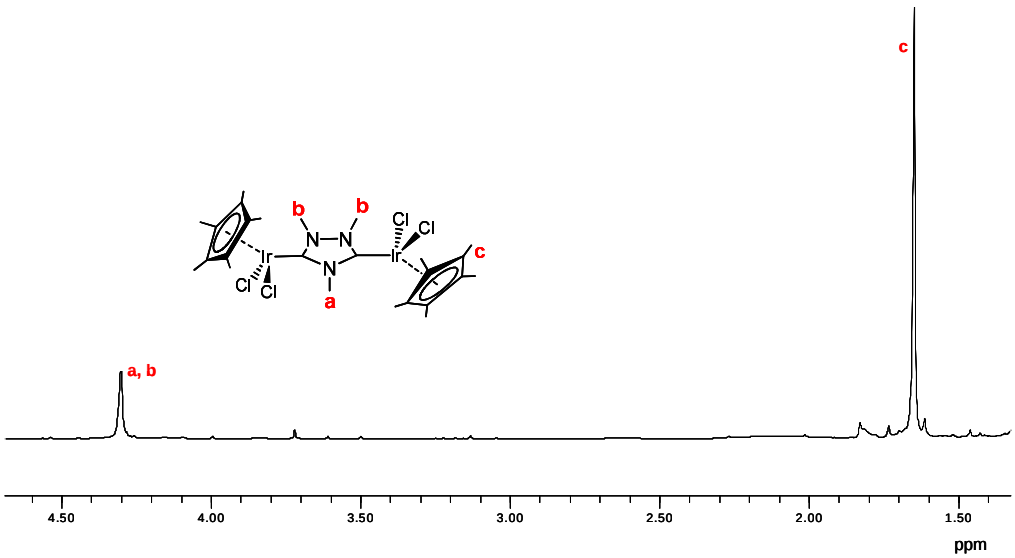

Figure 2.1. ^{1}H NMR spectrum of complex **3L**.

*^{13}C {^{1}H} NMR spectrum of complex **3L**.*

The ^{13}C{^{1}H} NMR spectrum of **3L** (**Figure 2.2**) provides a more direct evidence of the metalation, as seen by the signal at 168.9 ppm (**1**), assigned to the two metallated carbene carbons. The signals due to the methyls at the 1 and 2 positions of the triazole ring appear as a singlet at 38.2 ppm (**3**), while the signal of the methyl at the C4 is observed at 41.4 ppm (**2**). The resonances due to the Cp* are observed at 90.4 ppm ($C_5(CH_3)_5$) (**4**) and at 9.2 ppm ($C_5(CH_3)_5$) (**5**).

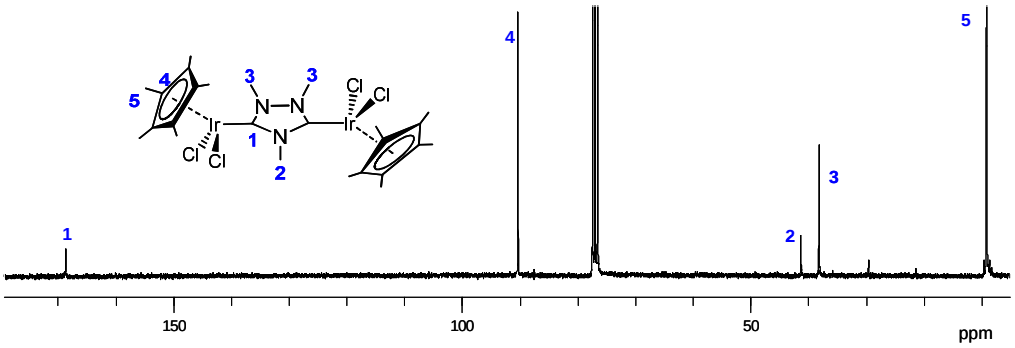

Figure 2.2. ^{13}C {^{1}H} NMR spectrum of complex **3L**

At this point, we decided to extend the coordination of "***ditz***" (**L**) to palladium and platinum with the aim to obtain new homobimetallic compounds with potential catalytic activity. Compound **4L** is prepared by refluxing palladium acetate and [**L**H_2](BF_4) in the presence of NaCl in acetonitrile, as shown in **Scheme 2.14**. In this reaction, the acetate ligand acts as an internal base, and is lost as acetic acid upon deprotonation of the triazolium NHC precursor.

The use of NaCl in the reaction mixture facilitates the coordination of the chloride ligands to the palladium in the formation of the final product.

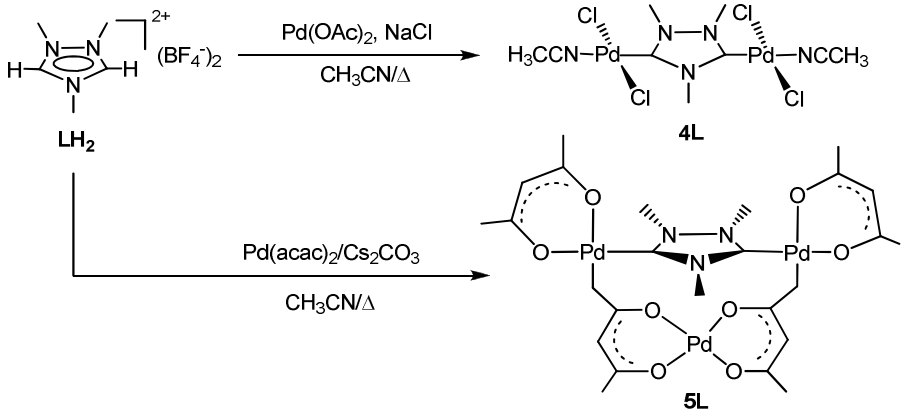

Scheme 2.14. Synthesis for complexes **4L** ad **5L**.

In the synthesis for complex **4L**, the reaction was stirred overnight and then filtered through Celite to eliminate the excess of NaCl and the $NaBF_4$ formed during the reaction; the solvent was then evaporated at reduced pressure. The crude was dissolved in CH_3CN and purified by column cromatography. The pure compound **4L** was eluted with a mixture of dichloromethane/methanol (3:1) and precipitated form *n*-hexane to give an orange solid in high yield (81%). Compound **4L** was then characterized by NMR (^{1}H and ^{13}C) spectroscopy, high resolution mass spectrometry and X-Ray diffraction.

The reaction of $[\mathbf{L}H_2](BF_4)$ with palladium acetylacetonate in the presence of an excess of Cs_2CO_3 in refluxing acetonitrile allows the preparation of **5L**, as shown in **Scheme 2.14**. The mixture was filtered through Celite to eliminate the excess of Cs_2CO_3 and the $NaBF_4$ formed during the reaction; the solvent was then removed under reduced pressure. The resulting crude was purified by column chromatography. The pure compound **5L** was eluted with a mixture of dichloromethane/acetone (3:1) and precipitated from a mixture of dichloromethane/diethyl ether to give a yellow solid. Compound **5L** was characterized by NMR spectroscopy, high resolution mass spectrometry and X-ray diffraction.

Although a large variety of coordination modes are known for β-diketonate (acac) ligands, just a few examples have been described in which the "acac" ligand activates one of the CH bonds of the terminal methyl groups to afford a bridging coordination between two metal fragments, and we just found only one example in which two of such activations provide an open trimetallic structure.[24, 25, 26] As we will discuss with the crystallographic details of the molecule, compound **5L**, represents a rare example of a trimetallic 12-membered palladacycle.

*^{1}H NMR spectrum of complex **5L***

The ^{1}H NMR spectrum of **5L** (**Figure 2.3**) shows the signals due to the non-equivalent geminal protons of the metallated CH_2 groups from the acetylacetonate ligands, at 2.67 and 2.36 (**Hc** and **Hc'**) ($^2J_{HH}$ = 5.1 Hz). The two signals at δ 4.38 and 4.76 (2:1 ratio) due to the protons of the three methyl groups at the azole ring are in accordance with the two-fold symmetry of the complex. The –C*H*– protons of the acetylacetonate ligand display two distinct resonances, one at 5.42 ppm and another at 5.32 ppm. Finally, three different signals assigned to the methyl groups of the acetylacetonate ligands are observed: 2.00, 1.95 and 1.87 ppm (**Figure 2.3**).

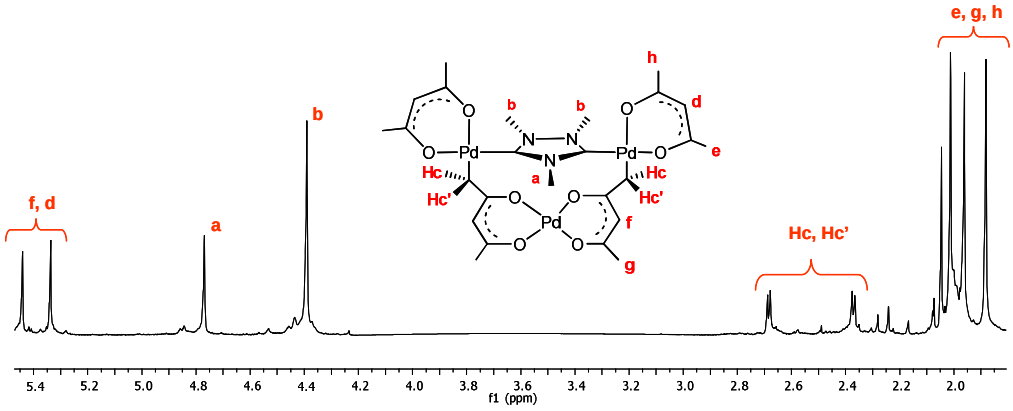

Figure 2.3. ^{1}H NMR spectrum of **5L**.

*$^{13}C\ \{^1H\}$ NMR spectrum of complex **5L***

The ^{13}C NMR (**Figure 2.4**) spectrum of **5L** displays the signals due to the metallated $C_{carbene}$ (178.2 ppm, **1**) and CH_2 (24.8 ppm, **1'**) carbons. The four quaternary carbonyl carbons show their resonances at 194.7, 187.1, 185.5 and 182.8 ppm. The two –*C*H– groups display their signals at 100.6 and 99.9 ppm (**4'** and **4**) while those due to the methyls of the triazole ring appear at 39.7 (**3**) and 37.2 ppm (**2**).

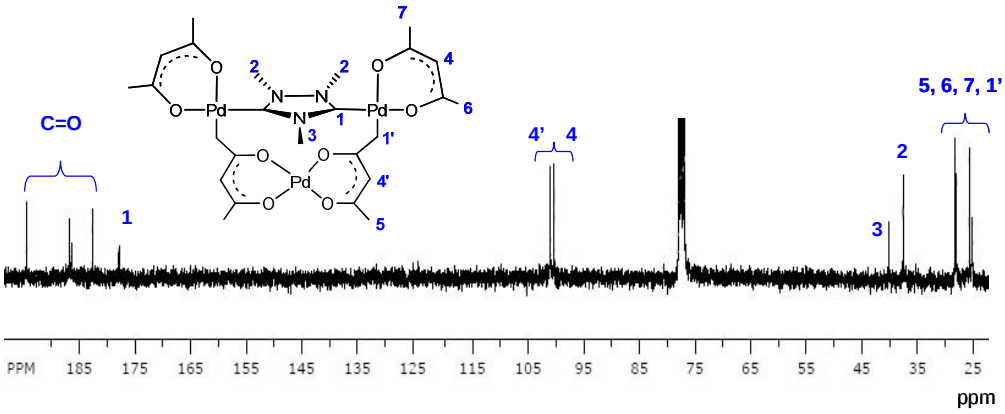

Figure 2.4. $^{13}C\ \{^1H\}$ NMR spectrum of **5L**.

X-Ray diffraction studies of 3L, 4L and 5L

Crystals of **3L** and **5L** suitable for X-ray diffraction analysis were obtained by slow evaporation from concentrated solutions in dichloromethane, while crystals of **4L** were obtained by slow evaporation from a concentrated solution in acetonitrile.

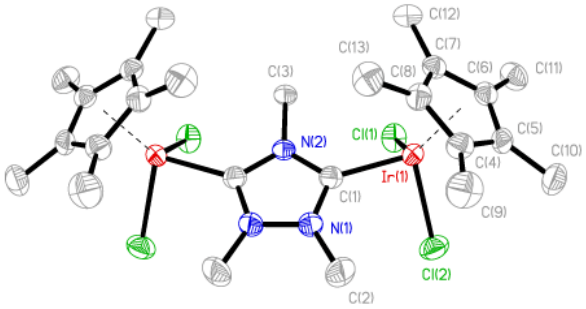

Figure 2.5. Molecular Diagram of complex **3L**. Ellipsoids are at 50% probability. Hydrogen atoms and solvent (H_2O) have been omitted for clarity.

The molecular structure of **3L** (**Figure 2.5**) consists of two fragments of Cp^*IrCl_2 connected by a triazolyl-di-ylidene bridge. The two metal fragments are disposed in a *syn* conformation, so there is a mirror plane perpendicular to the azole ring and along the N(2) and C(3) axis.

The Ir-$C_{carbene}$ distance of 2.033 Å lies in the expected range for Cp*Ir(NHC) complexes.[19] The distance between the two iridium atoms is 6.17 Å.**Table 2.1** displays the most representative bond distances and angles of complex **3L**.

Tabla 2.1. Selected bond lenghts (Å) and angles (º) of complex **3L**.

Bonds	(Å)	Angles	(º)
Ir(1)-C(1)	2.033(8)	C(1)-Ir(1)-Cl(1)	91.5(2)
Ir(1)-Cl(1)	2.442(2)	C(1)-Ir(1)-Cl(2)	90.5(2)
Ir(1)-Cl(2)	2.411(2)	Cl(2)-Ir(1)-Cl(1)	85.31(8)
Ir(1)-Cp*$_{centred}$	1.869	N(1)-C(1)-Ir(1)	127.2(6)
		N(2)-C(1)-Ir(1)	129.1

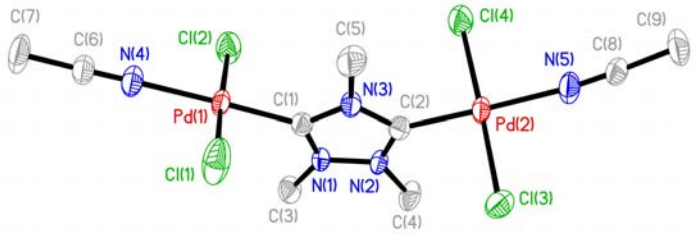

Figure 2.6. Molecular Diagram of complex **4L**. Ellipsoids are at 50% probability. Hydrogen atoms have been omitted for clarity.

The molecular structure of **4L** (**Figure 2.6**) consists of two $PdCl_2(CH_3CN)$ fragments connected by a triazolyl-di-ylidene bridge. The two metal fragments present a *trans*-conformation relative to the two chloro ligands. The two coordination planes about the two metal centers are disposed at angle of 32.3º, according to the Cl(1)-Pd(1)-Pd(2)-Cl(3) torsion angle. The distance between the two palladium atoms is 5.97 Å. The Pd-$C_{carbene}$ distance is of 1.949 Å. **Table 2.2** shows the most representative bond distances and angles of complex **4L**.

Tabla 2.2. Selected bond lenghts (Å) and angles (º) of complex **4L**.

Bonds	(Å)	Angles	(º)
Pd(1)-C(1)	1.949(5)	C(1)-Pd(1)-N(4)	178.9(2)
Pd(1)-N(4)	2.070(4)	C(1)-Pd(1)-Cl(1)	89.17(15)
Pd(1)-Cl(1)	2.282(17)	N(4)-Pd(1)-Cl(1)	90.06(15)
Pd(1)-Cl(2)	2.288(16)	Cl(1)-Pd(1)-Cl(2)	176.76(7)

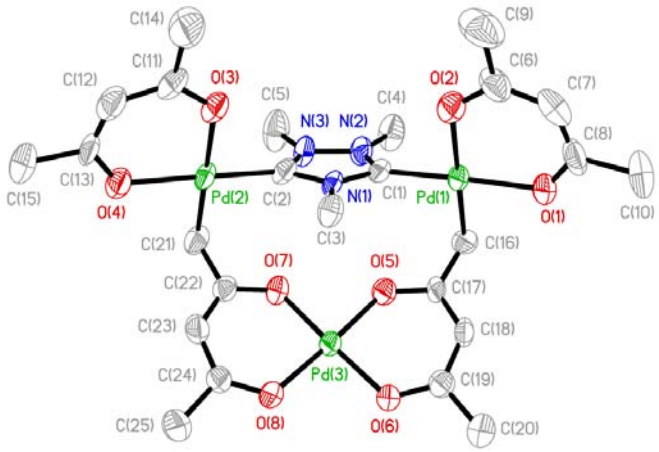

Figure 2.7. Molecular Diagram of complex **5L.** Ellipsoids at 50% probability level. Hydrogen atoms and solvent molecules have been omitted for clarity.

The molecular structure of **5L** (**Figure 2.7**) confirms that the triazolyl-di-ylidene ligand is bridging two palladium fragments. A third palladium fragment with two acetylacetonate ligands is bridging the other two palladium centers through two terminal carbons of the two different *acac* ligands, as a consequence of a double CH activation at the terminal methyl groups. One *acac* ligand completes the coordination sphere about each palladium center bound to the triazolyl-di-ylidene. The three palladium centers are forming part of a 12-membered metallacycle, with the shape of a double-seat-chair, folded by the two metallated CH_2 groups. The two palladium fragments bound to *ditz* are disposed in a *syn* conformation, so there is a mirror plane perpendicular to the azole ring and along the N(1) and C(3) axis. The Pd-$C_{carbene}$ distance is 1.955 Å, similar to that found in **4L**, and the Pd-CH_2 distance is 2.048 Å. The coordination planes about the two palladium centers coordinated to *ditz* are disposed at an angle of 72.3º and 70.7º with respect to the azole plane. The distance between the two palladium atoms bridged by the triazolyl-di-ylidene ligand is 5.96 Å. **Table 2.3** shows the most representative bond distances and angles of complex **5L**.

Table 2.3. Selected bond lenghts (Å) and angles (º) of complex **5L**.

Bonds	(Å)	Angles	(º)
Pd(1)-C(1)	1.955(10)	C(1)-Pd(1)-C(16)	89.0(4)
Pd(1)-C(16)	2.048(10)	C(1)-Pd(1)-O(1)	177.4(4)
Pd(1)-O(1)	2.056(7)	C(16)-Pd(1)-O(1)	88.4(4)
Pd(1)-O(2)	2.116(8)	C(1)-Pd(1)-O(2)	91.4(4)
C(2)-Pd(2)	1.957(11)	C(16)-Pd(1)-O(2)	179.3(4)
Pd(2)-C(21)	2.043(11)	N(2)-C(1)-Pd(1)	128.4(7)
Pd(2)-O(4)	2.059(8)	C(8)-O(1)-Pd(1)	123.9(8)
Pd(2)-O(3)	2.086(8)	O(7)-Pd(3)-O(8)	94.8(3)

2.3.2 Catalytic behaviour of complexes 4L and 5L

As a preliminary test, we observed that both palladium compounds **4L** and **5L** showed good activity in the Heck C-C coupling of styrene and 4-bromoacetophenone, affording full yields to the corresponding substituted stylbene at 100ºC (**Table 2.4**). We understand that 4-bromoacetophenone is not a very challenging substrate for the study of the Heck coupling reaction, but we considered that this preliminary catalytic study may constitute a good starting point for the evaluation of the catalytic activity of our new complexes. We actually did not aim to study the very well stablished Heck process in detail, but to apply our complexes to more novel catalytic processes instead.

Table 2.4. Heck reaction of aryl bromide and styrene.[a]

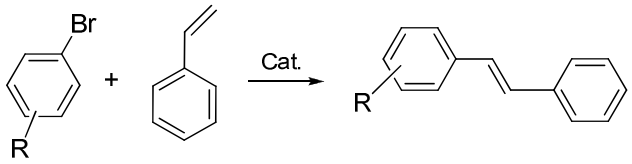

Entry	R	Catalyst	Time (h)	Yield (%)
1	$C(O)CH_3$	**4L**	15	> 95
2	$C(O)CH_3$	**5L**	15	> 95

[a] Reaction Conditions: Styrene (0.6 mmol) was added to a solution of Arylbromide (0.4 mmol), Cs_2CO_3, TBABr (0.04 mmol), catalyst. (1 mol %) in 1 ml of toluene. The mixture was heated at 100 ºC. Yields were determined by ^1H NMR spectroscopy. Ferrocene (0.04 mmol) was used in all cases as internal standard.

In order to widen the scope of these two catalysts, we decided to study their activity in a more novel reaction, namely the direct acylation of aryl halides with aldehydes (**Scheme 2.15**).

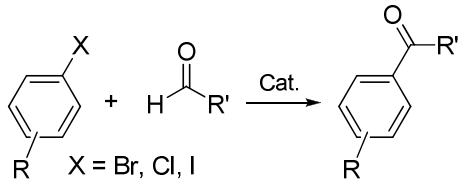

Scheme 2.15. Direct acylation of aryl halides with aldehydes

There are only very few reported examples on the acylation of aryl iodide with aldehydes.[27, 28] The reaction was recently described by Xiao and co-workers, who used a $Pd(dba)_2$-phosphine catalyst precursor,[27] allowing the direct preparation of alkyl-aryl ketones This procedure avoids the traditional Friedel-Crafts method that involves hazardous reagents and does not work when electron-deficient arenes are used.[29] In this case the presence of an organic base is essential, presumably because it acts as co-catalyst for the convertion of the aldehyde into a

highly reactive electron-rich olefin (**2.16**), which then participates in a palladium Heck-reaction with the haloarene.[27] The base is also responsible to neutralize the HBr released (**Scheme 2.16**).

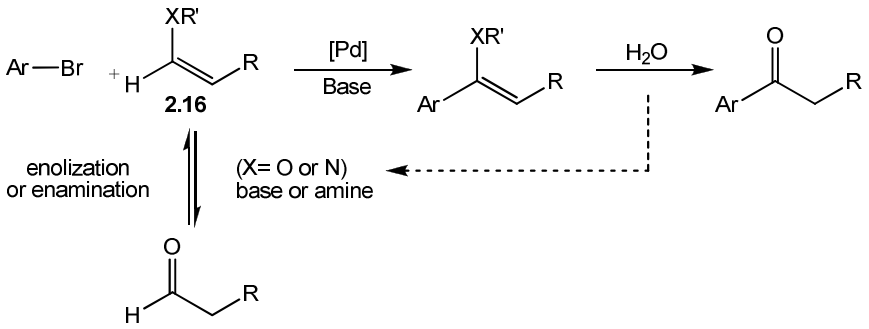

Scheme 2.16. Mechanism proposed by Xiao et al. for the acylation reaction.[29]

Interestingly, the reaction between the same two substrates (aryl halide and aldehyde) can also afford the α-arylation of the aldehydes, a palladium catalysed process using inorganic bases, recently described by Hartwig,[30] which proceeds under similar conditions to Xiao's acylation of aryl halides.

Our experiments on the acylation of arylhalides with aldehydes were carried out in DMF using a 1:1.2 aldehyde/arylhalide ratio. The catalytic experiments were monitored by ^{1}H NMR, monitoring the yields at fixed times using an internal standard (Ferrocene). The evolution of the reaction was analyzed comparing one signal due to the starting aldehyde with one due to the new ketone formed, according to previously published results.[27]

The experiments were carried out under anaerobic conditions, using a 2 mol % catalyst loading at 115 ºC. To facilitate the monitoring of the reaction, standard substrates were used to facilitate the comparison with data previously reported in the literature. As an example, the reaction between 1-hexanal and iodobenzene will be described in detail (**Scheme 2.17**).

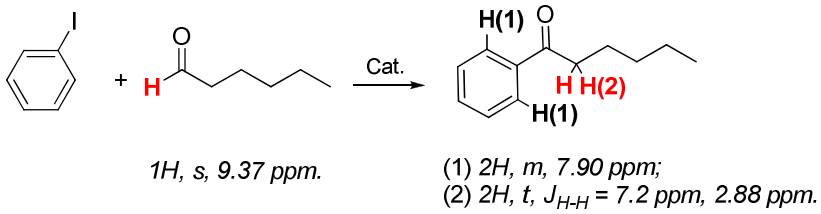

Scheme 2.17. ^{1}H NMR signals used for the monitoring of the reaction between 1-hexanal and iodobenzene.

The advance of this reaction is observed by the progressive disappearance of the aldehydic proton O=C–*H* relative to hexanal (singlet at 9.73 ppm), and the subsequent formation of a

triplet at 2.88 ppm (–C*H*$_2$– protons in α position to the carbonyl) and a multiplet at 7.90 ppm corresponding to the two –C*H*– benzene protons at the ortho positions. In the monitoring of this reaction, and under the reaction conditios that we used in all other related experiments, we never obtained the α-arylated product, so the reaction was very selective to the acylation process.

We observed that compound **5L** showed negligible activity in the acylation of aryl halides with aldehydes, but **4L** showed good activity in the coupling of several substrates. The results are shown in **Table 2.5**.

Table 2.5. Direct acylation of aryl halides with aldehydes with **4L**.[a]

Entry	Ar-X	Aldehyde	Time (h)	Yield (%)[b]
1	iodobenzene	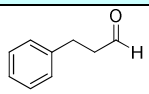	20	> 95
2	4-bromoanisole	$CH_3(CH_2)_2CHO$	48	70
3	4-bromoanisole	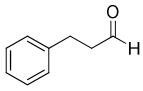	48	23
4	3-bromoanisole	$CH_3(CH_2)_4CHO$	48	34
5	4-bromotoluene	$CH_3(CH_2)_4CHO$	26	>95
6	bromobenzene	$CH_3(CH_2)_4CHO$	6	90
7	4-bromotoluene	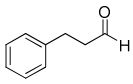	20	40
8	4-bromotoluene	$CH_3(CH_2)_4CHO$	6	90
9	4-bromotoluene	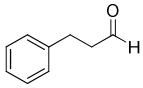	20	50

[a] Reaction Conditions: Arylhalide (0.5 mmol) was added to a solution of Aldehyde (0.6 mmol), pyrrolidine (1 mmol), TBABr (0.05 mmol), catalyst. (2 mol %) in 2 ml of DMF and 4Å MS (1g). The mixture was heated at 115 ºC. [b] Yields were determined by ^{1}H NMR spectroscopy. Ferrocene (0.05 mmol) was used in all cases as internal standard.

As expected, iodobenzene was the arylhalide that showed best performances for this reaction. The reaction of iodobenzene and hydrocinnamaldehyde afforded 95 % yield to the ketone in 20h (entry 1, **Table 2.5**). From the bromosubstituted aryls, 4-bromotoluene is the one furnishing better yields, while aliphatic aldehydes seem to provide better results than those containing aryl groups. Although these results only compare well with the previously reported data for the best performances achieved (**Table 2.5**, entries 5, 6 and 8), we have to take into account that the use of **4L** has the advantage that no addition of phosphine is needed for the catalytic activity of the palladium compound, thus we may reduce the generation of potentially

toxic residues and allow a more simplified method of separation of the final products from the reaction mixture.

The catalytic activity of complexes **4L** and **5L** were tested in the C-C coupling reaction showing good activity when *p*-bromoacetophenone and styrene were used. Only complex **4L** showed good activity in the acylation of arylhalides with aldehydes,[27] a recently reported reaction that we carried out in the absence of addition of phosphine. It is also to mention that the reaction is selective only for the obtention of the resulting ketone and no α-arylation of the aldehyde were observed.

In order to confirm the mechanism proposed by Xiao,[27] we also performed the catalytic experiments without adding pyrrolidine and we did not observe any transformations. This result suggests that the pyrrolodine indeed acts as a co-catalyst, presumably converting the aldehyde into a highly reactive electron-rich olefin for palladium cross-coupling and as a base to neutralize the HBr released from the Heck reaction, as proposed by Xiao according to the process depicted in **Scheme 2.16**.[27]

2.3.3 Synthesis and characterization of new bimetallic and monometallic NHC-Palladium and Platinum pyridine stabilized complexes

Because the introduction of pyridine ligands has been demonstrated to provide highly active catalysts for various Pd-mediated C-C reactions, by the so-called PEPPSI effect (Pyridine Enhanced Precatalyst Preparation, Stabilization and Initiation),[31, 32] we have prepared a series of pyridine-substituted NHC-Pd complexes. The reactions of palladium dichloride or platinum diiodide with the corresponding azolium salts in refluxing pyridine in the presence of K_2CO_3, afforded the corresponding NHC-M-Py (M = Pd or Pt) complexes in high yield (**Scheme 2.18**). The mixture was then concentrated at reduced pressure, redissolved in dichloromethane and filtered trough Celite in order to eliminate the excess of base and potassium salts formed during the reaction. Pure compounds **6L**, **7L**, **8L** and **9L** were obtained after recrystallization from dichloromethane/*n*-hexanes solutions. All four complexes were fully characterized by NMR spectroscopy (^{1}H and ^{13}C), high resolution mass spectrometry and X-ray diffraction.

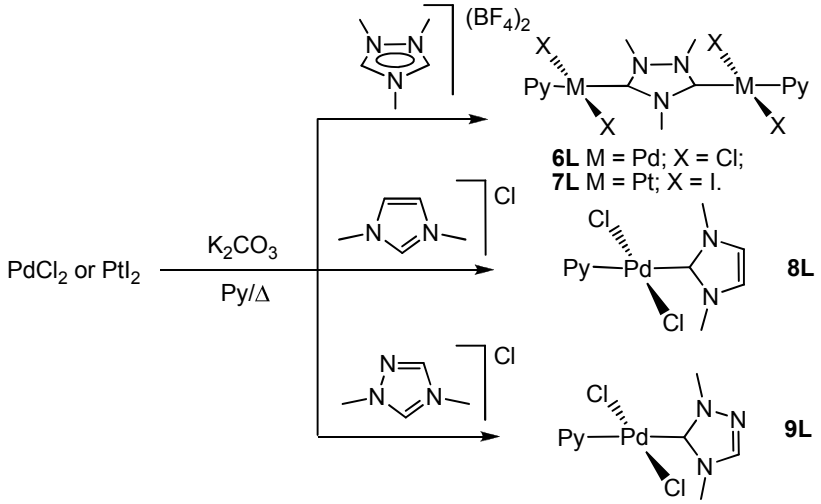

Scheme 2.18. Reaction synthesis for complexes **6L**, **7L**, **8L** and **9L**.

*^{1}H NMR spectrum of complex **6L***

The ^{1}H NMR spectrum of **6L** shows that the signal due to the two acidic HC*H*N protons has disappeared, thus providing the first evidence that the coordination has occurred. The spectrum shows two distinctive signals (relative ratio 2:1) assigned to the three methyl groups of the triazolyl-di-ylidene ligand, suggesting a two-fold symmetry for the molecule (**Figure 2.8**). The singlet due to the methyl groups at the 1 and 2 positions of the triazole ring appears at 4.46 ppm (**b**) while the resonance due to the methyl at the 4 position appears at 4.69 ppm (**a**). The pyridine protons show three distinctive signals: a doblet at 8.84 ppm and two triplets at 7.78 and 7.33 ppm.

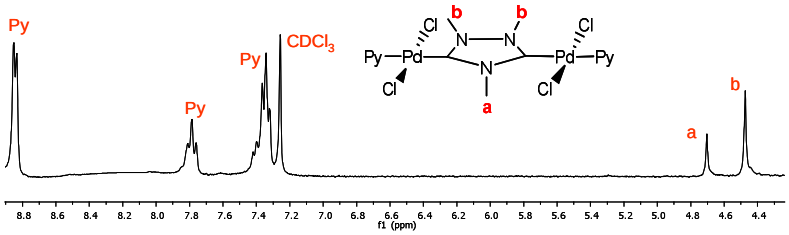

Figure 2.8. ^{1}H NMR spectrum of **6L**.

The ^{13}C NMR spectrum provides direct evidence of the metallation of the ligand, as seen by the signal at 164.9 ppm assigned to the Pd-$C_{carbene}$. The methyl groups at the 1 and 2 positions of the triazolium ring generate a singlet at 37.8 ppm and the signal attributed to the methyl at the 4 position is displayed at 40.9 ppm. The signals due to the protons of the coordinated pyridine appear at 153.9, 151.6, 138.8, 125.2 and 125 ppm. A selection of the most representative signals of the ^{1}H and ^{13}C {^{1}H} NMR spectra of complexes **7L**, **8L** and **9L** are displayed in **Table 2.6** and **Table 2.7**.

Table 2.6 ^{1}H signals for complexese **7L**, **8L** and **9L**.

^{1}H	**δ (ppm) 7L**	**δ (ppm) 8L**	**δ (ppm) 9L**
C-H_{py}	8.91 (d, $^{3}J_{H-H}$= 5.0 Hz, 2H) 6.55 (t, $^{3}J_{H-H}$= 7.5 Hz, 2H) 6.27 (t, $^{3}J_{H-H}$= 6.5 Hz, 1H)	9.06 (d, $^{3}J_{H-H}$= 4.8Hz, 2H) 7.74 (t, $^{3}J_{H-H}$= 5.4 Hz, 2H) 7.35 (t, $^{3}J_{H-H}$= 6.6 Hz, 1H)	8.97 (d, $^{3}J_{H-H}$ = 6.6 Hz, 1H) 8.83 (d, $^{3}J_{H-H}$ = 6.6 Hz, 1H) 7.75 – 7.80 (m, 1H) 7.31 – 7.40 (m, 2H)
NC*H*C*H*N or NCHN	-	6.92 (s)	7.94 (s)
NCH_3	4.63 (s), 3.38 (s)	3.97 (s)	4.32 (s), 4.15 (s)

Table 2.7 ^{13}C signals for complexese **7L**, **8L** and **9L**.

^{13}C	**δ (ppm) 7L**	**δ (ppm) 8L**	**δ (ppm) 9L**
$C_{carbene}$-Pd or $C_{carbene}$-Pt	164.1	153.9	143.4
$C_{Pyridine}$	153.5, 138.2, 125.2	152.4, 138.3, 124.9	153.6, 138.8, 125.2, 124.8
NCHCHN or NCHC	-	121.5	121.6
NCH_3	40.4, 37.0	40.5	40.3, 35.7

X-Ray diffraction studies of 6L, 7L and 8L

Crystals of **6L**, **7L** and **8L** suitable for X-ray diffraction analysis were obtained by slow evaporation from the corresponding concentrated dichloromethane/*n*-hexanes solutions. **Figures 2.9**, **2.10** and **2.11** show the ORTEP diagrams of complexes **6L**, **7L** and **8L**, respectively. Compounds **6L** and **7L** are isostructural, with the only difference that the Pd atom is replaced by Pt and Cl atoms by I.

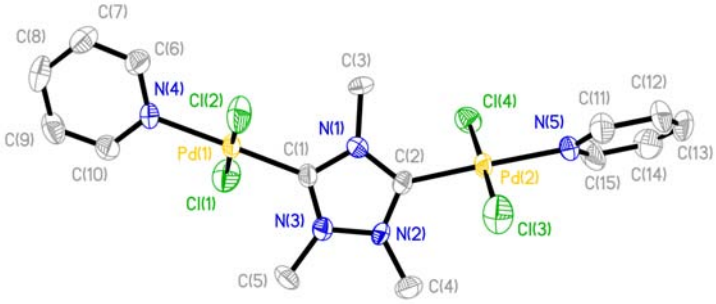

Figure 2.9. Molecular Diagram of complex **6L**. Ellipsoids are at 50% probability. Hydrogen atoms have been omitted for clarity.

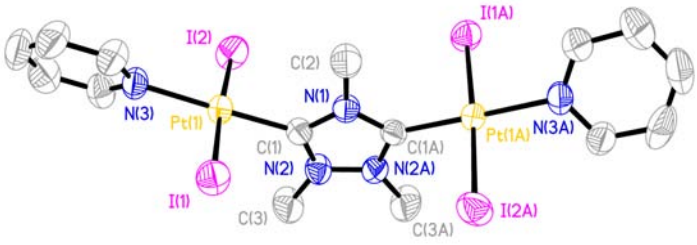

Figure 2.10. Molecular Diagram of complex **7L**. Ellipsoids are at 50% probability. Hydrogen atoms have been omitted for clarity.

The molecular structure of **6L** consists of two $PdCl_2$(pyridine) fragments connected by a ditz bridge (**Figure 2.12**). The two metal fragments present a *trans*-conformation related to the chloro ligands. The two coordination planes about the metal centers are disposed at an angle α of 60.1º and 67.5º. The distance between the two palladium atoms is 6.03 Å, and the average Pd-C distance is 1.960 Å, similar to the same parameters shown by [*trans*-$PdCl_2$(MeCN)]$_2$(μ-ditz) (**4L**), described before.**Tables 2.8** and **2.9** show the most representative bond distances and angles of complexes **6L** and **7L**.

Tabla 2.8. Selected bond lenghts (Å) and angles (º) of complex **6L**.

Bonds	(Å)	Angles	(º)
Pd(1)-C(1)	1.951(4)	C(1)-Pd(1)-N(4)	178.9(3)
Pd(1)-N(4)	2.079(5)	C(1)-Pd(1)-Cl(1)	89.8(2)
Pd(1)-Cl(1)	2.290(2)	N(4)-Pd(1)-Cl(1)	90.58(17)
Pd(1)-Cl(2)	2.296(2)	Cl(1)-Pd(1)-Cl(2)	178.48(8)

Tabla 2.9. Selected bond lenghts (Å) and angles (º) of complex **7L**.

Bonds	(Å)	Angles	(º)
Pt(1)-C(1)	1.955(7)	C(1)-Pt(1)-N(3)	178.5(3)
Pt(1)-N(3)	2.085(6)	C(1)-Pt(1)-I(2)	88.4(2)
Pt(1)-I(1)	2.5994(6)	N(3)-Pt(1)-I(1)	91.99(17)
Pt(1)-I(2)	2.6030(7)	I(1)-Pt(1)-I(2)	176.30(2)

The structure of **8L** (**Figure 2.12**) consists of a pseudo-square planar molecule with a palladium center surrounded by a 1,3-dimethylimidazolylidene, two chloride ligands in a *trans* configuration and a pyridine.

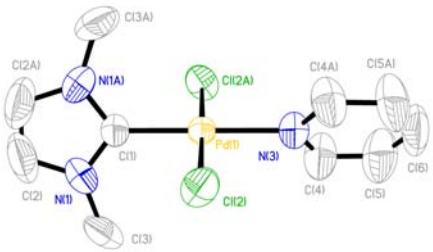

Figure 2.11. Molecular Diagram of complex **8L**. Ellipsoids are at 50% probability. Hydrogen atoms have been omitted for clarity.

The azole plane deviates from the coordination plane of the molecule by an angle of 74.8º. The Pd-C distance is 1.972 Å, similar to that shown by other palladium related species.[32] The Pd-N(pyridine) distance is 2.084 Å, almost identical to that shown by **6L** for the same bond (2.080 Å). These distances are longer than those shown for other related complexes with non-NHC ligands, indicating the high trans influence of NHC in **8L**.[33] **Table 2.10** shows the most representative bond distances and angles of complex **8L**.

Tabla 2.10. Selected bond lenghts (Å) and angles (º) of complex **8L**.

Bonds	(Å)	Angles	(º)
Pd(1)-C(1)	1.972(8)	C(1)-Pd(1)-N(3)	180.0 (1)
Pd(1)-N(3)	2.084(8)	C(1)-Pd(1)-Cl(2)	89.43(5)
Pd(1)-Cl(2)	2.3325(15)	N(3)-Pd(1)-Cl(2)	90.57(5)

2.3.4 Tandem catalysis with Pd complexes

The new complexes that we have described in this chapter (**6L**, **8L** and **9L**) were tested in a series of catalytic reactions between *o*-halohydroxyarenes (or *o*-halobenzylalcohols) and phenylacetylene to afford benzofurans (or (*Z*)-1-alkylidene-1,3-dihydroisobenzufurans), in a tandem process that comprises a Sonogashira coupling (**Step 1**, **Scheme 2.19**) followed by an intramolecular cyclic hydroalkoxylation (**Step 2**, **Scheme 2.19**).

Substituted benzofurans can be found as the key structural unit of many biological active compounds with pharmaceutical applications. For example, they show high activities as blood coagulation factor-Xa inhibitors, and as antagonist of angiotensin II receptors and potent calcium blockers.[34, 35, 36] Several methods for the preparation of benzufurans are known,[37] but there are just a few examples in the literature reporting the reaction of o-hydroxyaryl halides and terminal alkynes to afford directly benzufurans. [38, 39, 40]

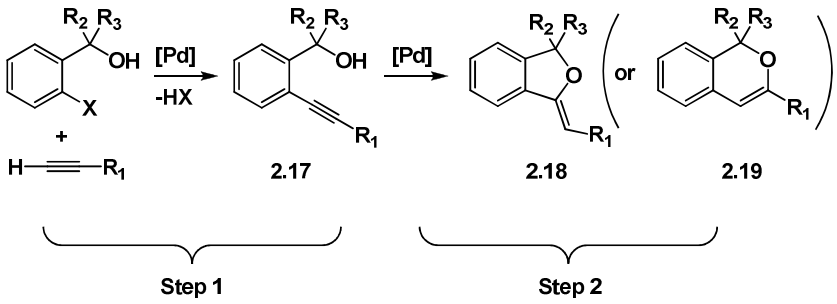

Scheme 2.19. Tandem sonogashira/hydroalcoxylation reactions catalyzed by Pd-NHC complexes.

A closer look at the overall process reveals that the two steps may find some incompatibilities regarding the nature of the catalyst, base, solvent and additives used for each individual step, so in most cases the isolation of the alkynylbenzyl alcohol (product **2.17**, **Scheme 2.19**) (or alkynylphenols) intermediate is needed prior to the cyclization process.

The Sonogashira cross-coupling reactions (**Step 1**, **Scheme 2.19**), for example, suffer from many limitations, like requiring stringent anaerobic conditions, and often yields unwanted homocoupled side products alongside with the desired cross-coupled products. The mechanism of the Sonogashira process, when copper and amine are added to the reaction, implies two independent cycles: one for the production of the cuprous acetylides (**Cycle B**) and the other for their coupling with the desired aryl or alkyl species (**Cycle A**). **Scheme 2.20** shows the two linked catalytic cycles.

A careful scrutiny of the mechanism pathway of the Sonogashira coupling reveals that the coupling reactions proceed via the formation of a Cu–acetylide species, wich are extremely explosive and yields unwanted homocoupled products in the presence of oxygen or under oxidizing conditions.[40]

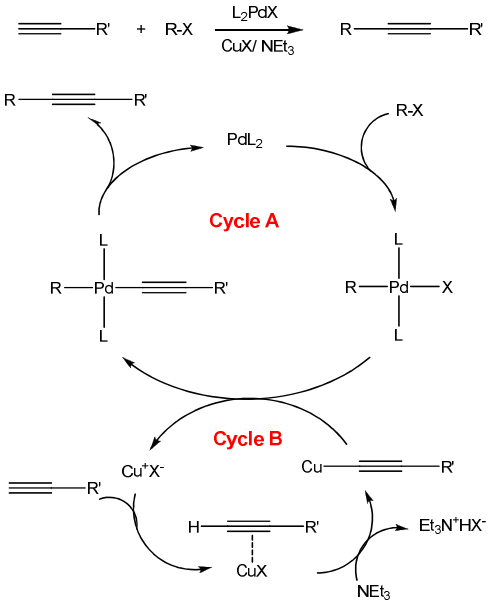

Scheme 2.20. General Sonogashira Cross-Coupling mechanism.

Hence, it is not surprising that the Cu-free-Sonogashira coupling is becoming increasingly popular in these days. However, many of the Cu-free Sonogashira couplings involve the use of amines that are not considered environmentally friendly.[40] Recently Ghosh and co-workers showed that a series of NHC-Pd-pyridine complexes are good catalysts for the Sonogashira coupling in Cu-free and amine-free conditions.[40]

Transition metal catalyzed annulation of *o*-alkynyphenols (or *o*-alkynyl benzylalcohol) (**Step 2**, **Scheme 2.19**, product **2.18** or product **2.19**) has been used to prepare heterocycles,[41] but also this cycloisomerization can occur under only basic conditions, with NaOH,[42] NaH, or TBAF (tetrabutylammonium fluoride).[43] Intramolecular ring closure reactions, which can be carried out between the nuclephilic part and carbon-carbon multibond in the same molecules, are one of the useful methods for costructing cyclic compounds. Sometimes, the ring size of the products could be predicted by the famous Baldwin´s Rule,[44] which was an empirically proposed rule based on stereoelectronic effects. For example, for the substrates (**i**) which have a triple bond as the counterpart, both the "*6-Endo-dig*" mode (**2i**) and "*5-Exo-dig*" mode (**3i**) are allowed by Baldwin's Rule (**Scheme 2.21**).

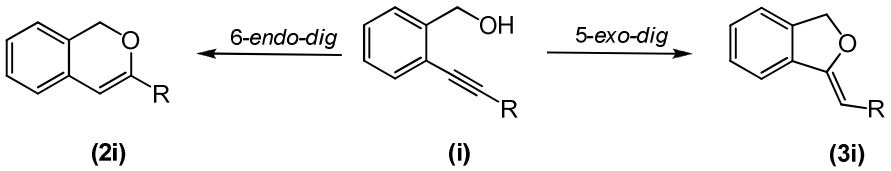

Scheme 2.21. Baldwin's Rule.[44]

Our studies on the tandem reaction between *o*-hydroxyaryl halides and phenylacetylene to afford benzofurans, aimed us to find the best conditions to achieve maximum yields under the mildest reaction conditions and minimum addition of additives. We initially thought that our catalysts fulfilled the requirements to be active in both, the Sonogashira coupling and the cyclization of the alkynyl-alcohol, because our complexes are stable and robust enough to stand the conditions of both catalytic processes.

The catalytic experiments were monitored by Gas-Chromatography, registering yields at fixed times and using anisole as internal standard. The catalytic studies were carried out under aerobic conditions, employing 1 mol % of paladium catalyst. **Scheme 2.22** shows the catalysts that we used.

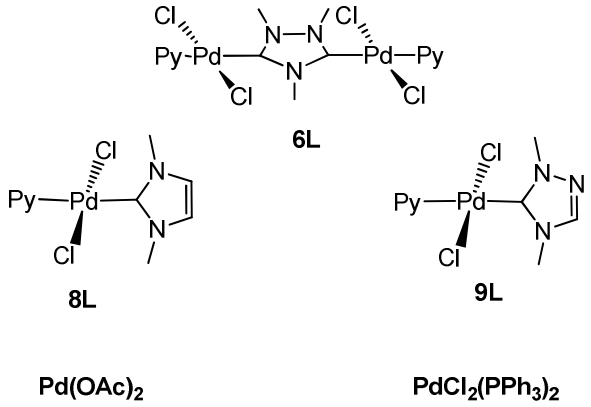

Scheme 2.22. Catalysts used in the tandem process that comprises a Sonogashira coupling followed by an intramolecular cyclic hydroalkoxylation.

In order to optimize the reaction conditions, we first screened a series of solvents and bases using **6L** as catalyst in the reaction between *o*-iodobenzyl alcohol and phenylacetylene. As shown in **Table 2.11**, the best combination of solvent and base is obtained when using DMSO and Cs_2CO_3, for which full yield to the final product is obtained. Remarkably, additives other than the base (CuI, amine, KI, etc.) were not needed in order to achieve high reaction outcomes, a result that is more relevant if we take into account that the overall reaction comprises two steps for which normally different additives are needed. For all the reactions tested, the "*5-Exo-dig"* product was the only product observed, and we never detected the formation of the "*6-Endo-dig*" cyclization product.

Table 2.11. Base/solvent evaluation in the formation of benzofuran.[a]

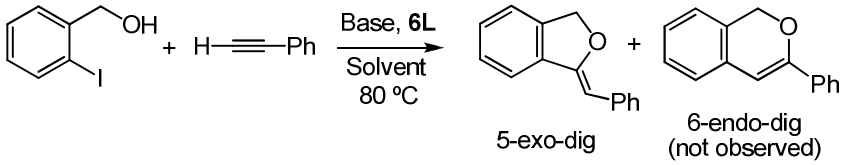

Entry	Base	Solvent	Yield (%)
1	Cs_2CO_3	DMSO	99
2	Cs_2CO_3	MeCN	59
3	Cs_2CO_3	Toluene	30
4	K_2CO_3	DMSO	25
5	NaOH	DMSO	36
6	NaOAc	DMSO	5

[a] Reaction Conditions: Phenylacetylene (0.75 mmol), iodobenzylalcohol (0.525 mmol), Cs_2CO_3 (1.57 mmol), catalyst **6L** (1 % mol palladium), solvent (3 mL) and anisole as internal standard (0.525mmol). Mixture heated at 80 ºC for 3h. Yields determined by GC.

Then we performed a evaluation of the activities of our new three complexes, **6L**, **8L** and **9L** including $PdCl_2(PPh_3)_2$ and $Pd(OAc)_2$ for comparative purpose. All the reactions were carried out at 80ºC in DMSO and with Cs_2CO_3. The results are summarized in **Table 2.12**. All three NHC-Pd complexes achieved full yield to the final product (**B**) when *o*-iodobenzyl alcohol was used (entries 3-5). Under the same reaction conditions, $Pd(OAc)_2$ and $PdCl_2(PPh_3)_2$ afforded poor yields, although the Sonogashira coupling seemed to have proceeded with quite good progress, a result that is not surprising if we take into account that $PdCl_2(PPh_3)_2$ is normally used for the preparation of the intermediate **A**.[45]

This result clearly illustrates that a good catalyst for the Sonogashira coupling may not be good for the cyclic hydroalkoxylation, so that if we are pursuing good outcomes for the overall reaction, we have to finely tune the catalysts to make them active in the two consecutive transformations.

Table 2.12. Catalyst evaluation of the Sonogashira/Cyclic hydroalkoxylation reaction[a]

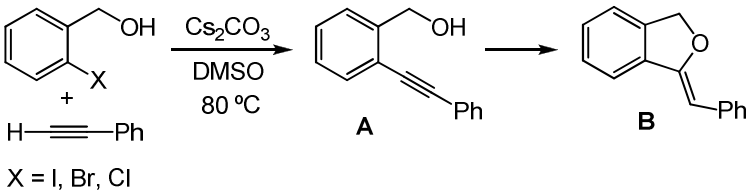

Entry	X	Catalyst	Time (h)	Yield % (isolated)	
				A	B
1	I	**$PdCl_2(PPh_3)_2$**	1	68	28
2	I	**$Pd(OAc)_2$**	1	58	19
3	I	**6L**	1	0	99 (85)
4	I	**8L**	1	0	98 (80)
5	I	**9L**	1	0	98 (84)
6	Br	**6L**	12	0	43
7	Br	**8L**	12	0	77
8	Br	**9L**	12	0	45
9	Cl	**6L**	12	0	7
10	Cl	**8L**	12	0	5
11	Cl	**9L**	12	0	3

[a] Reaction Conditions: Phenylacetylene (0.75 mmol), halobenzylalcohol (0.525 mmol), Cs_2CO_3 (1.57 mmol), catalyst (1 % mol palladium), DMSO (3 mL) and anisole as internal reference (0.525mmol). The mixture was heated at 80 ºC. Yields determined by GC (isolated yields in parenthesis).

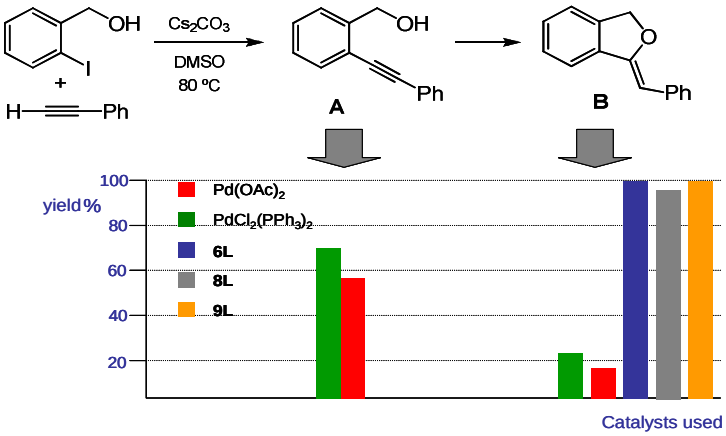

Scheme 2.23

Scheme 2.23 shows a Schematic comparison of the catalytic activity of the five catalysts when *o*-iodobenzyl alcohol and phenylacetylene were used. As can be seen, both $PdCl_2(PPh_3)_2$ and $Pd(OAc)_2$, resulted active only for the first step of the global process (production of **A**), while

the NHC-complexes complete the overall reaction producing in high yield compound **B**. Catalysts **6L**-**9L**, were tested for other halobenzyl alcohols (halo=bromo, chloro). The activation of *o*-bromobenzyl alcohol was moderate for **6L** and **9L** (yields 43 and 45 %, respectively, entries 6 and 8) and very good for **8L** (77%, entry 7). When *o*-chlorobenzyl alcohol was used the formation of the final product **B** was almost negligible (entries 9-11). Despite the moderate to low yields displayed by the bromo- and chloro- derivatives to compound **B** (except for the result shown in entry 7), we did not detect any amount of the intermediate **A**, meaning that the activation of the C-X bond is the rate limiting step for these cases.

In order to widen the applicability of this tandem process, we decided to carry out a similar reaction between *o*-iodophenol and phenylacetylene using compounds **6L**-**9L** as catalysts. The results are summarized in **Table 2.13.** The dimetallic catalyst **6L** afforded the best activity, with almost full conversion to the final product in a "*5-Endo-dig*" cyclization (2-phenylbenzofuran, **C**) in 8h. No "*4-Exo-dig*" (**D**) cyclization product was detected. The triazolyl-di-ylidene complex **8L** also afforded an excellent yield (88%) although in a longer reaction time (16h, entry 3). The replacement of *o*-iodophenol by *o*-bromophenol in this reaction resulted in an important decrease of the reaction outcome, affording yields below 20 % (best yield: 19% for catalyst **9L**; entry 6, **Table 2.13)**.

The time dependent reaction profiles of these three reactions are shown in **Figure 2.12**. As can be seen catalyst **6L** provides the best activity both in terms of overall yield and reaction rate, while **9L** affords a very poor outcome. It is worth mentioning, that the catalyst that showed the best activation for the Sonogashira coupling (catalyst **8L**) as seen for the activation of the C-Br bond in *o*-bromobenzyl alcohol (**Table 2.11**, entry 7) now provides the poorest yields in the formation of **C**, again illustrating that tuning the catalyst for a good performance in the Sonogashira coupling may result in its deactivation toward the cyclic hydroalkoxylation.

Table 2.13. Sonogashira/Cyclic hydroalkoxylation reaction between *o*-iodophenol and phenylacetylene[a]

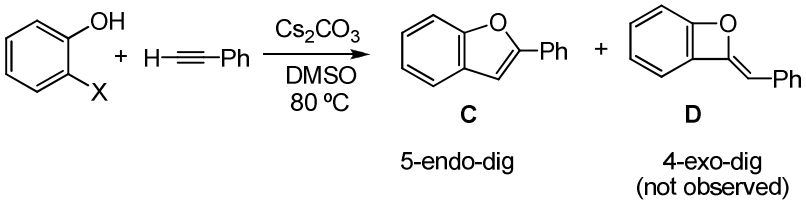

C 5-endo-dig **D** 4-exo-dig (not observed)

Entry	X	Cat.	Time (h)	Yield C %
1	I	**6L**	8	93
2	I	**8L**	20	16
3	I	**9L**	16	88
4	Br	**6L**	20	10
5	Br	**8L**	20	0
6	Br	**9L**	20	19

[a] Reaction Conditions: Phenylacetylene (0.75 mmol), halophenol (0.525 mmol), Cs_2CO_3 (1.57 mmol), catalyst (1 % mol palladium), DMSO (3 mL) and anisole as internal reference (0.525mmol). The mixture was heated at 80 ºC. Yields determined by GC.

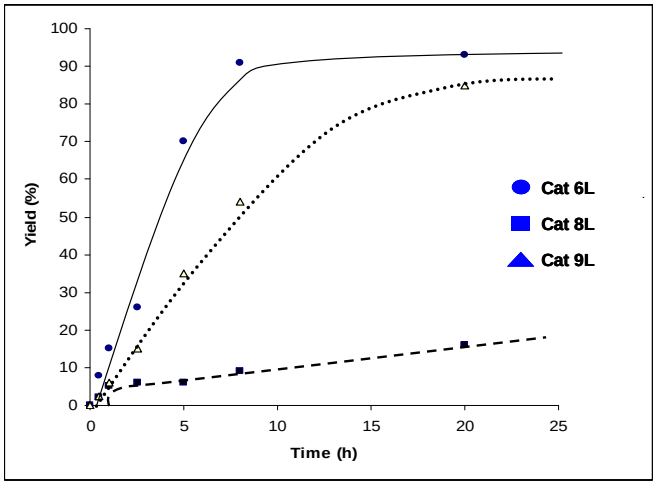

Figure 2.12. Time course of the formation of 2-phenylbenzofuran by the consecutive Sonogashira/Cyclic hydroalkoxylation reactions between *o*-iodophenol and phenylacetylene.

In conclusion, the catalytic activity of three different NHC-Pd-pyridine complexes have been tested in the consecutive Sonogashira/cyclic hydroalkoxylation reactions between *o*-hydroxyaryl halides and phenylacetylene to directly afford benzofurans. All three catalysts provide excellent yields on the final products when *o*-iodobenzylalcohol or *o*-iodophenol were used.

For other halosubstituted arenes, we obtained poor outcomes, except for the case of *o*-bromobenzylalcohol for which moderate to high yields were achieved. The same reactions

performed with $Pd(OAc)_2$ and $PdCl_2(PPh_3)_2$ stopped after the Sonogashira coupling, providing very low activity in the second reaction (cyclic hydroxyalkoxylation).

The palladium complex with the more basic NHC (**8L**) is the one to provide better yields when *o*-bromobenzylalcohol alcohol is used, as a consecuence of its better efficiency in the activation of the Sonogashira reaction. On the contrary, for the reactions with *o*-iodophenol, the reaction outcome is favored for the complexes with the less basic NHC ligands, with a variation of the overall catalytic activity in the order **6L** (NHC = ditz) > **9L** (NHC = triazolyl-di-ylidene) > **8L** (NHC = imidazolylidene). Assuming that for this latter process the cyclization is the rate limiting reaction (the Sonogashira coupling is assumed to be fast for C-I activations), it seems that less basic NHCs favour this second reaction of the sequence. This means that the basicity of the ligand may be playing an opposite effect in the trends of the catalytic activities for the two reactions comprising this overall process, so it is difficult to find an accurate balance of the electronic properties of the ligand to afford a catalyst that is active in both reactions at a time.

This tandem process provides a clear benefit compared to the traditional methods for the preparation of benzofurans that implies the same sequence of reactions but with the isolation of the Sonogahira coupling intermediate followed by the cyclic hydroalkoxylation, which usually requires different reaction conditions including a different catalyst.

2.4 Heterometallic complexes

2.4.1 Synthesis and characterization of heterobimetallic Ir^{III}/Ir^{I} and Ir^{III}/Rh^{I} complexes using triazolyl-di-ylidene ligand

Once we obtained the *ditz*-based homobimetallic complexes described in the previous sections we decided to design a general strategy for the preparation of heterobimetallic *ditz*-based complexes. The starting idea was to activate or deprotonate only one of the two C*H* bonds at the 1,2,4-trimethyltriazolium precursor, in order to facilitate the selective coordination of just one metal fragment. Thus, we decided to obtain the methanolic adduct starting from the triazolium salt [**L**H_2](BF_4)$_2$, [**L**H·MeOH]BF_4, with the procedure described in the literature (**Scheme 2.24**),[18] which implies the addition of one equivalent of NaH (60 % in *mineral oil*) to [**L**H_2](BF_4)$_2$ in MeOH. After two hours, the solution was concentrated and washed with diethyl ether. The crude was then dissolved in dichloromethane and filtered to eliminate the $NaBF_4$ generated. The methanolic adduct [**L**H·MeOH]BF_4 is an air-stable compound and can be stored for several days, although we generally generated it *in situ*, so that its isolation was not necessary.

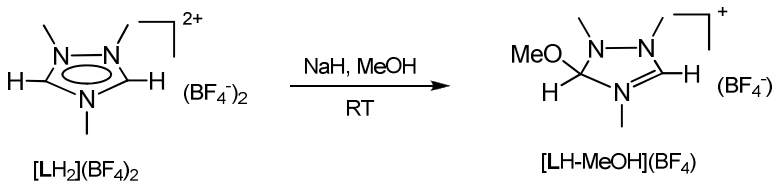

Scheme 2.24. Synthesis of [**L**H·MeOH]BF_4.

The reaction of the methanolic adduct [**L**H-MeOH]BF_4 with [Cp*$IrCl_2$]$_2$ (1:1, **L**H-MeOH:Ir) in refluxing methanol, afforded the cationic compound **10L,** in which the azole ligand is acting as a triazolium-ylidene (**Scheme 2.25**).

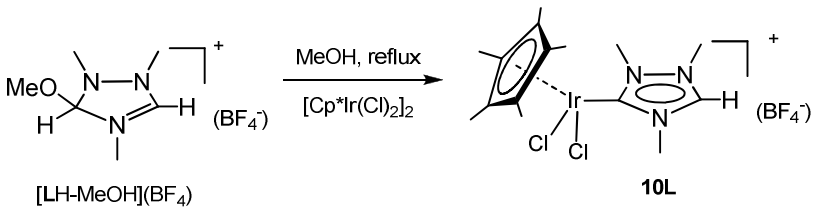

Scheme 2.25. Synthesis of complex **10L**.

Compound **10L** is soluble in polar solvents, as methanol, acetonitrile or acetone, and insoluble in non-polar solvents, like diethyl ether and *n*-hexanes. Pure compound **10L** was obtained after crystalization in cold acetonitrile. The resulting solution was concentrated at reduced pressure and precipitated as an orange solid with acetone/diethyl ether in 69% yield.

Alternatively, a more convenient route to the synthesis of **10L** can be performed generating the methanolic adduct *in situ* starting from the triazolium salt [**L**H_2](BF_4)$_2$, and one equivalent of NaH (60 % in mineral oil) in MeOH. The reaction was stirred at room temperature for 1h and subsequentially an equimolecular amount of [Cp*$IrCl_2$]$_2$ was added (**Scheme 2.26**). The resulting mixture was refluxed at 70 ºC for 2h. Then the solution was filtered in order to eliminate the $NaBF_4$ formed and concentrated. Compound **10L** was obtained after precipitation in acetone/diethyl ether achieving a better yield, 85 %. Compund **10L** was characterized by NMR spectroscopy, high resolution mass Spectrometry and X-ray diffraction.

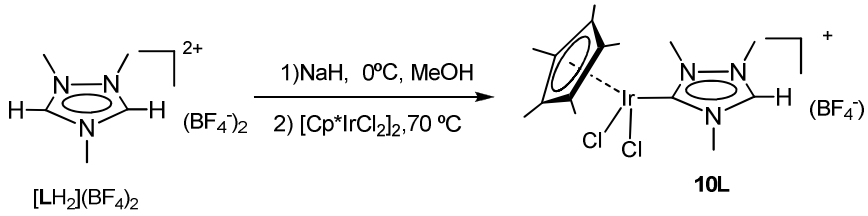

Scheme 2.26. Synthesis of complex **10L** from the dicationic salt.

*^{1}H NMR spectrum of complex **10L***

The ^{1}H NMR of **10L** (**Figure 2.13**) shows a singlet at δ 9.51(**a**), due to the NC*H*N acidic proton, with a relative integral of 1, compared to the three signals due to the methyl groups at 4.32, 4.18, and 4.13 (**b**, **c** and **d**) ppm, thus indicating that only one of the two NC*H*N protons was lost upon coordination to the metal. The signals attributed to the methyls of the Cp*****(**e**) appear as a singlet at 1.64 ppm

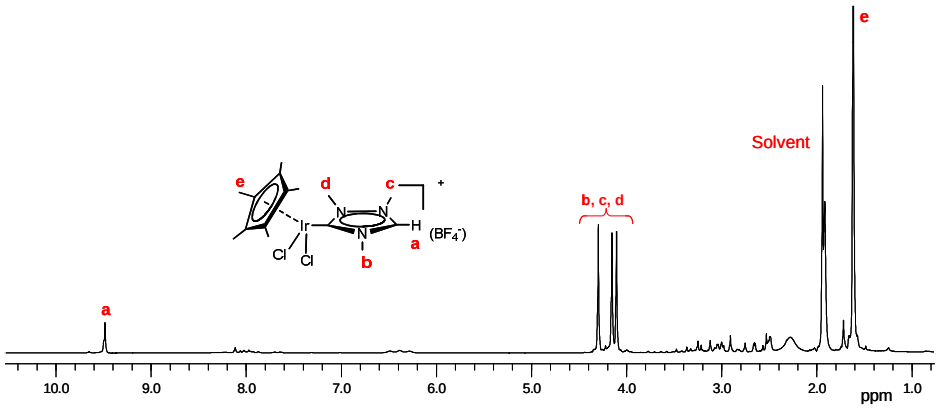

Figure 2.13. ^{1}H NMR spectrum of **10L**.

The most relevant feature of the ^{13}C NMR spectrum is the signal at 169.0 ppm, which provides evidence of the metalation to the Ir^{III} fragment.[21]

Using the same synthetic procedure but adding $[IrCl(cod)]_2$ instead over the solution of [**L**H·MeOH]BF_4, we obtained compound **11L** in a 87% yield, which also shows the monocoordination of the carbene ligand (**Scheme 2.27**).

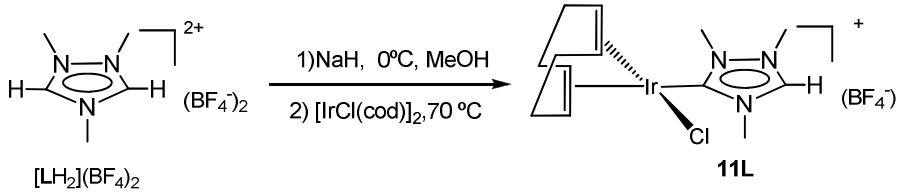

Scheme 2.27. Synthesis of complex **11L**.

The ^1H NMR of **11L** shows the signal due to the NC*H*N proton at δ 9.36, and the ^{13}C NMR shows the signal of the metalated carbene at 189.2, indicating the coordination to the Ir^I fragment.

Both **10L** and **11L** are highly valuable synthons for the preparation of heterometallic dicarbene species, since both species have a remaining CH bond at the azole ring that can be activated to generate the second carbene. The reaction of **10L** in the presence of an equivalent amount of NaH in MeOH generates a metallic methanolic adduct *in situ*. The reaction was stirred at room temperature for 30 minuts and subsequently an equimolecular amount of the corresponding metal precursor $[MCl(cod)]_2$ (M = Rh, Ir) was added. The resulting mixture was then refluxed at 70ºC for additional 30 minuts. After solvent evaporation the crude solid was purified by column cromatography. When the Ir^I precursor was used, elution with dichloromethane/acetone (8:2) affords an orange-yellow band containing compound **12L**. Pure compound **12L** was obtained by precipitation from dichloromethane/*n*-hexanes solution as a yellow solid. When the Rh^I precursor was used, elution with dichloromethane/acetone (7:3) affords a yellow band containing compound **13L**. Pure compound **13L** was obtained by precipitation from dichloromethane/*n*-hexanes solution as a yellow solid. This method affords the mixed-valence complex of Ir/Ir **12L** (Ir^{III}/Ir^I) and the Ir/Rh heterobimetallic species **13L** (Ir^{III}/Rh^I).

We were also able to obtain compound **12L** in high yield from the other way around, this is, starting from **11L**, by addition of $[Cp^*IrCl_2]_2$ in the presence of NaH in MeOH (**Scheme 2.28**). This alternative procedure to the preparation of **12L** confirms the wide applicability of the stepwise metalation of 1,2,4-trimethyltriazolium, as a valuable way to prepare different homo- and heterobimetallic species.

The reaction can also be performed by preparing and using **10L** and **11L** *in situ*, by sequentially adding base, metal source, base and second metal source, so that the stepwise metalation of the ligand provides directly the heterobimetallic compounds **12L** and **13L** (**Scheme 2.28**, **[c]**). For example, for the synthesis of complex **12L** using method **[c]** (**Scheme 2.28**) firstly, in one reactor vessel, we prepare the NaOMe solution, add the [**L**H_2](BF_4) and let the reaction stirring for 1h. After addition of [Cp*$IrCl_2$]$_2$ the mixture was refluxed at 70ºC for 90 minuts and subsequently cooled to room temperature and stirred for additional 30 minuts. In a second reactor vessel, another solution containing 1eq. of NaH (60% in mineral oil) in methanol was prepared and added via cannula to the previous solution. The mixture was stirred for 1 h at room temperature.

After addition of [IrCl(cod)]$_2$ the mixture was refluxed at 70 °C for 1h. After solvent evaporation, the crude solid was purified by column chromatography. Elution with dichloromethane/acetone (8:2) afforded compound **12L** and analytically pure material was obtained by precipitation from dichloromethane/*n*-hexanes solution as a yellow solid.

This latter method is very convenient because it clearly simplifies the workups to the final products, together with a clear reduction of the amount of solvents used in the overall reaction and purification processes.

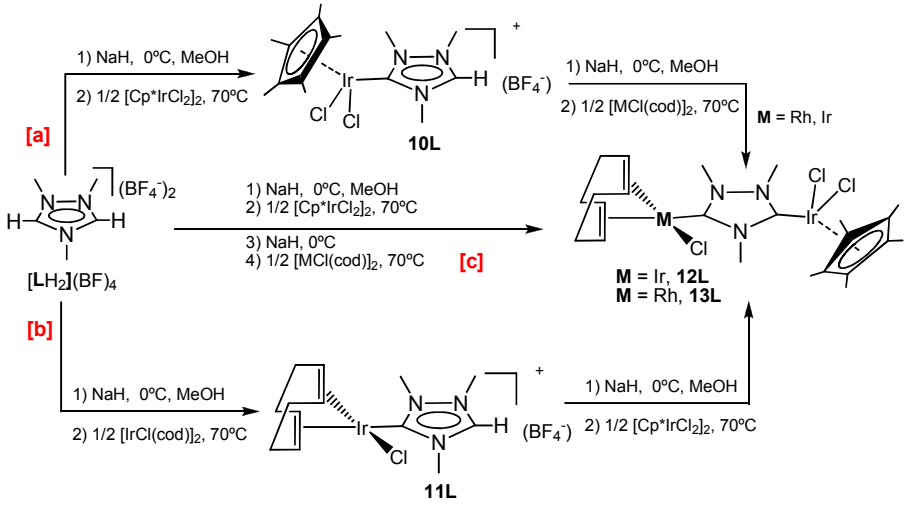

Scheme 2.28. Snthesis of heterobimetallic complexes 12L and 13L.

The yields achieved for the synthesis of the heterobimetallic complex **12L** using methods **[a]**, **[b]** and **[c]** (**Scheme 2.28**) were of 82%, 52 % and 40 % , respectively. Compound **13L** was obtained with the 66 % yield using method **[a]** and the 54 % using methos **[c]**. Compunds **12L** and **13L** were characterized by NMR spectroscopy (^{1}H and ^{13}C), high resolution mass spectrometry and X-ray diffraction.

*^{1}H NMR spectrum of complex **12L***

The ^{1}H NMR spectrum of compound **12L** is shown in **Figure 2.14**. The signals due to the protons at the cod ligand appear as broadbands at 4.77, 3.16, 2.95, 2.21, 1.84 and 1.71ppm. The signal attributed to the protons of the methyls of the Cp* appear as a singlet at 1.66 ppm, and those due to the methyls of the triazole ring appear as three singlets at 4.30 (**a**), 4.26 (**b**) and 4.24 (**c**) ppm.

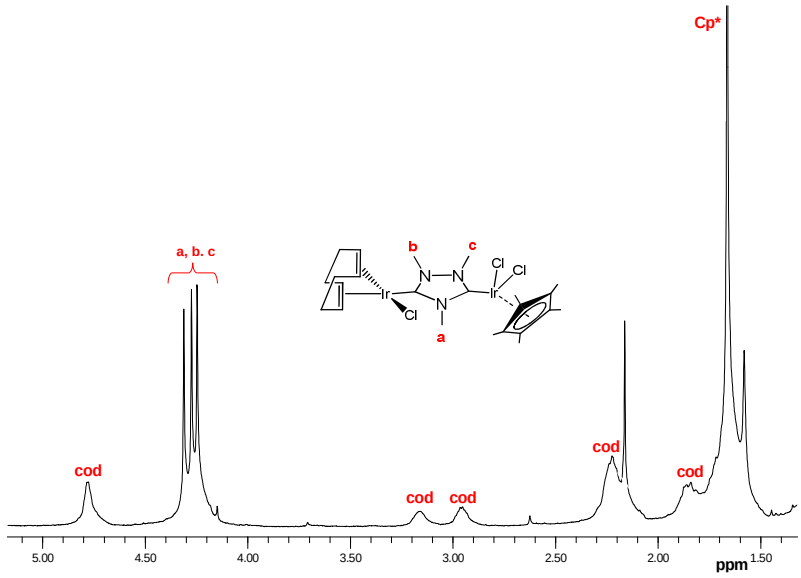

Figure 2.14. ^{1}H NMR spectrum of **12L**.

The ^{13}C NMR spectrum of **12L** shows two signals at 187.0 and 167.4 ppm**,** due to the two distinct metallated carbene-carbons, bound to Ir^{I} and Ir^{III}, respectively. The resonances of the carbons at the Cp* ligand appear at 90.4 ($C_5(CH_3)_5$) and 9,3 ppm ($C_5(CH_3)_5$). The olefinic carbons at the cod ligand display four signals between 89 and 53 ppm, and the four alkylic carbons display four resonances between 33 and 29 ppm confirming the asymmetry of the complex. The signals due to the carbons of the methyls of the triazole ring appear at 40.6, 37.2 and 36.8 ppm.

The ^{13}C NMR spectrum of **13L** confirms that the metallation of the two metallic fragments has occurred, showing two signals at 191.6 for Rh^{I}-C (d, $^{1}J_{Rh\text{-}C}$ = 52.1 Hz) and 167.3 for Ir^{III}-C.

The selected signals of the ^{1}H and ^{13}C {^{1}H}NMR spectra of complexes **12L** and **13L** are shown in **Tables 2.14** and **2.15**.

Table 2.14. ^{1}H NMR of compounds **12L** and **13L**.

^{1}H	**δ (ppm) 12L**	**δ (ppm) 13L**
cod	4.77 (m), 3.16 (m), 2.95 (m), 2.21 (m), 1.84 (m), 1.71 (m)	5.11 (m), 3.19 (m), 2.49 (m), 2.40 (m), 2.00 (m)
$C_5(CH_3)_5$	1.66 (s)	1.66 (s)
NCH_3	4.30 (s), 4.26 (s), 4.24 (s)	4.42 (s), 4.21 (s)

Table 2.15. ^{13}C NMR of compounds **12L** and **13L**.

^{13}C	**δ (ppm) 12L**	**δ (ppm) 13L**
$C_{carbene}$-Ir^{III}	167.4	167.3
$C_{carbene}$-M^{I} [M = Ir(**12**), Rh(**13**)]	187	191.6 (d, $^{1}J_{C\text{-}Rh}$ = 52.0 Hz)
cod	89.1, 88.9, 53.7, 53, 33.7, 33.4, 29.5, 29.4,	100.0 (d, $^{1}J_{C\text{-}Rh}$ = 7.1 Hz), 100.8 (d, $^{1}J_{C\text{-}Rh}$ = 6.8 Hz), 69.8 d, ($^{1}J_{C\text{-}Rh}$ = 9.1 Hz), 69.7 (d, $^{1}J_{C\text{-}Rh}$ = 8.8 Hz), 33, 32.8, 29, 28.9
NCH_3	40.6, 37.2, 36.8	40.8, 37.2
$C_5(CH_3)_5$	90.4	90.4
$C_5(CH_3)_5$	9.3	9.3

X-Ray diffraction studies of 10L, 12L and 13L

Crystals of **10L** were obtained after counter ion exchange with KPF_6. The ion exchange was realized dissolving compound **10L** in acetone and adding an excess of KPF_6. The solution was heated for 2h at 50ºC and then cooled to room temperature. The resulting mixture was then filtered, in order to eliminate the excess of salt, and then concentrated. Precipitation with diethylether afforded pure complex **10L[PF_6^-]**. The presence of the PF_6^- was confirmed by ^{31}P NMR analysis. Suitable crystals of **10L[PF_6^-]** were obtained by slow evaporation from a concentrated acetone solution. Crystals of **12L** and **13L** suitable for X-ray diffraction analysis were obtained by slow evaporation from the corresponding concentrated dichloromethane-acetone solutions. **Figures 2.15, 2.16** and **2.17** show the molecular diagrams of complexes **10L[PF_6^-]**, **12L** and **13L**, respectively.

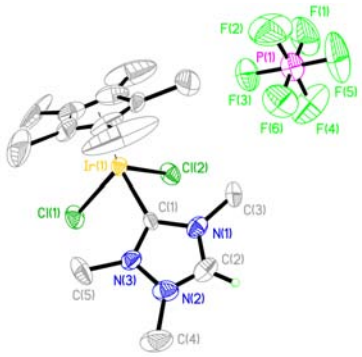

Figure 2.15. Molecular diagram of complex **10L[PF_6^-]**. Ellipsoids at 50% probability level. Hydrogen atoms (except H-2) have been omitted for clarity.

The molecular structure of **10L[PF_6^-]** can be regarded as a three-legged piano-stool. Together with the triazolium-ylidine ligand, two chloride ligands and a Cp* ring complete the coordination sphere about the Ir center. The cationic nature of the complex is confirmed by the presence of a PF_6^- counter ion. The Ir-$C_{carbene}$ distance is 2.048 Å, in the range of other analogue Cp*Ir(NHC) complexes,[23, 46] and also similar to that shown in the bimetallic complex **3L** (**Figure 2.5**, page 35) in which the *ditz* ligand is bridging two Cp*Ir fragments (2.023 Å, **Table 2.1**, page 36)).[22] The rest of distances (Ir-Cp*$_{centered}$, 1.76 Å; Ir-Cl, 2.442 and 2.430 Å) are in the expected range. **Table 2.16** shows the most representative bond distances and angles of complex **10L[PF_6^-]**.

Table 2.16. Selected bond lenghts (Å) and angles (º) of complex **10L[PF_6^-]**.

Bonds	(Å)	Angles	(º)
Ir(1)-C(1)	2.048(11)	C(1)-Ir(1)-Cl(1)	90.0(3)
Ir(1)-Cl(1)	2.442(3)	C(1)-Ir(1)-Cl(2)	88.8(3)
Ir(1)-Cl(2)	2.430(3)	Cl(2)-Ir(1)-Cl(1)	85.76(11)

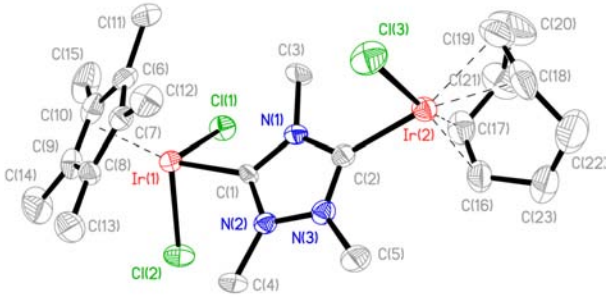

Figure 2.16. Molecular Diagram of complex **12L**. Ellipsoids at 50% probability level. Hydrogen atoms and solvent (CH_2Cl_2) have been omitted for clarity.

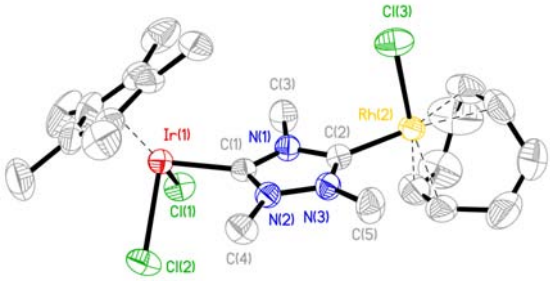

Figure 2.17. Molecular Diagram of complex **13L**. Ellipsoids at 50% probability level. Hydrogen atoms and solvent (CH_2Cl_2) have been omitted for clarity.

Compounds **12L** and **13L** are isostructural, despite the fact that **12L** contains an IrCl(cod) fragment while **13L** has RhCl(cod). The molecular structure of compound **12L** consists of a Cp^*IrCl_2 moiety connected to IrCl(cod) by the triazol-diylidene ligand (**Figure 2.17**). The structure offers a unique opportunity to compare the bond distances to Ir^{III} and Ir^{I} by the same ligand within the same compound. These distances are 2.023 and 2.006 Å for the Ir^{III}-$C_{carbene}$ and Ir^{I}-$C_{carbene}$, respectively, thus showing a slightly shorter distance for the Ir^{I}-C bond. Probably, the shorter distance may be due to the more sterically released geometry in the square-planar part of the molecule than in the pseudotetrahedral fragment, thus allowing a closer approach of the ligand to the metal.

The azole ring adopts an almost perpendicular orientation with respect to the coordination plane of the Ir^{I} metal fragment, as indicated by the torsion angles Cl(3)-Ir(2)-C(2)-N(3) and Cl(3)-Ir(2)-C(2)-N(1) of 90.8° and 86.9°, respectively, while the α angle corresponding is 87.9 º. The distances of the Ir^{I} center to the carbons of the olefin *trans* to the carbene are longer than for the other olefin (*trans* Ir-C_{olefin} 2.19, and *cis* Ir-C_{olefin} 2.13, average distances) as a consequence of the high *trans* influence of the carbene ligand.

Compound **13L** consists of a Cp^*IrCl_2 fragment connected to RhCl(cod) by the *ditz* ligand (**Figure 2.18**). Most structural parameters are similar to those shown by compound **12L**, regarding angles and distances. Even the M-$C_{carbene}$ distances are very similar, 2.032 (M = Ir) and 2.006 Å (M = Rh). **Tables 2.17** and **2.18** show the most representative bond distances and angles of complexes **12L** and **13L**.

Table 2.17 Selected bond lenghts (Å) and angles (º) of complex **12L**.

Bond	12L (Å)	Angles	13L (º)
Ir(1)-C(1)	2.023 (7)	C(1)-Ir(1)-Cl(1)	91.69 (19)
Ir(2)-C(2)	2.006 (7)	C(1)-Ir(1)-Cl(2)	91.05 (19)
Ir(1)-Cl(1)	2.412 (18)	C(2)-Ir(2)-Cl(3)	87.11 (19)
Ir(1)-Cl(2)	2.418 (19)	N(1)-C(1)-Ir(1)	129.0 (5)
Ir(2)-Cl(3)	2.349 (19)	N(2)-C(1)-Ir(1)	127.9 (5)
Ir(2)-C(16)	2.131 (8)	N(1)-C(2)-Ir(2)	127.2 (5)
Ir(2)-C(17)	2.125 (8)	N(3)-C(2)-Ir(2)	129.3 (5)
Ir(2)-C(20)	2.182 (10)		
Ir(2)-C(21)	2.196 (9)		

Table 2.18 Selected bond lenghts (Å) and angles (º) of complex **13L**.

Bond	13L (Å)	Angles	13L (º)
Ir(1)-C(1)	2.032 (4)	C(1)-Ir(1)-Cl(1)	91.58 (11)
Rh(2)-C(2)	2.006 (4)	C(1)-Ir(1)-Cl(2)	91.16 (11)
Ir(1)-Cl(1)	2.417 (10)	C(2)-Rh(2)-Cl(3)	86.12 (11)
Ir(1)-Cl(2)	2.419 (11)	N(1)-C(1)-Ir(1)	128.5 (3)
Rh(2)-Cl(3)	2.360 (12)	N(2)-C(1)-Ir(1)	127.7 (3)
Rh(2)-C(16)	2.102 (5)	N(1)-C(2)-Rh(2	127.0 (3)
Rh(2)-C(17)	2.118 (5)	N(3)-C(2)-Rh(2)	128.9 (3)
Rh(2)-C(20)	2.209 (5)		
Rh(2)-C(21)	2.222 (5)		

2.4.2 Catalytic evaluation of the heterobimetallic species 12L and 13L: initial attempts to build tandem processes up.

Once we obtained the heterobimetallic complexes **12L** and **13L**, we thought that we should try to design a tandem process by combining catalytic cycles tipically facilitated by Ir^{III} and Ir^{I} or Rh^{I}. For this purpose, we thoroughly used the database provided by the *Royal Society of Chemistry* at the:

http://www.rsc.org/Publishing/CurrentAwareness/CCR/CCRSearchPage.cfm

site. Although our initial thought was that this design should not be very complicated, we found many difficulties due to the inherent similarities in the catalytic properties of Ir^{III} and Ir^{I}/Rh^{I} species.

In order to test the catalytic activity of our new dimetallic compounds (**12L** and **13L**), we found it convenient to design a *tandem* process including two different catalytic reactions catalyzed by M^{I} (M=Rh and Ir) and Ir^{III} complexes.

Our initial idea was to perform the hydrosilylation of ketones, a reaction normally catalyzed for complexes of Ir^{I} and Rh^{I}, followed by the β-alkylation of the resulting secundary alcohol with a primary alcohol, a reaction which is tipically catalyzed by Ir^{III} or/and Ru^{II}(**Scheme 2.29**).[47, 48]

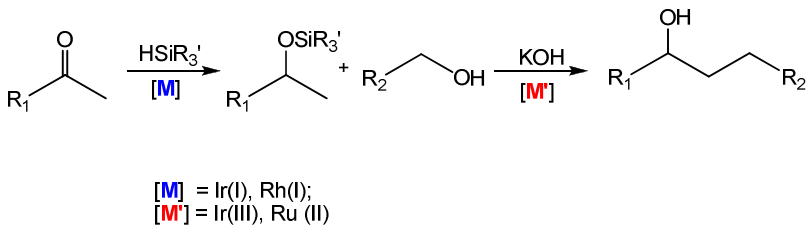

Scheme 2.29. General scheme of tandem Hydrosilylation/β-alkylation reaction.

Our results were fine in the sense that we were able to detect the final products in quantitative yields, but the design of this catalytic sequence was not the right one due to a series of factors that we should have taken into account. Mecanistically, the reaction between a secondary and primary alcohols imply: i) catalytic oxidation of both alcohols to generate the corresponding ketone and aldehyde, ii) aldolic condensation of the carbonilic compounds to produce the α,β-unsaturated ketone, and iii) catalytic reduction of the ketone to obtain the saturated secondary alcohol (**Scheme 2.30**).

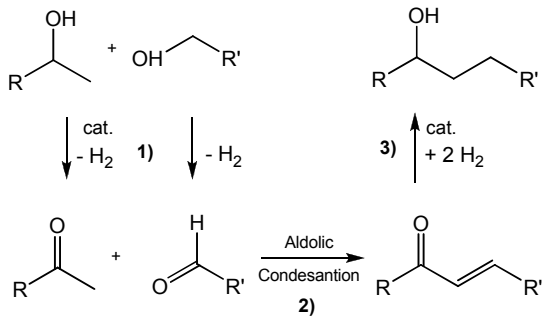

Scheme 2.30. β-alkylation reaction

Taking this into account, the mechanism shown in **Scheme 2.30**, the first hydrosilylation step should not be necessary, because the resulting secundary alcohol has to be further oxidized back to the ketone prior to the β-alkylation step. To confirm this point, we performed a reaction with acetophenone and an excess of *n*BuOH, using 3 equivalents of KOH, and we obtained the resulting β-alkylated secondary alcohol as major product.

Taking these initially misleading results into account, we considered another sequence implying the sequential cyclization of 2-aminophenyl ethyl alcohol (a reaction typically catalyzed by $[Cp^*IrCl_2]_2$),[49] followed by the alkylation of the resulting indole with a series of primary alcohols (a process tipically catalyzed by Ir,[50] Rh, [51] Ru,[52] and In compounds).[53] Because indole-based compounds are found in many natural products with an enormous number of pharmaceutical applications (in fact, indole has been called *the lord of the rings*), new environmentally benign and efficient methods for indole synthesis and its functionalization continue to attract attention.[54] Although there is a large list of articles describing the alkylation of indoles with ketones and aldehydes,[55, 56] the number of works in which alcohols are used instead is scarce and recent, and most respond to the development of new catalytic processes implying transition metal complexes.[50-54, 57] The one-pot tandem strategy to directly obtain alkylated indoles/bisindoles from the reaction of 2-aminophenyl ethyl alcohol and a series of alcohols (**Scheme 2.30**) is a challenging process because it will allow us to compare the different activities of our dimetallic catalysts in two different and consecutive processes.

In the course of our research, a work by Grigg and co-workers described for the first time this same reaction, using $[Cp^*IrCl_2]_2$ as catalyst for the overall process.[50] In this work they observed the selective formation of the 3-alkylated indole (**B**) with only traces of the bisindolylmethane (**A**) (**Scheme 2.30**).[50] In any case, the results described by Grigg and co-workers illustrate the catalytic similarities between M^I (M = Rh, Ir) and Ir^{III}, which actually make our compounds not as suitable as we initially thought for the design of a tandem process comprised by mechanistically distinct reactions catalysed by the two different metals. Not feeling very disappointed by this finding, we carried out a detailed catalytic study of our complexes in this interesting tandem process.

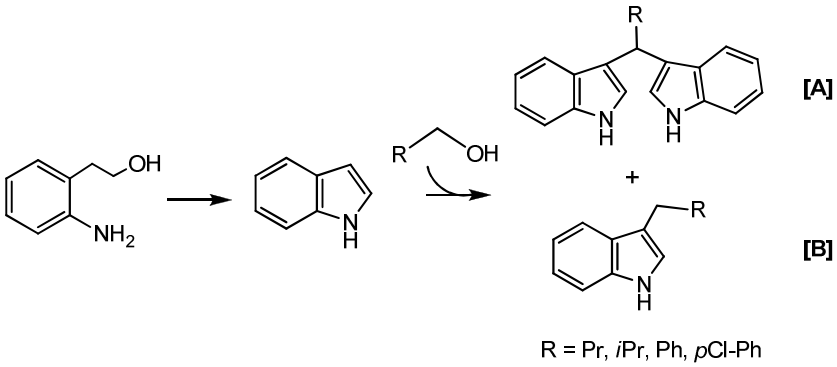

Scheme 2.31

We first studied the activity of a set of catalysts shown in **Scheme 2.32** in the reaction between the amino alcohol and benzylic alcohol. We also studied the activities of $[Cp^*IrCl_2]_2$, and $[IrCl(cod)]_2$ for comparative purposes. The reactions were carried out at 110 ºC, using KOH and an amino alcohol/primary alcohol ratio of 1:1, and using toluene as solvent.

This first set of data is displayed in **Table 2.19** and allows us to compare the activities of our catalysts in terms of yields and selectivities.

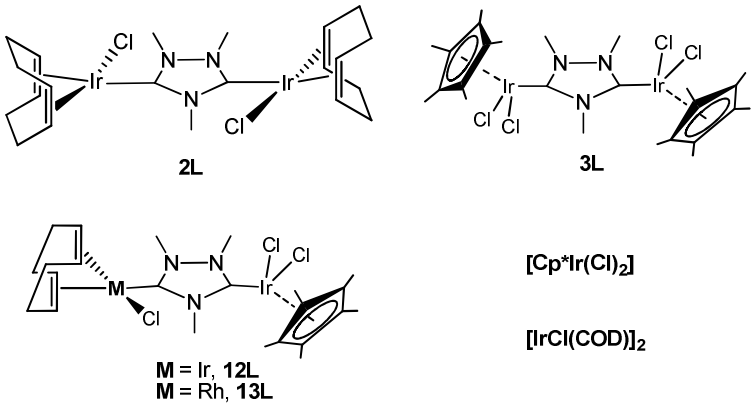

Scheme 2.32. Catalysts employed.

The catalytic experiments were monitored by ^{1}H NMR spectroscopy, extracting aliquots from the reaction medium. Yields were determined by comparing with the concentration of the internal standard (Ferrocene).

The evolution of the reaction was analyzed comparing the signal of the starting primary alcohol with the new signals due to the 3-benzyl-indole (**B**) or the bisindolyl-methane (**A**) formed, according to previously published results.[50] As an example, the reaction between 2-aminophenethyl alcohol and benzyl alcohol will be commented in detail (**Scheme 2.33**).

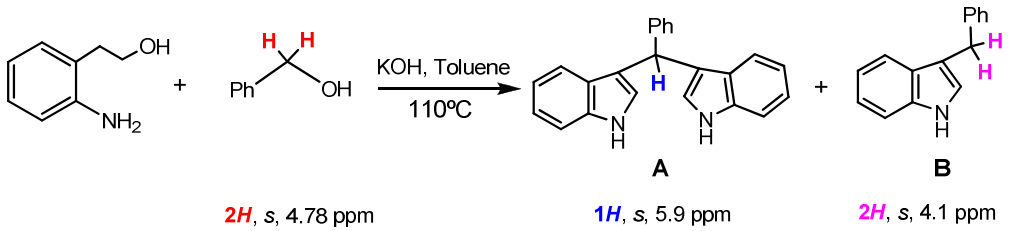

Scheme 2.33. ^{1}H NMR signals used for the study of the evolution of the reaction between an amino alcohol an benzylacohol.

The advance of this reaction is monitored by the progressive disappearance of the signal corresponding to the benzylic protons Ph-C***H*$_2$**-OH (singlet at 4.8 ppm), and the subsequent formation of a singlet at 5.9 ppm (C-***H*** proton at the bridge between the two indole fragments of the bisindolylmethane product) and/or another singlet at 4.1 ppm (C***H*$_2$** protons of the monoindole species). In our experiments, we did not detect any formation of the N-Alkylated indole.

As can be observed fom the data shown in **Table 2.19**, under the reaction conditions applied (equimolar amounts of alcohol and amino alcohol, catalyst loading of 1 mol %, toluene at 110 °C), a clear preference for the bisindolyl product **A** is observed for all catalysts except **13L**, which affords an **A**:**B** ratio of 50:50 (entry 4). The catalyst containing the Ir^{III}/Ir^{I} couple (**12L**) offers the best selectivity in the production of the bisindole **A** (compare entry 3 with entries 1, 2 and 4). In terms of yields, the triazol-diylidene-bridged complexes **2L** and **12L** showed higher activity than **3L** and **13L** (compare entries 1 and 3 with entries 2 and 4). The complex $[Cp^*IrCl_2]_2$ also showed a high activity toward the alkylated complexes, although it afforded a lower selectivity to **A** (entry 5).

These preliminary results show that the catalytic activity of all the complexes used cannot be assigned to any of the individual metal fragments that compose each dimetallic catalyst. For example, based on the high catalytic performances of **2L** we should assume that the good results are due to the Ir^{I}(cod) fragment. This would be consistent with the good activities shown by **12L**, which contains the Ir^{I}(cod)/Cp^*Ir^{III} couple. The same argument can be applied to the Cp^*Ir^{III} fragment, by comparing the results obtained by **3L** and **12L**. However, the Rh^{I}/Cp^*Ir^{III} compound **13L** shows a very low activity, a result that contrasts with those shown by the other Cp^*Ir^{III}-containing complexes **3L** and **12L**.

Table 2.19. Catalytic Tandem Cyclization/Alkylation of 2-Aminophenyl Ethyl Alcohol and Benzyl Alcohol[a]

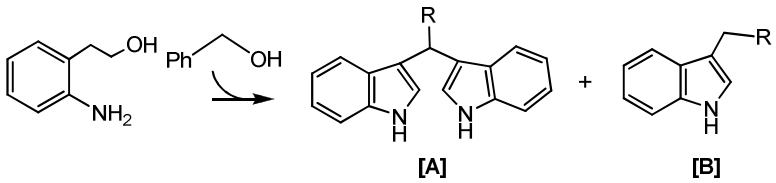

[A] [B]

Entry	Catalyst	Time (h)	Yield (%)	A:B[b]
1	**2L**	7	>95	77:23
2	**3L**	7	84	87:13
3	**12L**	7	>95	90:10
4	**13L**	20	30	50:50
5	**$[Cp^*IrCl_2]_2$**	7	>95	60:40
6	**$[IrCl(cod)]_2$**	7	58	70:30

[a]Reaction Conditions : 0.25 mmol of amino alcohol, 0.25 mmol of benzyl alcohol, 0.5 mmol of KOH, 1 mol % catalyst, 0.3 mL of toluene. *T*=110 °C. Yields determined by ^{1}H NMR spectroscopy using ferrocene (0.025 mmol) as standard. [b] Product distribution.

Since compounds **2L**, **12L**, and $[Cp^*IrCl_2]_2$ showed the best catalytic performances, they were tested using a wider range of primary alcohols. We also performed the reactions with a lower catalyst loading (0.1 mol %) in order to carefully determine the differences in the catalytic activities of all compounds used.

These data are shown in **Table 2.20**. According to these new results, it seems clear that all catalysts afford better activities when benzyl alcohols are used compared to the activity shown with *i*BuOH and *n*BuOH, in accordance with the previously reported data.[50] For a catalyst loading of 1 mol %, **12L** is the most effective catalyst in terms of both yields and selectivity, even achieving full conversion to the bisindolylmethane when *n*BuOH is used (entries 9, 11 and 13).

On the other hand, when *i*BuOH is used, long reaction time is needed to achieve moderate yield, without any alteration in selectivity to the product **A** (entry 15). Reducing the catalyst loading to 0.1 mol % results in a significant lowering of the catalytic productivity, although the yields were still moderate (~50%) when catalyst **12L** and the benzyl alcohols were used (entries 12 and 14).

Tabla 2.20 Catalytic Cyclization/Alkylation of 2-Aminophenyl Ethyl Alcohol with Different Primary Alcohols[a]

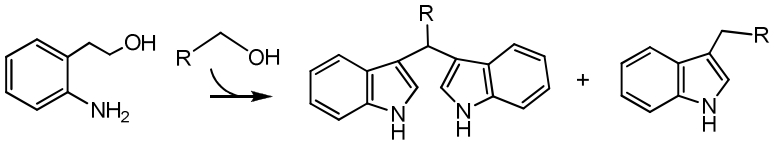

[A] [B]

R = Pr, *i*Pr, Ph, *p*Cl-Ph

Entry	Catalyst	R	[Cat] (mol %)	Time (h)	Yield (%)	A:B[b]
1	**2L**	Pr	1	20	61	100:0
2			0.1	12	10	100:0
3		Ph	1	7	>95	77:23
4			0.1	12	21	60:40
5		*p*Cl-Ph	1	7	>95	90:10
6			0.1	12	44	90:10
7		*i*Pr	1	36	15	100:0
9	**12L**	Pr	1	20	>95	100:0
10			0.1	12	14	100:0
11		Ph	1	7	>95	90:10
12			0.1	12	50	90:10
13		*p*Cl-Ph	1	7	>95	80:20
14			0.1	12	45	80:20
15		*i*Pr	1	36	50	100:0
17	**[Cp*IrCl$_2$]$_2$**	Pr	1	20	13	100:0
18		Ph	1	7	>95	60:40
19			0.1	20	40	70:30
20		*i*Pr	1	36	21	100:0

[a] Reaction conditions: 0.25 mmol of amino alcohol, 0.25 mmol of primary alcohol, 0.5 mmol of KOH, 0.3 mL of toluene. T=110 °C. Yields determined by ^{1}H NMR spectroscopy using ferrocene (0.025 mmol) as standard. [b] Product distribution.

Scheme 2.34 shows the different product ratios upon variation of the amount of alcohol added when **12L** was used.

As can be seen, upon increasing the alcohol/amino alcohol molar ratios, an inversion of the selectivity is observed, so that the monoalkylated compound **B** is the only product obtained for alcohol/amino alcohol molar ratios higher than 10. In order to discard that the activity of complex **12L** may be due to the activity of a mixture of **3L** and **2L** as a consequence of the disproportionation reaction of **12L**, we decided to test the stability of the complex at high temperatures in different solvents. Long standing solutions (>2 h) of **12L** in

$CDCl_3$, toluene-*d*8, and DMSO*d*6, at 80 and 110 °C, respectively, using an excess of base, showed that the complex did not decompose, according to the NMR spectra recorded during and after the experiment. In principle, this stability test supports the idea that the dimetallic structure of the complex is maintained during the catalytic cycle, although we are aware that the experiment does not reproduce the conditions supported by the catalyst in the catalytic reaction.

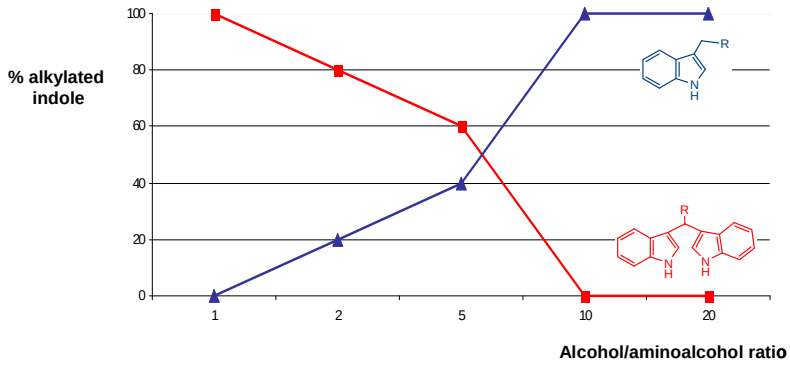

Scheme 2.34. Selectivity experiments using **12L** as catalyst upon variation of the amount of alcohol added.

According to the proposed mechanism for the alkylation of indole with alcohols,[52] the formation of the bisindolylmethane product (**A**, **Scheme 2.35**) arises from the Michael addition of indole to the intermediate **C**. This intermediate may also evolve to the monoalkylated species **B** after being hydrogenated by the alcohol in the presence of the base by a metal-mediated transfer hydrogenation process, as depicted in the mechanism shown in **Scheme 2.35**.

The selectivity of the reaction, leading to products **A** and **B** from the intermediate **C** is controlled by the amount of the alcohol used. Because the transfer hydrogenation is a relatively slow process, it is not surprising that **A** is the major compound formed when low amounts of the primary alcohol are used, because the Michael addition is the kinetically preferred process.

Since the alcohol is acting as both an alkylating agent and reductant, an excess of alcohol should favor the formation of the monoalkylated species **B**. The presence of an excess of base and the aerobic conditions would stimulate the oxidation of the primary alcohol and the continuing regeneration of the metal-hydride.

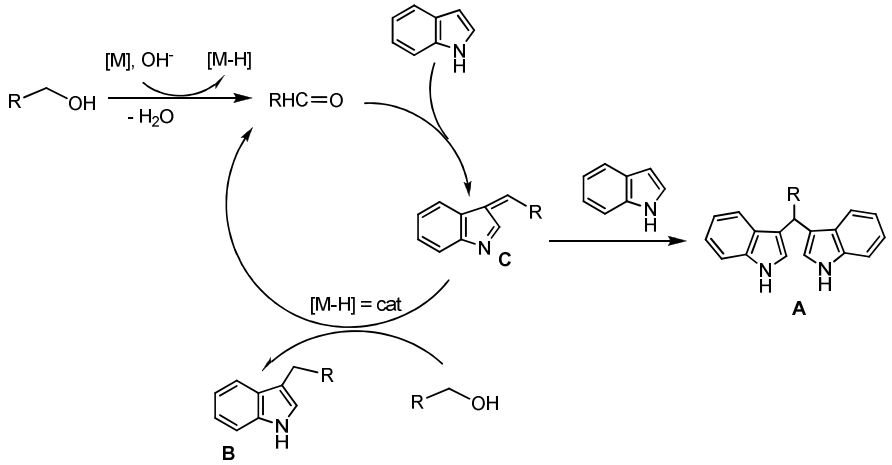

Scheme 2.35. Proponed mechanism for the oxidative cyclization/alkylation of indole with primary alcohols.

In conclusion, the catalytic activities of our new compounds have been tested in a tandem reaction implying the oxidative cyclization of an amino alcohol to produce indole that is alkylated by a primary alcohol to selectively produce the 3-alkylated species or the bisindolylmethane compound.

We performed a detailed study and proposed a mechanism that is slightly different from the previously proposed one.[52] Our results show not only that our compounds are highly effective for this tandem process but also that the activity of the heterometallic catalysts cannot be regarded as the sum of the individual components of the compound, thus implying that the connection of two different metal fragments through an aromatic bridging ligand may have important consequences in catalytic cooperativity.

2.4.3 Synthesis and characterization of heterobimetallic Ir^{III}/M^{II} (M = Pd, Pt) complexes using *ditz*

The preparation of the Ir/Pd and Ir/Pt heterobimetallic complexes was performed starting from the previously described compound **10L** as shown in the reactions depicted in Scheme **2.36**.

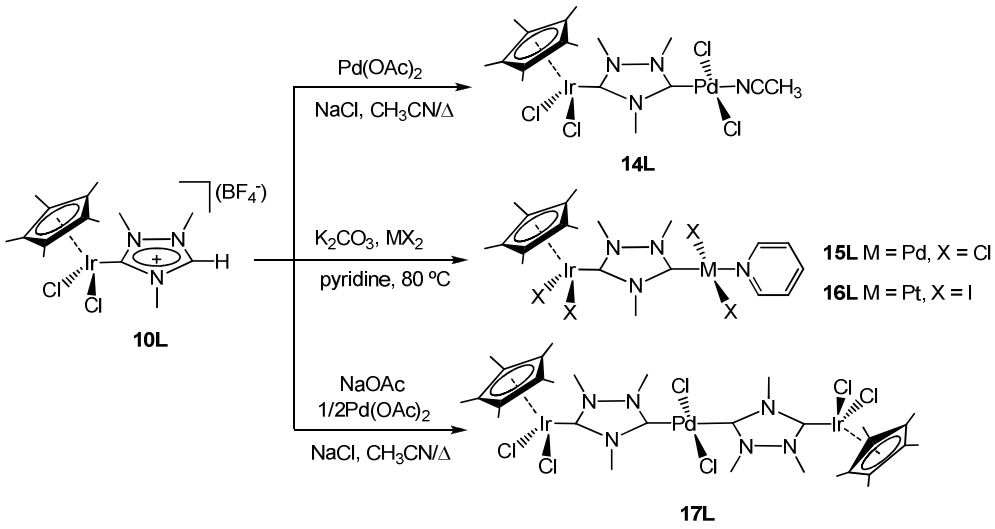

Scheme 2.36. Synthesis of complexes **14L**, **15L**, **16L** and **17L**.

Compound **14L** is prepared from the reaction between **10L** and $Pd(OAc)_2$ in refluxing acetonitrile overnight in the presence of NaCl, wich is used to supply the chloride ligands to the final products. The reaction mixture was then filtered through Celite, and the volatiles were removed under vacuum. The crude solid was dissolved in CH_2Cl_2 and purified by column chromatography. Compound **14L** was eluted as a pale-yellow band with dichloromethane/methanol (10:1) and precipitated from a mixture of acetone/diethylether to give a pale yellow solid in 68% yield.

An analogue complex but with a pyridine instead of the acetonitrile ligand, complex **15L**, can be obtained from the reaction of **10L** and $PdCl_2$ in pyridine as solvent in the presence of K_2CO_3 (yield, ca. 80%). Using the same procedure, the Ir^{III}/Pt^{II} complex **16L** was obtained by reaction of PtI_2 with the triazolium-ylidene-Iridium complex **10L**, with an excess of NaI, in order to accomplish the halide exchange. The pure compounds **15L** and **16L** were obtained as yellow and orange solids, respectively, after recrystallization from dichloromethane/*n*-hexanes.

The trimetallic compound **17L**, which contains two Ir-based fragments and one Pd, is prepared from the reaction between **10L** and $Pd(OAc)_2$ (2:1) in refluxing acetonitrile in the presence of NaCl, which is used in order to supply the chloride ligands to the final product. The reaction mixture was filtered through Celite, and the solvent was removed under vacuum.

The crude solid was dissolved in CH_2Cl_2 and purified by column chromatography. Compound **17L** was eluted with acetone /dichloromethane (7:3), and was isolated in low yield (ca. 15%). All four new complexes were characterized by NMR spectroscopy (^{1}H and ^{13}C), electrospray mass spectrometry (ESI-MS), elemental analysis and X-ray diffraction studies.

The ^{1}H NMR spectrum of **14L** shows that the signal due to the acidic HC*H*N proton has disappeared, thus providing the first evidence that the coordination on the palladium fragment has occurred. The signals attributed to the protons of the methyls of the Cp* appear as a singlet; three distinctive resonances due to the three methyl groups at the azole bridge are observed, indicating the lack of symmetry.

*^{13}C {^{1}H } NMR spectrum of **14L***

The more representative signals observed on the ^{13}CNMR spectrum (**Figure 2.18**), are the ones assigned to the metalated carbenes, at δ 169.0 (**1**) ($C_{carbene}$-Ir) and 158.7 (**2**) ($C_{carbene}$-Pd).

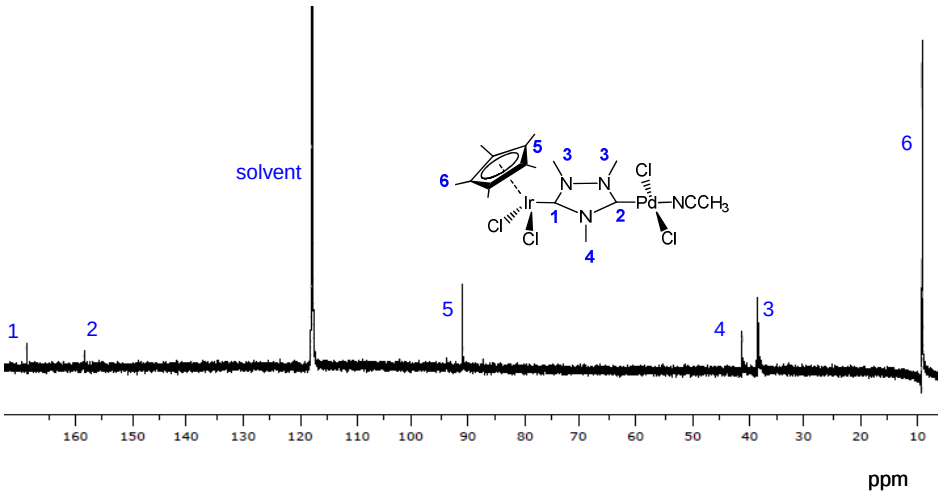

Figure 2.18. ^{13}C {^{1}H} NMR spectrum of **14L**.

The signals attributed to the carbons of the Cp* ligand appear at 91.1 (**5**) ($C_5(CH_3)_5$) and 8,8 ppm (**6**) ($C_5(CH_3)_5$). The resonances due to the carbon of the methyls at the 1 and 2 positions of the triazolium ring appear at 38.1 and 38.3 ppm (**3**), and the one due to the methyl at the 4 position is seen at 41.9 ppm (**4**).

The ^{1}H and ^{13}C {^{1}H} NMR spectra of complexes **15L** and **16L** are qualitatively similar. The data of the ^{1}H and ^{13}C {^{1}H} NMR spectra of the two complexes are summarized in **Tables 2.21** and **2.22**.

Table 2.21. ^{1}H NMR signals of compounds **15L** and **16L**.

^{1}H	δ (ppm) 15L	δ (ppm) 16L
C-H_{py}	9.0 (d, $^{3}J_{H-H}$= 5.5 Hz, 2H) 7.87 (t, $^{3}J_{H-H}$= 7.0 Hz, 1H) 7.45 (t, $^{3}J_{H-H}$= 6.5 Hz, 2H)	8.90 (d, $^{3}J_{H-H}$= 5.0 Hz, 2H) 7.75 (t, $^{3}J_{H-H}$= 7.0 Hz, 1H) 7.33 (t, $^{3}J_{H-H}$= 6.5 Hz, 2H)
$C_5(CH_3)_5$	1.73 (s)	1.79 (s)
NCH_3	4.60 (s), 4.58 (s), 4.41 (s)	4.27 (s), 4.24 (s), 4.23 (s)

Table 2.22. ^{13}C NMR signals of compounds **15L** and **16L**.

^{13}C	δ (ppm) 15L	δ (ppm) 16L
$C_{carbene}$-Ir^{III}	168.4	164.0
$C_{carbene}$-M^{II} [M = Pd(**15**), Pt(**16**)]	163.4	155.5
$C_{Pyridine}$	151.3, 151.1, 138, 124.9, 124.6	153.5, 138.1, 125.2
NCH_3	40.7, 38.1, 37.5	45.4, 41.8
$C_5(CH_3)_5$	90.6	91.6
$C_5(CH_3)_5$	9.0	8.9

*^{1}H NMR spectrum of **17L***

The ^{1}H NMR spectrum of the trimetallic complex **17L** (**Figure 2.19**) shows two resonances at 4.46 ppm (**a**) and 4.31 ppm (**b**) (2:1 integral ratio) due to the three methyl groups at the two azole bridges. The singlet due to the protons of the methyls groups of the two Cp* ligands appears at 1.65 ppm (**c**).

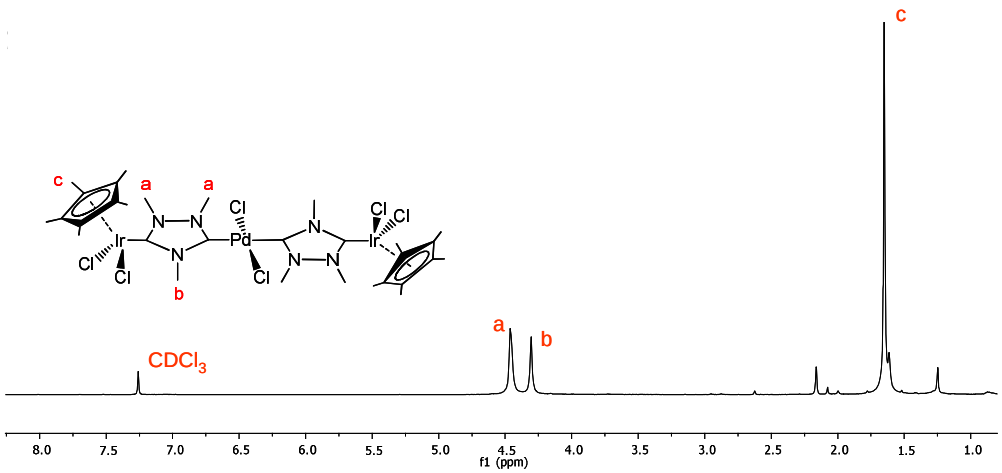

Figure 2.19. ^{1}H NMR spectrum of complex **17L**.

Due to the insolubility of the compound, we could not to get a proper ^{13}C NMR spectrum because concentrated solutions of **17L** in all ordinary deuterated solvents afforded insoluble crystals after several minutes.

X-Ray molecular structures of 15L, 16L and 17L

Suitable crystals of **15L**, **16L** and **17L** for X-ray diffraction analysis were obtained by slow evaporation from the corresponding concentrated dichloromethane solutions. **Figure 2.20, 2.21** and **2.22** show the ORTEP diagrams of complexes **15L**, **16L** and **17L**, respectively. Compounds **15L** and **16L** are isostructural with the only difference that the Pd is replaced by Pt and Cl atoms are replaced by I atoms.

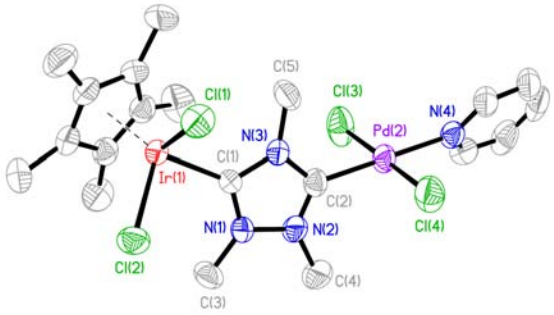

Figura 2.20. Molecular Diagram of complex **15L** . Ellipsoids at 50% probability level. Hydrogen atoms have been omitted for clarity.

The molecular structure of compound **15L** (**Figure 2.20**) consists of a Cp^*IrCl_2 fragment connected to $PdCl_2Py$ by the triazolyl-di-ylidene ligand. The structure allows a comparison between the bond distances to Ir^{III} and Pd^{II} by the same ligand within the same compound. These distances are 2.019 and 1.972 Å for Ir^{III}-$C_{carbene}$ and Pd^{II}-$C_{carbene}$, respectively.

The two chloro ligands on the Pd fragment adopt a *trans* configuration. The Pd-$N_{pyridine}$ distance is 2.070 Å, in the range of other similar bonds trans to NHCs (for comparison, see *section 2.3.3* at pag.47 and 49 of this thesis),[56, 57] and longer than those shown for other related complexes with non-NHC ligands,[58] indicating the high trans influence provided by the triazolyl-di-ylidene ligand.

The Ir-Pd distance is 6.039 Å. The azole ring adopts an almost perpendicular orientation with respect to the coordination plane of the Pd fragment, with an angle of 83º.

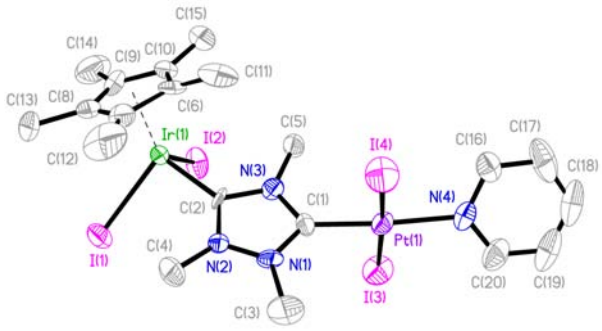

Figure 2.21. Molecular diagram of complex **16L.** Ellipsoids at 50% probability level. Hydrogen atoms have been omitted for clarity.

Compound **16L** consists of a Cp*IrI_2 fragment connected to PtI_2(Py) by the ditz bridging ligand (**Figure 2.21**). Most structural parameters are similar to those shown by compound **15L**, regarding angles and distances.

The M-$C_{carbene}$ distances are 2.011 (M = Ir) and 1.932 Å (M = Pt). The two iodide ligands on the Pt fragment adopt a *trans* configuration. The distance between the two metal centers is 6.04 Å. **Tables 2.23** and **2.24** show the most representative bond distances and angles of complexes **15L** and **16L**.

Table 2.23 Selected bond lenghts (Å) and angles (º) of complex **15L**.

Bond	15L (Å)	Angles	15L (º)
Ir(1)-C(1)	2.019 (6)	C(1)-Ir(1)-Cl(1)	90.31 (17)
Ir(1)-Cl(1)	2.425 (17)	C(1)-Ir(1)-Cl(2)	92.08 (17)
Ir(1)-Cl(2)	2.406 (17)	C(2)-Pd(2)-Cl(3)	87.2 (2)
Pd(2)-C(2)	1.972 (6)	C(2)-Pd(2)-Cl(4)	91.2 (2)
Pd(2)-Cl(3)	2.301 (2)		
Pd(2)-Cl(4)	2.290 (2)		
Pd(2)-N(4)	2.070 (5)		

Table 2.24 Selected bond lenghts (Å) and angles (º) of complex **16L**.

Bond	16L (Å)	Angles	16L (º)
Ir(1)-C(2)	2.011 (10)	C(2)-Ir(1)-I(1)	96.3 (4)
Ir(1)-I(1)	2.721 (11)	C(2)-Ir(1)-I(2)	91.4 (3)
Ir(1)-I(2)	2.719 (11)	C(1)-Pt(1)-I(3)	89.1 (4)
Pt(1)-C(1)	1.932 (12)	C(1)-Pt(1)-I(4)	88.0 (4)
Pt(1)-I(3)	2.604 (12)		
Pt(1)-I(4)	2.598 (12)		
Pt(1)-N(4)	2.077 (11)		

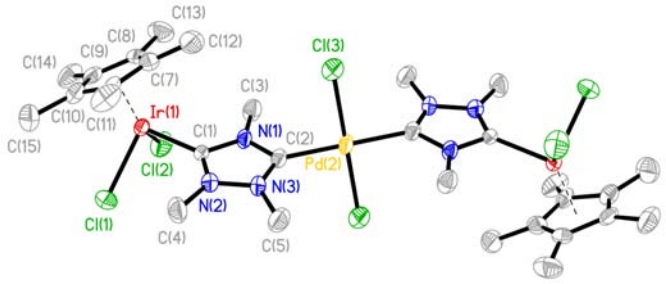

Figura 2.22. Molecular diagram of complex **17L**. Ellipsoids at 50% probability level. Hydrogen atoms have been omitted for clarity.

The molecular structure of **17L** can be regarded as two Cp*$IrCl_2$(triazolyl-di-ylidene) fragments connected by a *trans*-$PdCl_2$ bridge (**Figure 2.22**). The molecule shows an inversion center at the Pd atom, so the two Cp*$IrCl_2$ fragments are symmetry related. This makes the two azole rings to be essentially coplanar, with an *anti* configuration of the two Cp*Ir fragments along the Ir-Pd-Ir axis. The Ir-$C_{carbene}$ distance is 2.029 Å, similar to the same distance in other Cp*Ir fragments connected to *ditz*.[22] The Pd(2)-C(2) distance is 2.030 Å, longer than the distances shown for other previously reported Pd(II) complexes bound to *ditz*,[31, 57] and to the Pd(2)-C(2) distance shown by compound **15L** (1.972 Å), probably due to the mutually *trans* influence produced by the two triazolyl-di-ylidene ligands in **17L**. The intermetallic through-space distances in the molecule are 6.115 (Pd-Ir) and 12.229 Å (Ir-Ir). The azole rings deviate from the coordination plane of the Pd^{II} fragment, as seen from the angle (64º). **Table 2.25** shows the most representative bond distances and angles of complex **17L**.

Table 2.25. Selected bond lenghts (Å) and angles (º) of complex **17L**.

Bonds	(Å)	Angles	(º)
Ir(1)-C(1)	2.029(6)	C(1)-Ir(1)-Cl(1)	92.29(17)
Ir(1)-Cl(1)	2.3959(18)	C(1)-Ir(1)-Cl(2)	92.23(17)
Ir(1)-Cl(2)	2.424(17)	C(2)-Pd(2)-Cl(3)	88.96(17)
Pd(2)-C(2)	2.038(6)		
Pd(2)-Cl(3)	2.315(18)		

2.5 Tandem catalysis using Ir-Pd complexes

Aiming to search for a catalyst able to mediate two fundamentally different reactions now we will describe the catalytic activity of heterobimetallic species of Ir/Pd. In the design of a tandem catalytic process for which these heterobimetallic complexes of Ir/Pd can be used, we can combine the large and distinct library of transformations for wich Ir and Pd are potentially active.

In this chapter, we will discuss two of such tandem transformations, namely the dehalogenation/transfer hydrogenation of halo-acetophenones and the reduction of nitroarenes to anilines/coupling with primary alcohols to afford imines.

2.5.1 Dehalogenation/transfer hydrogenation of halo-acetophenones

For the first study of a tandem catalytic process for our Ir/Pd complexes, we thought that 4-halo-acetophenones would be very good substrates to start with, because they have two distinct functionalities tipically activated by Ir and Pd. The C-X bond is tipically activated by Pd catalysts, while the C=O bond is generally activated by Ir complexes, mainly in borrowing-hydrogen transformations (**Scheme 2.37**).

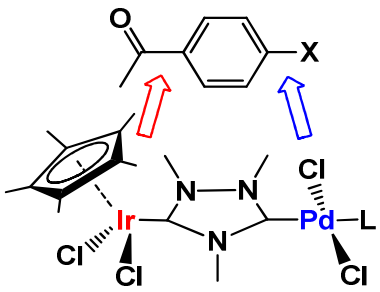

Scheme 2.37

In this section, we will discuss our results on the study of three transformations, namely: **i)** dehalogenation and transfer hydrogenation, **ii)** Suzuki coupling and transfer hydrogenation, and **iii)** Suzuki coupling and α-alkylation of the ketone with primary alcohols.

i) Dehalogenation/transfer hydrogenation of halo-acetophenones.

For the study of the catalytic properties of our Ir/Pd complexes, we thought that a simple sequence implying the dehalogenation/transfer hydrogenation of halo-acetophenones would be a very good process to start with. We thought that the *a priori* chances of compatibility between these two reactions should be high, because both are carried out in the presence of base and an alcohol.

The dehalogenation of aryl-halides represents an important transformation in organic synthesis,[59] with special interest in environmental remediation taking into account the high

toxicity of polychlorinated arenes.[60] Pd-catalyzed dehalogenations of aryl-halides can take place in *i*PrOH in the presence of a strong base, [61] such as NaO*t*Bu, the same reaction medium that is often required for the transfer hydrogenation to ketones.

The catalytic transfer hydrogenation reaction [62, 63] consists of the the reduction of unsaturated species with a hydrogen source that is normally an alcohol. The catalyst takes protons from the hydrogen source and releases them to the unsaturated species.[63] The unsaturated compounds generally used for this kind of reaction are ketones, aldehydes and imines,[64] combined with hydrogen donors wich are alcohols,[65-67] normally *i*-Propanol (**Scheme 2.38**).

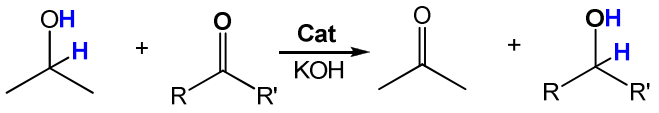

Scheme 2.38

The metals used in the transfer hydrogen reactions are complexes of Ru(II),[67, 68] Rh(III),[67, 69] Ir^{I} and Ir^{III}.[64, 70-71] In the last few years two catalytic mechanism have been proposed to describe the transfer hydorgenation reaction: 1) the direct transfer hydrogenation mechanism and 2) the hydride mechanism, which can occur *via* a mono- or a di-hydride intermediate.[72, 73]

Previous results have proved the activity of some Pd-NHC complexes in the dehalogenation of haloarenes,[74, 75] and Cp*Ir(NHC) complexes in the transfer hydrogenation to ketones.[23, 76-77] Taking this into account, we decided to study the one-pot dehalogenation/transfer hydrogenation of haloacetophenones in *i*PrOH under basic conditions. **Scheme 2.39** shows the catalysts used. For comparative purposes, we also used the homobimetallic compounds **3L,**[22] and **6L**[57] (see *section 2.3.1*at pag.31 and *2.3.3* at pag. 40, respectively) in this *tandem* catalytic process.

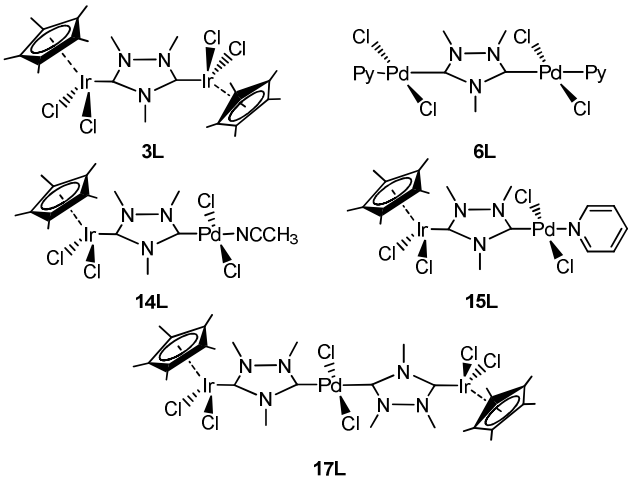

Scheme 2.39. Catalysts employed.

Table 2.26 summarizes the most representative data that we obtained for the tandem reaction under study. A first catalyst screening was performed in order to check which of the compounds tested afforded the best performances.

Table 2.26. Tandem dehalogenation/transfer hydrogenation of haloacetophenones.[a]

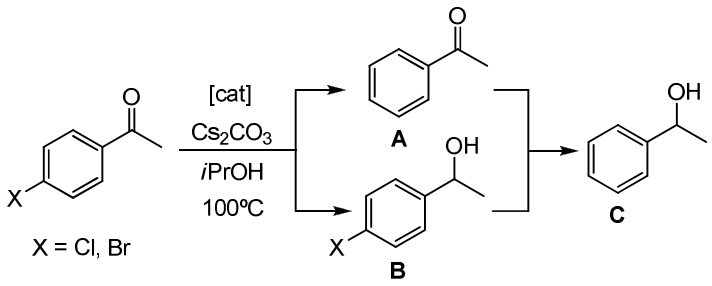

Entry	Catalyst	X	Time (h)	A (%)[b]	B (%)[b]	C (%)[b]
1	**14L**	Br	20	22	0	75
2	**15L**	Br	20	0	0	>99
3	**17L**	Br	20	0	0	95
4	**3L**	Br	20	0	89	0
5	**6L**	Br	20	95	0	0
6	**3L + 6L**[c]	Br	20	72	0	25
7	**15L**	Br	9	21	1	77
8	**15L**	Cl	25	3	12	83
9	**15L**	Cl	9	21	42	34

[a] Reaction Conditions: 4-haloacetophenone (0.36 mmol), Cs_2CO_3 (0.43 mmol), anisole as internal reference (0.36 mmol), catalyst (2 mol%) and 2 mL of 2-propanol. The solution was heated to 100 ºC in aerobic conditions. [b] Yields determined by GC chromatography. [c] 1 mol % of **3L** + 1 mol % of **6L**.

For the reaction with *p*-bromoacetophenone, in *i*PrOH and Cs_2CO_3, compound **15L** showed the best catalytic outcomes (**Table 2.26**, entry 2), when comparing the yields to the final product **C**. The homobimetallic complexes of Ir (**3L**) and Pd (**6L**) showed activities only in the reactions for which these two complexes were expected to be active, this is, the Ir complex produced only the hydrogenation transfer product (**B**, entry 4), while the Pd compound gave only the dehalogenation process (**A**, entry 5).

At a first glance this result may seem obvious, but we have to take into account that Fujita and Yamaguchi showed that $[Cp^*RhCl_2]_2$ is an effective catalyst in the dehalogenation of aryl chlorides,[78] so we could not discard that the same reaction may have been catalysed by the Ir complex **3L**. Interestingly, addition of the two homobimetallic species **3L** and **6L**

resulted in a much more ineffective catalytic system than any of the other three heterobimetallic species used (entry 6).

This result suggests that some catalytic cooperativity between the two metals of the heterobimetallic species, may be playing a role in the overall catalytic cycle, since the better activity of the well-defined heterobimetallic species is redundant in this and other related examples studied by us (see *section 2.4.2* at pag. 61).[22] Also, in a parallel experiment, we studied the stability of **14L**-**17L**, by dissolving them in *i*PrOH with an excess of base, and letting the solutions to be heated at 100ºC. The ^{1}H NMR spectra of the resulting solutions did not show any decomposition after 5h, and only after 20h a small amount of unidentified decomposition products (< 15%) could be observed. This experiment was intended to discard that the heterometallic species could evolve to a mixture of the two homobimetallic compounds (**3L** and **6L**) under the reaction conditions used in the catalytic assays.

Under the same conditions (*i*PrOH, 100ºC) an equimolecular mixture of **3L** and **6L** resulted in the partial decomposition of the palladium complex **6L**, as seen by NMR spectroscopy and by the deposition of some Pd-black in the reaction vessel.

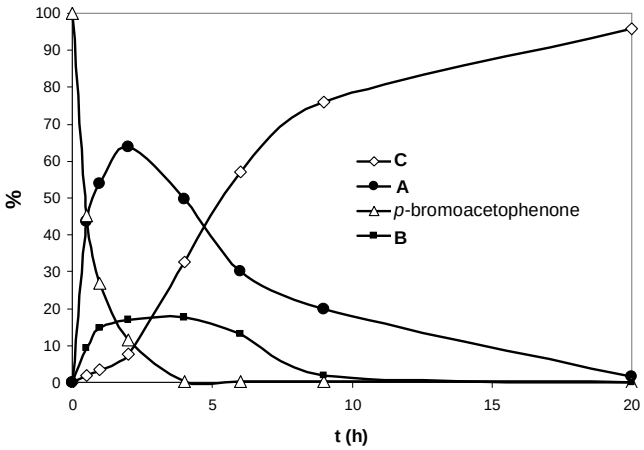

Figure 2.24. Time course of the transformation of *p*-bromoacetophenone with **15L** (*i*PrOH, 100ºC, cat. = 2 mol %).

Interestingly, the reaction is very clean, and we did not observe the formation of any other products apart from **A**, **B** and **C**. This gave us a very good opportunity to study the reaction time course. **Figure 2.24** shows the evolution of the reaction of *p*-bromoacetophenone using catalyst **15L**.

As can be seen, both the dehalogenation and transfer hydrogenation are simultaneous processes that afford the two reaction intermediates **A** and **B**, although the debromination is faster as seen by the formation of acetophenone (**A**) in a maximum yield of 65% after 2.5h of reaction (the maximum yield for **B** is 17 %). The formation of the 1-phenylethanol, **C**, is

gradual, although a clear acceleration of the reaction is observed after 2.5 h, at the point where the maximum amount of **A** has been produced, suggesting that the transfer hydrogenation is faster for acetophenone than for *p*-bromoacetophenone, in agreement with previously published results.[79]

ii-iii) Suzuki coupling of *p*-bromoacetophenone in the presence of different alcohols. Given the activity shown by catalysts **14L**, **15L** and **17L** in the dehalogenation/transfer hydrogenation of haloacetophenones, we decided to extend the catalytic studies to see if other related transformations could be coupled. Nolan and co-workers recently showed that the catalytic dehalogenation and the Suzuki-Miyaura reaction are intertwined, sharing the oxidative addition step (**Scheme 2.40**) .[61]

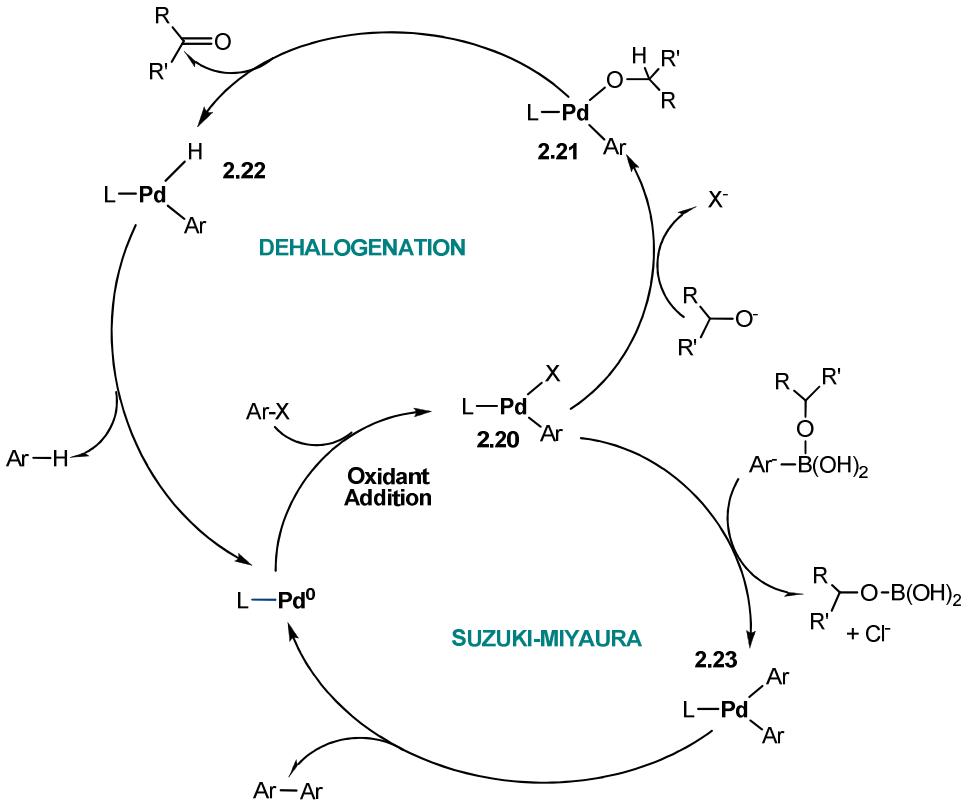

Scheme 2.40

For the general mechanism of the palladium-catalyzed dehalogenation, Pd(0) is the catalytically active species that generates the oxidative adduct complex (**Scheme 2.40**, **2.20**) after reaction with the arylhalide. A metal alkoxide (**2.21**) is generated *in situ* from the reaction with the alcohol under basic conditions. The palladium hydride (**2.22**) is produced

from the β-hydride elimination of the palladium-alkoxide, and the corresponding arene is finally formed by reductive elimination of the aryl group and the hydride.
Also for the palladium-catalyzed Suzuki-Miyaura cross coupling, the Pd^0 is the catalytically active species, which again generates the oxidative addition complex (**2.20**) by reaction with the arylhalide. The transmetallation from the phenyl boronic acid affords the corresponding complex intermediate **2.23**. Finally, a reductive elimination generates the bis-aryl compound and the Pd^0 catalyst.

Many transfer hydrogenation catalysts are active in a variety of 'borrowing-hydrogen' processes. Among all borrowing-hydrogen processes,[80] those implying the formation of C-C bonds such as the α-alkylation of ketones with primary alcohols,[81, 82] constitute valuable examples of environmental friendly processes that facilitate the formation of complex organic structures. We also took into account that both processes (the Suzuki-Miyaura coupling and the α-alkylation of ketones) are usually performed in the presence of alcohols and in basic medium, therefore the *a priori* chances of compatibility are high. Based on these, we decided to combine two C-C coupling reactions typically catalyzed for palladium and iridium. For this catalytic study, we only used compound **15L**, because it showed the best outcomes compared to those studied in the dehalogenation/transfer hydrogenation process described above (**Table 2.30**). This model reaction has a straight-forward application, because the resulting biphenyl substituted ketones are known to behave as non steroidal inhibitors of 5α-reductase, the enzyme that catalyzes the conversion of testosterone to dihydrotestosterone.[83]

Table 2.27 shows the results for the Suzuki coupling of *p*-bromoacetophenone in the presence of secondary and primary alcohols. The reactions were performed using a 2 mol % catalyst loading, at 100 ºC in a sealed tube containing a solution of the substrate in 1:1 mixtures of THF and alcohol. As seen from the results shown, the Suzuki C-C coupling reaction is fast, affording almost quantitative yields on the formation of **D** after 0.5h. The Ir-catalyzed process needs longer reaction times, and it can be directed toward the transfer hydrogenation product **E**, when the secondary alcohol (*i*PrOH) is used, or to the α-alkylated ketone (**F**), for the reactions performed in the presence of primary alcohols (benzyl alcohol, *n*BuOH or *i*BuOH).

For all four reactions studied the process afforded very high yields (80-90%) on either of the reaction products (**Table 2.27**, entries 2, 4, 6 and 8), a result that is even more remarkable if we take into account that the overall yields are due to a combination of inherently distinct catalytic processes. As minor byproducts (less than 8%), small amounts of biphenyl were formed, due to the coupling of phenylboronic acid. Again, mixtures of **3L** and **6L** were tested in order to compare their activity with that shown by **15L**. As seen from the data shown in **Table 2.27** (entries 9 and 10), the mixture of the two homobimetallic compounds display lower activity than that shown by **15L**, proving one more time the better activity of the well-defined heterobimetallic species.

Interestingly, the reaction is carried out in the presence of a weak base (Cs_2CO_3), instead of the strong bases that are often needed for the activation of both C-C coupling processes. It is also important to point out that, apart from the base, no further additives are needed for the activation of the catalyst, thus reducing the presence of undesired contaminating species that can interfere in either of the catalytic steps of the overall process and also reduce the atomic economy of the reaction.

Table 2.27. Suzuki coupling of *p*-bromoacetophenone in the presence of alcohols.[a]

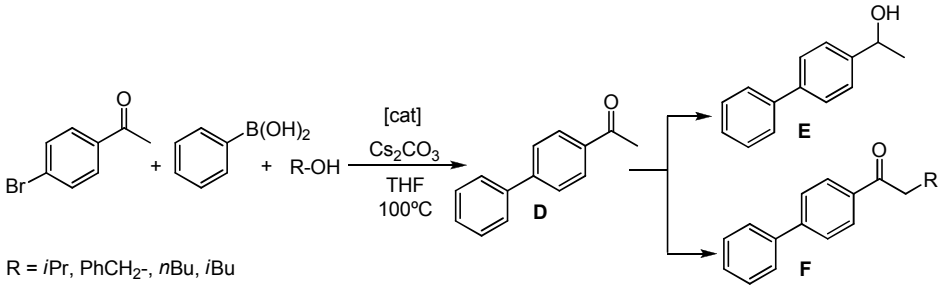

R = *i*Pr, $PhCH_2$-, *n*Bu, *i*Bu

Entry	Catalyst	Time(h)	R-OH	D (%)[b]	E (%)[b]	F (%)[b]
1	**15L**	4	*i*PrOH	58	28	0
2	**15L**	7	*i*PrOH	2	88	0
3	**15L**	0.5	$PhCH_2OH$	93	1	3
4	**15L**	20	$PhCH_2OH$	5	1	80 (72)
5	**15L**	0.5	*n*BuOH	94	0	4
6	**15L**	20	*n*BuOH	4	2	92 (86)
7	**15L**	0.5	*i*BuOH	96	1	1
8	**15L**	20	*i*BuOH	7	3	77 (69)
9[c]	**3L + 6L**	4	*i*PrOH	55	5	0
10[c]	**3L + 6L**	20	*n*BuOH	21	13	29

[a] Reaction Conditions: 4-bromoacetophenone (0.36 mmol), phenylboronic acid (0.55mmol), Cs_2CO_3 (1.08 mmol), anisole as internal reference (0.36 mmol), catalyst (2 mol%), 2 mL of R-OH and 2mL THF. The solution was heated to 100 ºC. [b] Yields determined by GC chromatography (isolated yields in parentheses). Less than 8% (based on Ph-$B(OH)_2$) of Ph-Ph formed. [c] 1 mol % of **3L** + 1 mol % of **6L**.

In conclusion, three different heterometallic complexes of Ir/Pd, in which the metals are connected through a triazolyl-di-ylidene ligand proved to be active catalysts in three different tandem processes, namely the dehalogenation/transfer hydrogenation of haloacetophenones, Suzuki-coupling/transfer hydrogenation of *p*-bromoacetophenone, and Suzuki-coupling/α-alkylation of *p*-bromoacetophenone.

The selection of the tandem reaction is performed by very small changes in the reaction conditions, which are directing the reaction to one of the three possible reaction products. All these tandem reactions are valuable catalytic transformations that have not been

reported before, and constitute a clear advance over the synthetic procedures to the same final products, that would imply the use of two different catalysts and complicated workups requiring the isolation of all reaction intermediates. Connected to this point, the fact that the use of a single well-defined catalyst (either **14L**, **15L** or **17L**) yields a better catalytic outcome than a mixture of two homobimetallic compounds (**3L** + **6L**), results in a clear benefit provided by the heterometallic species, not only because it affords a more atom-efficient process, but because it also suggests that the heterometallic species can improve its catalytic outcome due to catalytic cooperativity or, at least, it avoids any interference between the two active metal fragments (an alternative possible explanation to the poorer outcome shown by the mixture of catalysts).

All three tandem reactions reported constitute efficient methods for the generation of organic molecules by one-pot procedures, combining two different processes typically catalyzed by distinct metal complexes. Heterobimetallic complex **15L**, present high stability in three different catalytic processes. ^{1}H NMR experiments of deuterated solutions containing **15L** did not show any decomposition after 5h, and only after 20h a small amount of unidentified decomposition products (< 15%) could be observed. This experiment discard that the heterometallic species could evolve to a mixture of the two homobimetallic compounds (**3L** and **6L**) under the reaction conditions used in the catalytic assays.

Among the examples reported here, the one-pot preparation of biphenyl-substituted ketones, provides a much easier route to species with potential pharmaceutical applications.[83]

2.5.2 Tandem catalysis reduction of nitroarenes to anilines/coupling with primary alcohols to afford imines

As seen in the latter section, the Ir/Pd complex **15L** proved to be an efficient catalyst for a series of tandem reactions comprising different transformations of haloacetophenones, typically catalyzed by Ir and Pd. In order to extend the large and distinct library of transformations for which Ir and Pd precatalysts are potentially active, we decided to extend its use to other tandem processes, such as the preparation of imines by the reaction of alcohols and nitroarenes.

Imines are intermediates that are often detected in the N-alkylation of amines by alcohols in *borrowing-hydrogen* methodologies,[80, 84-85] although their selective preparation has been rarely studied.[86, 87] Imines are an important class of carbon-nitrogen compounds because they have a diverse reactivity and afford multiple applications in laboratory and industrial synthetic processes.[88] The traditional preparation of imines implies the reaction of ketones or aldehydes with amines, in the presence of lewis acid catalysts. They can also be obtained by the oxidative condensation of amines and by oxidation of amines.[89-91] In the past few years, the oxidative coupling of alcohols and amines in the presence of oxygen to provide imines was reported,[87, 92-93] but the catalytic outcomes were rather low. Very recently, Milstein and co-workers reported an efficient method for the oxidative coupling of amines and alcohols that produced imines in very high yields.[86]

The selective reduction of nitro-arenes is a useful method for the preparation of amines.[94, 95] In the study of this reaction, the development of catalytic methodologies that afford high chemo- and regioselectivity under mild reaction conditions is an intriguing area of research.[96] The reduction nitro compounds to anilines is a mechanistically complex process. A generally accepted mechanistic pathway is described in **Scheme 2.41**, in wich the aniline can be obtained via either the direct reduction or the condensation followed by reduction;[97] the latter route is favoured under the basic conditions.

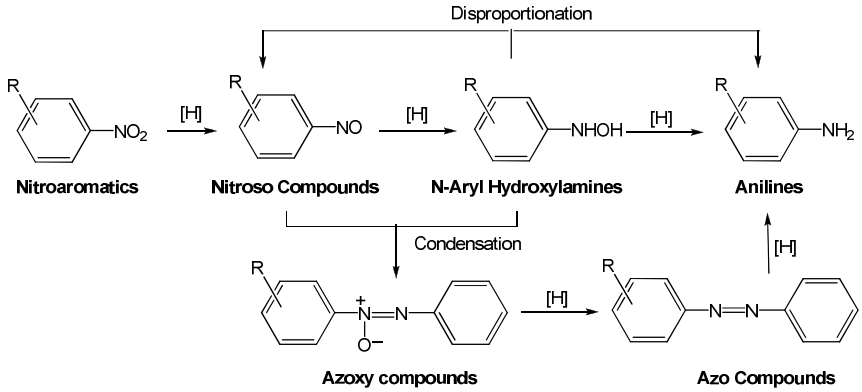

Scheme 2.41. Proposed reaction pathways for the hydrogenation of nitroaromatics.

Because the reduction of nitroarenes with hydrogen is known to be catalysed by some Pd systems,[98] we decided to combine this process with the oxidation of primary alcohols to aldehydes, which is known to be catalysed by certain 'Cp*Ir' complexes described in our group[23d, 77a] following the pioneering works performed by Fujita and co-workers.[49]

The oxidation of the alcohol generates hydrogen, which can be further used by the palladium fragment of the heterometallic species to reduce the nitroarene to aniline. Then the final step of the process would be the non metal-mediated condensation beween the aniline and the aldehyde to afford the final imine as shown in **Scheme 2.42**.

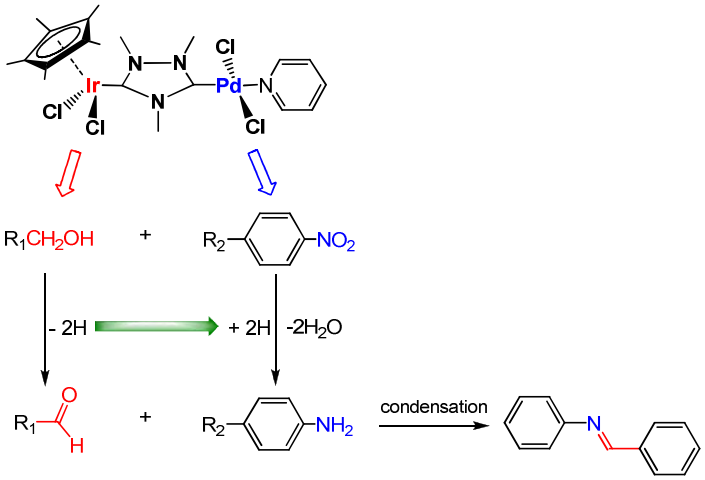

Scheme2.42

Scheme 2.43 shows the catalysts used, including $PdCl_2$ and $[Cp^*IrCl_2]_2$ for comparative purposes.

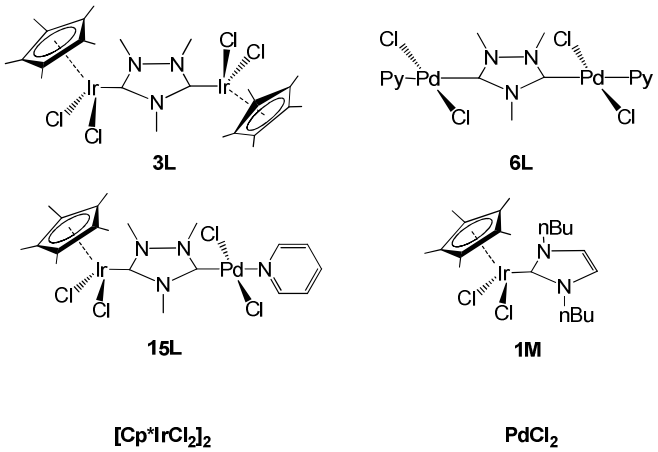

Scheme 2.43. Catalysts employed

In order to determine the ability of a series of homogeneous catalysts toward the reduction of nitroarenes, we first studied the reduction of nitrobenzene with molecular hydrogen. This experiment would tell us whether the Ir or the palladium or both metal fragments are able to catalyse the reduction of the nitroarene in the presence of molecular hydrogen. The catalytic experiments were monitored by Gas-Cromatography, registering yields at fixed times and using anisole as internal standard. Catalytic studies were carried out under aerobic conditions, employing 2 mol % of catalyst and Cs_2CO_3 as base.

All the reactions were carried out at 100ºC, with 1 atm of H_2. As can be seen from the data shown in **Table 2.28**, all the palladium-containing complexes used showed an excellent outcome in this reaction. On the contrary, the iridium complexes **[Cp*IrCl$_2$]$_2$** and **3L**, afforded negligible amounts of aniline, which actually confirms that the reduction of the nitroarene in the presence of hydrogen is exclusevily facilitated by the palladium fragment.

Table 2.28. Reduction of nitrobenzene to aniline.[a]

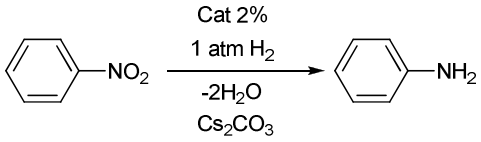

Catalyst	t(h)	Aniline (%)[b]
[Cp*IrCl$_2$]$_2$	20	10
PdCl$_2$	10	93
3L	20	5
6L	10	97
15L	10	90

[a] Reaction Conditions: Nitrobenzene (0.3 mmol), Cs_2CO_3 (0.3 mmol), anisole as internal reference (0.3 mmol), catalyst (2 mol%) in 500 μL of toluene. Hydrogen was added with a balloon filled with one atmosphere of gas. Three cycles of vacuum/H_2 were made before putting the reaction vessel in an oil bath at 100 ºC. [b] Yields determined by GC chromatography.

Having proved the ability of our Pd complexes to facilitate the reduction of the nitroarene to aniline, we decided to study the overall tandem process, implying i) reduction of a nitroarene to an amine, ii) oxidation of an alcohol to an aldehyde and iii) condensation of the aldehyde and the amine to form the corresponding imine.

Table 2.29 shows the results of the reaction between nitrobenzene and benzylalcohol used as reagent and solvent at 110 ºC in the presence of Cs_2CO_3.

Table 2.29. Catalyst screening for the reaction of nitrobenzene and benzylalcohol.[a]

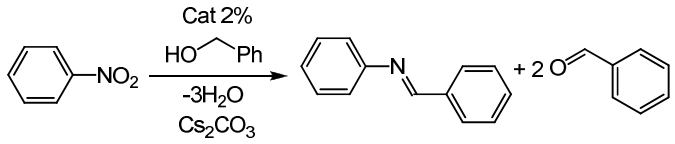

Entry	Catalyst	Cat. (mol%)[c]	t(h)	N-Benzylidene-aniline (%)[b]
1	**$[Cp^*IrCl_2]_2$**	2	3	81
2	**$[Cp^*IrCl_2]_2$**	0.5	20	60
3	**$PdCl_2$**	2	18	12
4	**$[Cp^*IrCl_2]_2$ + $PdCl_2$**	2	3	72
5	**15L**	2	3	87
6	**15L**	0.5	20	76
7	**6L**	2	3	16
8	**6L**	0.5	20	7
9	**3L**	2	3	85
10	**3L**	0.5	20	35
11	**3L + 6L**	0.5	20	73
12	**1M**	0.5	20	52

[a] Reaction Conditions: Nitrobenzene (0.3 mmol), benzylalcohol (5 mmol) used as solvent and reagent, Cs_2CO_3 (0.3 mmol), anisole as internal reference (0.3 mmol). The solution was heated at 110 ºC under aerobic conditions. [b]Yields determined by GC chromatography. [c] Based on metal amount.

As can be seen from the results shown in **Table 2.29**, all iridium-containing complexes provided good yields to the imine (see entries 1, 2, 5 and 9), while the catalysts that only contain palladium afforded negligible activities (see entries 3 and 7). This result is not surprising since the palladium catalysts are not expected to oxidize the alcohol to aldehyde and release the required amount of hydrogen to reduce the nitrobenzene to aniline. On the other hand, those catalysts containing only iridium provide high yields of N-benzylideneaniline (entries 1, 2 and 9).

This result is remarkable, because it suggests that, for these catalysts, the reduction of the nitrobenzene may be due to rare example of a transfer-hydrogenation mechanism, rather than the direct reduction with released molecular hydrogen from the alcohol. The fact that the 'Cp*Ir' fragment may reduce the nitro group by means of a hydrogen transfer process in the presence of *i*PrOH, was previously pointed out by Fujita and co-workers, although the yields to aniline were very low.[49, 98]

In a similar experiment, we performed the reduction of nitrobenzene to aniline with *i*PrOH using catalyst **15L** (2 mol%). After 20 h, we obtained a quantitative yield of aniline. The Ir-Pd heterobimetallic complex **15L** provides the best catalytic outcomes in this reaction (entries 5 and 6), although a mixture of the homobimetallic complexes **3L** and **6L** (entry 11),

also affords good yields. As a consequence of the stoichiometry of the process, in all the reactions under study, benzaldehyde was always detected in an amount over two equivalents with respect to the imine.

In order to test the general applicability of the process, we decided to study the catalysts previously described in the condensation of different nitroarenes with a series of primary alcohols. The results are shown in **Table 2.30**. The reactions were carried out using the primary alcohol as reagent and solvent at 110ºC, with a catalyst loading of 2 mol % in the presence of Cs_2CO_3.

The catalytic activity of **$[Cp^*IrCl_2]_2$** was very low after 3 hours (entries 1 and 3) compared to the other catalytic systems tried in this series of reactions. Longer reaction times afforded better yields to the final imines, although these were still moderate (60 % yield after 30 h, see entries 2 and 4). As expected, the general activity of the only-iridium based system is less prone to induce nitro reduction. The mixture of compounds **3L** and **6L** afforded a very good outcome for the coupling of *p*-nitrotoluene with benzylalcohol (entry 5), but provided only a moderate yield when *p*-nitroanisole was used (entry 6). Catalyst **15L** showed a wider applicability, providing very good yields in the reactions of several nitroarenes and benzylalcohols. Some aliphatic primary alcohols were also used (1-hexanol, 1-butanol), but we did not observe the formation of the imines. On the contrary, 2-phenylethanol provided an excellent outcome in the condensation with nitrobenzene (entry 10).

Table 2.30. Catalytic condensation of nitroarenes and primary alcohols.[a]

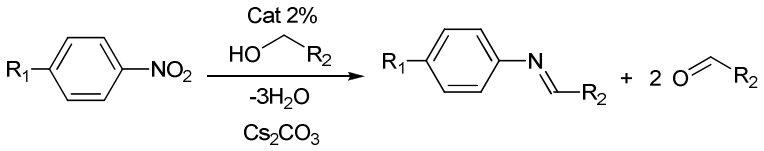

Catalyst	Entry	R_1	R_2	t(h)	Product	Yield (%)[b]
$[Cp^*IrCl_2]_2$	1	4-Me	C_6H_5	3	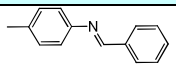	16
	2	4-Me	C_6H_5	30	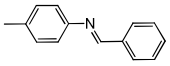	60
	3	4-MeO	C_6H_5	3	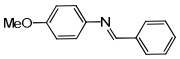	32
	4	4-MeO	C_6H_5	30	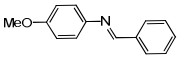	63
3L + 6L	5	4-Me	C_6H_5	3	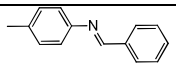	83
	6	4-MeO	C_6H_5	3	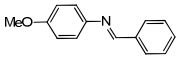	55
15L	7	H	4-Me-C_6H_5	5	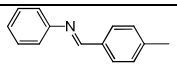	90
	8	H	4-MeO-C_6H_5	20	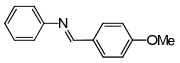	50 (43)
	9	H	$C_6H_5CH{=}CHCH_2$	20	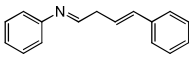	17
	10	H	$C_6H_5CH_2$	12	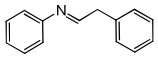	92
	9	4-Me	C_6H_5	3	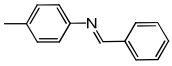	82
	10	4-Me	4-Me-C_6H_5	12	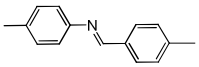	89
	11	4-Me	4-MeO-C_6H_5	12	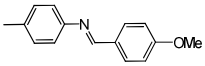	83
	12	4-MeO	C_6H_5	3	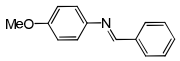	75
	13	4-MeO	4-Me-C_6H_5	12	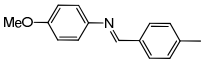	84
	14	4-MeO	4-MeO-C_6H_5	12	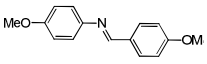	70 (65)

[a]Reaction Conditions: Nitroarene (0.3 mmol), benzylalcohol (5 mmol) used as solvent and reagent, Cs_2CO_3 (0.3 mmol), anisole as internal reference (0.3 mmol), catalyst (2 mol%). The solution was heated at 110 ºC under aerobic conditions. [b] Yields determined by GC chromatography (Isolated yields in parenthesis).

The different catalytic performances of **15L** and **3L** can be illustrated by the oxidative condensation of *p*-bromonitrobenzene and benzylalcohol. The results are shown in **Table**

2.31. Interestingly, each catalyst leads to the formation of a different product. While **3L** affords the expected N-benzylidene-*p*-bromoaniline (**A**), catalyst **15L** provides the dehalogenated imine (**B**). Pd-catalyzed dehalogenations of aryl-halides can take place in *i*PrOH in the presence of a base, such as Cs_2CO_3, and we have also previously observed that this process can be promoted by catalyst **15L** (see *section 2.5.1* at page 77).[74]

Because the catalytic dehalogenation and the Suzuki-Miyaura reaction are intertwined (as we have previously shown in *section 2.5.1*, pag. 81) sharing the oxidative addition step, we decided to combine this reaction with the oxidative condensation of *p*-bromonitrobenzene and benzylalcohol, by adding phenylboronic acid to the reaction mixture. This new reaction provided a very good yield of the corresponding bisarylated imine **C** (**Table 2.31**, entry 3), in a reaction where the two individual actions of the iridium- and palladium fragments imply clearly distinct fundamental catalytic processes.

Table 2.31. Oxidative condensation of *p*-bromonitrobenzene and benzylalcohol.[a]

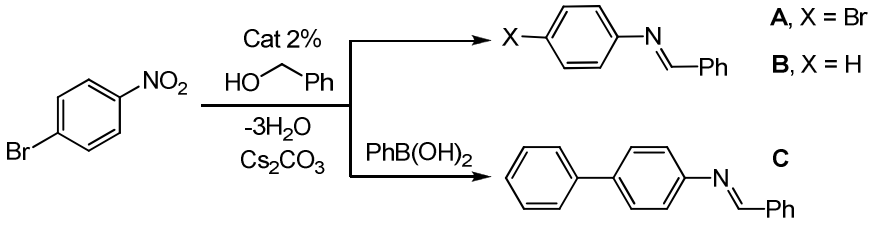

Entry	Catalyst	Additive	t(h)	Product	Yield (%)[b]
1	**3L**	None	3	A	78
2	**15L**	None	20	B	71
3	**15L**	$PhB(OH)_2$	40	C	77[c]

[a] Reaction Conditions: Nitrobenzene (0.3 mmol), benzylalcohol (10 mmol) used as solvent and reagent, Cs_2CO_3 (0.3 mmol) and catalyst (2 mol %). T = 110 ºC. [b] Yields determined by GC chromatography using anisole as internal standard (Isolated yields in parenthesis). [c] Nitrobenzene (0.3 mmol), benzylalcohol (10 mmol), phenylboronic acid (0.3 mmol) Cs_2CO_3 (0.6 mmol) and THF (1mL).

Based on these results, we believe that the overall tandem reaction may occur through two different mechanistic pathways (**Scheme 2.45** and **Scheme 2.46**), depending on whether iridium/palladium or 'only-iridium' catalysts are used. As expected, for the Ir/Pd catalyst **15L**, we would have the combined action of the Ir and Pd fragments, both acting separatedly in the two mechanistically distinct catalytic reactions.

In a first step, the oxidation of the alcohol to aldehyde would be promoted by the iridium fragment with the release of hydrogen, either in the form of molecular hydrogen or a Ir-bis-hydride. In the second step, the hydrogen is transferred to the palladium fragment, which facilitates the reduction of the nitroarene to aniline (**Scheme 2.45**).

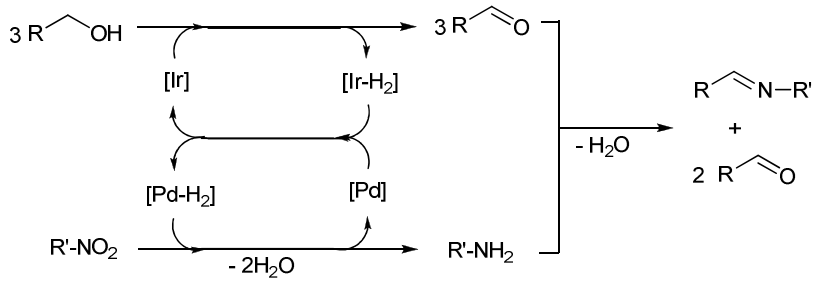

Scheme 2.45

For the 'only-iridium' catalysts, the reduction of the nitro group to the amino group only proceeds in good yield for nitrobenzene through a general *borrowing-hydrogen* mechanism (**Scheme 2.46**).

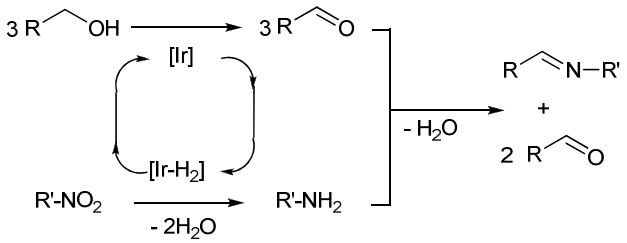

Scheme 2.46

Based on our experience,[23d] the initial stage of the reaction would be the oxidation of the benzyl alcohol to benzaldehyde and the generation of a metal-hydride. The metal-hydride will reduce the nitrobenzene to aniline. The benzaldehyde condensates with the aniline to produce the final imine.

In order to obtain any experimental evidences that the reduction of the nitroarene by **15L** is facilitated by molecular hydrogen or by an in situ formed Ir-bis-hydride, we decided to carry out some experiements (**Scheme 2.47**). First we carried ut the oxidant-free oxidation of benzylalcohol using catalyst **3L**, in a flask that was connected through a rubber tube to another flask in wich 1,2-cyclooctene and a catalytic amount of **6L** in toluene were placed (**Scheme 2.47**).

Our idea was to canalize the hydrogen produced in the oxidation of benzylalcohol to the reaction vessel where the reduction of 1,2-cyclooctene was to be produced. The catalytic experiments were monitored by Gas-Cromatography, exctracting aliquots, from the flask containing the olefin, at fixed times. This experiment was carried out under anaerobic conditions, employing 5 mol % of Ir^{III} and 2 mol % of Pd^{II} catalysts, respectively, and Cs_2CO_3 (0.3 mmol) as base. Both reactions were carried out at 110ºC.

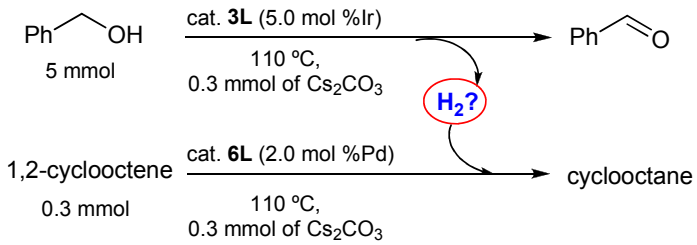

Scheme 2.47

After 24 hours we did not detect any amount of the desired hydrogenated alkane. We also performed the same reaction several times, changing reaction conditions, Cp*Ir catalysts and also using other alcohols in order to improve the catalytic oxidation with the concomitant evolution of hydrogen, but we did not obtain any significant results.

Although these experiments did not allow us to detect molecular hydrogen, we have found in the litereature that Fujita and co-workers were able to detect it under certain conditions, although its concentration in solution was found to be low.[99] Under these circumstances, we decided to leave this point unconclusive.

In conclusion, we have extended the general *borrowing-hydrogen* procedure in the N-alkylation of amines using alcohols. The amine has been generated *in situ* by reduction from a nitroarene. We have evaluated the activity of a series of catalysts in the oxidative coupling of nitroarenes with benzylalcohols to afford the corresponding imines. For this reaction, four homo- and hetero-bimetallic catalysts of Ir and Pd have been tested. The results provided by the bis-iridium complexes are remarkable, although limited to several substrates. However, the presence of the palladium fragment in the Ir/Pd complex **15L** improves the catalyst activity widening its applicability, most probably because the presence of the Pd opens a new reaction pathway in the reduction of the nitro group by using the hydrogen released in the oxidation of the alcohol by the iridium moiety. Catalyst **15L** has been used for the preparation of different products using the same substrates and changing the additives. In a new illustration of the wide applicability of the Ir/Pd heterobimetallic catalyst, we have also combined the oxidative coupling of *p*-bromonitrobenzene with benzylalcohol, with the Suzuki-Miyaura C-C coupling, by adding phenylboronic acid in the reaction medium. This reaction provides the corresponding bisarylated imine in high yield. This catalytic study provides a new example of tandem catalysis using dimetallic complexes bearing the *ditz* ligand. The use of only one catalyst with two different metal fragments is an interesting option for the design of catalytic sequential reactions with fundamentally distinct mechanisms. For these types of processes, a mixture of two catalysts can also be used, but the utilization of a heterobimetallic catalyst provides a series of advantages. We recently suggested that the linkage through the *ditz* ligand may provide some catalytic cooperativity between the two metals, but other advantages have to be taken into account, as the lower atomic efficiency achieved when two catalysts are used instead of one, and the obvious reduction of waste in the preparation of only one catalyst.

2.6 Tandem catalysis with the Ir/Pt complex 16L

Platinum is a metal that can afford the preparation of a wide variety of catalysts for many organic transformations. In its combination with iridium, platinum can allow the design of very interesting tandem processes, so the study of the catalytic activity of the Ir-Pt heterobimetallic complex **16L** may bring very important findings.

We previously described the catalytic reults carried out with the Ir compound **12L** for the preparation of functionalized indoles (see *section 2.4.2*, pag. 63).[22] Taking these results into account, we decided to study a tandem process for the Ir/Pt complex **16L**, implying three consecutive catalytic reactions, namely the oxidative cyclization of aminoalcohols to form indole (iridium-catalyzed), the intramolecular hydroalcoxylation of an alkynyl alcohol to afford a cyclic enol ether (platinum-catalyzed) and the addition of the C-H bond of indole to the unsaturated moiety of the cyclic enol ether (platinum-catalyzed), as shown in **Scheme 2.48**. The latter platinum catalysed reactions were rencently reported by Cheng and co-workers using $PtCl_2$ as catalyst.[100]

The overall process has a tremendous added value, because indole has become a privileged structure in many research areas due to their applications in pharmaceuticals, fragrances, agrochemicals, pigments and material science.[101] During the last few years many efforts are currently devoted to the catalytic construction and functionalization of indole rings.[102] Due to its broad spectrum of applications, indole has been lately being addressed as *the lord of the rings*.[102a]

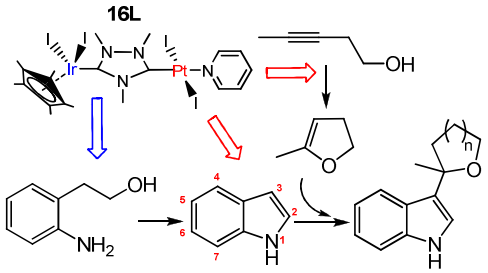

Scheme 2.48. General tandem reaction catalyzed by complex **16L**.

Obviously, as we have done in all the design of our tandem processes, in the choice of these reactions, we had to consider the catalyst compatibility with the residual materials from the catalytic steps comprising the overall process. In principle, the reactions that we chose seemed to fulfill the requirements for compatibility in terms of solvent, temperature and additives.

In the first place, we studied the multistep reaction of indoles with 4-pentyn-1-ol, which yields an indole derivative with five member cyclic ether at C3 (**Scheme 2.49**).

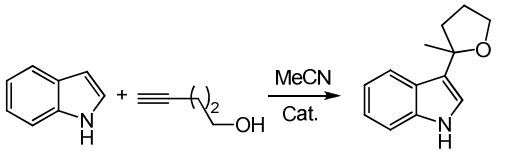

Scheme 2.49. Reaction of indole and 4-pentyn-1-ol

The catalytic experiments were monitored by Gas-Cromatography, registering yields at fixed times and using anisole as internal standard. The catalytic studies were carried out under aerobic conditions, employing 1 mol % of paladium catalyst and 3% of $AgSO_3CF_3$ as additive. **Scheme 2.51** shows the catalysts used.

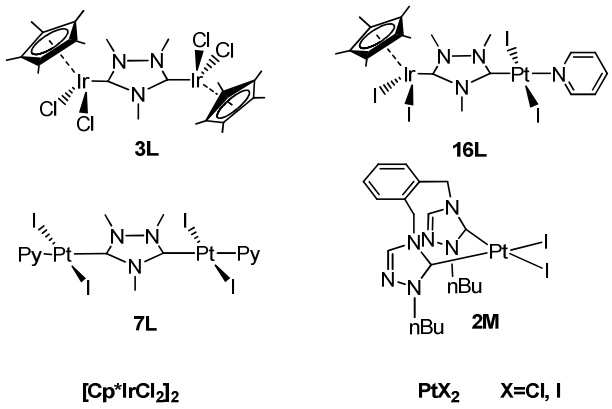

Scheme 2.51. Catalysts employed.

Table 2.32 shows some representative data that we obtained for the reaction under study. In order to obtain a representative catalyst screening, for this first set of experiments we used the platinum complexes depicted in **Scheme 2.51** (the iridium complex **3L** will be used later on).

The preparation and characterization of the bis-triazolyl-di-ylidene complex of Pt, **2M**, are detailed in Chapter 4 (page 164).

Table 2.32. Catalyst screening for the reaction of indole and pent-4-yn-1-ol[a]

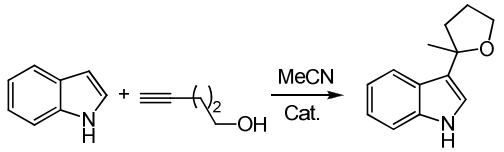

Entry	Catalyst[b]	[Cat] (mol %)	T (ºC)	Time (h)	Yield (%)[c]
1[d,e]	**$PtCl_2$**	5	25	12	36
2[e]	**7L**	5	25	12	73
3[e]	**2M**	5	25	12	62
4	**$PtCl_2$**	5	80	0.5	84
5[d]	**$PtCl_2$**	5	25	2	22
6[d]	**$PtCl_2$**	1	80	1	77
7[d]	**$PtCl_2$**	1	25	27	46
8[d]	**PtI_2**	5	80	0.5	66
9[d]	**PtI_2**	1	80	1	80
10[d]	**PtI_2**	1	25	27	36
11	**7L**	5	80	0.5	> 95
12	**7L**	1	25	27	58
13	**7L**	5	25	2	71
14	**16L**	5	80	0.5	> 95
15	**16L**	1	25	27	58
16	**16L**	5	25	2	18
17	**2M**	5	80	0.5	> 95
18	**2M**	1	25	27	75
19	**2M**	5	25	2	46

[a]Reaction Conditions: 0.3 mmol indole, 0.36 mmol 4-pentyn-1-ol, anisole as internal reference (0.3 mmol), AgO_3SCF_3 (3 mol%) in 1.5 ml of CH_3CN. [b] Based on amount of metal. [c] Yields determined by GC chromatography. [d] Without addition of AgO_3SCF_3. [e] Reactions carried out in toluene.

As can be seen in the data shown in **Table 2.32**, all NHC-based platinum catalysts **7L**, **16L** and **2M**, afford better catalytic performances than $PtCl_2$ and PtI_2, although they need the addition of $AgSO_3CF_3$ in order to facilitate the process.

Catalysts **7L**, **16L** and **2M** afford quantitative yields to the final product in only 30 minutes, when the reaction is carried out at 80 ºC with a 5 mol % of catalyst loading (entries 11, 14 and 17). The same catalysts afforded moderate to high yields (58-75 %) when the reaction was performed at room temperature with a catalyst loading of 1 mol %, although longer reaction times were needed (27 h). These catalytic results prompted us to widen the number of substrates used in this catalytic reaction. **Table 2.33** shows the most representative data that we obtained for the reaction of a series of substituted indoles and substituted alkynyl alcohols. In general, catalyst **7L** provided the best catalytic outcomes, affording almost quantitative yields for all the reactions carried out with N-methylindole (entries 1, 5 and 9). The heterobimetallic complex **16L**, also afforded excellent outcomes in all the reactions under

study, providing better yields than catalyst **7L**. We also proved that the activity of complex **16L** is also high when toluene is used as solvent, with catalytic outcomes very close to those shown for the reactions carried out in acetonitrile (see entries 14 and 16). This result is interesting because we have observed that toluene is a good solvent for the iridium-catalyzed oxidative cyclization of amino alcohols to form indole (see section *2.4.2* on page 61),[22] so the combination of the Pt- and Ir-catalyzed process seems to be warranted, at least in terms of solvent compatibility.

Table 2.33. Catalytic addition reaction between indoles and alkynyl alcohols.[a]

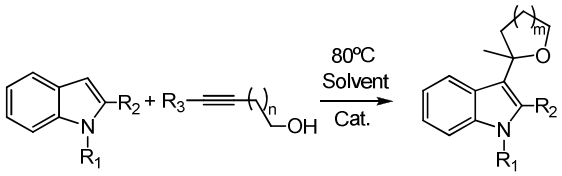

Entry	R^1	R^2	R^3	n	m	[Cat.][b]	Time (h)	Yield (%)[c]
1	Me	H	H	2	1	**7L**	3	> 99
2	Me	H	H	2	1	**2M**	6	67
3	H	H	Me	1	1	**7L**	6	80
4	H	H	Me	1	1	**2M**	6	81
5	Me	H	Me	1	1	**7L**	3	> 99
6	Me	H	Me	1	1	**2M**	3	> 99
7	H	H	H	3	2	**7L**	8	67
8	H	H	H	3	2	**2M**	8	28
9	Me	H	H	3	2	**7L**	12	93(86)[d]
10	Me	H	H	3	2	**2M**	12	52
11	H	Me	Me	1	1	**7L**	15	60
12	H	Me	Me	1	1	**2M**	15	60
13	Me	H	H	2	1	**16L**	5	84
14[e]	H	H	Me	1	1	**16L**	10	81
15	Me	H	Me	1	1	**16L**	10	77(72)[d]
16[e]	H	H	H	3	2	**16L**	10	71
17	Me	H	H	3	2	**16L**	10	74(73)[d]
18	H	Me	Me	1	1	**16L**	12	50(46)[d]

[a]Reaction Conditions: 0.3 mmol indole, 0.36 mmol, alkynyl alcohol, silver triflate (3%), and catalysts (1 mol %) in 1.5 mL of solvent. Anisole was used as internal standard (0.3 mmol). The solution was heated at 80 ºC under aerobic conditions. [b] Based on amount of metal. [c] Yields determined by GC chromatography. [d] Isolated Yields in parenthesis. [e] Reactions carried out in toluene.

Having proved the activity of our Pt catalysts in the catalytic additions between indoles and alkynyl alcohols, we thought that the combination of this multistep process with the oxidative cyclization of aminoalcohols to form indoles, may constitute a valuable illustration of the ability of our Ir/Pt complex **16L** to incorporate a further step into the already complex catalytic reaction. Despite the great interest shown by indole derivatives and the efforts that are currently being made for the search of catalytic processes in the construction and

functionalization of indole rings, we found very few examples in which functionalized indoles are obtained from multistep reactions implying aminoalcohols.[24, 52] The reactions were carried out in a single pot following a sequential procedure. First we allowed 2-aminophenylethylalcohol to form the molecule of indole, and then we added the corresponding alkynyl alcohol, to provide the corresponding functionalized molecule. The reactions were carried out in toluene at 110ºC, leaving 12h for the first process (cyclization of the aminoalcohol) and a variable time for the second (functionalization of indole). **Table 2.34** summarizes the most representative results that we obtained for this tandem process.

Table 2.34. Tandem cyclization of 2-aminophenyl ethyl alcohol and addition of an alkynyl alcohol.[a]

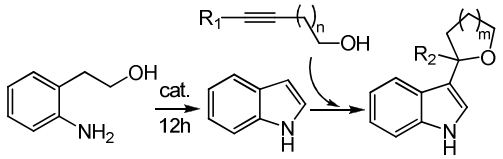

Entry	Catalyst (cat. load)[b]	R^1	R^2	n	m	Indole[c,d]	Time (h)[e]	Yield (%)[c]
1	**7L** (2)	Me	Me	1	1	0	15	0
2	**16L** (2)	Me	Me	1	1	77	15	74
3	**3L** (2)	Me	Me	1	1	67	15	56
4	**3L** + **7L** (2)	Me	Me	1	1	51	15	44
5	**3L** + **7L** (2)	H	Me	2	1	ND	15	16
6	**3L** + **7L** (5)	H	Me	2	1	ND	12	35
7	**$[Cp^*IrCl_2]_2$** (2)	Me	Me	1	1	38	15	29
8	**$[Cp^*IrCl_2]_2$** (5)	Me	Me	1	1	ND	12	32
9	**16L** (2)	H	Me	2	1	ND	15	60
10	**16L** (5)	H	Me	2	1	ND	15	81(77)
11[f]	**16L** (2)	H	Me	3	2	ND	15	15
12[f]	**16L** (5)	H	Me	3	2	ND	12	24
13[f]	**16L** (2)	Pr	Pr	1	1	ND	24	80(74)

[a] Reaction Conditions: 0.33 mmol 2-aminophenethyl alcohol, silver triflate (0.03 mmol), anisole as internal reference (0.25 mmol) in 800 μL of toluene at 110ºC. After 12h addition of 0.38 mmol of alkynyl alcohol. [b] Based on amount of metal. [c] Yields determined by GC chromatography. [d] Yield of indole-intermediate determined before addition of the alkynyl alcohol . ND = Not Determined [e] Total time, referred to the two steps (first step is always 12h). [f] Reaction temperature 80 ºC.

As can be seen from the data shown in **Table 2.34**, catalyst **16L** provided good yields to the final functionalized indoles when different alkynyl alcohols were used (yields in the range 60-81 %). These data are remarkable, especially if we take into account the complexity of the overall process. As expected, complex **7L** did not afford the formation of the final products, due to its incapability to facilitate the oxidative cyclization of the amino alcohol. A mixture of the two homobimetallic complexes of Pt (**7L**) and Ir (**3L**), afforded a much lower yield than

that provided by the heterobimetallic complex **16L** (compare entries 4-6 with entries 2, 9 and 10). This result is redundant with the catalytic outcomes shown by other ditz-based heterobimetallic complexes reported by us, compared to the mixtures of their homobimetallic counter parts,[22, 104, 105] and supports the idea that some catalytic cooperativity between the two vicinal metals may be at play. The results shown for the iridium complexes **3L** and $[Cp^*IrCl_2]_2$, which afford low (ca. 30 %, for $[Cp^*IrCl_2]_2$) to moderate (56 %, for complex **3L**, entry 3) yields to the final products, are remarkable (entries 3 and 7 and 8) since, contrary to what we expected, they demonstrate that these complexes also show activity in the final step of the reaction.

We also emphasize that the activity of complex **16L** is entirely unaffected by the addition of metallic Hg,[106] rending support to an homogeneous mechanism. Selective poisoning experiments require the addition of a poisonous component, specific either for homogeneous or heterogeneous catalysts. The early use of this concept was developed with mercury poisoning of noble metal heterogeneous catalysts by *amalgamating* their solid surface.[107] This experiment was performed by adding Hg^0 to the reaction mixture. The inhibition of catalysis is attributed then to a heterogeneous process, while conversely if no suppression of activity is noted a homogeneous process should be involved. For this purpose, we prepared a catalytic experiment putting two capped vessels in parallel and using for both the same reaction conditions. The reaction studied was the oxidative cyclization of the 2-aminophenylethylalcohol to form the molecule of indole, and the cyclization/alkylation with the corresponding alkynyl alcohol, to provide the corresponding functionalized molecule. In only one of the two vessels prepared, few drops of Hg^0 were added. The catalytic tests were monitored by Gas-Cromatography, registering yields at fixed times and using anisole as internal standard. After the time required for complete conversion to the functionalized indole, both reactions achieve the same yield so suggesting that the activity of complex **16L** is entirely unaffected by adding metallic Hg.[106]

In conclusion, the easy access to the Ir-Pt heterobimetallic complex (**16L**) allowed us to study a novel tandem process implying the combination of three mechanistically distinct processes typically catalyzed by Ir and Pt. We have first proved that all our Pt-based complexes show high activity in the cyclization-addition reactions of alkynyl alcohols and indoles. The presence of the Ir-fragment in complex **16L** allows the addition of a further step to this reaction, which can be started from 2-aminophenylethylalcohol that is transformed to indole by an Ir-mediated oxidative cyclization process, and then react with the corresponding alkynyl alcohol in a Pt-mediated reaction. Addition of silver triflate represents a good additive for the activation of the catalyst in both processes. No use of additional base is needed in this tandem sequence. Finally, the use of **16L** provides better catalytic outcomes than the use of mixtures of the corresponding homobimetallic catalysts (**3L** and **7L**), suggesting that some catalytic cooperativity may be at play between the two vicinal metals.

References

(1) A. L. Leninger, *Principles of Biochemistry*, **1984** Worth Publishers, New York.

(2) A. J. Kirby, *Angew. Chim. Int. Ed. Engl*., **1996**, *35*, 707; P. A. Vigato, S. Tamburini, D. E. Fenton, *Coord. Chem. Rev.*, **1990**, *106*, 25; W. H. Chapman, R. Breslow, *J. Am. Chem. Soc.*, **1995**, *117*, 5462.

(3) M. J. Young, J. Chin, *J. Am. Chem. Soc*., **1995**, *117*, 10577; D. E. Wilcox, *Chem. Rev*., **1996**, 96, 2435.

(4) M. Shibasaki, H. Sasai, *Pure Appl. Chem.*, **1996**, *68*, 523; M. Shibasaki, T. Arai, H. Sasai, *Angew. Chem. Int. Ed. Engl*., **1997**, *36*, 1237.

(5) H. Steiinhagen, G. Helmchen, *Angew. Int. Ed. Engl.*, **1996**, *35*, 2339.

(6) K. Takasu, Y. Takemoto, N. Shindoh, *Chem. Eur. J.*, **2009**, 15, 12168.

(7) J. Zhu, H. Bienaymé, *Multicomponent Reactions*, **2005**, Wiley-VCH, Weinhem.

(8) L. F. Tietze, *Chem. Rev.*, **1996**, *96*, 115.

(9) C. Zhou, D. E. Emrich, R. C. Larock, *Org. Lett.*, **2003**, *5*, 1579.

(10) J.-C. Wasilke, S. J. Obrey, R. T. Baler, G. C. Bazan, *Chem. Rev*., **2005**, *105*, 1001.

(11) D. E. Fogg, E. N. dos Santos, *Coord. Chem. Rev.*, **2004**, *248*, 2365.

(12) N. Jeong, S. Seo, J. Y. Shin, *J. Am. Chem. Soc.*, **2000**, *122*, 10220.

(13) J. Louie, C. W. Bielawski, R. H. Grubbs, *J. Am. Chem. Soc.*, **2001**, *123*, 11312.

(14) W. A. Herrmann, C. Kocher, *Angew. Chem*. **1997**, *109*, 2256; *Angew. Chem. Int. Ed. Engl*., **1997**, *36*, 2162; W. A. Herrmann, *Angew. Chem.*, **2002**, *114*, 1342; *Angew. Chem. Int. Ed*., **2002**, *41*, 1290; C. M. Crudden, D. P. Allen, *Coord. Chem. Rev*., **2004**, *248*, 2247; E. Peris, R. H. Crabtree, *Coord. Chem. Rev*., **2004**, 248, 2239; J.A. Mata, M. Poyatos, E. Peris, *Coord. Chem. Rev.*, **2007**, 251, 841.

(15) S. Gründemann, A. Kovacevic, M. Albrecht, J.W. Faller, R. H. Crabtree, *Chem. Commun.*, **2001**, *2274*; S. Gründemann, A. Kovacevic, M. Albrecht, J. W. Faller, R. H. Crabtree, *J. Am. Chem. Soc*., **2002**, *124*, 10 473; A. Kovacevic, S. Gründemann, J. R. Miecznikowski, E. Clot, O. Eisenstein, R. H. Crabtree, *Chem. Commun.*, **2002**, 2580; L. N. Appelhans, D. Zuccaccia, A. Kovacevic, A. R. Chianese, J. R. Miecznikowski, A. Macchioni, E. Clot, O. Eisenstein, R. H. Crabtree, *J. Am. Chem. Soc*., **2005**, 127, 16299.

(16) A. J. Boydston, C. W. Bielawski, *Dalton Trans*., **2006**, 4073; D. M. Khramov, A. J. Boydston, C.W. Bielawski, *Angew. Chem*., **2006**, *118*, 6332; *Angew. Chem. Int. Ed*., **2006**, *45*, 6186; A. J. Boydston, K. A. Williams, C.W. Bielawski, *J. Am. Chem. Soc*., **2005**, *127*, 12496.

(17) T. J. Curphey, K. S. Prasad, *J. Org. Chem.*, **1972**, *37* (14), 2259.

(18) O. Guerret, S. Sole, H. Gornitzka, G. Trinquier, G. Bertrand, *J. Organomet. Chem.*, **2000**, *600*, 112.

(19) O. Guerret, S. Sole, H. Gornitzka, M. Teichert, G. Trinquier, G. Bertrand, *J. Am. Chem. Soc.*, **1997**, *119*, 6668.

(20) E. Mas-Marzá, J. Mata, E. Peris, *Angew. Chem. Int. Ed.*, **2007**, *46*, 3729.

(21) M. Viciano, M. Sanaú, E. Peris, Organometallics, 2007, 26, 6050.

(22) A. Zanardi, R. Corberan, J. Mata, E. Peris, Organometallics, **2008**, *27*, 3570.

(23) (a) R. Corberan, M. Sanaú, E. Peris, *J. Am. Chem. Soc.*, **2006**, *128*, 3974; R. Corberan, M. Sanaú, E. Peris, *Organometallics*, **2006**, *25*, 4002; (b) R. Corberan, M. Sanaú, E Peris, *Organometallics*, **2007**, *26*, 3492; (c) V. Lillo, R. Corberan, J. Mata, E. Fernandez, E. Peris, *Organometallics*, **2007**, *26*, 4350; (d) A. Prades, R. Corberan, M. Poyatos, E. Peris, *Chem. Eur. J*, **2008**, *14*, 11474.

(24) S. Kawaguchi, *Coord. Chem. Rev*., **1986**, *70*, 51.

(25) N. Yanase, Y. Nakamura, S. Kawaguchi, *Inorg. Chem.* **1978**, *17*, 2874; S. Okeya, N. Yanase, Y. Nakamura, S. Kawaguchi, *Chem. Lett.*, **1978**, 699.

(26) B. Sahu, K. Misra, B. K Mohapatra, *Indian J. Chem. Sect A-Inorg. Phys. Theor. Anal. Chem.*, **1982**, *21*, 823.

(27) J. W. Ruan, O. Saidi, J. A. Iggo, J. L. Xiao, *J. Am. Chem. Soc.*, **2008**, *130*, 10510.

(28) S. Ko, B. Kang, S. Chang, *Angew. Int. Ed.*, **2005**, *44*, 455.

(20) G. A. Olah, *Friedel-Crafts Chemistry*. ed.; Wiley: New York, **1973**.

(30) G. D. Vo, J. E. Hartwig, *Angew. Chem. Int. Ed*., **2008**, *47*, 2127.

(31) M. G. Organ, M. Abdel-Hadi, S. Avola, N. Hadei, J. Nasielski, C. J. O'Brien and C. Valente, *Chem.-Eur. J.*, **2007**, *13*, 150-157; M. G. Organ, S. Avola, I. Dubovyk, N. Hadei, E. A. B. Kantchev, C. J. O'Brien and C. Valente, *Chem.-Eur. J.*, **2006**, *12*, 4749-4755; C. J. O'Brien, E. A. B. Kantchev, G. A. Chass, N. Hadei, A. C. Hopkinson, M. G. Organ, D. H. Setiadi, T. H. Tang and D. C. Fang, *Tetrahedron*, **2005**, *61*, 9723-9735

(32) C. Dash, M. Shaikh, P. Ghosh, *Eur. J. Inorg. Chem.*, **2009**, 1608; L. Ray, S. Barman, M. Shaikh, P. Ghosh, *Chem.-Eur. J.*, **2008**, 14, 6646.

(33) D. Jaganyi, F. Tiba, O. Q. Munro,.B. Petrovic, Z. D. Bugarcic, *Dalton Trans.* **2006**, 2943; Z. D. Bugarcic, B. Petrovic, E. Zangrando, *Inorg. Chim. Acta* **2004**, *357*, 2650; Q. D. Liu, L. Thorne, I. Kozin, D. T. Song; C. Seward, M. D'Iorio, Y. Tao, S. N. Wang,, *J. Chem. Soc.-Dalton Trans.* **2002**, 3234.

(34) T. Nagahara, Y. Yokoyama, K. Inamura, S. Katakura, S. Komoriya, H. Yamaguchi, T. Hara, M. Iwamoto, *J. Med. Chem.*, **1994**, *37*, 1200.

(35) K. A. Ohemeng, M. A. Appollina, V. N. Nguyen, C. F. Schwender, M. Singer, M. Steber, J. Ansell, G. Argentieri, W. Hageman, *J. Med. Chem.*, **1994**, *37*, 3663.

(36) A. P. Kozikowski, D. Ma, L. Du, N. E. Lewin, P. M. Blumberg, *J. Am. Chem. Soc.*, **1995**, *117*, 6666.

(37) S. Cacchi, G. Fabrizi, A. Goggiamani, *Curr. Org. Chem.*, **2006**, *10*, 1423; G. Zeni, R. C. Larock, *Chem. Rev.*, **2004**, *104*, 2285; V. Fiandanese, D. Bottalico, G. Marchese, A. Punzi, *Tetrahedron*, **2008**, *64*, 7301; B. Gabriele, G. Salerno, A. Fazio, R. Pittelli, *Tetrahedron*, **2003**, *59*, 6251; S. Cacchi, G. Fabrizi, L. Moro, *Synlett*, **1998**, 741;

(38) F. Colobert, A. S. Castanet, O. Abillard, *Eur. J. Org. Chem.*, **2005**, 3334.

(39) J.-H. Li, J.-J. Li, D.-P. Wang, S.-F. Pi, Y.-X. Xie, M.-B. Zhang, X.-C. Hu, *J. Org. Chem.*, **2007**, *72*, 2053.

(40) V. Fiandese, D. Bottalico, G. Marchese, A. Punzi, *Tetrahedron*, **2008**, *64*, 53.

(41) N. Isono, M. Lautens, *Org. Lett*., **2009**, *11*, 1329.

(42) A. Padwa, K. E. Krumpe, M. D. Weingarten, *J. Org. Chem*., **1995**, *60*, 5595.

(43) K. Hiroya, R. Jouka, M. Kameda, A. Yasuhara, T. Sakamoto, *Tetrahedron*, **2001**, *57*, 9697.

(44) J. E. Baldwin, *J. C. S Chem. Comm*., **1976**, 734.

(45) X. W. Li, A. R. Chianese, T. Vogel, R. H. Crabtree, *Org. Lett*. **2005**, *7*, 5437.

(46) F. Hanasaka, K. Fujita, R. Yamaguchi, *Organometallics*, **2005**, *24*, 3422.

(47) K.-I. Fujita, C. Asai, T. Yamaguchi, F. Hanasaka, R. Yamaguchi, *Org. Lett.*, **2005**, *7*, 4017.

(48) R. Martinez, D. J. Ramon, M. Yus, *Tetrahedron*, **2006**, *62*, 8992.

(49) K. Fujita, K. Yamamoto, R. Yamaguchi, *Org. Lett*., **2002**, *4*, 2691.

(50) S. Whitney, R. Grigg, A. Derrick, A. Keep, *Org. Lett.*, **2007**, *9*, 3299.

(51) S. Muthasamy, C. Gunanatan, *Synlett*, **2002**, *11*, 1783.

(52) A. B. Zaitsev, S. Gruber, P. S. Pregosin, *Chem. Commun.*, **2007**, 4692.

(53) J. S. Yadav, B. V. S. Reddy, S. Aravind, G. Kumar, A. S. Reddy, *Tetrahedron Lett.*, **2007**, *48*, 6117.

(54) J. T. Kuethe, *Chimia*, **2006**, *60*, 543.

(55) G. R. Humphrey, J. T. Kuethe, Chem. Rev., 2006, 106, 2875.; N. Azizi, L. Torkian, M. R. J. Saidi, *J. Mol. Catal. A: Chem.,* **2007**, *275*, 109; J. Azizian, F. Teimouri, M. R, Mohammadizadeh, *Catal. Commun.*, **2007**, *8*, 1117; M. A. Zolfigol, P. Salehi, M. Shiri, Z. Tanbakouchian, *Catal. Commun.*, **2007**, *8*, 173; S. Palaniappan, A. John, *J. Mol. Catal. A*: *Chem.,* **2005**, *242*, 168; W. J. Li, X. F. Lin, X. F.; J. Wang, G. L., Y. G. Wanf., *Synlett*, **2005**, 2003. M. Shi, S. C. Cui, Q. J. Li, *Tetrahedron*, **2004**, 60, 6679; M Mandini, A. Umani-Ronchi A., *AdV. Synth. Catal*., **2004**, *346*, 545.

(56) C. Dash, M. M. Shaikh, P. Ghosh, *Eur. J. Inorg. Chem.*, **2009**, 1608.

(57) A. Zanardi, J. A. Mata, E. Peris, *Organometallics*, **2009**, *28*, 4335.

(58) D. Jaganyi, F. Tiba, O.Q. Munro, B. Petrovic, Z. D. Bugarcic, *Dalton Trans.*, **2006**, 2943; Z. D. Bugarcic, B. Petrovic, E. Zangrando, *E. Inorg. Chim. Acta*, **2004**, *357*, 2650; Q. D. Liu, L. Thorne, I. Kozin, D. T. Song, C. Seward, M. D'Iorio, Y. Tao, S. N. Wang, *J. Chem. Soc.-Dalton Trans.*, **2002**, 3234.

(59) I. Terstiege, R. E. Maleczka, *J. Org. Chem.*, **1999**, *64*, 342; G. Dorman, J. D. Olszewski, G. D. Prestwich, Y. Hong, D. G. Ahern, *J. Org. Chem.*, **1995**, *60*, 2292; R. J. Parry, Y. Li, E. E. Gomez, *J. Am. Chem. Soc.*, **1992**, *114*, 5946; A. R. Pinder, *Synthesis-Stuttgart*, **1980**, 425.

(60) M. J. Morra, V. Borek, J. Koolpe, *J. Environ. Qual.*, **2000**, *29*, 706.

(61) Navarro, O.; Marion, N.; Oonishi, Y.; Kelly, R. A.; Nolan, S. P. J. Org. Chem. 2006, 71, 685.
(62) G. Brieger, T. J. Nestrick, *Chem. Rev.*, **1974**, *74*, 567.
(63) G. Zassinovich, G. Mestroni, S. Gladiali, *Chem. Rev.*, **1992**, *92*, 1051.
(64) J. R. Miecznikowski, R. H. Crabtree, *Polyhedron*, **2004**, *23*, 2857.
(65) M. Poyatos, E. Mas-Marza, J. A. Mata, M. Sanau, E. Peris, *Eur. J. Inorg. Chem.*, **2003**, 1215.
(66) M. Poyatos, J. A. Mata, E. Falomir, R. H. Crabtree, E. Peris, *Organometallics*, **2003**, *22*, 1110.
(67) E. Mas-Marza, M. Poyatos, M. Sanau, E. Peris, *Organometallics*, **2004**, *23*, 323.
(68) J. Takehara, S. Hashiguchi, A. Fujii, S. Inoue, T.; Ikariya, R. Noyori, R., *Chem. Commun.*, **1996**, 233.
(69) M. Albrecht, R. H. Crabtree, J. A. Mata, E. Peris, *Chem. Commun.*, **2002**, 32.
(70) D. Gnanamgari, A. Moores, E. Rajaseelan, R. H. Crabtree, *Organometallics*, **2007**, *26*, 1226.
(71) M. Albrecht, J. R. Miecznikowski, A. Samuel, J. W. Faller, R. H. Crabtree, *Organometallics*, **2002**, *21*, 3596.
(72) J. S. M. Samec, J. E. Bäckvall, P. G. Andersson, P. Brandt, *Chem. Soc. Rev.*, **2006**, *35*, 237.
(73) O. Pàmies, J.-E Bäckvall, *Chem. Eur. J.*, **2001**, *7*, 5052.
(74) O. Navarro, N. Marion, Y. Oonishi, R. A. Kelly, S. P. Nolan, *J. Org. Chem.*, **2006**, *71*, 685.
(75) M. S. Viciu, G. A. Grasa, S. P. Nolan, *Organometallics*, **2001**, *20*, 3607.
(76) R. Corberan, E. Mas-Marza, E. Peris, *Eur. J. Inorg. Chem.*, **2009**, 1700.
(77) (a) A. P. da Costa, M. Viciano, M. Sanau, S. Merino, J. Tejeda, E. Peris, B. Royo, *Organometallics*, **2008**, *27*, 1305; (b) F. Hanasaka, Y. Tanabe, K. Fujita, R. Yamaguchi, *Organometallics*, **2006**, *25*, 826; (c) F. Hanasaka, K. I. Fujita, R. Yamaguchi, *Organometallics*, **2004**, *23*, 1490.
(78) K. Fujita, M. Owaki, R. Yamaguchi, *Chem. Commun.*, **2002**, 2964.
(89) D. Cuervo, M. P. Gamasa, J. Gimeno, *Chem.-Eur. J.*, **2004**, *10*, 425.
(80) T. D. Nixon, M. K. Whittlesey, J. M. Williams, *Dalton Trans.*, **2009**, 753; M. G. Edwards, R. F. R. Jazzar, B. M Paine, D. J. Shermer, M. K. Whittlesey, J. M. Williams, D. D. Edney, *Chem. Commun.*, **2004**, 90.
(81) G. Guillena, D. J. Ramon, M. Yus, *Angew. Chem. Int. Ed.*, **2007**, *46*, 2358
(82) R. Martinez, D. J. Ramon, M. Yus, *Tetrahedron*, **2006**, *62*, 8988.
(83) A. R. McCarthy, R. W. Hartmann, A. D. Abell, *Bioorg. Med. Chem. Lett.*, **2007**, *17*, 3603; F. Picard, T. Schulz, R. W. Hartmann, *Bioorg. Med. Chem.*, **2002**, *10*, 437.
(84) G. E. Dobereiner, R. H. Crabtree, *Chem. Rev.*, **2010**, *110*, 681; G. Guillena, D. J. Ramon, M. Yus, *Chem. Rev.*, **2010**, *110*, 1611.

(85) M. Hamid, P. A. Slatford, J. M. J. Williams, *Adv. Synth. Catal*., **2007**, *349*, 1555; A. Tillack, D. Hollmann, D. Michalik, M. Beller, *Tetrahedron Lett.*, **2006**, *47*, 8881; K. I. Fujita, Y. Enoki, R. Yamaguchi, *Tetrahedron*, **2008**, *64*, 1943.

(86) B. Gnanaprakasam, J. Zhang, D. Milstein, *Angew. Chem.*, **2010**, *122*, 1510; *Angew. Chem. Int. Ed*., **2010**, *49*, 1468.

(87) M. S. Kwon, S. Kim, S. Park, W. Bosco, R. K. Chidrala, J. Park, *J. Org. Chem.*, **2009**, *74*, 2877.

(88) J. P. Adams, *J. Chem. Soc. Perkin Trans.*, **2000**, 125 –139; J. Gawronski, N. Wascinska, J. Gajewy, *Chem. Rev.*, **2008**, *108*, 5227 – 5252.

(89) K. Orito, T. Hatakeyama, M. Takeo, S. Uchiito, M. Tokuda, H. Suginome, *Tetrahedron*, **1998**, *54*, 8403; C. S. Yi, D. W. Lee, *Organometallics*, **2009**, *28*, 947.

(90) A. H. Ell, J. S. M. Samec, C. Brasse, J. E. Backvall, *Chem. Commun.*, **2002**, 1144; M. Largeron, A. Chiaroni, M. B. Fleury, *Chem. Eur. J.*, **2008**, *14*, 996.

(91) J. S. M. Samec, A. H. Ell, J. E. Backvall, *Chem. Eur. J.*, **2005**, *11*, 2327; S. I. Murahashi, Y. Okano, H. Sato, T. Nakae, N. Komiya, *Synlett*, **2007**, 1675; G. Jiang, J. Chen, J. S. Huang, C. M. Che, *Org. Lett.*, **2009**, *11*, 4568; X. Q. Gu, W. Chen, D. Morales-Morales, C.M. Jensen, *J. Mol. Catal. A*, **2002**, *189*, 119.

(92) J. W. Kim, J. He, K. Yamaguchi, N. Mizuno, *Chem. Lett.*, **2009**, *38*, 920.

(93) L. Blackburn, R. J. K. Taylor, *Org. Lett.*, **2001**, *3*, 1637.

(94) P. Rylander, *Catalytic Hydrogenation in Organic Synthesis*, Academic Press, New York, **1979**; H.-U. Blaser, U. Siegrist, H. Steiner, M. Studer, *Fine Chemicals through Heterogeneous Catalysis*, Wiley-VCH, Weinheim, **2001**; P. Baumeister, M. Studer, F. Roessler, *Handbook of Heterogeneous Catalysis*, Wiley-VCH, Weinheim, **1997**.

(95) F. Ragaini, S. Cenini, E. Gallo, A. Caselli, S. Fantauzzi, *Curr. Org. Chem.*, **2006**, *10*, 1479.

(96) K. Junge, B. Wendt, N. Shaikh, M. Beller, *Chem. Commun.*, **2010**, *46*, 1769; R. G. de Noronha, C. C. Romao, A. C. Fernandes, *J. Org. Chem.*, **2009**, *74*, 6960; Y. Sunada, H. Kawakami, T. Imaoka, Y. Motoyama, H. Nagashima, *Angew. Chem.*, **2009**, *121*, 9675; *Angew. Chem. Int. Ed.*, **2009**, *48*, 9511; L. He, L. C. Wang, H. Sun, J. Ni, Y. Cao, H. Y. He, K. N. Ean, *Angew. Chem.*, **2009**, *121*, 9702; *Angew. Chem. Int. Ed.*, **2009**, *48*, 9538.

(97) C. Y. Wang, C. F. Fu, Y. H. Liu, S. M. Peng, S. T. Liu, *Inorg. Chem.*, **2007**, *46*, 5779.

(98) M. Takasaki, Y. Motoyama, K. Higashi, S.-H. Yoon, I. Mochida, H. Nagashima *Org. Lett.*, **2008**, *10*(8), 1601; G. Wu, M. Huang, M. Richards, M. Poirier, X. Wen, R. W. Draper, *Synthesis*, **2003**, *11*, 1657; M. Rodel, F. Thieme, H. Buchholz, B. Konig, *Synth. Commun.*, **2002**, *32*(8), 1181.

(99) K. Fujita, N. Tanino, R. Yamaguchi, *Org. Lett.*, **2007**, *9*, 109; R. Yamaguchi, C. Ikeda, I. Takahashi, K. Fujita, *J. Am. Chem. Soc.*, **2009**, *131*, 8410.

(100) S. Bhuvaneswari, M. Jeganmohan, C.-H. Cheng, *Chem. Eur. J.*, **2007**, *13*, 8285.

(101) R. J. Sundberg, *The Chemistry of Indoles*, Academic Press, New York, **1970**; R. K. Brown, (Ed.: H. W. J.), Wiley-Interscience, New York, **1972**.

(102) (a) M. Bandini, A. Eichholzer, *Angew. Chem. Int. Ed.*, **2009**, *48*, 9608; (b) K. Kruger, A. Tillack, M. Beller, *Adv. Synth. Catal.*, **2008**, *350*, 2153.

(103) a) M. T. Reetz, K. Sommer, *Eur. J. Org. Chem.*, **2003**, 3485; b) J. Oamada, T. Kitamura, *Tetrahedron Lett.*, **2005**, *46*, 3823; c) C. Liu, X. Han, X. Wang, R. A. Widenhoefer, *J. Am. Chem. Soc.*, **2004**, *126*, 3700; d) A. Furstner, V. Mamane, *J. Org. Chem.*, **2002**, *67*, 6264; e) Z. Shi, C. He, *J. Org. Chem.*, **2004**, *69*, 3669; f) S. J. Pastine, S. W. Youn, D. Sames, *Org. Lett.*, **2003**, *5*, 1055; g) T. J. Harrison, G. R. Dake, *Org. Lett.*, **2004**, *6*, 5023; h) X. Han, R. A. Widenhoefer, *Org. Lett.*, **2006**, *8*, 3801; i) D. Karshtedt, A. T. Bell, T. D. Tilley, *Organometallics*, **2004**, *23*, 4169; j) J. Oyamada, T. Kitamura, *Tetrahedron*, **2006**, *62*, 6918; k) N. Chatani, H. Inoue, T. Ikeda, S. Murai, *J. Org. Chem.*, **2000**, *65*, 4913; l) Z. Li, Z. Shi, C. He, *J. Organomet. Chem.*, **2005**, *690*, 5049.

(104) A. Zanardi, J. A. Mata, E. Peris, *J. Am. Chem. Soc.*, **2009**, *131*, 14531.

(105) A. Zanardi, J. A. Mata, E. Peris, *Chem. Eur. J.*, **2010**, *16*, 10502.

(106) D. R. Anton, R. H. Crabtree, *Organometallics*, **1983**, *2*, 855; P. Foley, R. Dicosimo, G. M. Whitesides, *J. Am. Chem. Soc.*, **1980**, *102*, 6713.

(107) G. M. Whitesides, M. Hackett, R. B. L. Brainard, J.- P. P. M. Lavalleye, A. F. Sowinski, A. N. Izumi, S. S. Moore, D. W. Brown, E. M. Staudt, *Organometallics*, **1985**, *4*, 1819.

Chapter 3

Synthesis, Reactivity and Catalytic Properties of Iridium Complexes with Alkenyl-NHC ligands

3.1 Introduction: Hydrosilylation of terminal alkynes

Hydrosilylation is the addition of a Si-H bond to a multiple C-C or C-heteroatom bond as illustrated in **Scheme 3.1**.

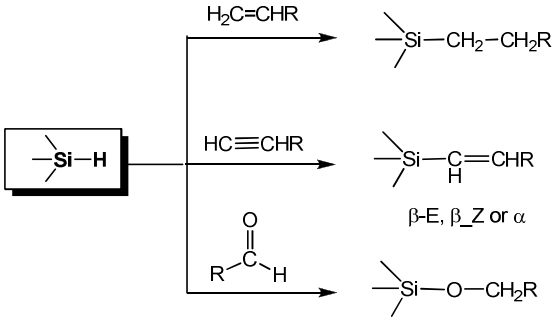

Scheme 3.1

This reaction has a wide applicability in industry.[1] It is used for the synthesis of silicone derivatives as well as for the modification of surfaces in textile, glasses, stones and conservation of archaeological pieces.

In the addition of Si-H bonds to C≡C triple bonds to obtain vinylsilanes, the challenge is to design a catalyst that can promote the regioselective formation of the corresponding **α** or **β** isomers. Together with the hydrosilylated products, dehydrogenative silylated products may also be obtained (**Scheme 3.2**).

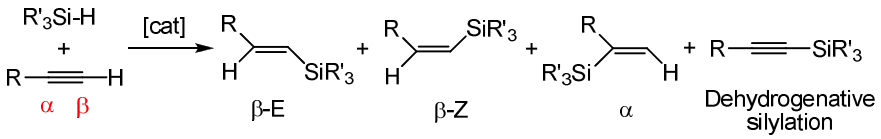

Scheme 3.2

The regioselectivity of the reaction can dramatically vary depending on many factors, such as the nature of the catalyst, the alkyne and/or hydrosilane and the reaction conditions (solvent, temperature and additives).

One of the most widely accepted mechanisms for this reaction was first reported by Chalk-Harrod in 1965,[2a] in which the insertion of a coordinated alkyne (or alkene) into a metal-hydrogen bond (hydrometalation) is followed by the reductive elimination of an alkyl (or alkenyl) and a silyl ligand to yield the hydrosilylation products (**Scheme 3.3**, pathway **a**).

The Chalk-Harrod mechanism can not explain the formation of the dehydrogenative silylation product, so a modified mechanism was proposed a few years later (1977).[2b, c] The so-called modified Chalk-Harrod mechanism involves the insertion of the alkene into the M-Si

bond (silylmetalation, intermediate **1.5**), followed by the reductive elimination of the β-silylalkenyl (or β-silylalkyl) and the hydride ligands to afford the hydrosilylation products, **1.6**. (**Scheme 3.3**, **pathway b**).[2b, c]

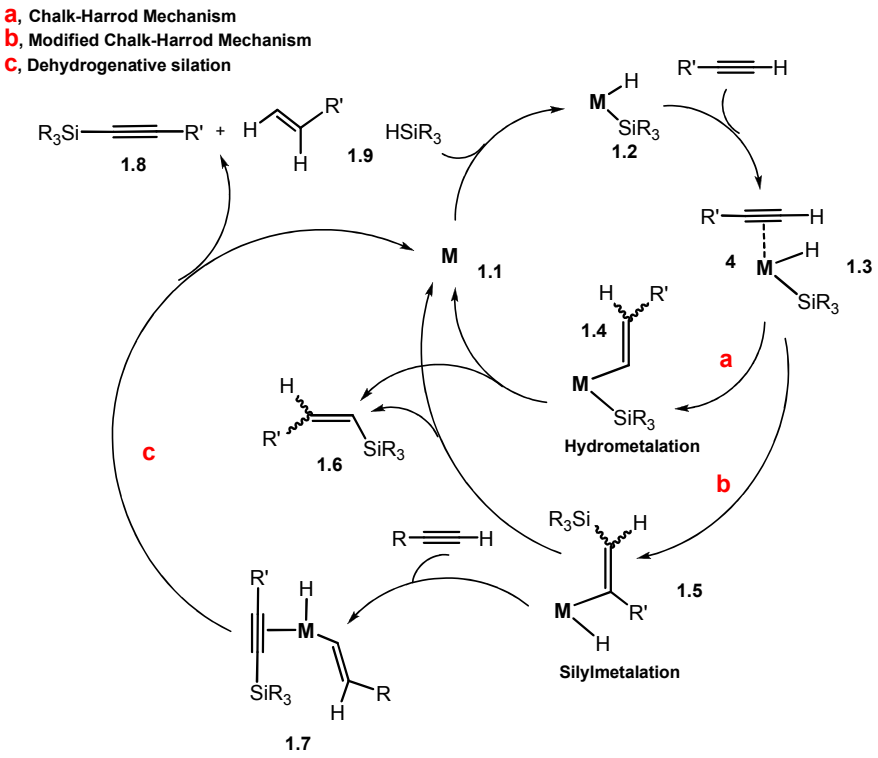

Scheme 3.3

If the reductive elimination is disfavoured for a second insertion of the alkyne, it could be possible to explain the formation of the alkynylsilane **1.8** and the corresponding alkene **1.9** that have been detected in some hydrosilylation processes.[3] This process is called dehydrogenative silylation (**Scheme 3.3**, pathway **c**).

The currently accepted mechanism was proposed to account for the unexpected predominant (> 99%) net trans hydrosilylation of RC≡CH by a rhodium or iridium catalyst. Both Ojima[4] and Crabtree[5] argued that initial insertion of the C≡C bond takes place exclusively into an Ir-Si bond of the catalyst to give an intermediate **1.10** (**Scheme 3.4**) that can rearrange to give the net trans hydrosilylation product.[6] Tanke and Crabtree[5] proposed that this occurs via a η^2-vinyl intermediate **1.11** while Ojima et al.[4] preferred a very closely related zwitterionic form. The bulky L groups on the metal cause the least hindered vinyl isomer to be preferred, and it is this isomer that leads to the trans addition product, **1.14**, after reductive elimination. Some interesting experiments showed that if the R' group in R'C≡CH is very

bulky, an equilibrium between the *pre-trans* **1.12** and *pre-cis* **1.10** species generates a mixture of *syn*- and *anti*-addition products in the resulting vinylsilanes. Otherwise, the steric bulkiness of the silyl group has a marginal influence, slightly favouring *syn*-addition for small R_3Si groups.[3] Increasing the temperature normally favours *syn*-addition resulting in the *trans*-isomer. This is probably because higher temperatures favour the reductive elimination of the product before the equilibrium between the pre-*trans* and pre-*cis* species is reached.[6, 7]

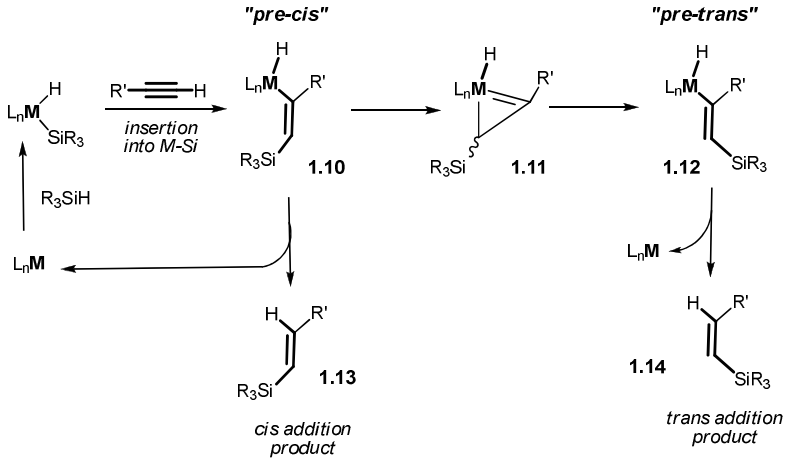

Scheme 3.4

Crabtree and co-workers also explored the generation of the dehydrogenative silylated product.[3] They found that the selectivity for this step (pathway **c**, **Scheme 3.3**) is higher when both R and R' are sterically demanding. Mechanistically, this finding is reasonable, because β-elimination is likely to be accelerated by bulky substituents that cause the vinyl C-H bond to approach the metal as a result of steric congestion between R' and SiR_3, as shown in **Scheme 3.5.**

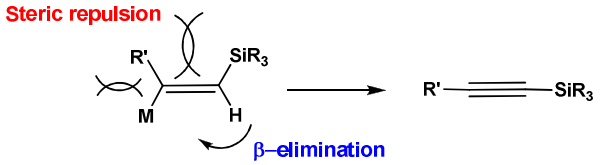

Scheme 3.5

The β-elimination is also strongly favoured when the alkyne/silane ratio is increased. A possible explanation could be that the formation of $R'C{\equiv}CSiR_3$ requires a hydrogen acceptor to remove the hydrogen liberated, and so having a high concentration of alkyne this process is favorable.[6]

3.2 Synthesis and characterization of Iridium complexes with alkenyl-imidazolyl-ylidene

N-alkenyl-imidazolyl-ylidene ligands have been recently used in our laboratories for the design of new Ir^{III} catalysts.[8, 9] The initial objective was to use these ligands as *hemicleaveable*.

An *hemicleaveable* ligand, consists of an initially chelating ligand that can irreversibly generate a coordination vacant site in the presence of a reactant (**Scheme 3.6**). It is important to point out that a *hemicleaveable* ligand is different from the traditionally known as *hemilabile* ligand, in which the decoordination of one of the two arms of the ligand is reversible.

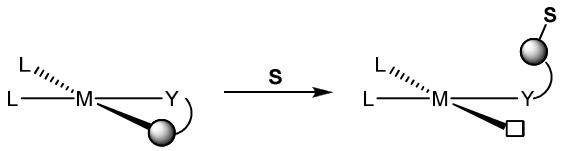

Scheme 3.6

For example, the π-coordination of an alkene can allow the stabilization of the coordination sites/vacancies of a precatalyst with respect to other precatalysts that generally use labile ligands (**Scheme 3.7**). It is easy to imagine that, under certain circumstances, we can force the irreversible decoordination of the alkenyl arm of the ligand, if we irreversibly cleave the M-alkene bond. This irreversible activation can take place by, for example, hydrogenenation of the alkenyl group, using any of the known hydrogenation methodologies. (**Scheme 3.8**).[8-11]

It is also noteworthy that the use of a *hemicleavable* ligand does not imply the generation of waste in the reaction media. There is no lost of labile ligand from the coordination sphere of the metal during the catalytic cycle.

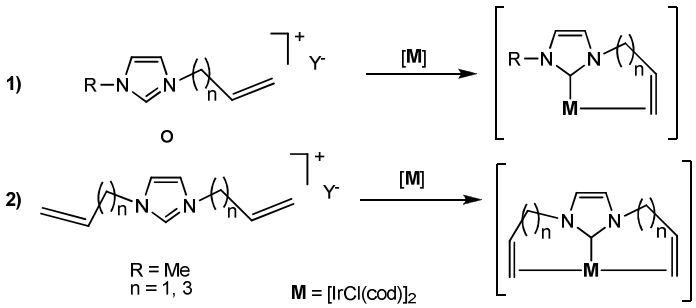

Scheme 3.7

In our case, the reactivity studies of this kind of compounds will be carried out with substrates that can be able to irreversibly nullify the coordination capacity of the olefines. The resulting

compounds will be used in reactions that imply the olefinic saturation generating reactive species. [9-12]

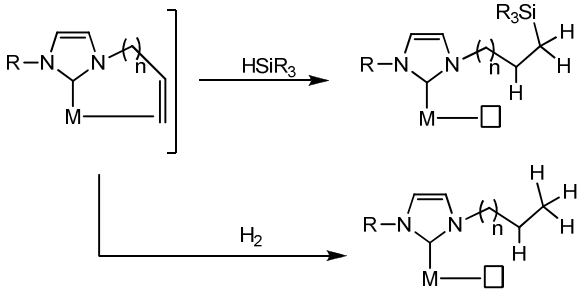

Scheme 3.8

Under these conditions we would have the *in situ* generation of a vacant site and the irreversible activation of the catalyst in the reaction medium of the catalytic system.

3.3. Synthesis and characterization of bisalkenyl-imidazolyl-ylidene ligands

Table 3.1 shows the labelling of the ligand precursors that will be used throughout this Chapter.

Table 3.1 Labelling of the precursor ligand salts **a-d**

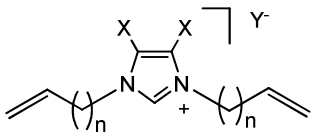

n	X	Y	label
1	H	Br	**a**
1	Cl	PF_6	**b**
1	Me	Cl	**c**
3	H	Br	**d**

Salts **a** and **c** were obtained following a one-step strategy that implied an intermolecular cyclocondensation of a primary amine, formaldehyde and glyoxal (or 2,3-butanedione)[11] as shown in **Scheme 3.9**.

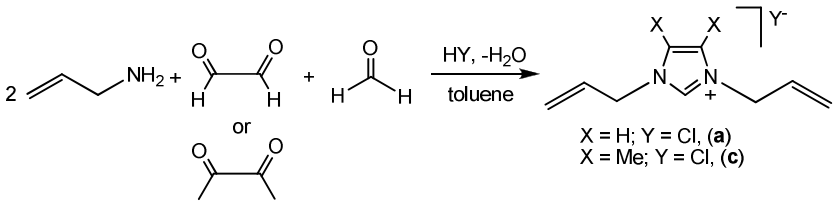

Scheme 3.9

The overall yields for the synthesis of salts **a**-**d**, were in the range of 86-100 %, as described in Chapter 4. Recently, Hahn and Oro, described the synthesis of the bisalkenyl-imidazolil-ylidene resulting from the deprotonation of the imidazolium salt **a**, and its coordination to Ir^{I}.[10, 11]

Salts **b** and **d** were obtained by a general procedure that implies two steps:

1- Synthesis of the alkenyl-imidazol: this step was carried out using a strong base (such as KOH) to deprotonate imidazole. A subsequent nucleophilic attack of the species so formed to an alkenyl-halide lead to the desired 1-alkenylimidazole (**Scheme 3.10**). The 1-alkenylimidazole was purified by extraction using CH_2Cl_2/H_2O. The organic phase was dried over Na_2SO_4 and the solvent was removed at reduced pressure, giving an oily product. Whereas salt **b** was isolated pure following this procedure, salt **d** required further purification by column chromatography.

2- Reaction of the alkenyl-imidazol with an alkenyl halide to obtain the 1,3-bisalkenyl-imidazole (**Scheme 3.10**). The reaction was carried out in the absence of solvent generating an oil that was purified with several washes using Et_2O.

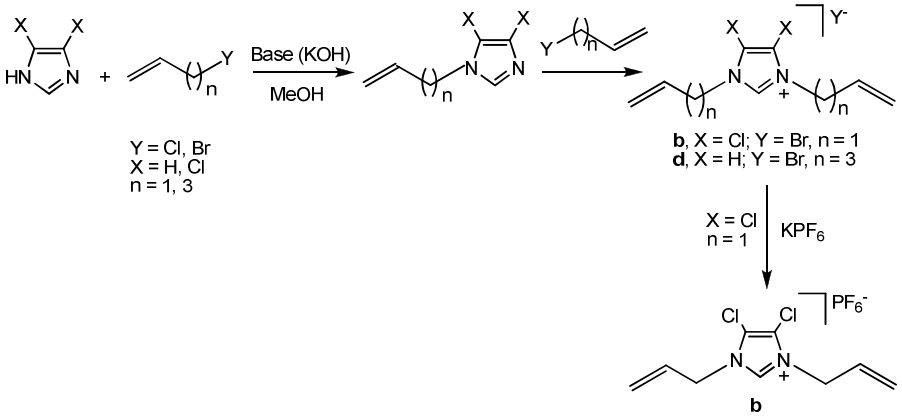

Scheme 3.10

Salt **b** (anion = PF_6^-) was obtained by addition of KPF_6 in acetone, and subsequent crystallization with Et_2O. Due to the similarity of the salts used, only the spectroscopic characterization of the ligand precursor **a** will be discussed in detail.

*^{1}H NMR spectrum of imidazolium salt **a***

Figure 3.1 shows the ^{1}H NMR spectrum of salt **a**. The number of signals that appears in the spectrum is consistent with the binary symmetry of the molecule. The signal due to the acidic proton at the C2 position (C2-*H*) appears as a singlet at 9.47 ppm (**a**). The signal attributed to the C4-H and C5-H imidazole protons is displayed as a singlet at 7.82 ppm (**b**). The signals due to the allyl moiety appear as a characteristic multiplet at 6.05 ppm (**d**), which corresponds to the -C*H*=CH_2- and a multiplet attributted to the -CH=CH_2, at 5.33 ppm (**e**). The -NCH_2- protons are shown as a doublet at 4.9 ppm (**c**) ($^2J_{H\text{-}H}$ = 6.0 Hz).

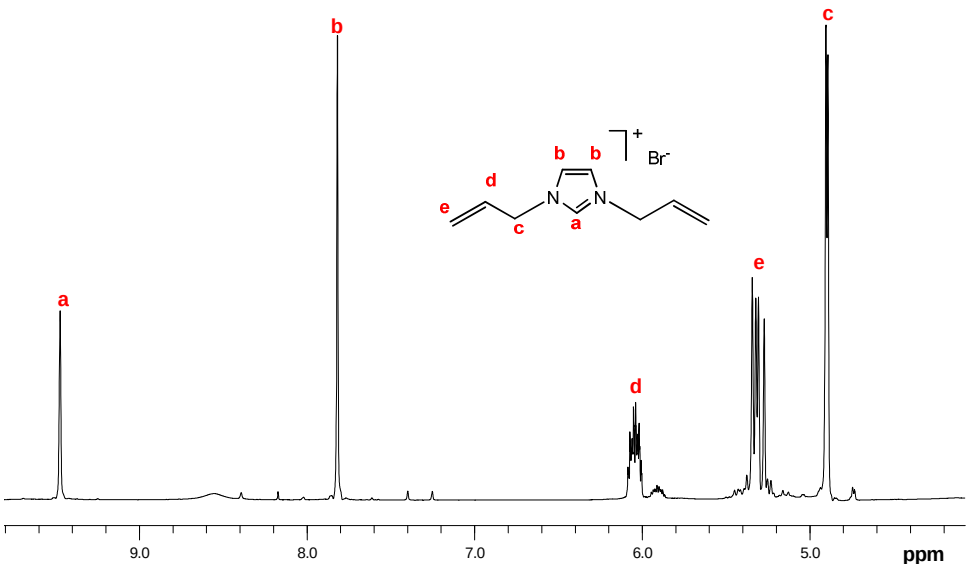

Figure 3.1. ^{1}H NMR spectrum of salt **a**.

*^{13}C {^{1}H} NMR spectrum of imidazolium salt **a***

Figure 3.2 shows the ^{13}C {^{1}H} NMR spectrum of salt **a**. The spectrum is consistent with the binary symmetry of the molecule. The signal corresponding to the *C*2 carbon appears at 136.2 ppm (**1**) while those due to *C*4-*C*5 appear at 122.5 ppm, (**4**). The signals attributed to the olefinic fragment are shown at 131.7 ppm (-*C*H=CH_2-,**2**); and at 120.1 ppm(-CH=*C*H_2-, **5**). Finally, the remaining signal at 50.7 ppm corresponds to the -N-*C*H_2 group (**3**).

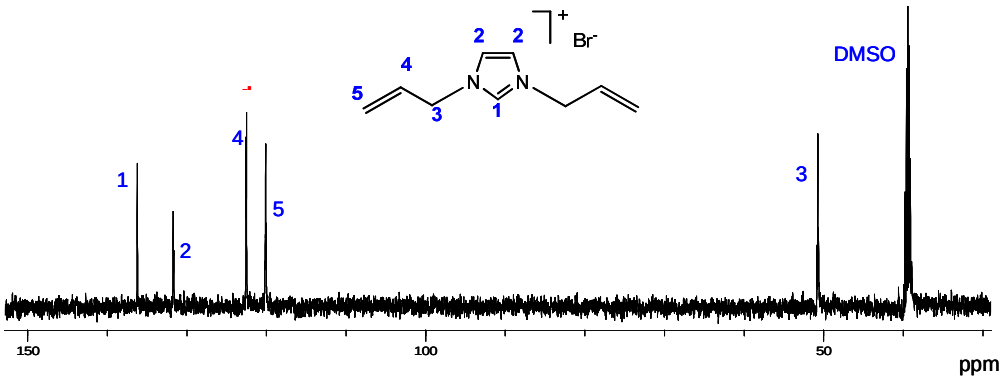

Figure 3.2 ^{13}C {^{1}H} NMR spectrum of salt **a**.

3.4 Synthesis of mono-coordinated, chelated and *pincer* alkenyl-NHC Iridium complexes

The ligand precursors **a**, **b, c** and **d** were coordinated to $[IrCl(cod)]_2$ (**Scheme 3.11**) by transmetallation from the corresponding pre-formed silver-NHC complexes. The silver-NHC complexes were obtained by reaction of the corresponding imidazolium salt with Ag_2O at room temperature during 1h in methanol. The silver complex was filtered through Celite to eliminate the excess of Ag_2O and other insoluble by-products. The resulting solution was concentrated under reduced pressure and redissolved in dichloromethane. $[IrCl(cod)]_2$ was then added and the mixture was stirred for 1h at 45 ºC. The crude was filtered through Celite to eliminate the AgCl, and the solvent was removed under reduced pressure. Pure compounds **1a**, **1b** and **1c** were obtained after flash chromatography using dichloromethane/methanol (7:3) as eluent. The overall yields were of 80 % (**1a**), 70% for (**1b**) and 66% for (**1c**). Compounds **1a**, **1b** and **1c** show a chelating coordination form, (η^2-alkenyl-NHC), in which the ligand is coordinated to the metal through the C2 of the NHC ring and the olefin (**Scheme 3.11**).

When using precursor salt **d,** with the longest alkenyl arm (n = 3), the olefin does not coordinate to the metal, so a monocoordinated species is formed (complex 2d, **Scheme 3.11**). In this case, the coordination of the olefin would form an eight membered metallacycle, which is more unstable and reactive than the related metallacycles formed. Complex **2d** was isolated as pure oil (yield 72%) and further purification was not required.

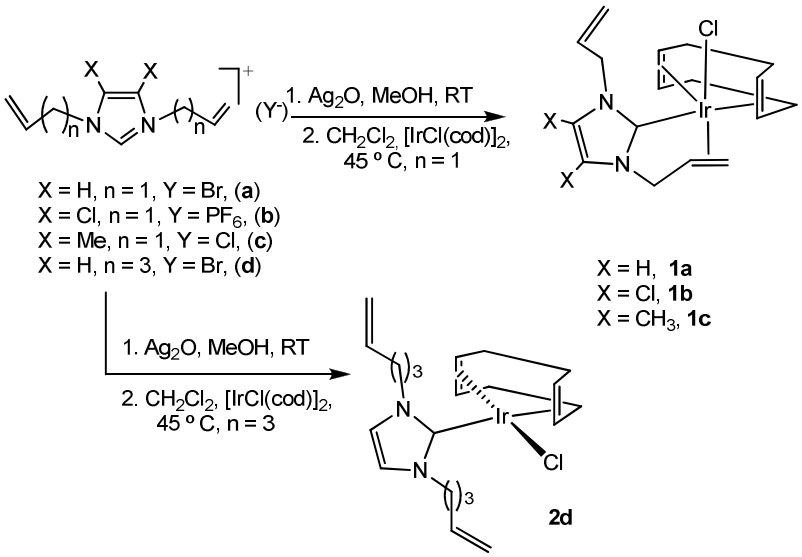

Scheme 3.11

All the new complexes were characterized by NMR (^{1}H and ^{13}C), and Mass Spectrometry analysis. The ^{1}H NMR spectra of complexes **1a**, **1b** and **1c**, are very similar and show an interesting fluxional behaviour. The evaluation of the kinetic and thermodynamic parameters concerning this process will be discussed in this section. As an example, the NMR spectrum of complex **2d** is described in detail.

*^{1}H NMR spectrum of complex **2d**.*

The ^{1}H NMR spectrum of complex **2d** is shown in **Figure 3.3**. The absence of the singlet corresponding to the acidic proton of precursor **d**, is the first evidence that metalation has taken place. The protons at the 4 and 5 positions of the imidazole ring are displayed as a singlet at 6.83 ppm (**a**) due to the binary symmetry of the compound. The signals corresponding to the olefinic protons are shown as two multiplets, -C*H*=CH$_2$ (**b**) at 5.8 ppm and -CH=C*H*$_2$, and 5.1 ppm (**c**). The COD ligand displays three distinctive signals: 4.5 ppm (singlet), 2.8 ppm (multiplet) and 2.0 ppm (multiplet). The resonances due to the protons at the N-wingtips appear at 4.3 ppm (-NC*H*$_2$-, m) while the remaining signals, -C*H*$_2$- protons, appear as two multiplets at 1.9 and 1.6 ppm.

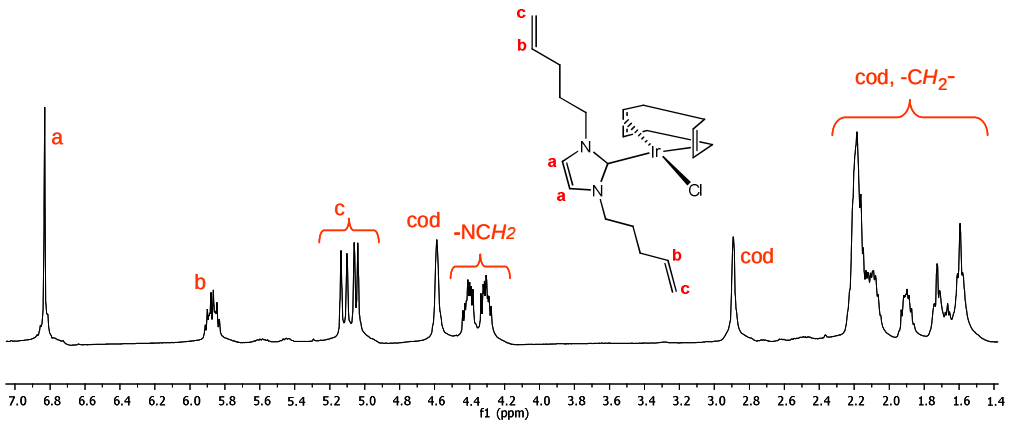

Figure 3.3 ^{1}H NMR spectrum of complex **2d**

*$^{13}C\{^{1}H\}$ NMR spectrum of complex **2d**.*

Figure 3.4 show the $^{13}C\{^{1}H\}$ RMN spectrum of complex **2d**. The signal due to the metallated carbon (180.2 ppm, **1**), confirms that the coordination to the *C*2 to Iridium was achieved.

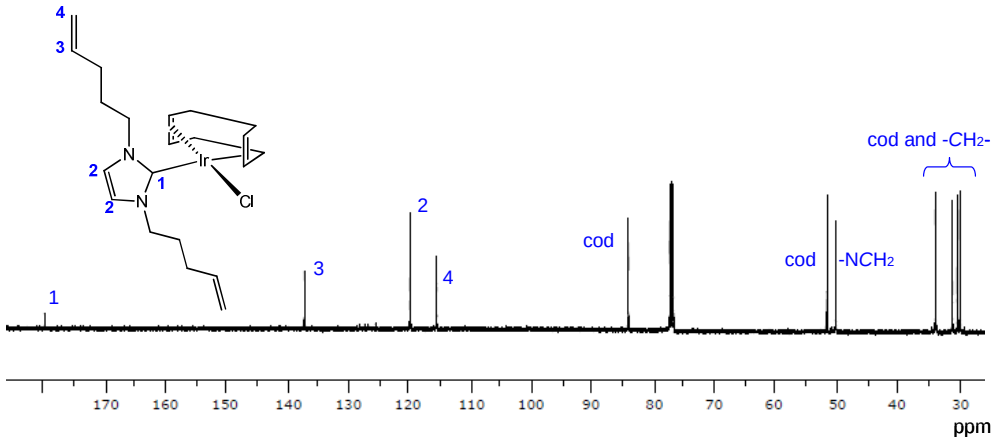

Figure 3.4 $^{13}C\{^{1}H\}$ NMR spectrum of complex **2d**

The other peaks appear in a range of chemical shift similar to other Ir^{I} complexes: the *C*4 and *C*5 carbons of the imidazolium ring, 115.8 ppm (**2**), olefinic carbons, 137.5 ppm -*C*H=CH$_2$ (**3**), and 120.2 ppm (**4**), –CH=*C*H$_2$. The COD ligand displays its signals at 84.3, 51.6, 33.8 and 31.0 ppm. The signal corresponding to the –N*C*H$_2$– carbons appear at 50.8 ppm. Finally the remaining signals at 30.2 and 29.7 ppm correspond to the –*C*H$_2$– carbons.

Variable-Temperature NMR studies

The room temperature ^{1}H NMR spectrum of complex **1a** showed a different environment for the two azole-ring protons at 6.89 (**H$_a$**) and 6.67 (**H$_b$**) ppm (**Figure 3.5**). This observation and the low frequency resonances due to the alkene-protons are consistent with the coordination of one of the two olefins. The upper and lower side of the iridium complex is different making all the protons magnetically inequivalent. The line width of the signals at room temperature is broad (e.g. 6.89 ppm, $w_{1/2}$ = 9.43 Hz; solvent $CDCl_3$ $w_{1/2}$ = 0.98 Hz) suggesting that a fluxional process is involved, probably implying the coordination/decoordination of the olefin. This dynamic process involves the exchange of Ha and Hb, as indicated in **Scheme 3.12**.

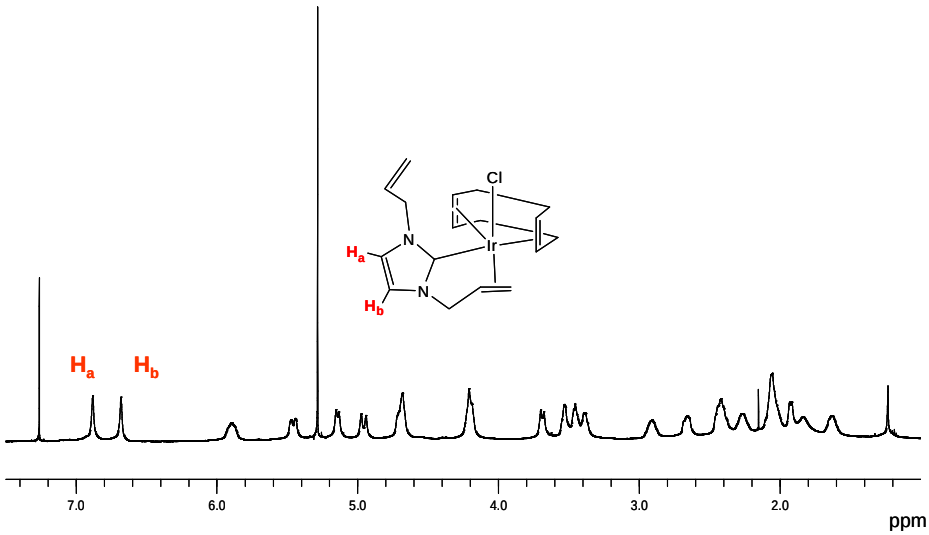

Figure 3.5 ^{1}H NMR spectrum of complex **1a** at 25ºC.

The metal-carbene rotation is not feasible as observed previously in analogous rhodium complexes.[12, 13] Previous studies by Enders demonstrated that the rotation about the Rh-$C_{carbene}$ bond is hindered when bulky cyclooctadiene or norbornadiene ligands are present.[14]

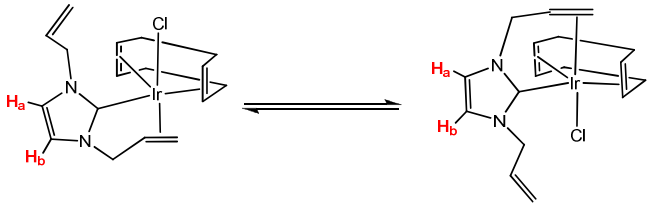

Scheme 3.12

Compound **1a** shows a sharp AB pattern for the azole-ring protons at -15 ºC (**Figure 3.6**). At this temperature, a complete NMR assignment has been made by HETCOR and COSY

experiments (**Figure 3.8**). As example, **Figure 3.7** shows the assignments of the non coordinated olefinic fragment due to a monodimensional correlation experiment.

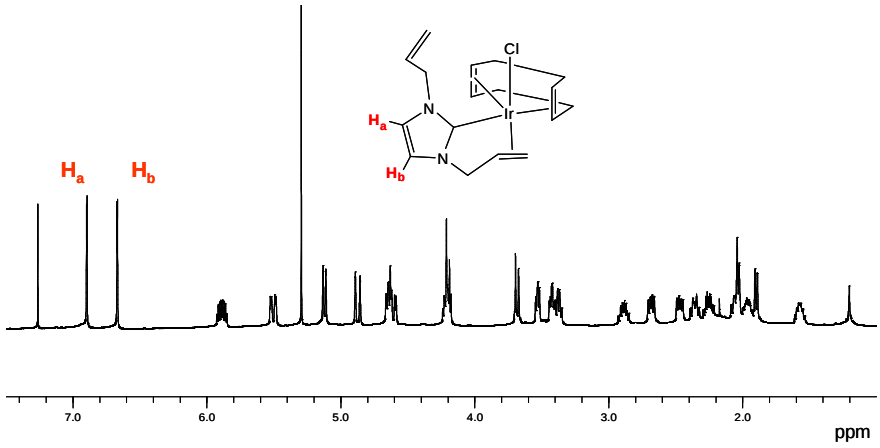

Figure 3.6. ^{1}H NMR spectrum of complex **1a** at – 15 ºC.

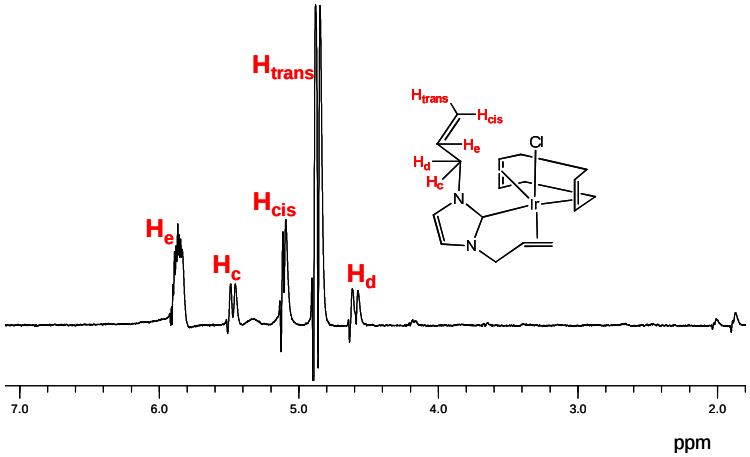

Figure 3.7. TOCSY 1D NMR spectrum of complex **1a** at – 10 ºC showing the signals corresponding to the non coordinated olefinic fragment.

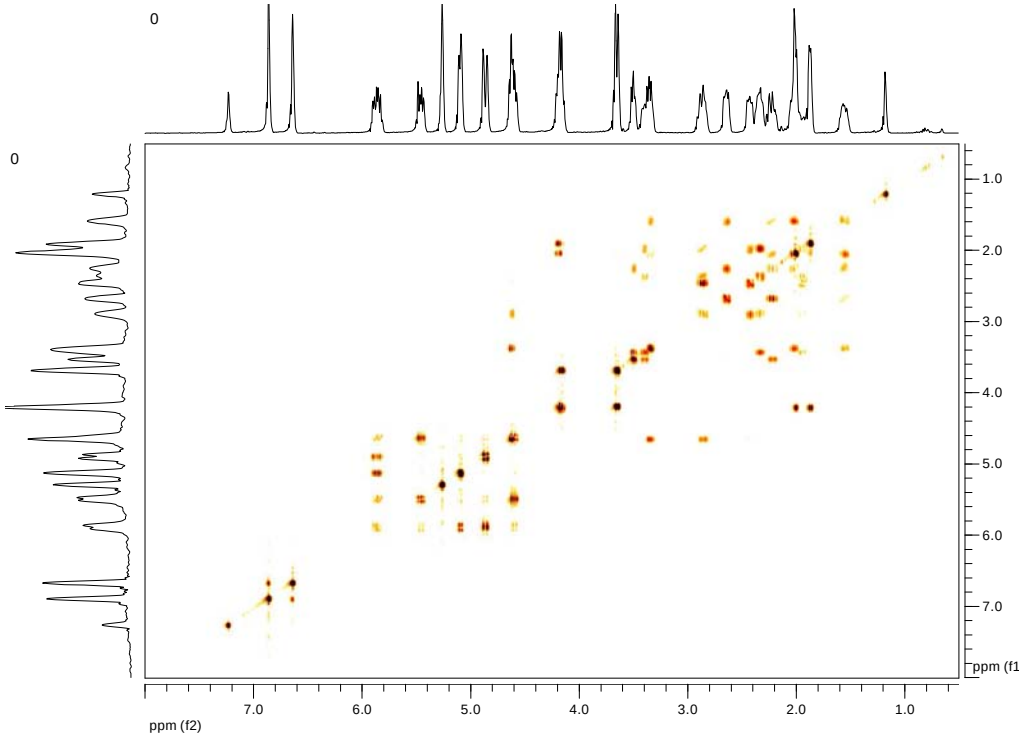

Figure 3.8. COSY NMR experiment of complex **1a** at -5 ºC.

As the temperature is raised, the peaks corresponding to **Ha** and **H_b** of the imidazole ring broaden and coalesce into a singlet at 50ºC. At this point we can calculate the free energy of activation at the coalescence temperature using equation (**1**):[15]

$$\Delta G^{\neq} = RT[23.759 + \ln(k/T)] \qquad (\mathbf{1})$$

Where the rate constant *k* can be obtained using equation (**2**):

$$k = \pi \Delta\nu / \sqrt{2} \qquad (\mathbf{2})$$

In equation (**2**), $\Delta\nu$ corresponds to the separation expressed in Hz of the two protons at the C-4,5 positions, **Ha** and **Hb**, taken from the spectra where no dynamic process is observed. This equation is only valid provided that the dynamic process is first order, the two singlets have equal intensities and the exchanging nuclei are not coupled to each other.

A series of ^{1}H NMR spectra of **1a** at different temperatures is shown in **Figure 3.9**. At -15 ºC, all the signals are relatively sharp and reveal two nonequivalent azole-ring protons at 6.89 and 6.67 ppm, in the ratio 1:1 (**Figure 3.8** and **3.9**). A line-shape analysis[16] from the data of **Figure 3.9** (-15 ºC to 50 ºC in $CDCl_3$) allows to determine the kinetic parameters governing this process.

As previously mentioned, equation (**1**) allows the calculation of $\Delta G^{\neq}$ at the coalescence temperature. The determination of the kinetic constants at temperatures below the coalescence were determined by line-shape analysis according to equation (**3**), by measuring the linewidths of the signals due to the azole-ring protons (ω) compared to the linewidth in the absence of exchange (ω_0).

$$k = (\omega - \omega_0)/\pi \qquad (3)$$

Table 3.2 shows de lineshape analysis data of the ^{1}H NMR signal at 6.89 ppm of compound **1a**.

Table 3.2. Calculated kinetics constants from 5 ºC to 40 ºC.

Temp (K)	w (Hz)	k= π (ω - ω_o)	1/T	ln(k/T)
278,15	3,89	1,31946889	0,00359518	-5,35093124
283,15	4,47	3,1415926	0,0035317	-4,50124692
288,15	5,15	5,27787557	0,00347041	-3,99995752
293,15	6,27	8,79645928	0,00341122	-3,50633514
298,15	9,43	18,7238919	0,00335402	-2,76779637
303,15	14,09	33,3637134	0,0032987	-2,20675885
308,15	20,75	54,2867201	0,00324517	-1,73630705
313,15	42,03	121,139811	0,00319336	-0,94973697

ω_o (Hz) = 3,47 Hz

Once the kinetic constants at different temperatures were determined, the corresponding $\Delta G^{\neq}$ values could be calculated. The representation of ln(k/T) = f(1/T) (Eyring plot), allows the deconvulsion of the $\Delta H^{\neq}$ and $T\Delta S^{\neq}$ values, as shown in **Figure 3.10**.

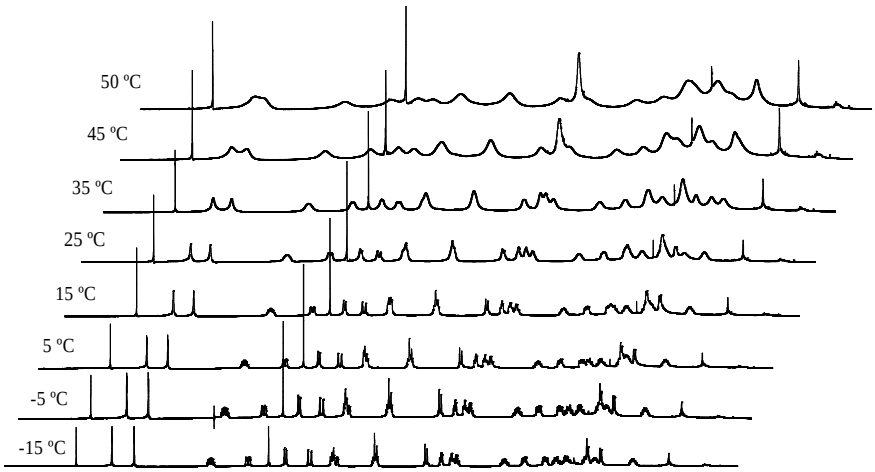

Figure 3.9. Variable temperature analyses for compound **1a** from -15 ºC to 50 ºC.

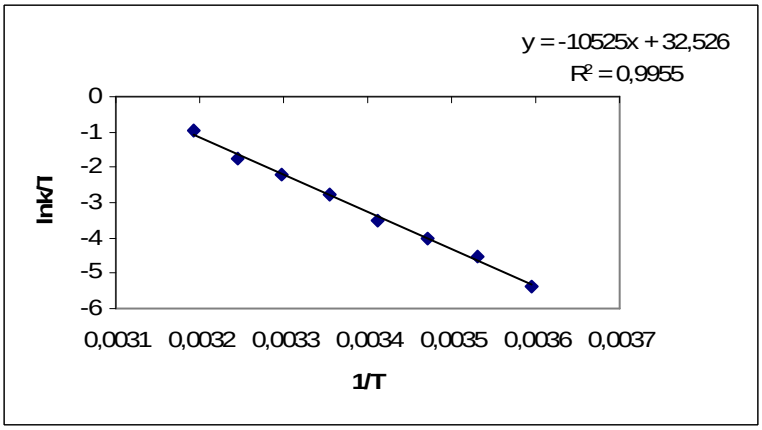

Figure 3.10. Complex **1a** line shape Analysis. Selected signal at 6.89 ppm, H_{imid}. Linear regression from Eq. $\ln(k/T) = -(\Delta H^{\neq}/R)(1/T) + \Delta S^{\neq}/R + 23.76$. Results: $\Delta H^{\neq} = 20.9$ Kcal/mol; $\Delta S^{\neq} = 17.4$ Kcal/mol.

A similar variable temperature study of complex **1a** has been done using ^{13}C NMR (75 MHz). The two different signals from the carbons attach directly to the azole ring appear at 52.6 and 52.2 ppm. As the temperature is increased, the peaks broaden and coalesce into a singlet at 35 ºC. This implies that at this temperature, the rate constant (determined from eq. (**1**)) is $k = 62.9$ s^{-1} and the free activation energy $\Delta G^{\neq} = 15.5$ Kcal/mol. The results agree well with the ones obtained previously using ^{1}H NMR.

This kinetic parameters are in good agreement with experimental and theoretical data for olefin coordination.[17-19] Our results indicate that the fluxional behaviour is governed through an enthalpic process corresponding to the cooordinaton/decoordination of the olefin. The positive entropic value suggests a highly disordered transition state associated to the

decoordination of the olefin, so the exchange process probably occurs through a dissociative mechanism implying a pseudo-square-planar 16e species.

*Reactivity of complexes **1a**, **1b** and **1c***

In order to remove the chloride from the coordination sphere of the rhodium centre, we reacted the neutral compounds **1a**, **1b** and **1c** with $AgBF_4$. This process facilitated the coordination of the second olefinic group as shown in **Scheme 3.13**.

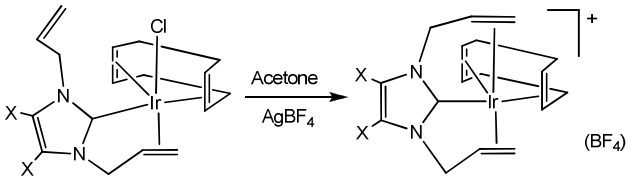

X = H, n =1, (**1a**);
X = Cl, n = 1, (**1b**);
X = CH_3, n = 1, (**1c**).

X = H, n = 1, (**2a**);
X = Cl, n = 1, (**2b**);
X = CH_3, n = 1, (**2c**).

Scheme 3.13

The reaction was carried out in acetone at room temperature. The solution was then filtered through Celite in order to eliminate the excess of unreacted $AgBF_4$ and AgCl. After the volatiles were removed, the complexes were isolated by precipitation using diethyl ether. For complexes **2b** and **2c**, anion exchange was necessary to facilitate the purification (see Chapter 2, *section 2.4.1* at pag. 59 of this Thesis, for anion exchange procedure with KPF_6). Complexes **2a**, **2b** and **2c** were isolated as white solids with yields of: 82, 92 and 68 %, respectively. In the case of the mono-coordinated species, **2d**, the addition of the silver salt did not allow the formation of the corresponding *pincer* analogue. The isolation of the cationic complexes **2a**, **2b** and **2c** was confirmed by high-resolution mass spectrometry and NMR spectroscopy. The ^1H NMR spectra of complexes **2a**, **2b** and **2c**, are very similar and confirm the binary symmetry of the NHC ligand. The spectroscopic characterization of complex **2a** will be discussed in detail.

*^{1}H NMR spectrum of complex **2a**.*

The ^{1}H NMR spectrum of complex **2a** (**Figure 3.11**) confirms the coordination of the ligand in the *pincer* form. Both olefins are bound to the metal resulting in an increase of symmetry with respect to compound **1a**.

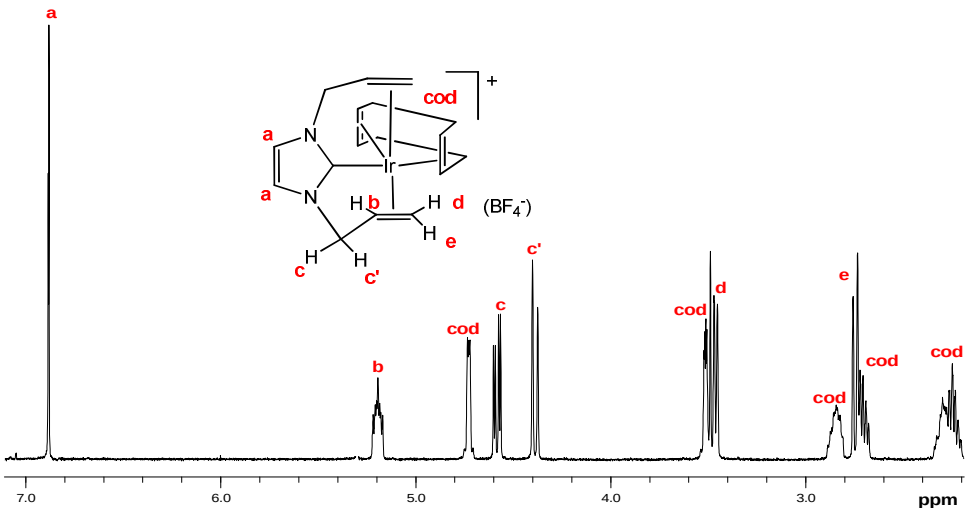

Figure 3.11. ^{1}H NMR spectrum of complex **2a**.

Scheme 3.14 represents the orientation of one propenyl fragment coordinated to the metal.

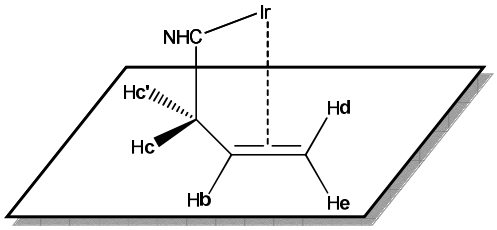

Scheme 3.14

The methylenic protons (Hc y Hc') are diastereotopic with a coupling constant $^{2}J_{H,H}$= 13.0 Hz. The spatial arrangement of the propenyl substituents causes that protons Hc and Hb are coupled ($^{3}J_{H,H}$= 5.0 Hz), and the corresponding signal assigned to Hc' appear as a double doublet at 4.60 ppm (**c**) while the signal corresponding to the Hc appear as a doublet at 4.40 ppm (**c'**). The other olefinic protons (Hb, Hd and He) appear at lower frequencies than the corresponding protons of the imidazolium salt precursor, due to the coordination to the metal.

The signal corresponding to the Hb appears at 5.2 ppm (**b**) as a multiplet, as consequence to the coupling with protons Hc, Hd and He. The resonances relative to the proton Hd appear at 3.47 ppm (**d**) as a doublet due to the *cis* coupling with He ($^{3}J_{H,H}$ = 9.0

Hz). The signal corresponding to He appear at 2.75 ppm (**e**) like a doublet due to the *trans* coupling with Hb ($^3J_{H,H}$ = 11.5 Hz). The protons at the 4 and 5 positions of the imidazole ring appeared as a singlet at 6.88 ppm (**a**).The remaining signals corresponding to the **cod** ligand.**Table 3.3** summarizes the signals of the ^{13}C {^1H} NMR spectra of complexes **2a**, **2b** and **2c**.

Table 3.3 ^{13}C signals for complexes **2a**, **2b** and **2c**.

^{13}C	δ (ppm) 2a	δ (ppm) 2b	δ (ppm) 2c
N*C*N	Not observed	161.2	Not observed
NC*X*CXN X=H, Cl, Me	120.6	114.6	124.7
$NCH_2CH{=}CH_2$	64.9	63.7	63.9
$NCH_2CH{=}CH_2$	51.6	51.1	49.2
$NCH_2CH{=}CH_2$	42.6	42.6	42.2

X-Ray diffraction studies of 2a, 2b and 2d

Suitable Crystals of **2a**, **2b** and **3** suitable for X-ray diffraction analysis were obtained by slow evaporation from concentrated dichloromethane-hexanes solutions. **Figure 3.12** shows the ORTEP diagram of complexes **2a** and **2b**.

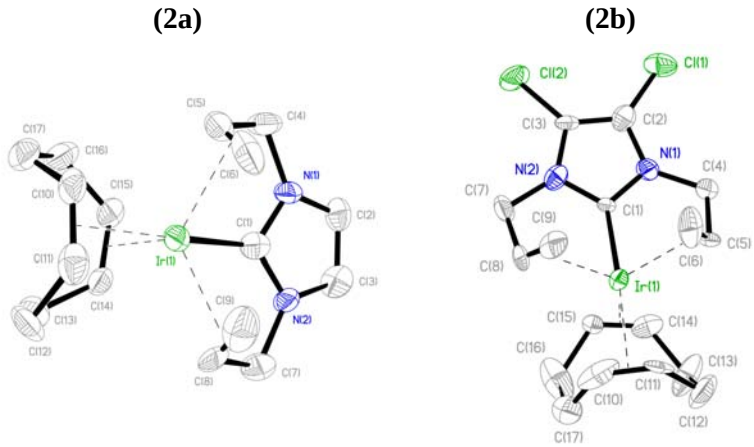

Figure 3.12. The ORTEP diagram of **2a** and **2b**. Ellipsoids are at 50% probability. Hydrogen atoms and the counterion have been omitted for clarity.

The molecular structures of complexes **2a** and **2b** confirm the *pincer* coordination of the NHC ligand as a result of the two olefins binding. The geometry about the iridium center (**Figure 3.12**) is best described as distorted trigonal bipyramidal. The equatorial plane is defined by the two olefinic fragments of the NHC-bis-allyl ligand and one C=C from COD, while the axial

axis is occupied by the other C=C from COD and the carbene-carbon. The relative orientation of the olefin fragments of the bisallyl ligand is *syn*, with the two olefins symmetry related by a plane perpendicular to the azole ring.

The *pincer* coordination of the NHC-bisallyl ligand seems to push the azol ring closer to the metal center, shortening the Ir-$C_{carbene}$ distance in ca. 0.1 Å. As a consequence, the iridium-carbene distance is in the expected range for complex **2d** (Ir-$C_{carbene}$ = 2.030(10) Å), but slightly shorter for complexes **2a** (1.934(9) Å) and **2b** (1.944(12) Å). All metal coordinated olefins show a longer C=C distance compared with the free alkene ($d_{C=C}$, 1.337 Å) as a consequence of the metal back-bonding into the olefin π^* orbital.**Table 3.4** summarizes the selected bond distances and angles of the molecular structure of **2a** and **2b**.

Table 3.4. Selected lenghts (Å) and angles (º) for **2a** and **2b**.

Bond	2a (Å)	2b (Å)	Angles	2a (º)	2b (º)
Ir(1)-C(1)	1.934(9)	1.944(12)	N(1)-C(1)-Ir(1)	123.9(7)	124.5(9)
Ir(1)-C(5)	2.214(8)	2.221(14)	N(1)-C(4)-C(5)-C(6)	57.7(11)	-56.8(17)
Ir(1)-C(6)	2.225(9)	2.248(18)			
Ir(1)-C(8)	2.308(8)	2.247(12)			
Ir(I)-C(9)	2.261(9)	2.203(12)			

Figure 3.13 shows the ORTEP diagram of compound **2d**.

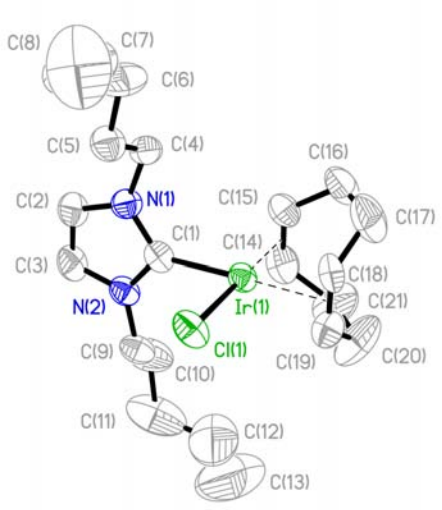

Figure 3.13. The ORTEP diagram of **2d**. Ellipsoids are at 35% probability. Hydrogen atoms have been omitted for clarity.

The structure of compound **2d** confirms that the two olefin fragments of the NHC remain unbound. The geometry about the iridium center is pseudo-square planar. The iridium-carbene

distance is in the expected range for complex **2d** (Ir-$C_{carbene}$ = 2.030(10) Å). **Table 3.5** includes the selected bond distances and angles for complex **2d**.

Table 3.5. Selected bond lenghts (Å) and angles (º) for **2d**.

Bond	Å	Ángles	(º)
Ir(1)-C(1)	2.030(10)	C(1)-Ir(1)-C(15)	93.4(4)
Ir(1)-Cl(1)	2.358(3)	C(1)-Ir(1)-Cl(1)	87.0(3)
		N(1)-C(1)-Ir(1)	127.6(7)
		C(14)-Ir(1)-Cl(1)	160.8(4)
		C(18)-Ir(1)-Cl(1)	92.2(3)

3.5 Catalytic Hydrosilylation

Before the results presented in this manuscript, our research group had carried out hydrosilylation studies with a series of Rh^I and Ir^I complexes using N-heterocyclic biscarbene ligands, bridging one or two metal unit (complexes **3.1**-**3.3**, **Scheme 3.15**), and compounds of Rh^I and Ir^I using N-heterocyclic tripodale ligands (complexes **3.4** and **3.5**, **Scheme 3.15**).[20,-22] Complex **3.1** is a good catalysts in the hydrosislylation of terminal alkynes like phenylacetylene or 1-Hexyne, at room temperature. In few cases, *dehydrogenative silylation* products were detected.[23]

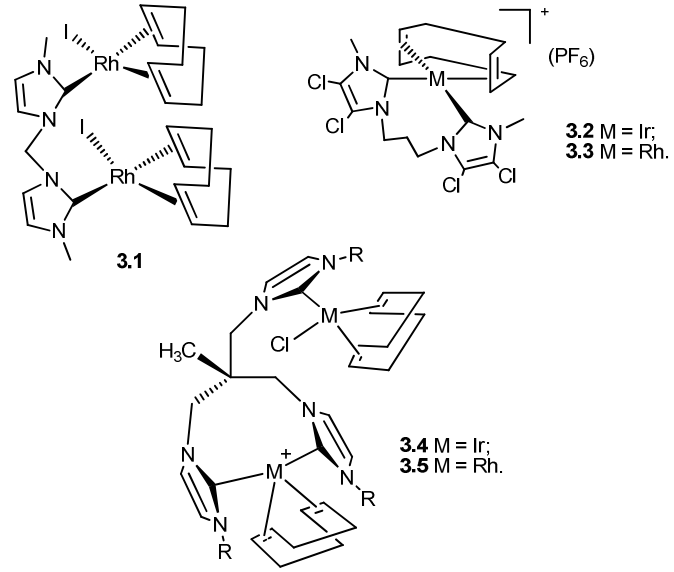

Scheme 3.15. Catalyst used in hydrosilylation reactions by our group.

In our laboratory, mechanistic studies in the hydrosilylation of acetylene were carried out with Ir^I complex **3.6**, using pyridine-functionalized carbene ligand (**Scheme 3.16**) [23]. Oxidant

addition tests were produced in order to analyze possible reaction intermediates during the catalytic cycle. This study showed that, under stoichiometric conditions, only the hydrosilylation product was formed. However, when the conditions were closer to those during catalysis, both hydrosilylation and silylation mechanisms were operative. This study was carried by means of trough Spectrometry Mass Experiments.[23]

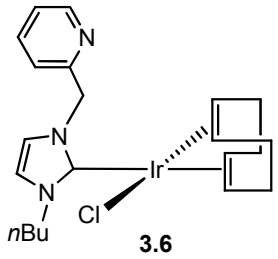

3.6

Scheme 3.16. Complex of Ir^{I} pyridine-functionalized carbene ligand.

Based on these previous results, the activity for addition of Si-H to alkynes of a series of NHC–Ir^{I} complexes functionalized with terminal olefins (**Scheme 3.17**) is now reported.

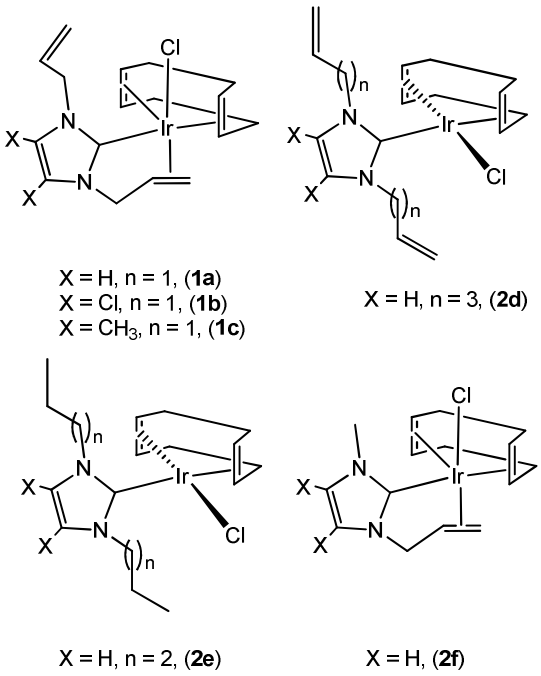

Scheme 3.17. Complexes used in the catalytic studies.

The hydrosilylation of terminal alkynes was carried out in $CDCl_3$ using a 1:1 hydrosilane/alkyne ratio. Catalytic experiments were monitored by ^{1}H NMR, registering yields at fixed times. The reaction evolution was analyzed comparing the signal of the starting

alkyne with the new olefins signals formed (β-E and β-Z), according to the results published previously.[6, 22]

Catalytic studies were carried out under aerobic conditions, employing different catalyst loadings (0.01, 0.1 y 1 mol %) and different temperatures (25 ºC and 60 ºC) in order to test the catalyst activity. To facilitate the monitoring evolution, standard substrates were used. As an example, the reaction of 1-hexyne and dimethylphenylsilane will be commented (**Scheme 3.18**). The evolution of this reaction is monitored by the progressive disappearance of the alkynic proton -C≡C*H* relative to 1-hexyne (triplet at 1.93 ppm), and the appearance of the signals corresponding to the products (doublet of triplets at 6.4 ppm, olefinic hydrogen of β-Z isomer and a double triplet at 6.1 ppm, olefinic hydrogen of β-E isomer). In our case we did not observed the formation of α isomer (two doublets into 5.38 and 5.83 ppm, corresponding to geminal protons).

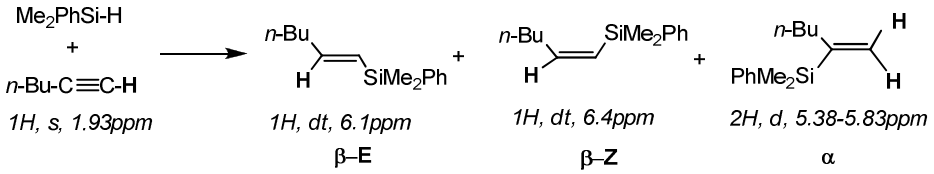

Scheme 3.18

Table 3.6 summarizes the catalytic results for the hydrosilylation of 1-hexyne and phenylacetylene at room temperature after 1h of reaction. For comparative reasons, in the catalytic studies we found convenient to obtain complexes **2e**[12] and **2f**[11] following the procedures reported in the bibliography.

All the studied compounds showed some activity under the reaction conditions used (1 mol% cat. loading); the best yields (68-92 %) were obtained for catalysts **1a** and **2f**. In general, the reaction proceeded with higher yields for the reduction of phenylacetylene, although catalysts **2d** and **2e** seem to present the reverse tendency. The 4,5-substituted azoles (**1b** and **1c**), present a lower activity than their unsubstituted analogue (**1a**), although this behaviour does not seem to follow a logical tendency if we consider the electronic modification of the ligands implied (compare, i. e. entries 1, 2, 3 and 7, 8, 9 in **Table 3.6**).

Noteworthy, high selectivity was achieved, with a clear preference to the *Z*-isomer, which in some cases is obtained as the only product. This selectivity was higher when catalysts **1** (**1a**, **1b** and **1c**) were used, compared to the selectivities shown by **2f** (compare, i.e. entries 1-3 and 6 in **Table 3.6**).

We believe that the second alkenyl branch of the catalyst in **1** (**1a**, **1b** and **1c**), may be having some steric influence in the selectivity of the reaction. Compound **2f**, with a small methyl group as a wingtip, has a reduced steric influence that seems to reduce the selectivity of the process (although high). In general, the selectivity obtained when using these catalysts, is

higher than that achieved with similar Ir^I and Rh^I species,[21, 24, 25] and lies among the highest reported to date for Ir complexes. Remarkably, the alpha isomer was not obtained in any of the experiments. Degradation of the catalytically active species was not observed in the hydrosilylation process, even at the end of the catalytic reaction. Employing catalyst **1a**, after the initial batch, two more runs were carried out without a measurable deactivation of the system, confirming the high stability of the NHC-metal complexes (**Table 3.6**, entries 8, 12).

Table 3.6. Hydrosilylation of alkynes at room temperature (hydrosilane = $HSiMe_2Ph$)[a].

Entry	Catalyst	Alkyne	Yield (%)[b]	α[d]	E[d]	Z[d]
1	**1a**	*n*BuC≡CH	68	--	7	93
2	**1b**	*n*BuC≡CH	21	--	--	100
3	**1c**	*n*BuC≡CH	25	--	--	100
4	**2d**	*n*BuC≡CH	71	--	12	88
5	**2e**	*n*BuC≡CH	46	--	9	91
6	**2f**	*n*BuC≡CH	55	--	17	83
7[c]	**1a**	PhC≡CH	92	--	28	72
8	**1b**	PhC≡CH	57	--	34	66
9	**1c**	PhC≡CH	45	--	20	80
10	**2d**	PhC≡CH	18	--	7	93
11	**2e**	PhC≡CH	0	--		
12[c]	**2f**	PhC≡CH	80	--	20	80

[a] Experimental conditions: Temperature 25 ºC, Time 1 h, Solvent $CHCl_3$. Alkyne (1eq), dimethylphenylsilane (1eq), catalyst loading (1 mol%) and ferrocene as internal reference (0.1 eq); [b] Yields determined by ^1H NMR spectroscopy. [c] Catalyst active at least for three runs. [d] Product distribution.

Table 3.7 shows the results on the catalytic hydrosilylation of phenylacetylene at 60 ºC. As expected, an increase of the reaction temperature results in an increase of the reaction yields with, again, catalysts **1a** and **2f** achieving the highest efficiencies in terms of yields. The selectivity on the *Z* hydrosilylated isomer was reduced, but still the reaction is highly selective, with yields between 65-90% leading to this reaction product, and only the β-isomers were obtained. Catalyst loadings as low as 0.1 and 0.01 mol % also provide high activity at 60 ºC, although slow kinetics were found (**Table 3.7**, entries 13, 14).

Table 3.7. Hydrosilylation of phenylacetylene at 60 ºC (hydrosilane = $HSiMe_2Ph$)[a].

Entry	Catalyst	Time (h)	Yield (%)[b]	α[f]	E[f]	Z[f]
1	**1a**	1	100	--	23	77
2	**1b**	1	70	--	10	90
3	**1c**	1	67	--	12	88
4	**2d**	1	36	--	21	79
5	**2e**	1	55	--	26	74
6	**2f**	1	100	--	27	73
7	**1a**	2	100	--	17	83
8	**1b**	2	100	--	23	76
9	**1c**	2	100	--	20	80
10	**2d**	2	100	--	20	80
11	**2e**	2	100	--	31	69
12	**2f**	2	100	--	35	65
13	**1a**[c]	2	85	--	30	70
14	**1c**[d]	2	45[e]	--	35	65

[a] Reaction conditions:Temp 60 ºC, Solvent $CHCl_3$. phenylacetylene (1eq), dimethylphenylsilane (1eq), ferrocene as internal reference (0.1 eq) and catalyst loading (1 mol%) unless otherwise stated; [b] Yields determined by ^1H NMR spectroscopy. [c] Catalyst loading (0.1 mol%). [d] Catalyst loading (0.01 mol%). [e] Full conversion was achieved after 24 h. [f] Product distribution.

According to the results of this catalytic survey, olefin functionalized NHC iridium complexes constitute a new family of catalysts for the addition of Si-H to alkynes. The high activity and selectivity indicate the potential of these catalysts for future applications.

Compound **1a** is a highly active and robust catalyst for the hydrosilylation of alkynes because it combines the high activity of the iridium with the stability of NHC ligand. It is worth to mention that the catalytic activity performed with these catalysts achieved the best results obtained in our laboratory till the date.

References

(1) Ojima,I., *The Chemistry of Organic Silicon Compounds* ed.; Wiley: New York, **1989**; 'Vol.' p 1479; Ojima, I.; Li, Z.; Zhu, J. *The Chemistry Of Organic Silicon Compounds* ed. Wiley: New York, **1998**; 'Vol.' p 168.

(2) (a) A.J. Chalk, J. F. Harrod, *J. Am. Chem. Soc.*, **1965**, *87*, 16; (b) Harrod, J. F.; Chalk, A. J.; Wender, I.; Pino, P. *Organic Synthesis via Metals Carbonyls* ed.; Wiley: (c) New York, **1977**, 'Vol.' 2, p 673; Schroeder, M. A.; Wrighton, M. S. *J. Organomet. Chem.***1977**, *128*, *345*.

(3) Jun, C.H.;Crabtree, R. H. *J. Organom. Chem*. **1993**, *447*, 177.

(4) I. Ojima, N. Clos, R. J. Donovan and P. Ingallina, *Organometallics*, **1990**, *9*, 3127.

(5) R. S. Tanke and R. H. Crabtree, *J. Am. Chem. Soc.*, 1**990**, *112*, 7984.

(6) R. H. Crabtree, *New. J. Chem.*, **2003**, *27*, 771.

(7) I. Ojima, M. Kumagai and Y. Nagai, *J. Organomet. Chem.*, **1974**, 66, C14.

(8) A. Zanardi, J. A. Mata, E. Peris, *New J. Chem*. **2008**, *32*, 120.

(9) R. Corberán, M. Sanaú, E. Peris, *Organometallics* **2007**, *26*, 3492.

(10) F. E. Hahn, C. Haltgrewe, T. Pape, M. Martin, E. Sola, L. A. Oro, *Organometallics* **2005**, *24*, 2003.

(11) F. E. Hahn, B. Heidrich, T. Pape, M. Martin, M.; A. Hepp, E. Sola, L. A. Oro, *Inorg*. *Chim*. *Acta* **2006**, *559*, 4840.

(12) A. Chianese, X. W. Li, M. C. Janzen, J. W. Faller, R. H. Crabtree, *Organometallics* **2003**, 22, 1663.

(13) M. J. Doyle, M. F. Lappert, *J. Chem. Soc.-Chem. Commun.*, **1974**, 679.

(14) a)D. Enders, H. Gielen, *J. Organomet. Chem.* **2001**, *617*, 70; b) D. Enders, H. Gielen, K. Runsink, S. Breuer, S. Brode, K. Boehn, *Eur. J. Inorg. Chem*., **1998**, 913.

(15) J. W. Akitt, B. E. Mann, *NMR and Chemistry*, Edition Stanley Thornes, London, **2000**.

(16) J. Sandstrom, *Dynamic NMR Spectroscopy*, Academic Press, London, **1982**.

(17) F. A. Jalon, B. R. Manzano, F. Gomez-de la Torre, A. M. Lopez-Agenjo, A. M. Rodriguez, W. Weissensteiner, T. Sturm, J. Mahia and M. Maestro, *J. Chem. Soc.-Dalton Trans.*, **2001**, 2417-2424.

(18) C. P. Casey, M. A. Fagan and S. L. Hallenbeck, *Organometallics*, 1998, **17**, 287-289.

(19) M. V. Galakhov, G. Heinz and P. Royo, *Chem. Commun.*, **1998**, 17-18.

(20) M. Poyatos, E. Mas-Marza, J. A. Mata, M. Sanau, E. Peris, *Eur. J. Inorg. Chem*. **2003**, 1215.

(21) M. Poyatos, M. Sanau, E. Peris, *Inorg. Chem*., **2003**, *42*, 2572.

(22) E. Mas-Marza, M. Poyatos, E. Peris, *Inorg. Chem*., **2004**, *43*, 2213.

(23) C. Vicent, M. Viciano, E. Mas-Marzá, M. Sanaú, E. Peris, *Organometallics* **2006**, *25*, 3713.

(24) M. Poyatos, J. Uriz, J. Mata, C. Claver, E. Fernandez, E. Peris, *Organometallics*, **2003**, *22*, 440.

(25) M. Poyatos, A. Maisse-Francois, S. Bellemin-Laponnaz, L. H. Gade, *Organometallics*, **2006**, *25*, 2634.

Summary

Summary

The research described in this work concerns the design of new-homogeneous catalysts using two different types of ligands: triazolyl-di-ylidene and bis-alkenyl-NHCs. The aim of this work was to use these classes of ligands in order to obtain compounds with new fundamentally advantageous properties and also study repercussions in catalysis:

a) Triazolyl-di-ylidene:

The 1,2,4-trimethyltriazolium tetrafluoroborate was coordinated to a variety of metals in order to obtain stable homo- and hetero-bimetallic complexes. The synthesis and characterization of the heterobimetallic species represents a breakthrough in the design of tandem catalysts that can be applied in catalytic sequences formed by distinct reactions:

- We have described the synthesis of new palladium and platinum homobimetallic complexes (**4L**, **5L**, **6L** and **7L**) in which the triazolyl-di-ylidene (ditz) ligand is bridging two metallic fragments. The structure of compound **5L** consists of a 12-membered metallacycle formed by a double CH activation of two terminal methyl groups of a $Pd(acac)_2$ molecule, a situation that has no precedent in the literature. Complexes **4L** and **5L** showed activity in the C-C coupling reaction, while only **4L** showed good activity in the acylation of aryl halides with aldehydes, a recently reported reaction that we carried out in the absence of phosphines.
- Complex **6L** and other related Pd-NHC complexes (**8L** and **9L**), provided good results in the consecutive Sonogashira/cyclic hydroalkoxylation reactions between *o*-hydroxyaryl halides and phenylacetylene, to directly afford benzofurans. This tandem process provides a clear benefit compared to the traditional methods for the preparation of benzofurans that implies the same reactions sequence but with the isolation of the Sonogahira coupling intermediate followed by the cyclic hydroalkoxylation that usually requires different reaction conditions including a different catalyst.
- We have described the preparation of heterobimetallic complexes of Rh^{I}/Ir^{III} (**13L**) and mixed valence complex of Ir^{III}/Ir^{I} (**12L**) with the bridging triazolyl-di-ylidene ligand. The catalytic activities of our new compounds have been tested in a tandem reaction implying the oxidative cyclization of an amino alcohol to produce indole that is alkylated by a primary alcohol to selectively produce the 3-alkylated species or the bisindolylmethane compound. Our results show not only that our compounds are highly effective for this tandem process but also that the heterobimetallic complex (**12L**) show different activity than the homobimetallic species, in the sense, the activity of the heterometallic catalysts can not be regarded as the sum of the individual components of the complexes, thus implying that the connection of two different metal fragments through the *ditz* ligand may have important consequences in catalytic cooperativity.

- We have prepared a set of three different heterometallic complexes of Ir/Pd (**14L**, **15L** and **17L**), in which the metals are connected through the triazolyl-di-ylidene ligand. These complexes proved to be active catalysts in three different tandem processes, namely the dehalogenation/transfer hydrogenation of haloacetophenones, Suzuki-coupling/transfer hydrogenation of *p*-bromoacetophenone, and Suzuki-coupling/α-alkylation of *p*-bromoacetophenone. These tandem reactions are valuable catalytic transformations that have not been reported before and constitute a clear advance over the synthetic procedures to the same final products. The use of a single well-defined catalyst (either **14L**, **15L**, or **16L**) yields a better catalytic outcome than a mixture of two homobimetallic compounds (**3L** + **6L**). All three tandem reactions described previously constitute efficient methods for the generation of organic molecules by one-pot procedures, combining two different processes typically catalyzed by distinct metals.
- Complex **15L** was also used in another new tandem catalytic process. The process implies the unprecedented preparation of imines from the direct reaction of nitroarenes and primary alcohols. The oxidation of the alcohol (iridium-catalyzed) generates hydrogen, which can be further used by the palladium fragment of the heterometallic species to reduce the nitroarene to aniline. Then the final step of the process would be the non metal-mediated condensation beween the aniline and the aldehyde to afford the final imine. For this reaction, four homo- and heterobimetallic catalysts of Ir and Pd have been tested. The results provided by the bis-iridium complexes are remarkable, although limited to several substrates. However, the presence of the palladium fragment in the Ir/Pd complex **15L** improves the catalyst activity widening its applicability, most probably because the presence of the Pd opens a new reaction pathway in the reduction of the nitro group by using the hydrogen released in the oxidation of the alcohol by the iridium moiety.
- We synthesized a new Ir/Pt complex with the di-carbene ligand *ditz*. The easy access to the Ir-Pt heterobimetallic complex (**16L**) allowed us to study a tandem process implying three consecutive catalytic reactions, namely the oxidative cyclization of aminoalcohols to form indole (iridium-catalyzed), the intramolecular hydroalcoxylation of an alkynyl alcohol to afford a cyclic enol ether (platinum-catalyzed) and the addition of the C-H bond of indole to the unsaturated moiety of the cyclic enol ether (platinum-catalyzed). The ability of the Ir-Pt complex **16L** confirms the wide applicability of ditz-based heterobimetallic complexes in the design of new and complex tandem processes. The preparation of substituted indoles from the direct reaction of 2-aminophenylethylalcohol and alkynyl alcohols is an unprecedented process that may have some industrial applications. Again, the use of **16L** provides better catalytic outcomes than the use of mixtures of the corresponding

homobimetallic catalysts (**3L** and **7L**), suggesting that some catalytic cooperativity may be at play between the two vicinal metals.

b) bis-alkenyl NHCs:

A family of alkenyl-functionalized N-heterocyclic-carbene-Ir^{I} complexes were synthesized, providing a series of mono-coordinated, chelate and pincer alkenyl-NHC species. Olefin coordination is highly influenced by the nature of the substituents on the NHC ring, and on the length of the alkenyl branch. A fluxional process involving coordination/decoordination of the olefin in bis-allyl-NHC complexes has been studied, and the activation parameters have been determined by means of VT-NMR spectroscopy. The mono-coordinated complexes resulted highly active in the hydrosilylation of terminal alkynes, showing high selectivity for the Z-isomers, with no α-isomers or dehydrogenative silylation processes being observed

Chapter 4

Experimental Section

4.1 Analytical Techniques

NMR Spectra

NMR spectra were recorded on Varian spectrometers operating at 300 or 500 MHz (^{1}H NMR) and 75 and 125 MHz ($^{13}C\{^{1}H\}$ NMR), respectively, and referenced to $SiMe_4$ (δ in ppm and J in Hertz), using $CDCl_3$, CD_2Cl_2, CD_3CN, acetone-d_6 and DMSO-d_6 as solvents.

Electrospray MS and ESI-TOF-MS

Electrospray mass spectra (ESI-MS) were recorded on a Micromass Quatro LC instrument; nitrogen was employed as drying and nebulizing gas.

A QTOF I (quadrupole-hexapole-TOF) mass spectrometer with an orthogonal Z-spray-electrospray interface (Micromass, Manchester, UK) was used. The drying gas as well as nebulizing gas was nitrogen at a flow of 400 L/h and 80 L/h respectively. The temperature of the source block was set to 120 °C and the desolvation temperature to 150 °C. A capillary voltage of 3.5 KV was used in the positive scan mode, and the cone voltage was set to 30 V. Mass calibration was performed using a solution of sodium iodide in isopropanol: water (50:50) from *m*/*z* 150 to 1000 amu. Sample solutions (aprox 1 × 10-4 M) in dichlormethane:methanol (50:50) were infused via a syringe pump directly connected to the interface at a flow of 10 μL/min. A 1 μg/mL solution of 3,5-diiodo-L-tyrosine was used as a lock mass.

Elemental Analysis

Elemental analyses were carried out on a EuroEA3000 Eurovector analyzer.

GC and GC/MS

A gas chromatograph GC-2010 (Shimadzu) equipped with a FID and a Teknokroma (TRB-5MS, 30m × 0.25 mm × 0.25 μm) column and Gas chromatograph/Mass spectrometer GCMS-QP2010 (Shimadzu) equipped with a Teknokroma (TRB- 5MS, 30m × 0.25 mm × 0.25 μm) column were used.

GC-FID calibration was performed using an internal standard (normally anisole) and known concentrations of products versus reagents. The calibration curve was obtained using the same range and conditions used in the catalytic experiments. The final product concentration was confirmed by ^{1}H NMR using anisole as standard and, in some cases, by isolation of the products.

X-Ray Diffraction studies

Single crystals were obtained mainly with slowly diffusion of a mixture of solvents and evaporation to dryness. Then, they were mounted on a glass fiber in a random orientation. Data collection was performed at low or at room temperature on a Siemens Smart CCD

diffractometer using graphite monochromated Mo KR radiation (λ) 0.71073 Å) with a nominal crystal to detector distance of 4.0 cm. Space group assignment was based on systematic absences, E statistics, and successful refinement of the structures. The structure was solved by direct methods with the aid of successive difference Fourier maps and were refined using the SHELXTL 6.1 software package.[1] All non-hydrogen were refined anisotropically. Hydrogen atoms were assigned to ideal positions and refined using a riding model. Details of the data collection, cell dimensions, and structure refinement are given at the end of this chapter. The diffraction frames were integrated using the SAINT package.[2]

4.2 Working Techniques and Reagents

The synthesis of monocarbene iridium complexes and the homo- and hetero- dimetallic species with the bis-carbene, were carried out under nitrogen atmosphere using the standard Shlenck techniques. Solvents were dried and degassed with the general procedures before used. $[IrCl(cod)]_2$[3], $[Cp^*IrCl_2]_2$[4], $[Pd(acac)_2]$[5] 1,3-Bis(2-propenil)imidazolium bromine[6], dimethyl-1,3-Bis(2-propenyl)-imidazolium hexafluorofosphate[6], 1,3-bis(N-methyl)imidazolium chloride and 1,4-bis(N-methyl)triazolium chloride[7] and 1,2,4-trimetiltriazolium tetrafluoroborate[8] were prepared following the procedures described in the bibliography. Metallic complexes such as $[RhCl(cod)]_2$, $PdCl_2$, $Pd(OAc)_2$, $PtCl_2$ and PtI_2 were acquired from commercial suppliers without any further purification.

All other reagents were used as received from commercial suppliers (Aldrich, Alfaesar or Merck). Chromatography purifications were performed on silica gel (silica gel 60, Merck, particle size 0.063-0.200 mm). Pressurized nitrogen was used to accelerate the purification.

4.2.1 Hydrosilylation of terminal alkynes:

In a Schlenk tube and under aerobic conditions, alkyne (1 eq.), dimethylphenylsilane (1 eq.), catalyst (1 mol %), Ferrocene (0.1 eq.; internal standard) were dissolved in 10 ml of $CHCl_3$. The mixture was stirred at room temperatur or at 60 ºC during 24h. Conversions and concentrations of isomers were monitored by ^{1}H NMR spectroscopy taking aliquots (0.5 ml) at the appropriate time.

4.2.2 One-Pot Synthesis of 3-Substituted Indoles from 2-Aminophenyl Ethyl Alcohol and Primary Alcohols:

A mixture of 2-aminophenyl ethyl alcohol (0.25 mmol), primary alcohol (0.25 mmol), catalyst (1 or 0.1 mol %), KOH (0.5 mmol), and toluene (0.3 mL) was combined in a thick-walled glass tube. The mixture was stirred at 110 °C. The reaction mixture was analyzed by ^{1}H NMR spectroscopy, and products were characterized according to previously reported spectroscopic data.[9, 10, 11] Ferrocene (0.025 mmol) was used in all cases as an internal standard.

4.2.3 Heck Reaction:

In a typical run an oven-dried tube containing a stirrer bar was charged with 4-bromoacetophenone (0.4 mmol), styrene (0.6 mmol), Cs_2CO_3 (0.8 mmol), TBABr (0.04 mmol), catalyst (1 mol %), and 750 μL of toluene. The solution was heated to 100 °C for 15 h. Conversions were determined by ^{1}H NMR spectroscopy. Ferrocene (0.04 mmol) was used as an internal standard.

4.2.4 Direct Acylation of Aryl Bromides with Aldehydes:

An oven-dried tube containing a stirrer bar was charged with an aryl bromide or iodide (0.5 mmol), catalyst (2 mol%), TBABr (0.05 mmol), and 4 Å molecular sieves (1 g). After degassing three times with nitrogen, dry *N*,*N*-dimethylformamide (DMF) (2 mL), aldehyde (0.6 mmol), and pyrrolidine (1 mmol) were injected sequentially. The reaction mixture was stirred at 115 °C for 6-22 h. After cooling to room temperature, 8 mL of EtOAc was added, and the mixture was washed with H_2O (3 × 2.5 mL) to remove the DMF, dried over Na_2SO_4, and concentrated under vacuum. Conversions were determined by ^{1}H NMR spectroscopy.

4.2.5 Consecutive Sonogashira/Cyclic Alkyne Hydroalkoxylation:

In a typical run a capped vessel containing a stirrer bar was charged with the corresponding halobenzyl alcohol (0.53 mmol), phenylacetylene (0.75 mmol), Cs_2CO_3 (1.57 mmol), anisole as internal reference (0.525mmol), catalyst (1% mol palladium) and DMSO (3 mL). The reaction mixture was stirred at 80 ºC for the appropriate time. Yields and conversions were determined by GC chromatography. Isolated yields were determined by ^{1}H NMR spectroscopy after column chromatography purification. Catalytic reactions were carried out under air and with regular solvents.

4.2.6 Dehalogenation/Transfer Hydrogenation of Halo-Acetophenones:

In a typical run a capped vessel containing a stirrer bar was charged with the corresponding 4-haloacetophenone (0.36 mmol), Cs_2CO_3 (0.43 mmol), anisole as internal reference (0.36 mmol), catalyst (2 mol %), and 2 mL of 2-propanol. The reaction mixture was stirred at 100 °C for the appropriate time. Reaction monitoring, yields, and conversions were determined by GC chromatography. Products and intermediates were characterized by GC/MS. Isolated products were characterized by ^{1}H NMR and ^{13}C NMR after column chromatography purification using *n*hexanes/ ethylacetate (9:1).

4.2.7 Suzuki-Miyaura Coupling/Transfer Hydrogenation or α-Alkylation of Ketones:

A capped vessel containing a stirrer bar was charged with 4-bromoacetophenone (0.36 mmol), phenylboronic acid (0.55 mmol), Cs_2CO_3 (1.08 mmol), anisole as internal reference (0.36

mmol), catalyst (2 mol %), 2 mL of alcohol, and 2 mL of THF. The solution was heated to 100 °C for the appropriate time. The resulting products were characterized by comparing the spectroscopic data of the isolated compounds with those reported in the literature.[12]

4.2.8 Reduction of nitrobenzene to aniline using H_2:

Molecular hydrogen was added with a balloon filled with one atmosphere of gas to a mixture of nitrobenzene (0.3 mmol), Cs_2CO_3 (0.3 mmol), anisole as internal reference (0.3 mmol) and catalyst (2 mol %) in 500 μL of toluene. Three cycles of vacuum/H_2 were made before putting the reaction vessel in an oil bath at 100 ºC for the appropriate time. Yields and conversions were determined by GC chromatography.

4.2.9 Condensation of nitroarenes and primary alcohols:

In a capped vessel containing a stirrer bar was charged with nitrobenzene (0.3 mmol), benzylalcohol (5.0 mmol), Cs_2CO_3 (0.3 mmol), anisole as internal reference (0.3 mmol) and catalyst (0.5 or 2 mol %). The solution was heated to 110 ºC for the appropriate time. Yields and conversions were determined by GC chromatography. Products and intermediates were characterized by GC/MS. Isolated products were characterized by ^{1}H NMR and ^{13}C NMR after column chromatography purification using mixtures of *n*-hexanes/ ethylacetate. The confirmation of the nature of the products was performed by comparison with the literature data.[13]

4.2.10 Cyclization-Addition reaction of Indole with Alkynyl alcohol: In a capped vessel containing a stirrer bar was charged with indole (0.3 mmol), alkynyl alcohol (0.36 mmol), silver trilate (3 %), anisole as internal reference (0.3 mmol), catalyst (1 %) in 1.5 mL of acetonitrile. The solution was heated to 80 ºC for the appropriate time. During the reaction monitoring, yields and conversions were determined by GC chromatography. Products and intermediates were characterized by GC/MS. Isolated products were characterized by ^{1}H NMR and ^{13}C NMR after column chromatography purification using mixtures of n-hexanes/ethylacetate.

4.2.11 Sequential Oxidation/Cyclization of Amino alcohol to Indole and functionalization with alkynyl alcohol:

In a capped vessel containing a stirrer bar was charged with 2-aminophenethyl alcohol (0.33 mmol), silver trilate (0.03 mmol), anisole as internal reference (0.3 mmol), catalyst (2 %) in 800 μL of toluene. The solution was heated to 110 ºC for the appropriate time. After complete conversion to indole, alkynyl alcohol (0.38 mmol) was added and the final solution was stirred at the same temperature for additional 3h. During the reaction monitoring, yields and

conversions were determined by GC chromatography. Products and intermediates were characterized by GC/MS. Isolated products were characterized by ^{1}H NMR and ^{13}C NMR after column chromatography purification using mixtures of *n*-hexanes/ethylacetate

4.3 Synthesis and characterization

SYNTHESIS OF IMIDAZOLIUM SALTS

1-(4-pentenyl)-imidazol: In a round bottom flask, imidazole (1.4 g, 20.6 mmol), KOH (1.4 g, 25.7 mmol), TBABr (200 mg, 0.62 mmol) and few drops of H_2O were added. The mixture was stired for 1 h at room temperature. After that, 4-pentenyl bromine (2.8 g, 24.7 mmol) was added. The reaction was stirred for addtional 24h at the same temperature. The mixture was then extracted with H_2O/CH_2Cl_2 (3 x 50 ml) and the organic fractions were dried on Na_2SO_4. The solvent was evaporated at reduced pressure and the crude was purified with a column chromatography using mixture acetone/CH_2Cl_2 (1:1). Yield: 2.34 g, 83 %, orange oil.
^{1}H NMR (500 MHz, $CDCl_3$): δ 7.43 (s, 1H, NC*H*N), 7.03 (s, 1H, NC*H*CHN), 6.87 (s, 1H, NCHC*H*N), 5.79 (m, 1H, -C*H*=CH_2), 5.05 (m, 2H, -CH=C*H*$_2$), 3.94 (m, 2H, NC*H*$_2$), 2.07 (m, 2H, -C*H*$_2$-), 1.90 (m, 2H, -C*H*$_2$-).

3-Bis(4-pentenil)-imidazol bromine (d). 4-pentenyl bromine (1 mL, 8,76 mmol) and N-4-pentenylimidazol (1g, 7.3 mmol) reacted without solvents for for 4 h at 80 ºC. The solid obtained was washed with diethyl ether (3 x 50 ml) and dried under vacuum. Yield: 1.8 g, 86 %.^{1}H NMR (500 MHz, $CDCl_3$): δ 10.59 (s, 1H, NC*H*N), 7.42 (s, 2H, NC*H*C*H*N), 5.76 (m, 2H, -C*H*=CH_2), 5.03 (m, 4H, -CH=C*H*$_2$), 4.38 (t, $^{3}J_{HH}$ = 7.2 Hz, 4H, NC*H*$_2$-), 2.15 (m, 4H, -C*H*$_2$-), 2.08 (m, 4H, -C*H*$_2$-). $^{13}C\{^{1}H\}$ NMR (75.4 MHz, $CDCl_3$): δ 136.5(N*C*N), 136.1 (-*C*H=CH2), 122.6 (N*C*H*C*HN), 116.2 (-CH=*C*H_2), 49.2 (NCH_2-), 30.0(-CH_2-), 29.2 (-CH_2-).

4, 5-dichloro-1-(2-propenyl)-imidazol. Allyl bromine (690 µl, 8 mmol) and KOH (616 mg, 11 mmol) were added to a solution of 4,5-dichloroimidazole (1g, 7.3 mmol) in MeOH (15 ml) and the mixture was refluxed for 24 h. The solution was then filtered and solvent was evaporated at reduced pressure. The crude was extracted with H_2O/CH_2Cl_2 (3 x 50 ml). The organic layer was dried on Na_2SO_4 and concentrated in vacuum. Yield: 1.07 g, 71 %.
^{1}H NMR (500 MHz, $CDCl_3$): δ 7.36 (s, 1H, NC*H*N), 5.94 (m, 1H, NCH_2C*H*=CH_2), 5.33 d, $^{2}J_{HH}$ = 10.2 Hz, NCH_2CH=CH*Hcis)*, 5.17 (d, 1H, NCH_2CH=CH*Htrans*,$^{2}J_{HH}$ = 15 Hz), 4.51 (d, 2H, NC*H*$_2$CH=CH_2, $^{3}J_{HH}$ = 5.7 Hz).

4, 5-dichloro-1,3-Bis(2-propenyl)-imidazol bromine (b). Allyl bromine (1.38 ml, 16 mmol) and 4, 5-dichloro-1-(2-propenyl)-imidazol (2.4 g, 14 mmol) reacted without solvent for 12 h at 70 ºC. The solid obtained was washed with diethyl ether (3 x 50 ml) and dried under vacuum.

Yield: 3.5 g, 85%.^{1}H NMR (300 MHz, $CDCl_3$): δ 8.82 (s, 1H, NC*H*N), 6.02 – 5.97 (m, 2H, -C*H*=CH_2), 5.54 – 5.47 (m, 4H, -CH=CH_2), 4.82 (d, 4H, $^{3}J_{HH}$ = 6.3 Hz, N-CH_2-).
^{13}C{^{1}H} NMR (75.4 MHz, $CDCl_3$): δ 136.8 (N*C*N), 128.1 (*C*-Cl),124.1 (-CH=*C*H_2), 123.9 (-CH=*C*H_2), 51.8 (NCH_2-).

SYNTHESIS OF ORGANOMETALLIC COMPLEXES

Synthesis of complex 1a

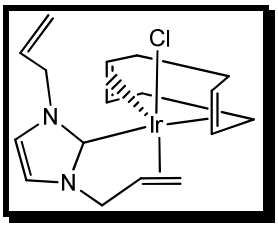

Silver oxide (63 mg, 0.27 mmol) was added to a solution of 1,3-bis(2-propenyl)imidazolium bromide (55 mg, 0.3 mmol) in MeOH. The solution was stirred at room temperature for 1 h and filtered through Celite. The solution was concentrated under reduced pressure and redissolved in dichloromethane. $[IrCl(COD)]_2$ (100 mg, 0.15 mmol) was added and the mixture was stirred for 1 h at 45º 1C. After solvent removal, the crude product was purified by flash chromatography using CH_2Cl_2/MeOH (7: 3) as the eluent (yield 117 mg, 80%).
^{1}H NMR (500 MHz, $CDCl_3$, T = - 15 ºC): δ 6.89 (s, 1H, NCHC*H*N), 6.67 (s, 1H, NCHC*H*N), 5.92 (m, 1H,NCH_2C*H*=CH_2, not coordinated), 5.52 (dd, $^{3}J_{HH}$ = 4.5 Hz, $^{2}J_{HH}$ = 17.0 Hz, 1H, NCH*H*CH=CH_2, not coordinated), 5.13 (d, $^{3}J_{HH}$ = 10.5 Hz, 1H, NCH_2CH=CHH_{cis}, not coordinated), 4.89 (d, $^{3}J_{HH}$ = 17 Hz, $NCH_2CH=CH_{Htrans}$, not coordinated), 4.66 (m, 2H, NC*H*HCH=CH_2, not coordinated and cod), 4.23 (m, 2H, NCH*H*CH=CH_2, coordinated y NCH_2C*H*=CH_2, coordinated), 3.70 (d, $^{3}J_{HH}$ = 15 Hz, NC*H*HCH=CH_2, coordinated), 3.54 (m, 1H, cod), 3.44 (m, 1H, cod), 2.93 (m, 1H, cod), 2.70 (m, 2H, cod), 2.49 (m, 1H, cod), 2.39 (m, 2H, cod), 2.08 (d, 1H, $^{3}J_{HHcis}$ = 7.5 Hz, NCH_2CH=CH*H*, coordinated), 1.93 (m, 2H, COD), 1.89 (d, 1H, $^{3}J_{HHtrans}$ = 9.0 Hz, NCH_2CH=C*H*H), 1.61 (m, 1H, cod).
^{13}C{^{1}H} NMR (75 MHz, $CDCl_3$): δ 161.9 (N*C*N), 135.4 (NCH_2*C*H=CH_2, not coordinated), 122.2 (N*C*HCHN), 118.0 (NCH*C*HN), 117.5 ($NCH_2CH=CH_2$, coordinated), 99.0, 97.7, 60.6, 55.6 (cod), 52.89 ($NCH_2CH=CH_2$, coordinated), 52.5 (NCH_2CHQCH_2, not coordinated), 47.27 (NCH_2*C*H=CH_2, coordinated), 41.0 (cod), 35.9 (N*C*H_2CH=CH_2, coordinated), 33.4, 29.6, 28.1 (cod). Electrospray Ms. (cone 25 V): m/z (fragment) 449.4 $[M - Cl]^{+}$.

Synthesis of complex 1b

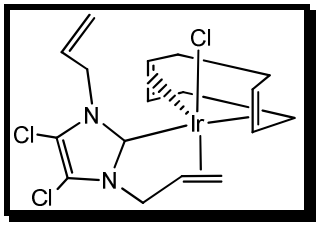

The synthesis of complex **1b** was carried out using the same general procedure as described for complex **1a** using silver oxide (76 mg, 0.33 mmol), 4,5-dichloro-1,3-bis(2-propenyl)imidazolium hexafluorophosphate (89 mg, 0.30 mmol) and $[IrCl(COD)]_2$ (100 mg, 0.15 mmol) (yield 114 mg, 70%).

^{1}H NMR (500 MHz, $CDCl_3$): δ 5.97 (d, 1H, $^2J_{HH}$ = 17 Hz, NCH*H*CH=CH_2, not coordinated), 5.78 (m, 1H, NCH_2CH=CH_2, coordinated), 5.08 (m, 1H, NCH_2CH=CH_2, not coordinated), 4.68 (m, 2H, NCH_2CH=CH_2, not coordinated), 4.46 (m, 1H, NCH*H*CH=CH_2, not coordinated), 4.13 (m, 2H, NCH*H*CH=CH_2, coordinated and NCH_2CH=CH_2, coordinated) , 3.77 (d, $^2J_{HH}$ = 11 Hz, NCH*H*CH=CH_2, coordinated), 3.59 (m, 1H, cod), 3.46 (m, 1H, cod), 3.34 (m, 1H, cod), 2.87 (m, 2H, cod), 2.68 (m, 1H, cod), 2.38 (m, 2H, cod), 2.28 (m, 1H, NCH_2CH=CH*H*, coordinated), 2.00 (m, 2H, cod), 1.91 (m, 1H, NCH_2CH=CH*H*), 1.58 (m, 2H, cod).

^{13}C{^{1}H} NMR (75 MHz, $CDCl_3$): δ 161.6 (N*C*N), 134.05 (NCH_2*C*H=CH_2, not coordinated), Cl–*C* not observed, 115.8 (NCH_2CH=*C*H_2, not coordinated), 99.41, 97.9, 61.2, 56.0 (COD–CH), 52.3 (NCH_2CH=*C*H_2, coordinated), 50.55 (N*C*H_2CH=CH_2, not coordinated), 44.5 (NCH_2*C*H=CH_2, coordinated), 40.9 (COD–CH2), 35.5 (N*C*H_2CH=CH_2, coordinated), 33.15, 28.80, 27.48 (cod). Electrospray Ms. (cone 25 V): m/z (fragment) 517.1 $[M - Cl]^+$.

Synthesis of complex 1c

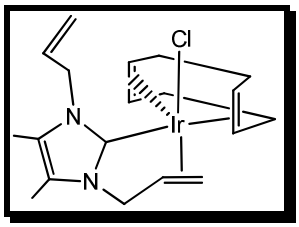

The synthesis of complex **1c** was carried out using the same general procedure as described for complex **1a** using silver oxide (94 mg, 0.45 mmol), 4,5-dimethyl-1,3-bis(2-propenyl)imidazolium chloride (95 mg, 0.45 mmol) and $[IrCl(COD)]_2$ (150 mg, 0.22 mmol) (yield 148 mg, 66%).

^{1}H NMR (500 MHz, $CDCl_3$): δ 5.85 (m, 2H, NCH*H*CH=CH_2, NCH_2CH=CH_2, not coordinated), 5.03 (d, $^2J_{HH}$ = 15.5 Hz, 1H, NCH_2CH=C*H*$_2$, not coordinated), 4.60 (m, 1H, NCH_2CH=C*H*$_2$, not coordinated), 4.18 (m, 2H, cod, NCH*H*CH=CH_2, not coordinated), 4.01 (m, 2H, NCH*H*CH=CH_2, coordinated and cod), 3.61–3.43 (m, 4H, NCH*H*CH=CH_2, NCH_2CH=CH_2, coordinated and cod), 3.30 (m, 1H, cod), 2.95 (m, 2H, cod), 2.85 (m, 2H, cod), 2.38 (m, 1H, cod), 2.28 (m, 1H, NCH_2CH=CH*H*, coordinated), 2.06 (s, 3H, C*H*$_3$), 1.91 (m, 1H, NCH_2CH=CH*H*, coordinated), 1.89 (s, 3H, C*H*$_3$), 1.54 (m, 2H, cod).

^{13}C{^{1}H} NMR (75 MHz, $CDCl_3$): δ 158.9 (NCN), 136.1 (NCH_2*C*H=CH_2, not coordinated), 125.8 (*C*–CH_3), 122.2 (*C*–CH3), 114.5 (NCH_2CH=*C*H_2, not coordinated), 98.3, 96.7, 60.1, 55.3 (cod), 50.3 (NCH_2CH=*C*H_2, coordinated), 49.4 (N*C*H_2CH=CH_2, not coordinated), 46.1 (NCH_2*C*H=CH_2, coordinated), 41.2 (cod), 35.8 (N*C*H_2CH=CH_2, coordinated), 33.3, 29.0, 27.5 (cod), 9.7 (*C*H_3), 8.9 (*C*H_3). Electrospray MS. (cone 25 V): m/z (fragment) 477.2 $[M - Cl]^+$

Synthesis of complex 2a

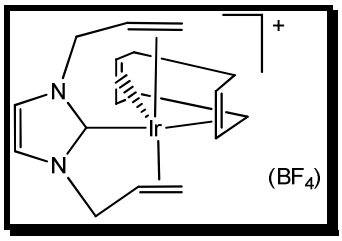

To a solution of complex **1a** (44 mg, 0.09 mmol) in acetone was added $AgBF_4$ (18 mg, 0.09 mmol), and the mixture was stirred at room temperature for 4 h. The suspension was filtered

through Celite and the solution concentrated under reduced pressure. Precipitation with diethyl ether (6 mL) afforded a solid (yield 40 mg, 82%).

^{1}H NMR (500 MHz, $CDCl_3$): δ 6.88 (s, 2H, NC*H*C*H*N), 5.19 (m, 2H, NCH_2CH=CH_2), 4.73 (m, 2H, cod), 4.60 (dd, $^{3}J_{HH}$ =5.0 Hz, $^{2}J_{HH}$ =13.0 Hz, 2H, NCH*H*CH=CH_2), 4.40 (d, 2H, $^{2}J_{HH}$ = 13.5 Hz, NCH*H*CH=CH_2), 3.52 (m, 2H, cod), 3.47 (d, $^{3}J_{HH}$ =9.0 Hz, 2H, NCH_2CH=CHH_{cis}), 2.85 (m, 2H, cod), 2.75 (d, $^{3}J_{HH}$ = 11.5 Hz, 2H, NCH_2CH=CHH_{trans}), 2.72 (m, 2H, cod), 2.29 (m, 4H, cod).

^{13}C{^{1}H} (75 MHz, $CDCl_3$): δ N*C*N not observed, 120.6 (N*C*H*C*HN), 93.7, 74.0 (cod), 64.9 (NCH_2CH=CH_2), 51.6 (N*C*H_2CH=CH_2), 42.6 (NCH_2CH=CH_2), 32.8, 31.4 (cod). Electrospray Ms. (Cone 25 V): m/z (fragment) 449.1 $[M]^+$.

Synthesis of complex 2b

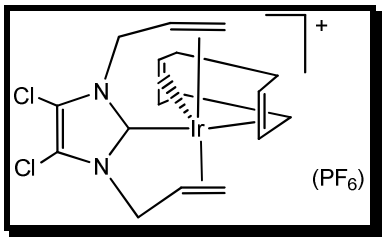

The synthesis of complex **2b** was carried out using the same general procedure as described for complex **2a** but followed by anion exchange (PF_6^-) using complex **1b** (75 mg, 0.13 mmol) and $AgBF_4$ (25 mg, 0.13 mmol) (yield 68 mg, 92%).

^{1}H NMR (500 MHz, $CDCl_3$): δ 5.22 (m, 2H, NCH_2CH=CH_2), 4.91 (m, 2H, cod), 4.55 (dd, $^{3}J_{HH}$ = 4.5 Hz, $^{2}J_{HH}$ = 13.5 Hz, 2H, NCH*H*CH=CH_2), 4.35 (d, $^{2}J_{HH}$ = 13.0 Hz, 2H, NCH*H*CH=CH_2), 3.59 (m, 2H, cod), 3.51 (d, $^{3}J_{HH}$ = 6.5 Hz, 2H, NCH_2CH=CHH_{cis}), 2.88 (d, $^{3}J_{HH}$ = 10 Hz, 2H, NCH_2CH=CHH_{trans}), 2.86 (m, 2H, cod), 2.73 (m, 2H, cod), 2.26 (m, 4H, cod).

^{13}C{^{1}H} NMR (125 MHz, acetone-*d6*): δ 161.2 (N*C*N), 114.6 (Cl–*C*), 94.8, 74.5 (cod), 63.71 (NCH_2CH=CH_2), 51.1 (N*C*H_2CH=CH_2), 42.6 (NCH_2CH=*C*H_2), 32.2, 30.8 (cod). Electrospray Ms. (Cone 25 V): m/z (fragment) 517.0 $[M]^+$.

Synthesis of complex 2c

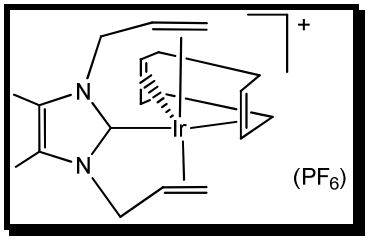

The synthesis of complex **2c** was carried out using the same general procedure as described for complex **2a** but followed by anion exchange (PF_6^-)
using complex 1c (40 mg, 0.08 mmol) and $AgBF_4$ (15 mg, 0.08 mmol) (yield 30 mg, 68%).
^{1}H NMR (500 MHz, $CDCl_3$): δ 5.17 (m, 2H, $NCH_2CH=CH_2$), 4.74 (m, 2H, cod), 4.44 (dd, $^3J_{HH}$ = 4.5 Hz, $^2J_{HH}$ = 13.0 Hz, 2H, $NCHHCH=CH_2$), 4.21 (d, $^2J_{HH}$ = 12.5 Hz, 2H, $NCHHCH=CH_2$), 3.47 (m, 2H, cod), 3.44 (d, $^3J_{HH}$=8.0 Hz, 2H, $NCH_2CH=CH_{cis}$), 2.85 (m, 2H, cod), 2.77 (d, $^3J_{HH}$ = 12.0 Hz, 2H, $NCH_2CH=CH_{trans}$), 2.70 (m, 2H, cod), 2.29 (m, 4H, cod), 1.98 (s, 6H, CH_3).
$^{13}C\{^1H\}$ NMR (125 MHz, $CDCl_3$): δ NCN no observado, 124.7 (*C*–CH3), 93.3, 74.2 (cod), 63.9 ($NCH_2CH=CH_2$), 49.2 ($NCH_2CH=CH_2$), 42.2 ($NCH_2CH=CH_2$), 32.7, 31.3 (cod), 9.4 (CH_3). Electrospray Ms. (Cone 25 V): m/z (fragmento) 477.3 $[M]^+$.

Synthesis of complex 2d

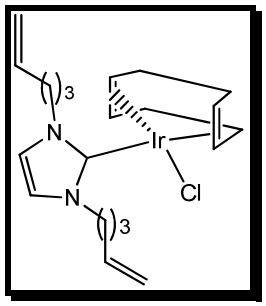

Silver oxide (63 mg, 0.27 mmol) was added to a solution of 1,3-bis(4-pentenyl) imidazolium bromide (85 mg, 0.30 mmol) in MeOH. The mixture was stirred at room temperature for 1 h and filtered through Celite. The solution was concentrated under reduced pressure and redissolved in dichloromethane. $[IrCl(COD)]_2$ (100 mg, 0.15 mmol) was added and the

mixture was stirred for 1 h at 45 1C. The volatiles were removed under reduced pressure. Compound **2d** was obtained as a yellow oil (yield 122 mg, 77%).

^{1}H NMR (500 MHz, $CDCl_3$): δ 6.83 (s, 2H, C*H* imidazol), 5.86 (m, 2H, –CH=CH_2), 5.14 (m, 4H, –C*H*=CH_2), 4.58 (s, 2H, cod), 4.36 (m, 2H, –NCH_2–), 4.30 (m, 2H, –NCH_2–), 2.88 (s, 2H, cod), 2.19 (m, 4H, cod), 2.0 (m, 4H, cod), 1.95 (m, 2H, –CH_2–), 1.87 (m, 2H, –CH_2–), 1.71 (m, 2H,–CH_2–), 1.67 (m, 2H, –CH_2–).

^{13}C{^{1}H} NMR (75 MHz, $CDCl_3$): δ 180.2 (N*C*N–Ir), 137.5 (–*C*H=CH_2), 120.2 (–N*C*H*C*HN–), 115.8 (–CH=*C*H_2), 84.3 (COD), 51.6 (cod), 50.8(2C, N*C*H_2), 33.8 (cod), 31.0 (cod), 30.2 (–*C*H_2–), 29.7(–*C*H_2–). Electrospray Ms. (Cone 25 V): m/z (fragment) 505.3 [M - Cl^+].

Synthesis of complex 3L

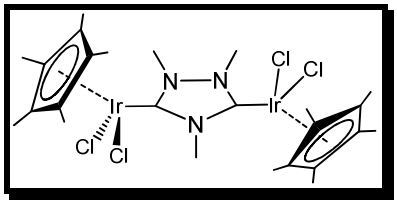

A mixture of 1,2,4-trimethyltriazolium tetrafluoroborate (43 mg, 0.15 mmol) and potassium *tert*-butoxide (51 mg, 0.45 mmol) was cooled to 0 °C in an ice bath. Freshly distilled THF (5 mL) was added, and the mixture was allowed to reach room temperature. To this suspension was added a solution of $[Cp^*IrCl_2]_2$ (120 mg, 0.15 mmol) in freshly distilled CH_2Cl_2 (5 mL). The mixture was stirred at room temperature for 1 h. Solvents were evaporated under reduced pressure, and the crude solid was redissolved in diethyl ether. The mixture was filtered through a pad of Celite, and after evaporation of the solvent, the crude solid was purified by column chromatography. The pure compound **3L** was eluted with dichloromethane/acetone (8:2) and precipitated in a mixture of dichloromethane/diethyl ether to give an orange solid. Yield: 82 mg (60%).

^{1}H NMR (500 MHz, $CDCl_3$): *δ* 4.32 (s, 3H, NCH_3), 4.31 (s, 6H, NCH_3), 1.67 (s, 15H, C_5(CH_3)$_5$).

^{13}C NMR (75 MHz, $CDCl_3$): *δ* 168.9 (*C*-Ir carbene), 90.5 (C_5(CH_3)$_5$), 41.5 (N*C*H_3), 38.4 (N*C*H_3), 9.3 (C_5(*C*H_3)$_5$). Electrospray MS (cone 30 V) (*m*/*z*, fragment) 872.1, [M- $Cl]^+$.

Elemental Analysis for for $C_{25}H_{39}Cl_4Ir_2N_3$ H_2O; Theoric: C, 32.43; H, 4.46; N, 4.54. Found: C, 32.32; H, 4.46;N, 4.55.

Synthesis of complex 4L

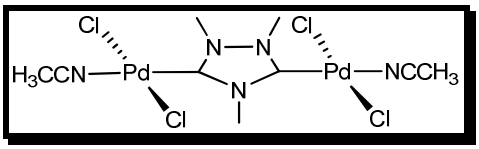

A mixture of 1,2,4-trimethyltriazolium tetrafluoroborate (82 mg, 0.28 mmol), $Pd(OAc)_2$ (140 mg, 0.62 mmol), and sodium chloride (162 mg, 2.8 mmol) was refluxed overnight in CH_3CN. The reaction mixture was filtered through Celite, and the solvent was removed under vacuum. The crude was dissolved in CH_3CN
and purified by column chromatography. The pure compound **4L** was eluted with dichloromethane/methanol (3:1) and precipitated with *n*-hexane to give an orange solid. Yield: 135 mg (81%).

^{1}H NMR (300 MHz, CD_3CN): δ 4.46 (s, 3H, NCH_3), 4.31 (s, 6H, NCH_3), (CH_3CN) not observed.

$^{13}C\{^1H\}$ NMR (125 MHz, CD_3CN): δ 164.9 (*C*carbene-Pd), 45.5 (N*C*H_3), 43.1 (N*C*H_3), *C*H_3*C*N not observed. *Elemental Analysis* for $C_9H_{15}Cl_4Pd_2N_5$; Theoric: C, 19.73; H, 2.76; N, 12.78. Found: C, 19.79; H, 2.93; N, 12.49. ESI-TOF-MS (positive mode): $[M - 2(CH_3CN) + Na]^+$ isotopic peak 489.7506; calculated 489.7500. ε_r = 1.6 ppm.

Synthesis of complex 5L

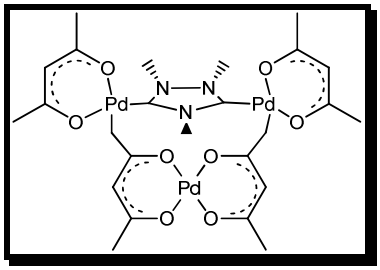

A mixture of 1,2,4-trimethyltriazolium tetrafluoroborate (61 mg, 0.21 mmol), $Pd(acac)_2$ (150 mg, 0.49 mmol), and Cs_2CO_3 (685 mg, 2.1 mmol) was heated to 85 °C for 2 h in CH_3CN. The reaction mixture was filtered through Celite, and the solvent was removed under vacuum. The crude was purified by column chromatography. The pure compound **5L** was eluted with dichloromethane/acetone (3:1) and precipitated in a mixture of dichloromethane/diethyl ether to give a yellow solid. Yield: 73 mg (54%).

^{1}H NMR (300 MHz, $CDCl_3$): δ 5.42 (s, 1H, -C*H*-), 5.32 (s,1H, -C*H*-), 4.76 (s, 3H, NCH_3), 4.38 (s, 6H, NCH_3), 2.67 (d,$^{2}J_{HH}$ = 5.1 Hz, 2H, -CH*H*-,), 2.36 (d, $^{2}J_{HH}$ = 5.1 Hz, 2H,-C*H*H-,), 2.00 (s, 3H, -CH_3), 1.95 (s, 3H, -CH_3), 1.87 (s, 3H, -CH_3).
^{13}C{^{1}H} NMR (125 MHz, $CDCl_3$): δ 194.7 (C, *C*=O), 187.1(C, *C*=O), 186.5 (C, *C*=O), 182.8 (C, *C*=O), 178.2 (*C*carbene-Pd), 100.6 (CH, C(O)-*C*H), 99.9 (CH, C(O)-*C*H), 39.7 (*C*H_3), 37.2 (*C*H_3), 27.8 (CH_3, C(O)-CH_3), 27.6 (CH_3, C(O)-CH_3), 25.9 (CH_3, C(O)-CH_3), 24.8 (CH_2, Pd-CH_2). *Elemental Analysis* for $C_{25}H_{35}O_8Pd_3N_3$; Theoric: C, 36.40; H, 4.28; N, 5.09. Found: C, 36.54; H, 4.38; N, 4.97. ESI-TOF-MS (positive mode): $[M + Na]^+$ isotopic peak 847.9464; calculated 847.9453. ε_r = 1.3 ppm.

Synthesis of complex 6L

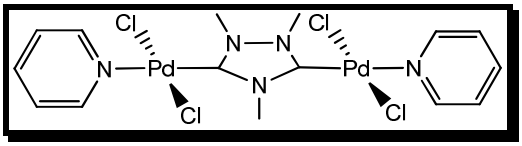

A mixture of 1,2,4-trimethyltriazolium tetrafluoroborate (60 mg, 0.21 mmol), $PdCl_2$ (75 mg, 0.42 mmol) and K_2CO_3 (221 mg, 1.6 mmol) was refluxed for three hours in pyridine (3 ml). The reaction mixture was filtered through Celite, and the solvent was removed under vacuum. Pure compound **6L** was obtained as a light yellow solid after recrystallization from dichloromethane/n-hexanes (2 times). Yield: 95 mg (75%).
^{1}H NMR (500 MHz, $CDCl_3$): δ 8.84 (d, $^{3}J_{H-H}$ = 6.0 Hz, 4H, Py), 7.78 (t, $^{3}J_{H-H}$ = 8.0 Hz, 2H, Py), 7.33 (t, $^{3}J_{H-H}$ = 6.8 Hz, 4H, Py), 4.69 (s, 3H, NCH_3), 4.46 (s, 6H, NCH_3).
^{13}C{^{1}H} NMR (75 MHz, $CDCl_3$): δ 164.9 (NCN-Pd), 153.6, 151.6, 138.8, 125.2, 125.0 (Py), 40.9, 37.8 (-CH_3). *Elemental Analysis* for $C_{15}H_{19}N_5Pd_2Cl_4$; Theoric: C, 28.87; H, 3.07; N, 11.22. Found: C, 28.97; H, 3.28; N, 11.35. Electrospray MS Cone 25V. (m/z, fragment): 646.6, $[M+Na]^+$.

Synthesis of complex 7L

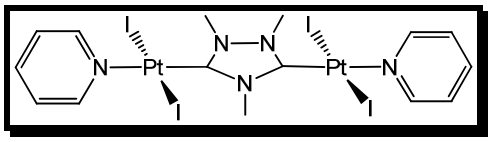

A mixture of 1,2,4-trimethyltriazolium tetrafluoroborate (60 mg, 0.21 mmol), PtI_2 (180 mg, 0.42 mmol) and K_2CO_3 (221 mg, 1.6 mmol) was refluxed for three hours in pyridine (3 ml). The reaction mixture was filtered through Celite, and the solvent was removed under vacuum. Pure compound **7L** was obtained as a light yellow solid after recrystallization from dichloromethane/n-hexanes (2 times). Yield: 170 mg (70%).

^{1}H NMR (500 MHz, C_6D_6): δ 8.91 (d, $^3J_{H-H}$ = 5.0 Hz, 4H, Py), 6.55 (t, $^3J_{H-H}$ = 7.5 Hz, 2H, Py), 6.27 (t, $^3J_{H-H}$ = 6.5 Hz, 4H, Py), 4.63 (s, 3H, NC*H*$_3$), 3.38 (s, 6H, NC*H*$_3$).

^{13}C NMR (75 MHz, $CDCl_3$): δ 164.1 (NCN-Pt), 153.5, 138.2, 125.2, (Py), 40.4, 37.0 (-CH_3).

ESI-TOF-MS (positive mode): monoisotopic peak 715.1340; calc. 715.1335. ε_r = 0.7 ppm.

Synthesis of complex 8L

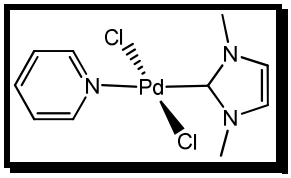

Compound **8L** was obtained following the procedure described for **6L** using 1,3-bis(N-methyl)imidazolium chloride (28 mg, 0.21 mmol). Yield: 61 mg (83%).

^{1}H NMR (300 MHz, $CDCl_3$): δ 9.06 (d, $^3J_{H-H}$ = 4.8 Hz, 2H, Py), 7.74 (t, $^3J_{H-H}$ = 5.4 Hz, 2H, Py), 7.35 (t, $^3J_{H-H}$ = 6.6 Hz, 4H, Py), 6.92 (s, 2H, NC*H*C*H*N), 3.97 (s, 6H, NC*H*$_3$).

^{13}C{^{1}H} NMR (75 MHz, $CDCl_3$): δ 153.9 (NCN-Pd), 152.4, 138.3, 124.9 (Py), 121.5 (N*C*H*C*HN), 40.5 (-CH_3). *Elemental Analysis* for $C_{10}H_{13}N_3PdCl_2$; Theoric: C, 34.10; H, 3.72; N, 11.92. Found: C, 34.23; H, 3.68; N, 11.35. Electrospray MS Cone 25V. (m/z, fragment): 357.1, $[M\text{-}Cl+MeCN]^+$.

Synthesis of complex 9L

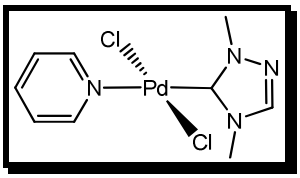

Compound **9L** was obtained following the procedure described for **6L** using 1,4-bis(N-methyl)triazolium chloride (28 mg, 0.21 mmol). Yield: 50 mg (67%).
^{1}H NMR (300 MHz, $CDCl_3$): δ 8.97 (d, $^{3}J_{H-H}$ = 6.6 Hz, 1H, Py), 8.83 (d, $^{3}J_{H-H}$ = 6.6 Hz, 1H, Py), 7.94 (s, 1H, NC*H*N), 7.80 - 7.75 (m, 1H, Py), 7.40 - 7.31 (m, 2H, Py), 4.32 (s, 3H, NCH_3), 4.15 (s, 3H, NCH_3).
^{13}C{^{1}H} NMR (75 MHz, $CDCl_3$): δ 143.4 (NCN-Pd), 153.6, 151.5, 138.8, 125.2, 124.8 (Py), 121.6 (N*C*HN), 40.3, 35.7 (-CH_3). *Elemenal Aalysis* for $C_9H_{12}N_4PdCl_2$ (353.6); Theoric: C, 30.63; H, 3.42; N, 15.92. Found: C, 30.43; H, 3.48; N, 16.03. Electrospray MS Cone 25V. (m/z, fragment): 358.0, $[M\text{-}Cl+MeCN]^+$.

Synthesis of complex 10L

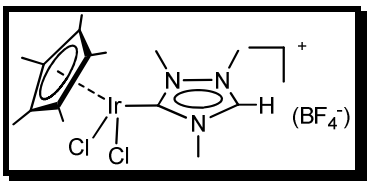

Method a): A mixture of methanolic aduct $[LHMeOH]BF_4$ (66 mg, 0.27 mmol) and $[Cp^*IrCl_2]_2$ (108 mg, 0.13 mmol) was refluxed in methanol (10 mL) for 2 h. Solvent removal afforded a mixture of compound **10L** and an excess of $[Cp^*IrCl_2]_2$.
The non reacted $[Cp^*IrCl_2]_2$ was eliminated by fractional recrystallization in cold CH_3CN (2 × 15 mL). Compound **10L** was obtained as an orange solid after precipitation in acetone/diethyl ether. Yield: 110 mg (69%).
Method b): A suspension of sodium hydride (60% in mineral oil, 17 mg, 0.42 mmol) in dry methanol was stirred at 0 °C under a nitrogen atmosphere until a clear solution of sodium methoxide was formed. 1,2,4-Trimethyltriazolium tetrafluoroborate (103 mg, 0.3 mmol) was added, and the mixture was stirred at room temperature for 1 h. After addition of $[Cp^*IrCl_2]_2$ (108 mg, 0.13 mmol) the mixture was refluxed at 70 °C for 2 h. The suspension was filtered

and the solution concentrated under reduced pressure. Compound **10L** was obtained as an orange solid after precipitation in acetone/diethyl ether. Yield: 136 mg (85%).
^{1}H NMR (500 MHz, CD_3CN): δ 9.51 (s, 1H, NC*H*N), 4.32 (s, 3H, NCH_3), 4.18 (s, 3H, NCH_3), 4.13 (s, 3H, NCH_3), 1.64 (s, 15H, $C_5(CH_3)_5$).
^{13}C{^{1}H} NMR (75 MHz, DMSO-d_6): δ 169.0 (*C*-Ir carbene), 145.6 (N*C*HN), 90.8 ($C_5(CH_3)_5$), 38.0 (N*C*H_3), 37.5 (N*C*H_3), 37.1 (N*C*H_3), 8.8 ($C_5(CH_3)_5$). *Elemental Analysis* for $C_{15}H_{25}BCl_2F_4IrN_3$; Theoric: C, 30.16; H, 4.22; N, 7.03. Found: C, 30.07; H, 4.20; N, 7.00.
Electrospray Ms. (Cone 20V): (m/z, fragment) 510.1, $[M]^+$.

Synthesis of complex 11L

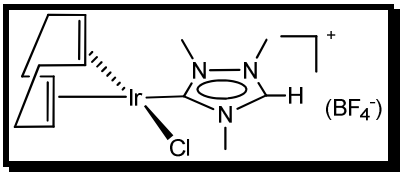

A suspension of sodium hydride (60% in mineral oil, 17 mg, 0.42 mmol) in dry methanol was stirred at 0 °C under a nitrogen atmosphere until a clear solution of sodium methoxide was formed. 1,2,4-Trimethyltriazolium tetrafluoroborate (103 mg, 0.3 mmol) was added, and the mixture was stirred at room temperature for 1 h. After addition of $[IrCl(cod)]_2$ (100 mg, 0.15 mmol) the mixture was refluxed at 70 °C for 2 h. The suspension was filtered and the solution concentrated under reduced pressure. Compound **11L** was obtained as an orange-yellow oil. Yield: 140 mg (87%).
^{1}H NMR (300 MHz, $CDCl_3$): δ 9.36 (s, 1H, NC*H*N), 4.85 (m, 2H, cod), 4.28 (s, 3H, CH_3), 4.1 (s, 6H, CH_3), 3.15 (m, 2H, cod), 2.27 (m, 5H, cod), 1.92 (m, 3H, cod), 1.76 (m, 3H, cod).
^{13}C{^{1}H} NMR (75 MHz, $CDCl_3$): δ 189.2 (C-Ir carbene), 144.4 (N*C*HN), 91.9 (cod), 91.8 (cod), 55.3 (cod), 54.6 (cod), 37.9 (*C*H_3), 37 (*C*H_3), 36.9 (*C*H_3), 33.5 (cod), 33.4 (cod), 29.4 (cod). Electrospray Ms. Cone 20V: (m/z, fragment) 448, $[M]^+$.

Synthesis of complex 12L

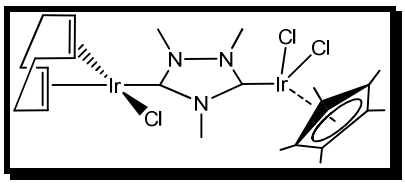

Method a): A suspension of sodium hydride (60% in mineral oil, 8 mg, 0.2 mmol) in dry methanol was stirred at 0 °C under a nitrogen atmosphere until a clear solution of sodium methoxide was formed. Compound **10L** (111 mg, 0.17 mmol) was then added, and the mixture was stirred at room temperature for 30 min. After addition of $[IrCl(cod)]_2$ (50 mg, 0.074 mmol) the mixture was refluxed at 70 °C for 30 min. Solvent was evaporated under reduced pressure, and the crude solid was purified by column chromatography. Elution with dichloromethane/acetone (8:2) afforded compound **12L**. Analytically pure material was obtained by precipitation from dichloromethane/hexanes as a yellow solid. Yield: 103 mg (82%).

Metodo b): A suspension of sodium hydride (60% in mineral oil, 26 mg, 0.6 mmol) in dry methanol was stirred at 0 °C under a nitrogen atmosphere until a clear solution of sodium methoxide was formed. Compound **11L** (305 mg, 0.57 mmol) was then added, and the mixture was stirred at room temperature for 30 min. After addition of $[Cp^*IrCl_2]_2$ (200 mg, 0.25 mmol) the mixture was refluxed at 70 °C for 30 min. Solvent was evaporated under reduced pressure, and the crude solid was purified by column chromatography. Elution with dichloromethane/acetone (8:2) afforded compound **12L**. Analytically pure material was obtained by precipitation from dichloromethane/hexanes as a yellow solid. Yield: 220 mg (52%).

Method c): A suspension of sodium hydride (60% in mineral oil, 16 mg, 0.4 mmol) in dry methanol was stirred at 0 °C under a nitrogen atmosphere until a clear solution of sodium methoxide was formed. 1,2,4-Trimethyltriazolium tetrafluoroborate (100 mg, 0.35 mmol) was then added, and the mixture was stirred at room temperature for 1 h. After addition of $[IrCl(cod)]_2$ (100 mg, 0.15 mmol) the mixture was refluxed at 70 °C for 90 min and subsequently cooled to room temperature and stirred for an

additional 30 min. Another solution of NaH (60% in mineral oil, 14 mg, 0.35 mmol) in methanol was prepared and added via cannula to the previous solution. The mixture was stirred for 1 h at room temperature. After addition of $[Cp^*IrCl_2]_2$ (100 mg, 0.12 mmol) the mixture was refluxed at 70 °C for 1 h. Solvent was evaporated under reduced pressure, and the crude solid was purified by column chromatography.

Elution with dichloromethane/acetone (8:2) afforded compound **12L**. Analytically pure material was obtained by precipitation from dichloromethane/hexanes as a yellow solid. Yield: 82 mg (40%).

^{1}H NMR (500 MHz, $CDCl_3$): δ 4.77 (m, 2H, cod), 4.30 (s, 3H, NCH_3), 4.26 (s, 3H, NCH_3), 4.24 (s. 3H, NCH_3), 3.16 (m, 1H, cod), 2.95 (m, 1H, cod), 2.21 (m, 4H, cod), 1.84 (m, 2H, cod), 1.71 (m, 2H, cod), 1.66 (s, 15H, $C_5(CH_3)_5$).

^{13}C{^{1}H} NMR (75 MHz, $CDCl_3$): δ 187.0 (*C*-Ir^{I} carbeno), 167.4 (*C*-Ir^{III} carbene), 90.4 ($C_5(CH_3)_5$), 89.1 (cod), 88.9 (cod), 53.7 (cod), 53.0 (cod), 40.6 (NCH_3), 37.2 (NCH_3), 36.8 (NCH_3), 33.7 (cod), 33.4 (cod), 29.5 (cod), 29.4 (cod), 9.3 ($C_5(CH_3)_5$). *Elemental Analysis* for $C_{23}H_{36}Cl_3Ir_2N_3 \cdot CH_2Cl_2$; Theoric: C, 30.99; H, 4.12; N, 4.52. Found: C, 31.12; H, 4.13; N, 4.50. Electrospray Ms. (Cone 25V): (m/z, fragmento) 810, $[M\text{-}Cl]^+$.

Synthesis of complex 13L

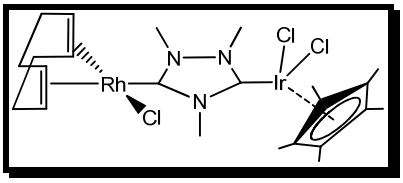

Method a): A suspension of sodium hydride (60% in mineral oil, 13 mg, 0.32 mmol) in dry methanol was stirred at 0 °C under a nitrogen atmosphere until a clear solution of sodium methoxide was formed. Compound **10L** (165 mg, 0.28 mmol) was then added, and the mixture was stirred at room temperature for 30 min. After addition of $[RhCl(cod)]_2$ (60 mg, 0.12 mmol) the mixture was refluxed at 70 °C for 30 min. Solvent was evaporated under reduced pressure, and the crude solid was purified by column chromatography. The pure compound **13L** was eluted with dichloromethane/acetone (7:3) and precipitated in a mixture of dichloromethane/ hexanes to give a pale yellow solid. Yield: 120 mg (66%).

Method b): A suspension of sodium hydride (60% in mineral oil, 22 mg, 0.54 mmol) in dry methanol was stirred at 0 °C under a nitrogen atmosphere until a clear solution of sodium methoxide was formed. 1,2,4-Trimethyltriazolium tetrafluoroborate (124 mg, 0.43 mmol) was then added, and the mixture was stirred at room temperature for 1 h. After addition of $[Cp^*IrCl_2]_2$ (150 mg, 0.18 mmol) the mixture was refluxed at 70 °C for 90 min and subsequently cooled to room temperature and stirred for an additional 30 min. Another solution of NaH (60% in mineral oil, 15 mg, 0.37 mmol) in methanol was prepared and added via cannula to the previous solution. The mixture was stirred for 1 h at room temperature. After addition of $[RhCl(cod)]_2$ (70 mg, 0.14 mmol) the mixture was refluxed at 70 °C for 1 h. Solvent was evaporated under reduced pressure, and the crude solid was purified by column

chromatography The pure compound **13L** was eluted with dichloromethane/ acetone (7:3) and precipitated in a mixture of dichloromethane/hexanes to give a pale yellow solid. Yield: 115 mg (54%).

^{1}H NMR (500 MHz, $CDCl_3$): δ 5.11 (m, 2H, cod), 4.42 (s, 6H, NCH_3), 4.21 (s, 3H, NCH_3), 3.19 (m, 1H, cod), 2.49 (m, 1H, cod), 2.40 (m, 4H, cod), 2.00 (m, 4H, cod), 1.66 (s, 15H, $C_5(CH_3)_5$).

^{13}C{^{1}H} NMR (75 MHz, $CDCl_3$): δ 191.6 (d, $^1J_{C\text{-}Rh}$ = 52.06 Hz, *C*-Rh carbeno), 167.3 (*C*-Ir carbeno), 100 (d, $^1J_{C\text{-}Rh}$ = 7.1 Hz, cod), 100.8 (d, $^1J_{C\text{-}Rh}$ = 6.8 Hz, cod), 90.4 ($C_5(CH_3)_5$), 69.8 (d, $^1J_{C\text{-}Rh}$ = 9.1 Hz, cod), 69.7 (d, $^1J_{C\text{-}Rh}$ = 8.8 Hz, cod), 40.8 (N*C*H$_3$), 37.2 (N*C*H$_3$), 33.0 (cod), 32.8 (cod), 29.0 (cod), 28.9 (cod), 9.3 ($C_5(CH_3)_5$).

Elemental Analysis for $C_{23}H_{36}N_3IrRhCl_3 \cdot CH_2Cl_2$; Theoric: C, 34.28; H, 4.55; N, 5.00. Found: C, 34.20; H, 4.56; N, 4.99. Electrospray Ms. (Cone 20V): (m/z, fragment) 720, $[M\text{-}Cl]^+$.

Synthesis of complex 14L

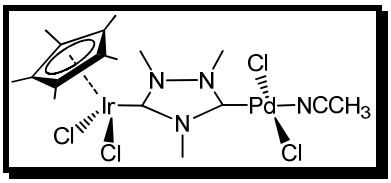

A mixture of compound **10L** (68 mg, 0.11 mmol), $Pd(OAc)_2$ (30 mg, 0.12 mmol), and sodium chloride (30 mg, 0.52 mmol) was refluxed overnight in CH_3CN. The reaction mixture was filtered through Celite, and the volatiles were removed under vacuum. The crude was dissolved in CH_2Cl_2 and purified by column chromatography. The pure compound **14L** was eluted with dichloromethane/methanol (10:1) and precipitated from a mixture of acetone/diethylether to give a pale yellow solid. Yield 60 mg (68%).

^{1}H NMR (300 MHz, CD_3CN): δ 4.45 (s, 3H, NCH_3), 4.37 (s, 3H, NCH_3), 4.27 (s, 3H, NCH_3), 1.58 (s, 15H, $C_5(CH_3)_5$), (CH_3CN) not observed.

^{13}C{^{1}H} NMR (125 MHz, CD_3CN): δ 169.0 (*C*carbene - Ir), 158.7 (*C*carbene - Pd), 91.1 ($C_5(CH_3)_5$), 41.1 (N*C*H$_3$), 38.3 (N*C*H$_3$), 38.1 (N*C*H$_3$), 8.8 ($C_5(CH_3)_5$). *Elemental Analysis* for $C_{17}H_{27}Cl_4N_4IrPd$; Theoric: C, 28.05; H, 3.74; N, 7.70. Found: C, 28.24; H, 3.78; N, 7.95.

Electrospray MS. Cone 20 V. (*m*/*z*, fragment): (692.8,$[M\text{-}Cl]^+$). ESI-TOF-MS (positive mode): monoisotopic peak 692.9963; calculated 692.9935. ε_r = 4.0 ppm.

Synthesis of complex 15L

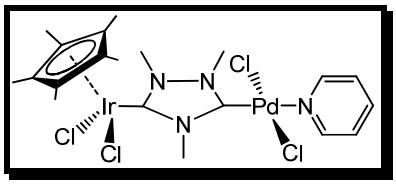

A mixture of compound **10L** (100 mg, 0.17 mmol), $PdCl_2$ (36 mg, 0.2 mmol), and K_2CO_3 (70 mg, 0.5 mmol) was heated overnight in pyridine (3 mL) at 80 °C. The reaction mixture was filtered through Celite, and the solvent was removed under vacuum.Pure compound **15L** was obtained as a light yellow solid after precipitation in dichloromethane/*n*-hexanes. Yield: 102 mg (78%).

^{1}H NMR (500 MHz, $CDCl_3$): δ 9.0 (d, $^3J_{H\text{-}H}$ = 5.5 Hz, 2H, Py), 7.87 (t, $^3J_{H\text{-}H}$ = 7.0 Hz, 1H, Py), 7.45 (t, $^3J_{H\text{-}H}$ = 6.5 Hz, 2H, Py), 4.60 (s, 3H, NCH_3), 4.58 (s, 3H, NCH_3), 4.41 (s, 3H, NCH_3), 1.73 (s, 15H, $C_5(CH_3)_5$).

$^{13}C\{^1H\}$ NMR (125 MHz, $CDCl_3$): δ 168.4 (*C*carbene - Ir), 163.4 (*C*carbene - Pd), 151.3, 151.1, 138, 124.9, 124.6 (Py), 90.6 ($C_5(CH_3)_5$), 40.7 (N*C*H_3), 38.1 (N*C*H_3), 37.5 (N*C*H_3), 9.0 ($C_5(CH_3)_5$). *Elemental Analysis* For $C_{20}H_{29}Cl_4N_4IrPd$ (765.9): C, 31.36; H, 3.82; N, 7.31. Found: C, 31.77; H, 3.88; N, 7.35. Electrospray MS. Cone 5 V. (*m*/*z*, fragment): (730.8, $[M\text{-}Cl]^+$). ESI-TOF-MS (positive mode): monoisotopic peak 731.0101; calculated 731.0106. εr = 0.7 ppm.

Synthesis of complex 16L

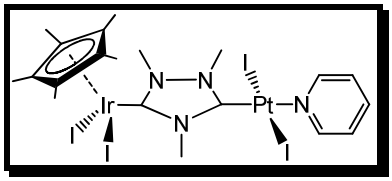

A mixture of compound **10L** (120 mg, 0.2 mmol), PtI_2 (100 mg, 0.22 mmol), NaI (150 mg, 1 mmol) and K_2CO_3 (83 mg, 0.6 mmol) was heated for three hours in pyridine (3 ml) at 80 ºC. The reaction mixture was filtered through Celite, and the solvent was removed under vacuum. The excess of salt was eliminated dissolving the crude in dichloromethane and filtering the solution. Pure compound **16L** was obtained as a light yellow solid after precipitation n-hexanes. Yield: 110 mg (41%).

^{1}H NMR (500 MHz, CD_2Cl_2): δ 8.90 (d, $^3J_{H-H}$ = 5.0 Hz, 2H, Py), 7.75 (t, $^3J_{H-H}$ = 7.0 Hz, 1H, Py), 7.33 (t, $^3J_{H-H}$ = 6.5 Hz, 2H, Py), 4.27 (s, 3H, NCH_3), 4.24 (s, 3H, NCH_3), 4.23 (s, 3H, NCH_3), 1.79 (s, 15H, $C_5(CH_3)_5$).
^{13}C NMR (125 MHz, $CDCl_3$): δ 164.0 ($C_{carbene}$ – Ir), 155.5 ($C_{carbene}$ – Pt), 153.5, 138.1, 125.2 (Py), 91.6 ($C_5(CH_3)_5$), 45.4 (NCH_3), 41.8 (NCH_3). ESI-TOF-MS (positive mode): monoisotopic peak 1092.8806; calc. 1092.8785. ε_r = 1.92 ppm.

Synthesis of complex 17L

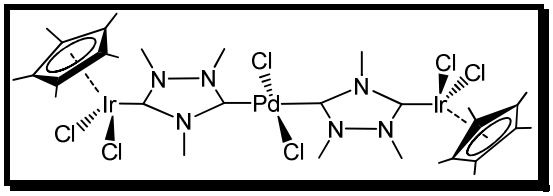

A mixture of compound **10L** (160 mg, 0.27 mmol), $Pd(OAc)_2$ (28 mg, 0.11 mmol), sodium acetate (12 mg, 0.14 mmol), and sodium chloride (78 mg, 1.35 mmol) was refluxed overnight in CH_3CN. The reaction mixture was filtered through Celite, and the solvent was removed under vacuum. The crude was dissolved in CH_2Cl_2 and purified by column chromatography. The pure compound **17L** was eluted with acetone/dichloromethane (7:3). Yield 40 mg (13%).
^{1}H NMR (500 MHz, $CDCl_3$): *δ* 4.46 (s, 12H, NCH_3), 4.31 (s, 6H, NCH_3), 1.65 (s, 30H, $C_5(CH_3)_5$).

Elemental Analysis for $C_{30}H_{48}Cl_6N_6Ir_2Pd$ (1196.3): C, 30.12; H, 4.04; N, 7.02. Found: C, 30.35; H, 4.19; N, 7.08. Electrospray MS. Cone 5 V. (*m*/*z*, fragment): (1161.1, $[M\text{-}Cl]^+$) and (562.1, $[M\text{-}2Cl]^{2+}$). ESI-TOFMS (positive mode): monoisotopic peak 563.0481; calculated 563.0477. ε_r = 0.7 ppm.

Synthesis of complex 2M

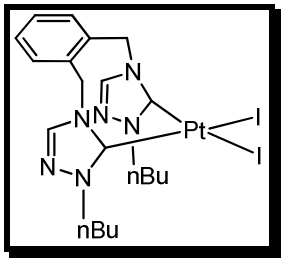

A mixture of *o*-xylenebis(N-*n*butyl)triazolium diiodide (200 mg, 0.47 mmol), PtI_2 (210 mg, 0. 47 mmol), and NaOAc (77 mg, 0.94 mmol) was refluxed for five hours in acetonitrile (5 ml). The reaction mixture was filtered through Celite, and the solvent was removed under vacuum. Pure compound **5** was obtained as a white crystalline solid after recrystallization from acetone/diethylether. Yield: 275 mg (73%).

^{1}H NMR (500 MHz, CD_3CN): δ 8.42 (s, 2H, NC*H*), 7.77 (m, 2H, Ph), 7.51 (m, 2H, Ph), 6.68 (d, $^{2}J_{H\text{-}H}$ = 14.5 Hz, 2H, CH_2), 5.15 (d, $^{2}J_{H\text{-}H}$ = 15.0 Hz, 2H, CH_2), 4.67 (m, 2H, CH_2, nBu), 4.18 (m, 2H, CH_2, nBu), 2.02 (m, 2H, CH_2, nBu), 1.97 (m, 2H, CH_2, nBu), 1.46 (m, 4H, CH_2, nBu), 0.98 (t, $^{3}J_{H\text{-}H}$ = 7.5 Hz, 6H, CH_3, nBu).

^{13}C NMR (125 MHz, CD_3CN): δ 156.6 (N*C*H), 143.5 ($J_{Pt\text{-}C}$ = 203.0 Hz, $C_{carbene}$–Pt), 135.6, 133.0, 131.7 (Ph), 52.7 (CH_2), 49.13, 31.1, 20.7, 14.0 (nBu). Electrospray MS Cone 25V. (m/z, fragment): 716.0 $[M - I + CH_3CN]^+$. ESI-TOF-MS (positive mode): monoisotopic peak 715.1340; calc. 715.1335. ε_r = 0.69 ppm.

4.4 Crystallographic data collection

- Complex 2a -

Empirical formula:	$C_{17}H_{24}BF_4IrN_2$
Mw:	535.39
Wave lenght:	Mo Kα (monochr); 0.71073 λ (Å)
Temperature(K):	293
Crystal system:	Monoclínic
Space group:	P2(1)/c (no 14)
a (Å):	8.1277(4)
b (Å):	36.568(2)
c (Å):	12.0502(6)
α (deg):	90
β (deg):	99.5350(10)
γ (deg):	99.5350(10)
V ($Å^3$):	3532.0(3)
Z:	8
Density Calculated (Mg/m^3):	2.014
Abosorption coefficient (mm^{-1}):	7.602
Reflections registered:	24 448
Goodness on fit on F^2:	1.047
R1:	0.0448
wR2:	0.0778

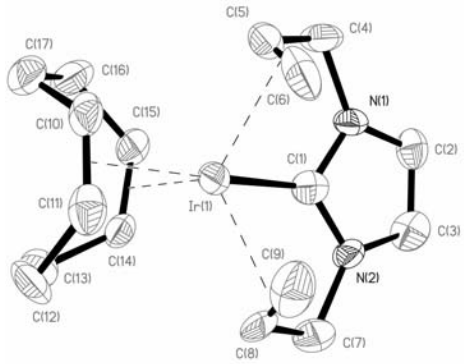

Figure 4.1. Molecular diagram of complex **2a.** Ellipsoids at 50% probability level. The ORTEP diagram of complex **2a**, showing 50% probability ellipsoids. Selected bond lengths (A˚) and angles (º): Ir(1)–C(1) = 1.934(9), Ir(1)–C(5) = 2.214(8), Ir(1)–C(9) = 2.261(9), Ir(1)–C(8) = 2.308(8), Ir(1)–C(6) = 2.225(9), C(5)–C(6) = 1.404(12), C(8)–C(9) = 1.373(13); N(1)–C(1)–Ir(1) = 123.9(7), N(1)–C(4)– C(5)–C(6) = 57.7(11).

- Complex 2b -

Empirical formula:	$C_{17}\ H_{22}\ C_{l2}\ F_6\ Ir\ N_2\ P$
Mw:	662.44
Wave lenght:	Mo Kα (monochr); 0.71073 λ (Å)
Temperature(K):	293
Crystal system:	Monoclinic
Space group:	P2(1)/c
a (Å):	15.2900(11)
b (Å):	10.7009(8)
c (Å):	12.7347(10)
α (deg):	90
β (deg):	96.789(2)
γ (deg):	90
V (Å^3):	2069.0(3)
Z:	4
Density Calculated (Mg/m^3):	2.127
Abosorption coefficient (mm^{-1}):	6.848
Reflections registered:	8374
Goodness on fit on F^2:	1.117
R1:	0.0525
wR2:	0.1315

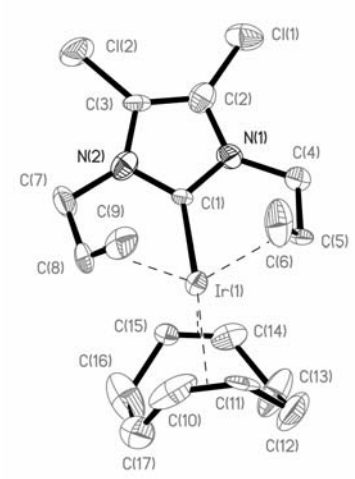

Figure 4.2. Molecular diagram of complex **2b.** Ellipsoids at 50% probability level. Selected bond lengths (A˚) and angles (º): Ir(1)–C(1) = 1.944(12), Ir(1)–C(5) = 2.221(14), Ir(1)–C(6) = 2.248(18), Ir(1)–C(8) = 2.247(12), Ir(1)–C(9) = 2.203(12), C(5)–C(6) = 1.38(2), C(8)–C(9) = 1.41(2); N(1)–C(1)–Ir(1) = 124.5(9).

- Complex 2d -

Empirical formula:	C_{21} H_{32} Cl Ir N_2
Mw:	540.14
Wave lenght:	Mo Kα (monochr); 0.71073 λ (Å)
Temperature (K):	293
Crystal system:	Triclinic
Space group:	P-1
a (Å):	12.0233(11)
b (Å):	13.9740(14)
c (Å):	14.7666(15)
α (deg):	64.168(2)
β (deg):	85.560(3)
γ (deg):	89.213(2)
V (Å^3):	2225.8(4)
Z:	4
Density Calculated (Mg/m^3):	1.612
Absorption coefficient (mm^{-1}):	6.124
Reflections registered:	12840
Goodness on fit on F^2:	1.005
R1:	0.0468
wR2:	0.1019

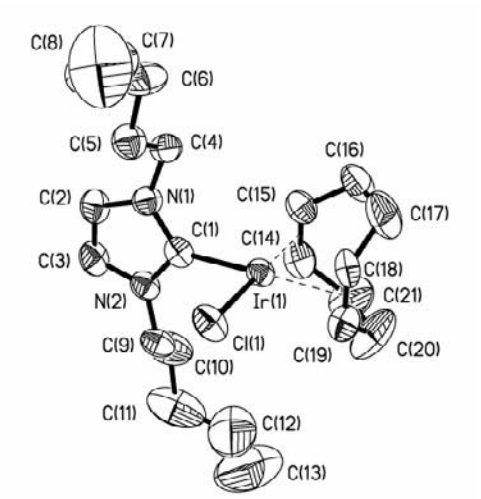

Figure 4.3. Molecular diagram of complex **2d.** Ellipsoids at 35% probability level. Selected bond lengths (A˚) and angles (º):Selected bond lengths (A˚) and angles (1): Ir(1)–C(1) = 2.030(10); N(1)–Ir(1)–C(1) = 127.6(7), N(1)–C(4)–C(5)–C(6) = -173.6(9).

- Complex 3L -

Empirical formula:	$(C_{25}H_{39}Cl_4Ir_2N_3)$ x H_2O
Mw:	925.79
Wave lenght:	Mo Kα (monochr); 0.71073 λ (Å)
Temperature (K):	298
Crystal system:	orthorhombic
Space group:	Pbcm
a (Å):	8.4528(3)
b (Å):	15.0376(3)
c (Å):	23.8627(9)
α (deg):	90
β (deg):	90
γ (deg):	90
V (Å^3):	3033.2(2)
Z:	4
Density Calculated (Mg/m^3):	2.023
Absorption coefficient (mm^{-1}):	9.141
Reflections registered:	16 412
Goodness on fit on F^2:	1.183
R1:	0.0297
wR2:	0.0807

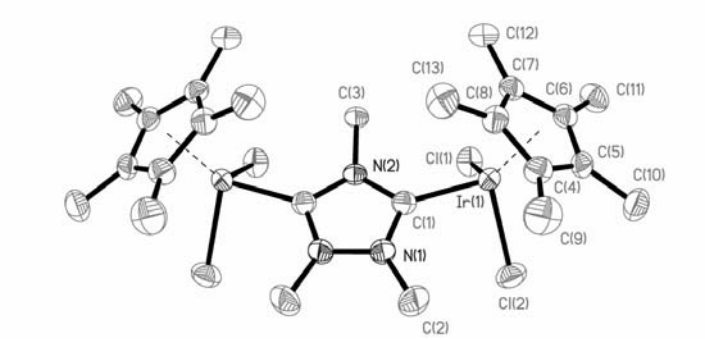

Figure 4.4. Molecular diagram of complex **3L.** Ellipsoids at 50% probability level. Selected bond distances (Å) and angles (deg): Ir(1)-C(1) 2.033(8),Ir(1)-Cl(1)2.442(2),Ir(1)-Cl(2)2.411(2),C(1)-Ir(1)-Cl(1) 91.5(2), C(1)-Ir(1)-Cl(2) 90.5(2), Cl(2)-Ir(1)-Cl(1) 85.31(8), N(1)-C(1)-Ir(1) 127.2(6), N(2)-C(1)-Ir(1) 129.1.

- Complex 4L -

Empirical formula:	$C_9\ H_{15}\ Cl_4\ N_5\ Pd_2$
Mw:	547.86
Wave lenght:	Mo Kα (monochr); 0.71073 λ (Å)
Temperature (K):	293
Crystal system:	monoclinic
Space group:	P21/n
a (Å):	8.1284(10)
b (Å):	10.1320(12)
c (Å):	22.069(3)
α (deg):	90
β (deg):	94.604(3)
γ (deg):	90
V (Å^3):	1811.7(4)
Z:	4
Density Calculated (Mg/m^3):	2.009
Absorption coefficient (mm^{-1}):	2.571
Reflections registered:	11822
Goodness on fit on F^2:	1.137
R1:	0.0381
wR2:	0.0887

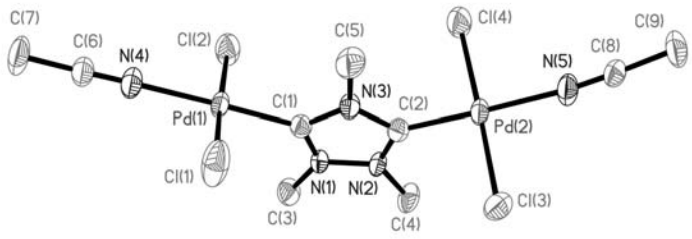

Figure 4.5. Molecular diagram of complex **4L.** Hydrogen atoms have been omitted for clarity. Selected bond lengths (Å) and angles (º): Pd(1)-C(1) 1.949(5), Pd(1)-N(4) 2.070(4), Pd(1)-Cl(1) 2.2825(17), Pd(1)-Cl(2) 2.2887(16), C(1)-Pd(1)-N(4) 178.9(2), C(1)-Pd(1)-Cl(1) 89.17(15), N(4)-Pd(1)-Cl(1) 90.06(15), Cl(1)-Pd(1)-Cl(2) 176.76(7).

- Complex 5L -

Empirical formula:	$C_{25}\ H_{35}\ N_3\ O_8\ Pd_3$, $2(C_3\ H_6\ O)$, O
Mw:	956.92
Wave lenght:	Mo Kα (monochr); 0.71073 λ (Å)
Temperature (K):	293
Crystal system:	monoclinic
Space group:	P21/n
a (Å):	14.854(2)
b (Å):	13.0012(18)
c (Å):	20.665(3)
α (deg):	90
β (deg):	104.379(3)
γ (deg):	90
V ($Å^3$):	3865.9(9)
Z:	4
Density Calculated (Mg/m^3):	1.644
Absorption coefficient (mm^{-1}):	1.436
Reflections registered:	25444
Goodness on fit on F^2:	1.079
R1:	0.0804
wR2:	0.2047

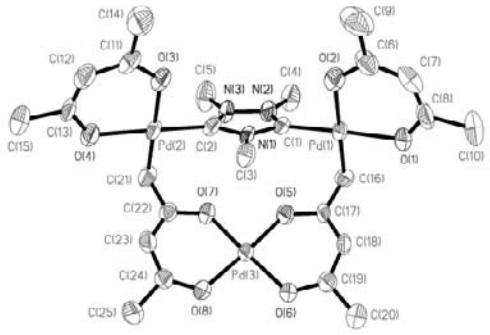

Figure 4.6. Molecular diagram of complex **5L.** Ellipsoids at 50% probability level. Hydrogen atoms and solvent molecules have been omitted for clarity. Selected bond lengths (Å) and angles (º): Pd(1)-C1 1.955(10), Pd(1)-C(16) 2.048(10), Pd(1)-O(1) 2.056(7), Pd(1)-O(2) 2.116(8), C(2)-Pd(2) 1.957(11), Pd(2)-C(21) 2.043(11), Pd(2)-O(4) 2.059(8), Pd(2)-O(3) 2.086(8), Pd(3)-O(7) 1.971(7), Pd(3)-O(6) 1.983(7), C(1)-Pd(1)-C(16) 89.0(4), C(1)-Pd(1)-O(1) 177.4(4), C(16)-Pd(1)-O(1) 88.4(4), C(1)-Pd(1)-O(2) 91.4(4), C(16)-Pd(1)-O(2) 179.3(4), N(2)-C(1)-Pd(1) 128.4(7), C(8)-O(1)-Pd(1) 123.9(8), O(7)-Pd(3)-O(8) 94.8(3), O(5)-Pd(3)-O(8) 177.1(3).

- Complex 6L -

Empirical formula:	$C_{15}\ H_{19}\ Cl_4\ N_5\ Pd_2$
Mw:	623.5
Wave lenght:	Mo Kα (monochr); 0.71073 λ (Å)
Temperature (K):	293
Crystal system:	Triclinic
Space group:	P1
a (Å):	8.4373(10)
b (Å):	9.2156(11)
c (Å):	14.2393(17)
α (deg):	84.508(3)
β (deg):	80.142(2)
γ (deg):	88.531(3)
V (Å^3):	1085.8(2)
Z:	2
Density Calculated (Mg/m^3):	1.909
Absorption coefficient (mm^{-1}):	2.158
Reflections registered:	7277
Goodness on fit on F^2:	1.029
R1:	0.0381
wR2:	0.0887

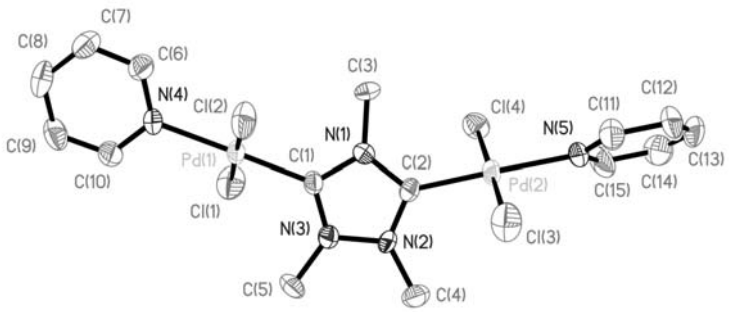

Figure 4.7. Molecular diagram of complex **6L.** Hydrogen atoms have been omitted for clarity. Selected bond lengths (Å) and angles (º): Pd(1)-C(1) 1.951(4), Pd(1)-N(4) 2.079(5), Pd(1)-Cl(1) 2.290(2), Pd(1)-Cl(2) 2.296(2), Pd(2)-C(2) 1.968(7), Pd(2)-N(5) 2.088(6), Pd(2)-Cl(3) 2.299(2), Pd(2)-Cl(4) 2.291(2), C(1)-Pd(1)-N(4) 178.9(3), C(1)-Pd(1)-Cl(1) 89.8(2), N(4)-Pd(1)-Cl(1) 90.58(17), Cl(1)-Pd(1)-Cl(2) 178.48(8), C(2)-Pd(2)-N(5) 178.1(3), C(2)-Pd(2)-Cl(4) 89.4(2), N(5)-Pd(2)-Cl(4) 89.8(2), Cl(4)-Pd(2)-Cl(3) 178.16(8).

- Complex 7L -

Empirical formula:	$C_{15}\,H_{19}\,I_4\,N_5\,Pt_2$
Mw:	1167.13
Wave lenght:	Mo Kα (monochr); 0.71073 λ (Å)
Temperature (K):	293
Crystal system:	Monoclinic
Space group:	C2/c
a (Å):	26.404(3)
b (Å):	10.9836(12)
c (Å):	8.9600(10)
α (deg):	90
β (deg):	90.232(2)
γ (deg):	90
V (Å^3):	2598.5(5)
Z:	4
Density Calculated (Mg/m^3):	2.983
Absorption coefficient (mm^{-1}):	15.517
Reflections registered:	2985
Goodness on fit on F^2:	1.037
R1:	0.0324
wR2:	0.0750

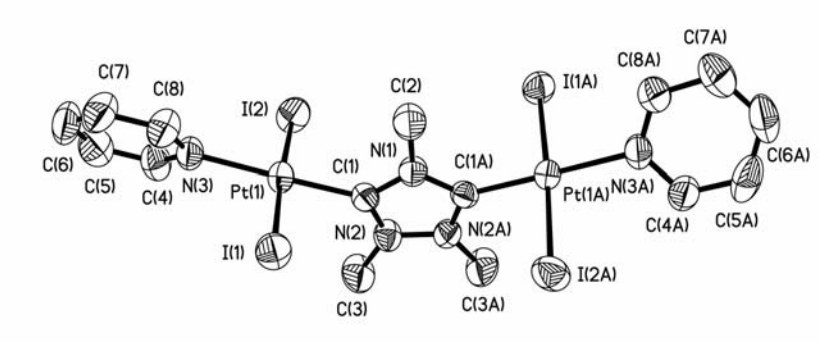

Figure 4.8. Molecular diagram of complex **7L**. Hydrogen atoms have been omitted for clarity. Selected bond lengths (Å) and angles (º): Pt(1)-C(1) 1.955(7), Pt(1)-I(1) 2.5994(6), Pt(1)-I(2) 2.6030(7), Pt(1)-N(3) 2.085(6), C(1)-Pt(1)-N(3) 178.5(3), N(3)-Pt(1)-I(1) 91.99(17), C(1)-Pt(1)-I(2) 88.4(2), N(3)-Pt(1)-I(2) 91.50(17), I(1)-Pt(1)-I(2) 176.30(2), N(2)-C(1)-Pt(1) 127.3(5).

- Complex 8L -

Empirical formula:	$C_{10}\ H_{13}\ Cl_2\ N_3\ Pd$
Mw:	352.5
Wave lenght:	Mo Kα (monochr); 0.71073 λ (Å)
Temperature (K):	293
Crystal system:	Hexagonal
Space group:	P6(1)22
a (Å):	9.0470(5)
b (Å):	9.0470(5)
c (Å):	29.203(3)
α (deg):	90
β (deg):	90
γ (deg):	120
V (Å^3):	2070.0(3)
Z:	6
Density Calculated (Mg/m^3):	1.697
Absorption coefficient (mm^{-1}):	1.710
Reflections registered:	14177
Goodness on fit on F^2:	1.080
R1:	0.0804
wR2:	0.2047

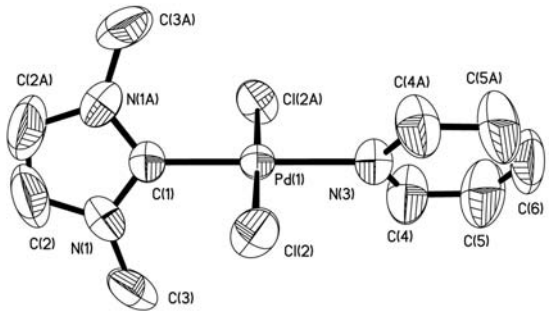

Figure 4.9. Molecular diagram of complex **8L.** Hydrogen atoms have been omitted for clarity. Selected bond lengths (Å) and angles (º): Pd(1)-C(1) 1.972(8), Pd(1)-N(3) 2.084(8), Pd(1)-Cl(2) 2.3325(15), C(1)-Pd(1)-N(3) 180.0 (1), C(1)-Pd(1)-Cl(2) 89.43(5), N(3)-Pd(1)-Cl(2) 90.57(5).

- Complex 10L -

Empirical formula:	$C_{15}\ H_{25}\ Cl_2\ F_6\ Ir\ N_3\ P$
Mw:	655.45
Wave lenght:	Mo Kα (monochr); 0.71073 λ (Å)
Temperature (K):	293
Crystal system:	Monoclinic
Space group:	P2(1)
a (Å):	9.1008(10)
b (Å):	8.8050(10)
c (Å):	14.0629(15)
α (deg):	90
β (deg):	105.996(2)
γ (deg):	90
V (Å^3):	1083.3(2)
Z:	2
Density Calculated (Mg/m^3):	2.009
Absorption coefficient (mm^{-1}):	6.540
Reflections registered:	4984
Goodness on fit on F^2:	1.008
R1:	0.0438
wR2:	0.0573

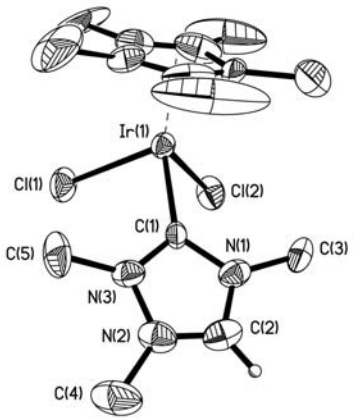

Figure 4.10. Molecular diagram of complex **10L.** Ellipsoids at 50% probability level. Hydrogen atoms and counter ion (PF_6^-) have been omitted for clarity. Selected bond lengths (Å) and angles (º): Ir(1)-C(1) 2.048(11), Ir(1)-Cl(1) 2.422(3), Ir(1)-Cl(2) 2.430(3), C(1)-Ir(1)-Cl(1) 90.0(3), Cl(1)-Ir(1)-Cl(2) 85.76(11), C(1)-Ir(1)-Cl(2) 88.8(3).

- Complex 12L -

Empirical formula:	$(C_{23}H_{36}Cl_3Ir_2N_3)$ x CH_2Cl_2
Mw:	930.22
Wave lenght:	Mo Kα (monochr); 0.71073 λ (Å)
Temperature (K):	293
Crystal system:	Monoclinic
Space group:	*P*2(1)/*n*
a (Å):	12.5314(6)
b (Å):	15.3256(7)
c (Å):	16.6218(8)
α (deg):	90
β (deg):	106.6410(10)
γ (deg):	90
V ($Å^3$):	3058.5(3)
Z:	4
Density Calculated (Mg/m^3):	2.020
Absorption coefficient (mm^{-1}):	9.148
Reflections registered:	20703
Goodness on fit on F^2:	1.027
R1:	0.0390
wR2:	0.0807

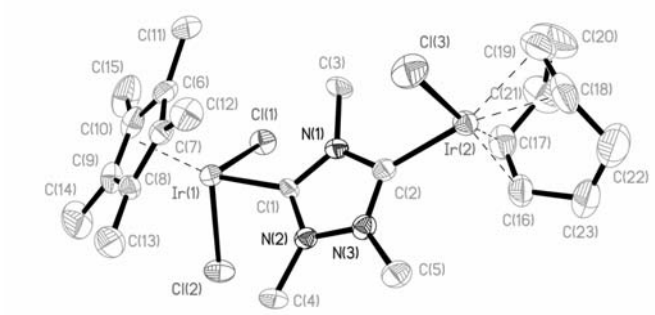

Figure 4.11. Molecular diagram of compound **12L**. Ellipsoids are at 50% probability level. Hydrogen atoms and solvent (CH_2Cl_2) have been omitted for clarity. Selected bond distances (Å) and angles (deg): Ir(1)-C(1) 2.023(7), Ir(2)-C(2) 2.006(7), Ir(1)-Cl(1) 2.4122(18), Ir(1)-Cl(2) 2.4180(19), Ir(2)-Cl(3) 2.3497(19), Ir(2)-C(16) 2.131(8), Ir(2)-C(17) 2.125(8), Ir(2)-C(20) 2.182(10), Ir(2)-C(21) 2.196(9), C(1)-Ir(1)-Cl(1) 91.69(19), C(1)-Ir(1)-Cl(2) 91.05(19), C(2)-Ir(2)-Cl(3)87.11(19), N(1)-C(1)-Ir(1)129.0(5), N(2)-C(1)-Ir(1) 127.9(5), N(1)-C(2)-Ir(2) 127.2(5), N(3)-C(2)-Ir(2) 129.3(5).

- Complex 13L -

Empirical formula:	$(C_{23}H_{36}Cl_3IrN_3Rh) \times CH_2Cl_2$
Mw:	840.93
Wave lenght:	Mo Kα (monochr); 0.71073 λ (Å)
Temperature (K):	298
Crystal system:	Monoclinic
Space group:	*P*2(1)/*n*
a (Å):	12.5908(4)
b (Å):	15.2228(6)
c (Å):	16.6788(6)
α (deg):	90
β (deg):	106.8130(10)
γ (deg):	90
V (Å^3):	3060.13(19)
Z:	4
Density Calculated (Mg/m^3):	1.825
Absorption coefficient (mm^{-1}):	5.338
Reflections registered:	20994
Goodness on fit on F^2:	1.034
R1:	0.0267
wR2:	0.0680

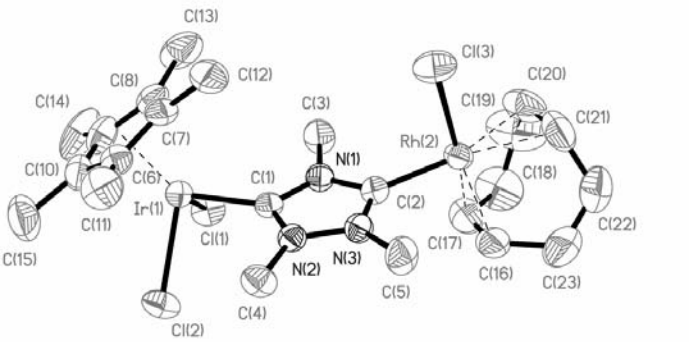

Figure 4.12. Molecular diagram of compound **13L**. Ellipsoids are at 50% probability level. Hydrogen atoms and solvent (CH_2Cl_2) have been omitted for clarity. Selected bond distances (Å) and angles (deg): Ir(1)-C(1) 2.032(4), Rh(2)-C(2) 2.006(4), Ir(1)-Cl(1) 2.4173(10), Ir(1)-Cl(2) 2.4198(11), Rh(2)-Cl(3) 2.3603(12), Rh(2)-C(16) 2.102(5), Rh(2)-C(17)2.118(5), Rh(2)-C(20)2.209(5), Rh(2)-C(21) 2.222(5), C(1)-Ir(1)-Cl(1) 91.58(11), C(1)-Ir(1)-Cl(2) 91.16(11), C(2)-Rh(2)-Cl(3)86.12(12), N(1)-C(1)-Ir(1)128.5(3), N(2)-C(1)-Ir(1) 127.7(3), N(1)-C(2)-Rh(2) 127.0(3), N(3)-C(2)-Rh(2) 128.9(3).

- Complex 15L -

Empirical formula:	$C_{46}\ H_{64}\ Cl_{25}\ Ir_2\ Pd_2\ N_8$
Mw:	2212.5
Wave lenght:	Mo Kα (monochr); 0.71073 λ (Å)
Temperature (K):	273
Crystal system:	Monoclinic
Space group:	C2/c
a (Å):	28.9630(8)
b (Å):	13.9348(4)
c (Å):	23.0014(7)
α (deg):	90
β (deg):	126.6400(10)
γ (deg):	90
V (Å^3):	7448.9(4)
Z:	4
Density Calculated (Mg/m^3):	1.973
Absorption coefficient (mm^{-1}):	4.972
Reflections registered:	10233
Goodness on fit on F^2:	1.039
R1:	0.0485
wR2:	0.0628

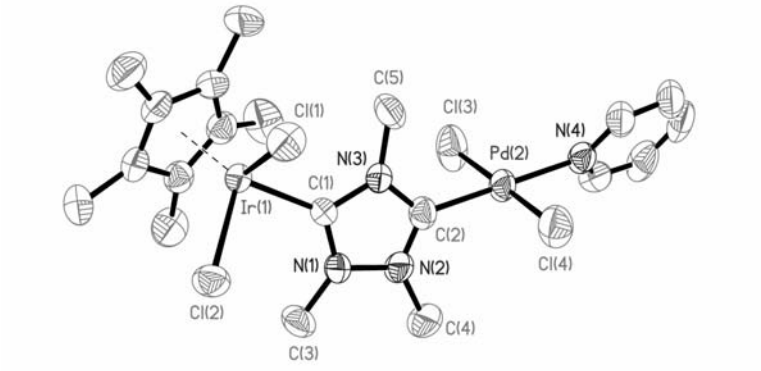

Figure 4.13. Molecular diagram of complex **15L.** Ellipsoids at 50% probability level. Hydrogen atoms and solvent molecules have been omitted for clarity. Selected bond lengths (Å) and angles (º): Ir(1)-C(1) 2.019(6), Ir(1)-Cl(1) 2.4256(17), Ir(1)-Cl(2) 2.4068(17), Pd(2)-C(2) 1.972(6), Pd(2)-Cl(3) 2.301(2), Pd(2)-Cl(4) 2.290(2), Pd(2)-N(4) 2.070(5), C(1)-Ir(1)-Cl(1) 90.31(17), C(1)-Ir(1)-Cl(2) 92.08(17), C(2)-Pd(2)-Cl(3) 87.2(2), C(2)-Pd(2)-Cl(4) 91.2(2).

- Complex 16L -

Empirical formula:	C_{20} H_{29} I_4 Ir Pt N_4
Mw:	1305.29
Wave lenght:	Mo Kα (monochr); 0.71073 λ (Å)
Temperature (K):	293
Crystal system:	Monoclinic
Space group:	P2(1)/n
a (Å):	14.7970(8)
b (Å):	9.2108(5)
c (Å):	23.6378(13)
α (deg):	90
β (deg):	98.665(1)
γ (deg):	90
V (Å^3):	3184.9(3)
Z:	4
Density Calculated (Mg/m^3):	2.722
Absorption coefficient (mm^{-1}):	12.624
Reflections registered:	7304
Goodness on fit on F^2:	1.068
R1:	0.0535
wR2:	0.1168

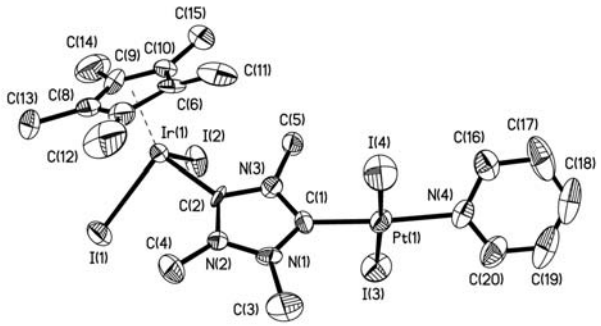

Figure 4.14. Molecular diagram of complex **16L.** Ellipsoids at 50% probability level. Hydrogen atoms and solvent molecules have been omitted for clarity. Selected bond lengths (Å) and angles (º): Ir(1)-C(2) 2.011(10), Ir(1)-I(1) 2.7213(11), Ir(1)-I(2) 2.7195(11), Pt(1)-C(1) 1.932(12), Pt(1)-I(3) 2.6044(12), Pt(1)-I(4) 2.5987(12), Pt(1)-N(4) 2.077(11), C(2)-Ir(1)-I(1) 96.3(4), C(2)-Ir(1)-I(2) 91.4(3), C(1)-Pt(1)-I(3) 89.1(4), C(1)-Pt(1)-I(4) 88.0(4).

- Complex 17L -

Empirical formula:	C_{32} H_{52} Cl_{10} Ir_2 Pd N_6
Mw:	1366.1
Wave lenght:	Mo Kα (monochr); 0.71073 λ (Å)
Temperature (K):	293
Crystal system:	Monoclinic
Space group:	P2(1)/c
a (Å):	8.6071(5)
b (Å):	17.8320(9)
c (Å):	14.8374(7)
α (deg):	90
β (deg):	99.2250(10)
γ (deg):	90
V (Å^3):	2247.8(2)
Z:	2
Density Calculated (Mg/m^3):	2.018
Absorption coefficient (mm^{-1}):	6.927
Reflections registered:	15388
Goodness on fit on F^2:	1.022
R1:	0.0373
wR2:	0.0697

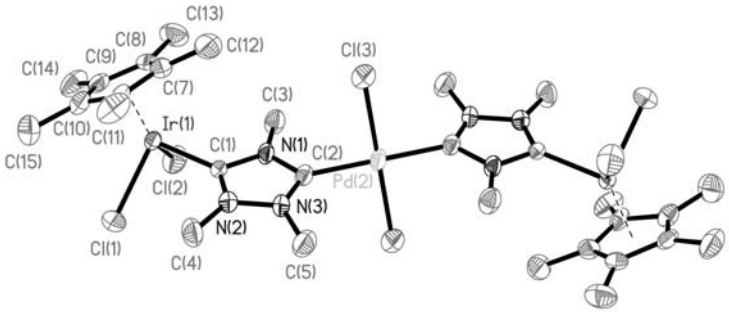

Figure 4.15. Molecular diagram of complex **17L.** Ellipsoids at 50% probability level. Hydrogen atoms and solvent molecules have been omitted for clarity. Selected bond lengths (Å) and angles (º): Ir(1)-C(1) 2.029(6), Ir(1)-Cl(1) 2.3959(18), Ir(1)-Cl(2) 2.4241(17), Pd(2)-C(2) 2.038(6), Pd(2)-Cl(3) 2.3159(18), C(1)-Ir(1)-Cl(1) 92.29(17), C(1)-Ir(1)-Cl(2) 92.23(17), C(2)-Pd(2)-Cl(3) 88.96(17).

4.5 Mass Spectrometry

Experimental and theoretical isotopic distribution of compound 4L.

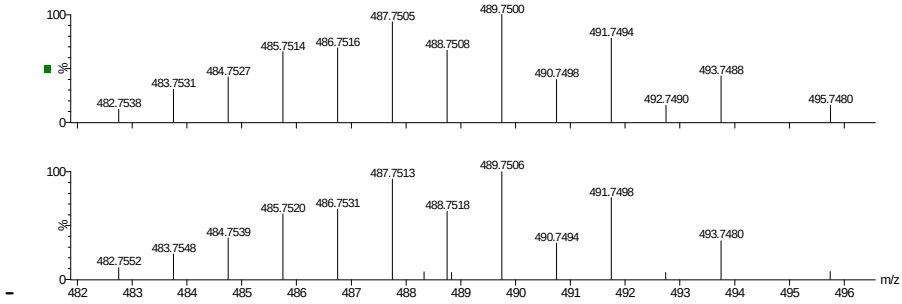

Figure 4.16. ESI mass spectrum of compound **4L** (bottom) and simulated peak for (top).

Experimental and theoretical peak of compound **4L**.

Experimental Mass	Theoretical Mass	Relative Error
487.7513	487.7505	1.6
488.7518	488.7508	2.0
489.7506	489.7500	1.2
490.7494	490.7498	0.8
491.7498	491.7494	0.8

Experimental and theoretical isotopic distribution of compound 5L.

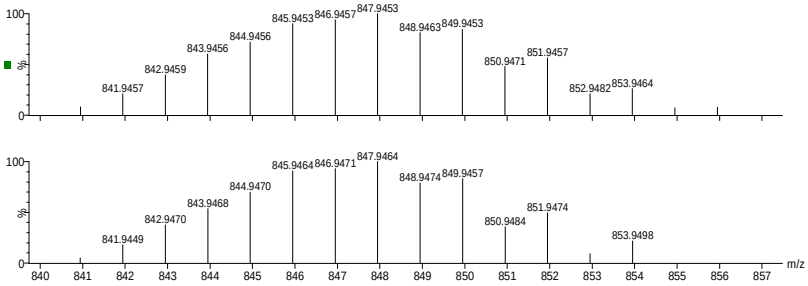

Figure 4.17. ESI mass spectrum of compound **5L** (bottom) and simulated peak for (top).

Experimental and theoretical peak of compound **5L**.

Experimental Mass	Theoretical Mass	Relative Error
845.9464	845.9453	1.3
846.9471	846.9457.	1.6
847.9464	847.9453	1.3
848.9474	848.9463	1.3
849.9457	849.9453	0.4

References

(1) G. M. Sheldrick, *SHELXTL, version 6.1, Bruker AXS, Inc*. ed; Madison, WI, **2000**; 'Vol.'p.

(2) *SAINT, Bruker Analytical X-ray System, version 5.0*. ed.; Madison, WI, **1998**.

(3) Y. Lin, K. Nomiya, R. G. Finke, R. G. *Inorg. Chem*., **1993**, *32*, 60.

(4) R. Ball, W. A. G. Graham, D. M. Heinekey, J. K. Hoyano, A. D. McMaster, B. M. Mattson, S. T. Michel, S. T. *Inorg. Chem.*, **1990**, *29*, 2023.

(5) S. I. Murahashi, Y. Tamba, M. Yamamura, N. Yoshimura, N. *J. Org. Chem.,* **1978**, *43*,4099.

(6) A. J. Arduengo, U. S. Patents 6 177 575, **2001**.

(7) T. J. Curphey, K. S. Prasad, *J. Org. Chem.*, **1972**, *37*, 2259; K. Ofele, *J. Organomet. Chem.*, **1968**, *12*, 42; H. W. Wanzlick, H. J. Schonher, *Angew. Chem. Int. Ed.*, **1968**, *7*, 141.

(8) T. J. Curphey, K. S. Prasad, K. S. *J. Org. Chem*., **1972**, *37*, 14, 2259.

(9) S. Whitney, R. Grigg, A. Derrick, A. Keep, *Org. Lett.*, **2007**, *9*, 3299.

(10)X. L. Mi, X. S. Z. Luo, J. Q. He, J. P. Cheng, *Tetrahedron Lett.*, **2004**, *45*, 4567.

(11) H. Chalaye-Mauger, J. N. Denis, M. T. Averbuch-Pouchot, Y. Vallee, *Tetrahedron*, **2000**, *56*, 791; M. Marzi, P. Minetti, G. P. Moretti, G. Giannini, E. Garattini, E. EP 1 337 511 AO, 2002-05-10, **2002**.

(12) R. J. Mohrbacher, N. H. Cromwell, *J. Am. Chem. Soc*., **1957**, *79*, 401; H. R. Henze, L. M. Long, *J. Am Chem. Soc.*, **1941**, *63*, 1941; L. M. Long, H. R. Henze, *J. Am. Chem. Soc*., **1941**, *63*, 1939.

(13) S. Chessa, N. J. Clayden, M. Bochmann, J. A. Wright, *Chem. Commun.* **2009**, 797; H. Naka, D. Koseki, Y. Kondo, *Adv. Synth. Catal.*, **2008**, *350*, 1901; H. Neuvonen, K. Neuvonen, F. Fulop, *J. Org. Chem.*, **2006**, *71*, 3141; D. A. Alonso, C. Najera, M. C. Pacheco, *J. Org. Chem.*, **2002**, *67*, 5588; S. Cabiddu, E. Cadoni, A. Ianni, G. Gelli, S. Melis, A. M. Bernard, M. G. Cabiddu, S. De Montis, C. Fattuoni, *Eur. J. Org. Chem.*, **2002**, 3393; K. Tomioka, M. Satoh, D. Taniyama, M. Kanai, A. Iida, *Heterocycles*, **1998**, *47*, 77; J. R. Wang, Y. Fu, B. B. Zhang, X. Cui, L. Liu, Q. X.Guo, *Tetrahedron Lett.*, **2006**, *47*, 8293.

Capítulo 5

Diseño de Catalizadores con Ligandos Ditópicos y Hemiactivables de Tipo Carbeno N-Heterocíclico

5.1 Introducción: Carbenos N-heterocíclico

El uso de ligando de tipo carbeno N-heterocíclico, NHC (**Esquema 5.1**), en el diseño de catalizadores homogéneos se ha desarrollado ampliamente en los últimos años.[1, 2] Desde el punto de vista electrónico, estos ligandos se comportan como dadores σ, con baja capacidad aceptora π.[1]

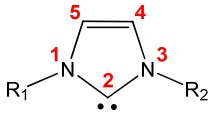

Esquema 5.1. Carbeno N-heterocíclico derivado de imidazol.

Desde que en el año 1995 Hermann utilizó este tipo de ligandos en el diseño de los primeros catalizadores homogéneos,[3] su uso y desarrollo ha experimentado un crecimiento casi exponencial. Algunas de las características que justifican este creciente interés son las que se especifican a continuación:

- Sus precursores, generalmente sales de azolio (**Esquema 5.2**), son fáciles de preparar mediante secuencias sintéticas que implican la utilización de reactivos de baja toxicidad.

- Presentan una gran versatilidad topológica, lo que permite diseñar derivados susceptibles de coordinar en forma quelato o pinza, e incluso introducir quiralidad.

- La introducción de diferentes sustituyentes en el anillo de azol permite modular las propiedades electrónicas y estéricas de los ligandos obtenidos. Así, la introducción de diferentes sustituyentes en las posiciones 4 y 5 permite modular principalmente las propiedades electrónicas del ligando, mientras que los sustituyentes en las posiciones 1 y 3 modifican sus propiedades estéricas.

- Una vez coordinados al metal, los compuestos obtenidos presentan una elevada estabilidad térmica, debido a la fortaleza del enlace M-NHC.

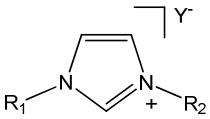

Esquema 5.2. Sal de imidazolio.

Los primeros carbenos N-heterocíclicos (**Esquema 5.3**) fueron descritos por Öfele[4] y Wanzlick[5] en 1968, y fueron coordinados a Hg y Cr. Sin embargo, puesto que se pensaba que

los carbenos eran especies muy reactivas, el desarrollo de este campo permaneció estancado hasta que en 1991 Arduengo[6] aisló el primer carbeno libre, cuya estructura cristalográfica fue determinada mediante difracción de rayos X. (**Esquema 5.4**).

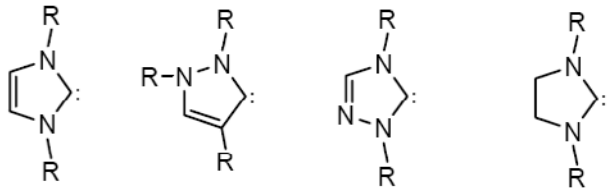

Esquema 5.3. Primeros carbenos N-heterocíclicos obtenidos por Öfele.[4]

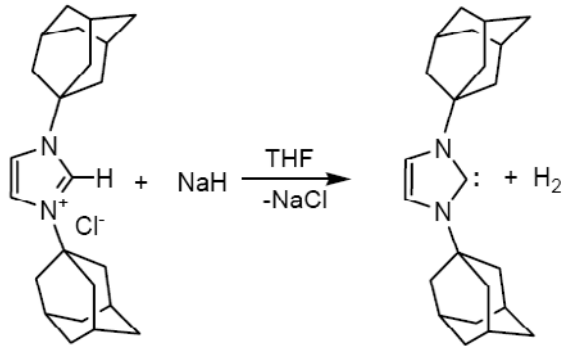

Esquema 5.4

Desde entonces, los carbenos N-heterocíclico se han utilizado ampliamente como ligandos estabilizadores de catalizadores homogéneos.[1, 2, 7]. El principal inconveniente en el empleo de estos ligandos es la necesidad de activar previamente la sal de imidazolio para que pueda llevarse a cabo su coordinación al metal. Las estrategias de metalación más utilizadas son [1, 8]: *a*) inserción del metal en el doble enlace de enetetraminas, (*b*) empleo de aductos carbeno o formas protegidas de carbenos N-heterociclico libres, (*c*) empleo de carbenos libres previamente aislados, (*d*) transmetalación a partir de un complejo de Ag-NHC preparado por reacción de Ag_2O en CH_2Cl_2 a temperatura ambiente y (*e*) adición oxidante vía activación del C-2X (X = Me, halógeno, H) de un cation de imidazolio.

Entre las metodologías de metalación citadas, la trasmetalación a partir de un carbeno de Ag^I y la formación de un aducto carbeno-metanol son las que se han empleado más habitualmente en la preparación de los complejos que se describen en esta memoria.

- *Trasmetalación a partir de un carbeno de Ag(I)*: esta metodologia fue desarrollada por Wang y Lin en 1998, [9] e implica una reacción de la correspondiente sal de imidazolio con Ag_2O en CH_2Cl_2 a temperatura ambiente (**Esquema 5.5**). El complejo Ag(NHC) generado puede aislarse o emplearse *in situ* como reactivo de transferencia

de carbeno a otro metal, como Pd, Rh, Ir y Au.[10] La reacción de transmetalación es favorecida por (*i*) la labilidad del enlace Ag-NHC y (*ii*) la baja solubilidad del haluro de plata formado (AgX).

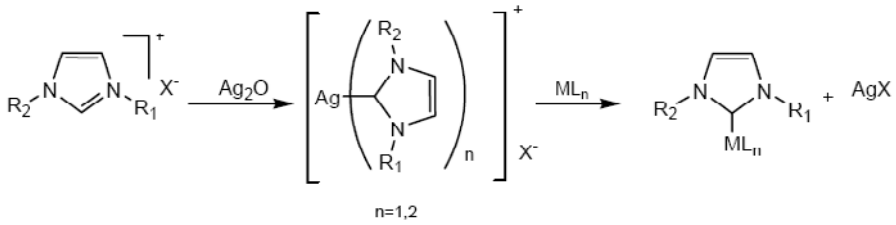

Esquema 5.5

- *Formación de un aducto carbeno*: el uso de formas protegidas de carbenos es una estrategia poco habitual en la preparación de complejos NHC. Anillos N-heterocíclicos que contienen grupos alcoxo o triclorometil como se muestra en el **Esquema 5.6**, pueden ser considerados como aductos-NHCs, puesto que la eliminación de alcohol o cloroformo libera el carbeno para que pueda producirse su coordinación al metal.[11]

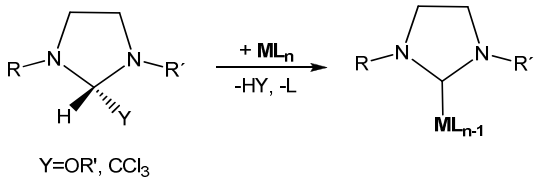

Esquema 5.6. Formación de un carbeno metálico a partir de un aducto de NHC.

Actualmente existe un gran numero de articulos de revisión relacionados con las propiedades estructurales, [12] catalíticas[13] y aplicaciones[14] de los ligandos carbenos N-heterocíclico.

5.2 Objetivos de la investigación

El **Esquema 5.7** muestra los dos tipos generales de ligandos empleados en la realización de este trabajo. La obtención del ligando 1,2,4-trimetil-triazol-di-ilideno (**L**) nos permitirá obtener compuestos bimetálicos conectados a través del dicarbeno, que actúa como puente (**Esquema 5.8-I**). Por otra parte, los ligandos alquenil-NHC permitirán su uso como ligandos de tipo hemiactivable, al permitir la descoordinación irreversible del fragmento olefínico en presencia de sustratos específicos (**Esquema 5.7).**

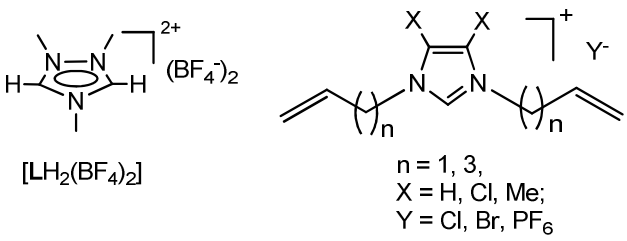

Esquema 5.7. Ligandos NHC empleados

Los ligandos de tipo N-alquenilimidazol se utilizaron para obtener compuestos de Ir^{I}, monocoordinados, bis-quelatos y trisquelato tipo pinza. Los sustituyentes en las posiciones 4 y 5 del imidazol (H, Cl, Me) modificarán las propiedades electrónicas del ligando permitiendo el estudio de las propiedades catalíticas de los complejos resultantes (**Esquema 5.8-II**).

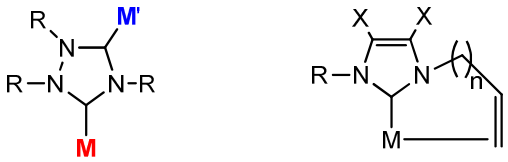

I **II**

Esquema 5.8. Modelos de complejos que serán obtenidos a partir de los ligandos **I** (triazolil-di-ilideno) y **II** (alquenilimidazol).

Los compuestos heterobimetálicos se probarán fundamentalmente en reacciones catalíticas *tándem*, es decir, en procesos consecutivos o concertados. En este sentido, se han realizado estudios en los que se dan procesos secuenciales que implican la acción combinada de los dos metales que constituyen el catalizador.

Los compuestos con ligandos N-alquenil-imidazolil-ilideno se probarán en la reacción de hidrosililación de alquinos terminales. La hidrosililación es un procedimiento catalítico muy importante en la funcionalización de compuestos orgánicos. En la evaluación de los resultados sobre la eficacia catalítica de nuestros compuestos, tendremos en cuenta tanto la eficacia de los catalizadores, es decir, la capacidad para obtener altas conversiones, como su selectividad a la hora de formar los correspondientes isómeros alquenilsilanos: el producto ***α***, y los productos β-***E*** y β-***Z***.

5.3 Discusión y Resultados

5.3.1. Uso de triazolil-di-ilidenos en la síntesis de catalizadores ditópicos

El diseño de catalizadores *tándem* efectivos en dos o más procesos catalíticos consecutivos es uno de los retos actuales en la investigación en catálisis homogénea. Habitualmente, el término *catálisis tándem* se refiere a aquéllas estrategias sintéticas que implican la acción secuencial de varias reacciones catalíticas sin que se produzca un cambio de las condiciones de reacción, o en las que el procedimiento operativo es muy simplificado.[15] Esto implica que el catalizador tiene que ser compatible con las reacciones catalíticas que componen la secuencia.

La llamada *catálisis tándem concurrente* (CTC), implica, además, que dos o más ciclos catalíticos ocurren dentro de un mismo reactor. En algunos casos, un catalizador monometálico es capaz de catalizar dos procesos consecutivos, aunque evidentemente esto exige que ambos procesos sean compatibles con la actividad catalítica del metal. Esto es, por ejemplo, lo que describe el Prof. Field con un catalizador de Ir capaz de catalizar dos reacciones distintas, que consisten en una hidroaminación y una hidrosililación de 4-pentin-1-amino para generar N-sililaminas cíclicas (**Esquema 5.9**). [16]

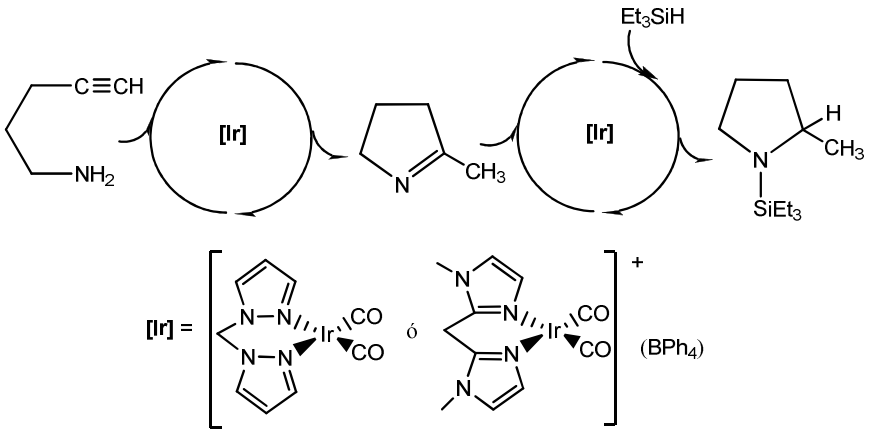

Esquema 5.9

Si lo que se pretende es catalizar dos procesos muy diferentes, normalmente se suele usar una mezcla de dos o más catalizadores (**Esquema 5.10**). Por ejemplo, Jeong y colaboradores muestran una alilación catalizada por Pd generando un intermedio enino, que es transformado, por medio de una reacción tipo Pauson-Khand catalizada por Rh, en una ciclopentenona (**Esquema 5.10**).[17]

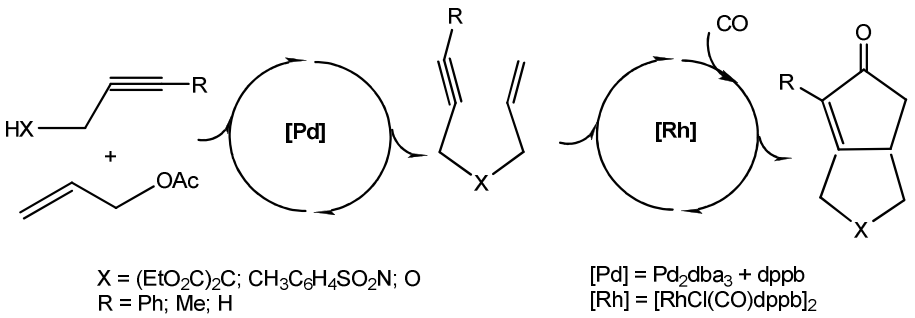

Esquema 5.10

Para este último tipo de catálisis *tándem*, sería extremadamente útil preparar catalizadores de naturaleza bimetálica, de forma que cada fragmento metálico fuera capaz de facilitar una reacción diferente. Para conseguir este objetivo, hace falta diseñar ligandos que sean capaces de unirse a dos o más metales a la vez, y que sean compatibles con las diferentes reactividades de éstos (**Esquema 5.11**).

Dado que los carbenos de tipo N-heterocíclico (NHC), son ligandos que se pueden coordinar a un gran número de metales, en varios estados de oxidación, nuestra hipótesis de partida consistió en utilizar este tipo de ligandos para el diseño de compuestos heterometálicos para su uso en catálisis tándem.

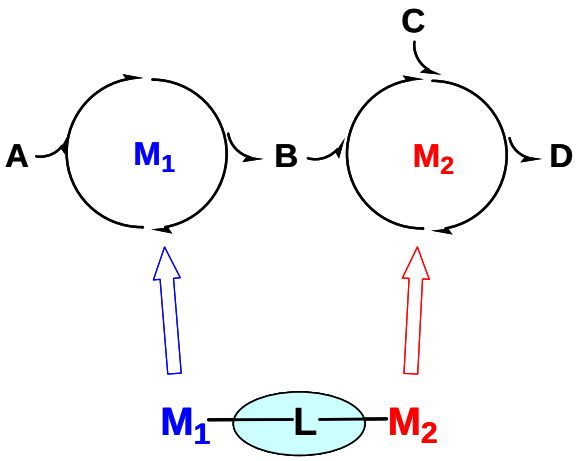

Esquema 5.11

Dentro de esta línea, recientemente, en nuestro grupo de investigación, se ha coordinado el dicarbeno monoazol (**L**) obteniendo compuestos homobimetálicos de Ru, Rh y Ir (**Esquema 5.12**).[18, 19]

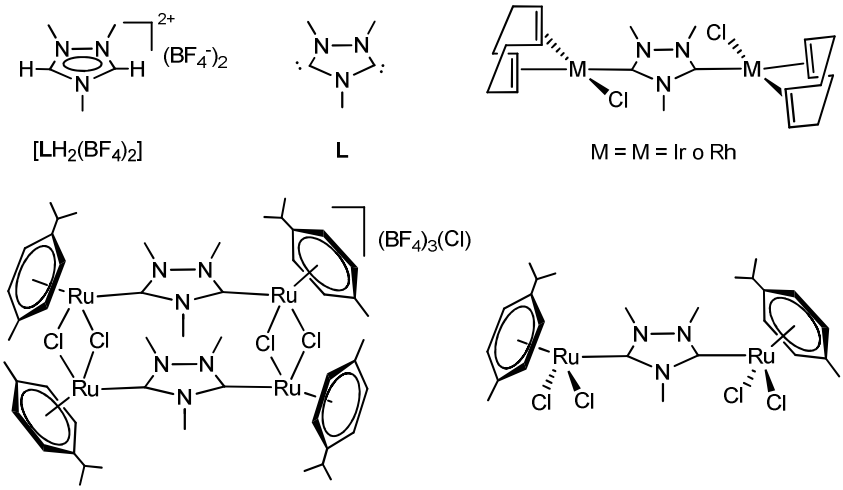

Esquema 5.12

Recientemente Bielawsky y col, prepararon una série de ligandos ditópicos de tipo benzobis(imidazolidenos), que coordinan a dos metales sobre las dos caras opuestas del ligando (coordinación tipo Janus-Head, **Esquema 5.13**). Con estos ligandos se obtuvieron compuestos homo-dinucleares de Rh, Pd, Pt y Ag. [20]

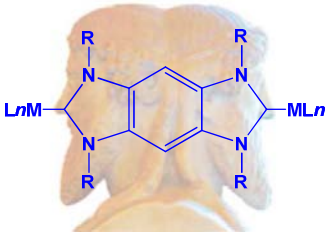

Esquema 5.13

Las sales de triazolio dicatiónicas mostradas en la **Esquema 5.7**, fueron descritas por Curphey en 1972.[21] Precisamente el hecho de ser dicatiónicas, sugiere que la doble desprotonación de los dos enlaces C-H del anillo debe ser fácil, por lo que la coordinación a dos metales debería ser posible. De hecho, Bertrand y col, [22, 23] describieron un biscarbeno polimérico de Ag en el que el ligando triazol-di-ilideno, actúa como puente entre los centros metálicos.[22]

Según estudios realizados en nuestro grupo de investigación,[18] el ligando **L** (**Esquema 5.12**) presenta propiedades electrónicas similares a las trisalquilfosfinas, pero con la topología propia de los ligandos NHC. Los estudios catalíticos en reacciones de ciclación de ácidos alquinóicos y transferencia de hidrógeno, muestran que sus propiedades son sensiblemente mejores que compuestos análogos con ligandos NHC tradicionales.[18] Para la obtención de compuestos heterobimetálicos de Ir^{I}/Rh^{I} se ha propuesto un procedimiento

secuencial como el que se muestra en el **Esquema 5.14**.[18] En una primera etapa, la reacción de la sal de triazolio con $[IrCl(cod)]_2$ en presencia de 1 equivalente de *t*BuOK conduciría a la formación de un intermedio monocarbeno coordinado a Ir. Este intermedio reaccionaría con el precursor metálico $[RhCl(cod)]_2$ tras añadir un segundo equivalente de base, para obtener el compuesto heterobimetálico con el ligando 1,2,4-trimetiltriazolil-diilideno (**L**) coordinado simultáneamente a los dos metales. Sin embargo, este procedimiento proporcionó muy bajos rendimientos en el compuesto heterobimetálico y no permitió aislar el intermedio de reacción monocarbénico.[18]

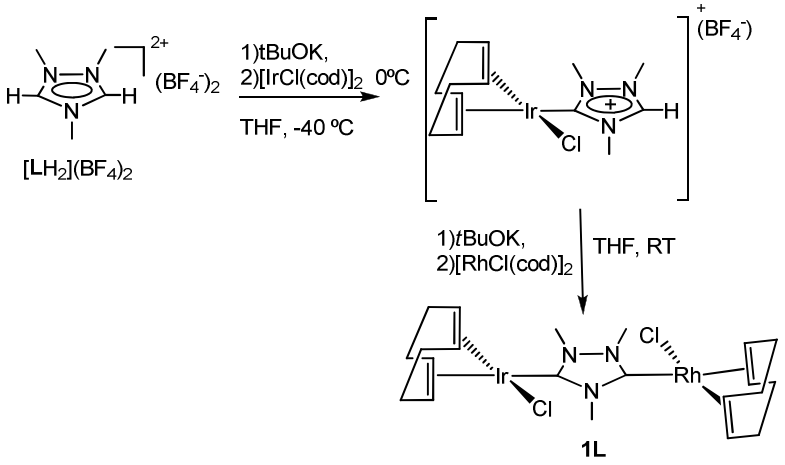

Esquema 5.14

Teniendo en cuenta los resultados obtenidos en la coordinación del ligando **L** a Rh^I e Ir^I se decidió extender su coordinación a otros metales.

5.3.2 Reactividad y propiedades cataliticas de compuestos de Pd^{II} y Pt^{II} con ligandos de tipo triazolil-di-ilideno

La coordinación del ligando **L** a Pd y Pt ha permitido preparar compuestos bimetálicos homonucleares de Pd y Pt (**Esquema 5.15**) a partir de la sal dicationica de triazolio $[\mathbf{L}H_2](BF_4)_2$:

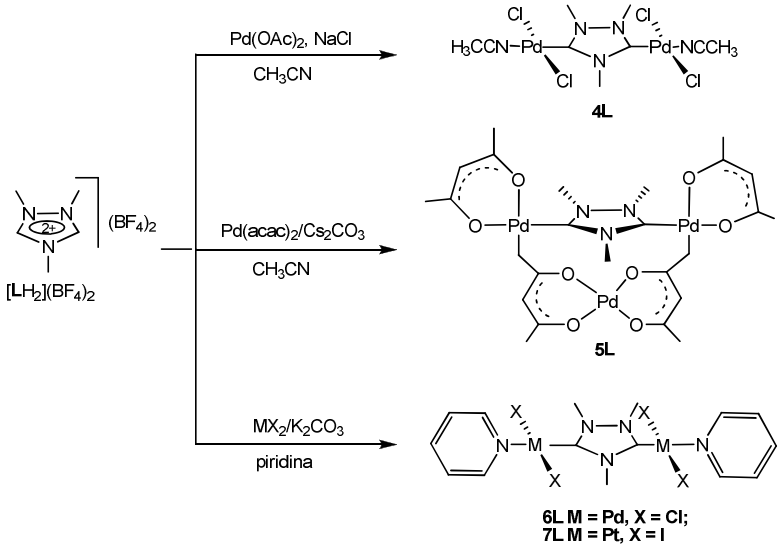

Esquema 5.15

Los compuestos obtenidos han sido caracterizados por las técnicas espectroscópicas habituales. El estudio estructural del compuesto **5L** mediante difracción de Rayos X ha permitido elucidar un palladaciclo trimetálico de 12 miembros. (**Figura 5.1**).

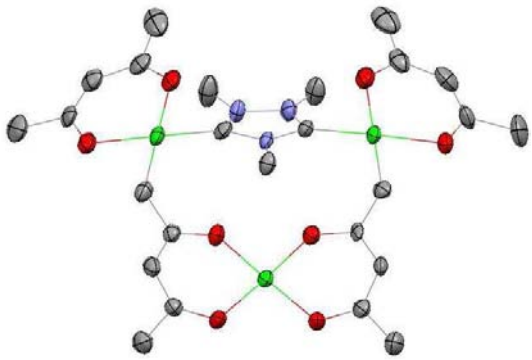

Figura 5.1. Diagrama Molecular del compuesto **5L**.

En la literatura existe un solo ejemplo anterior en el que se describe una coordinación puente del ligando 'acac' como la que muestra el compuesto **5L**.[24] Los compuestos **4L** y **5L** han sido

empleados como catalizadores en reacciones de acoplamiento C-C. Como test preliminar hemos comprobado la actividad de nuestros nuevos compuestos en la reacción de Heck. La reacción entre estireno y 4-bromoacetophenona nos ha proporcionado la conversión completa al estilbeno correspondiente.

La segunda reacción catalítica estudiada ha sido la acilación de aril-haluros con aldehidos (**Esquema 5.16**).[25]

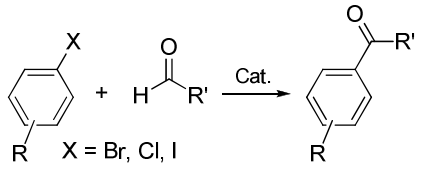

Esquema 5.16. Acilación directa de aril haluros con aldehidos.

En esta reacción se consigue directamente a la obtención de cetonas, evitando la clásica reacción de Friedel-Crafts que comportaría el uso de reactivos peligrosos. El catalizador **4L** presentó buenos resultados en la obtención de los productos deseados mientras que el catalizador **5L** no presentó ninguna actividad catalítica.

Esta reacción catalítica fue descrita muy recientemente por Xiao,[25] y nuestros resultados constituyen el segundo ejemplo de este tipo de catálisis. En comparación con el trabajo de Xiao,[25] nuestro catalizador resulta especialmente conveniente ya que no necesita el empleo de fosfinas adicionales, que podrían generar residuos tóxicos difíciles de eliminar a la hora de separar los productos finales de la mezcla de reacción.

El compuesto **6L** ha sido empleado como catalizador en un proceso tándem entre *o*-hidroxiaril haluros y fenilacetileno para generar benzofuranos (**Esquema 5.17**). Con objeto de comparar otros compuestos similares se emplearon también los compuestos de Pd(NHC), **8L** y **9L,** que se muestran en el **Esquema 5.18**. Es interesante observar que, a pesar de que ambos procesos suelen ser cataizados por catalizadores de Pd, en ninguna ocasión se ha descrito un proceso tándem que implique la realización consecutiva de ambas reacciones en el mismo medio de reacción. Nosotros decidimos plantear esta reacción tándem al considerar que la estabilidad de los catalizadores empleados (**Esquema 5.18**), podría permitir que estos soportaran las condiciones de reacción de ambos procesos.

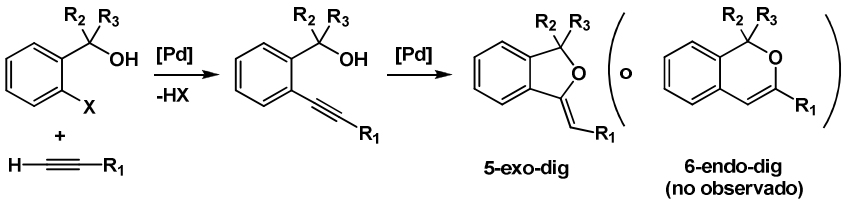

Esquema 5.17

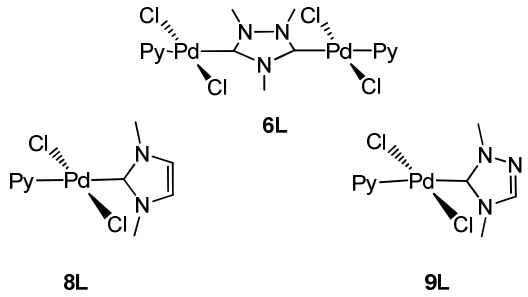

Esquema 5.18

La elección de los catalizadores empleados se realizó en base a la capacidad dadora σ de los ligandos utilizados, que disminuye en el orden: 1,3-dimetil-imidazolilideno > 1,4-dimetil-triazolilideno > 1,2,4-trimetiltriazolil-di-ilideno. Las propiedades estéricas de los tres ligandos son muy similares.

La secuencia catalítica (**Esquema 5.17**) implica como primer paso un acoplamiento de Sonogashira seguido por una hidroalcoxilación intramolecular del alquino resultante. Ambas reacciones son catalizadas por paladio a través de una estrategia tipo "one-pot", sin añadir algún tipo de aditivo o co-catalizador. En nuestro caso, la reacción ha sido selectiva para la ciclación en la forma 5-exo-dig. Los tres catalizadores muestran elevadas actividades; hay que destacar que la presencia de ligandos más dadores sigma (1,3-dimetil-imidazolilideno, complejo **8L**) favorecen la reacción de Sonogashira mientras que ligandos menos dadores sigma (1,2,4-trimetiltriazolil-di-ilideno, complejo **6L**) favorecen la reacción de ciclación.

5.3.3 Estudio de procesos catalíticos tipo *tándem* con compuestos heterobimetálicos de Ir^{III}/Ir^{I} y Ir^{III}/Rh^{I} con el ligando triazolil-di-ilideno

La obtención de compuestos heterobimetálicos se realizó de forma secuencial. A partir de un equivalente del precursor [**L**H_2](BF_4) y un equivalente de base se pudo obtener una especie monocarbeno (**10L**, **Esquema 5.19**). Posteriormente una segunda activación del enlace C-H nos proporcionó los compuestos de naturaleza heterobimetálica. El **Esquema 5.19** muestra el procedimiento empleado.

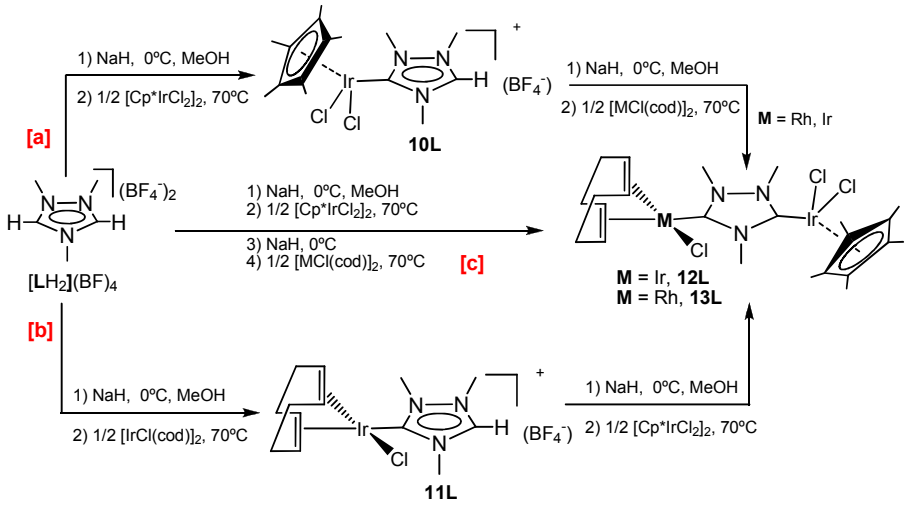

Esquema 5.19

La síntesis del compuesto **10L** pudo ser realizada a partir de un aducto metanólico de triazol o tambien pudo realizarse generando el aducto metanólico a partir de la sal de triazolio [**L**H_2]$(BF_4)_2$, y haciéndolo reaccionar *in situ* con el precursor metálico de Ir^{III} (**Esquema 5.19**), simplificando el procedimiento de síntesis. Usando la misma estrategia de síntesis pero utilizando $[IrCl(cod)]_2$, conseguimos aislar el complejo **11L** (**Esquema 5.19**).

La reacción del compuesto **10L** con $[MCl(cod)]_2$ (M = Rh, Ir) en presencia de NaH en MeOH nos permitió obtener los complejos bimetálicos **12L** (Ir^{III}/Ir^{I}) y **13L** (Ir^{III}/Rh^{I}). Estos dos nuevos complejos contienen dos fragmentos metálicos en diferente estado de oxidación. La síntesis pudo ser realizada también preparando **12L** y **13L** *in situ* sin necesidad de aislar los carbenos monometalados **10L** y **11L**. Esta estrategia es muy conveniente porque simplifica la preparación de los productos finales, a la vez que disminuye la cantidad de disolventes usados, tiempo de preparación y purificaciones posteriores. El compuesto **12L** también pudo prepararse haciendo reaccionar **11L** con $[Cp^*IrCl_2]_2$ en presencia de NaH en MeOH (**Esquema 5.19**). Los rendimientos obtenidos en la obtención de **12L** usando los metodos **[a]**, **[b]** y **[c]** (**Esquema 5.19**) han sido del 82 **[a]**, 52 **[b]** y 40 % **[c]**. El compuesto **13L** se obtuvo a su vez con el 66 **[a]** y el 54 % **[c]**.Los compuestos obtenidos han sido caracterizados por las técnicas espectroscópicas habituales, espectrometría de masas y por difracción de Rayos X.

Estos compuestos han resultado muy activos en un proceso catalítico secuencial que implica la oxidación/ciclación de 2-aminofenil-etil alcohol (una reacción típicamente catalizada por $[Cp^*Ir(Cl)_2]_2$)[26] y la alquilación del indol resultante con una serie de alcoholes primarios (reacción catalizada por compuestos de Ir[27], Ru[28], In[29] y Rh[30] **Esquema 5.20**). Los esqueletos de tipo indol se encuentran en muchos productos naturales con aplicaciones farmacéuticas, por lo que el desarrollo de nuevas metodologías para la síntesis de indoles funcionalizados es un campo de gran interés.[30]

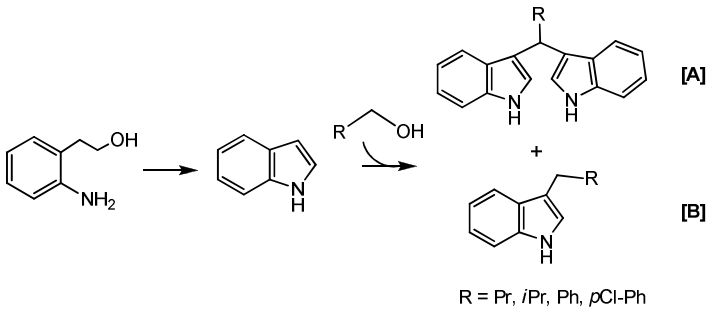

Esquema 5.20

La posterior alquilación del indol con un alcohol primario nos ha proporcionado la obtención selectiva de la especie bisindolilmetano [**A**] o la especie monoindol funcionalizada [**B**], según las condiciones de reacción empleadas.

La estrategia *one-pot tándem* para obtener, en un único paso, indoles o bisindoles funcionalizados a partir del 2-aminofenil-etil alcohol y alcoholes primarios, nos permite comparar la actividad de nuestros catalizadores bimetálicos en dos procesos diferentes y consecutivos. Los catalizadores estudiados se muestran en el **Esquema 5.21**.

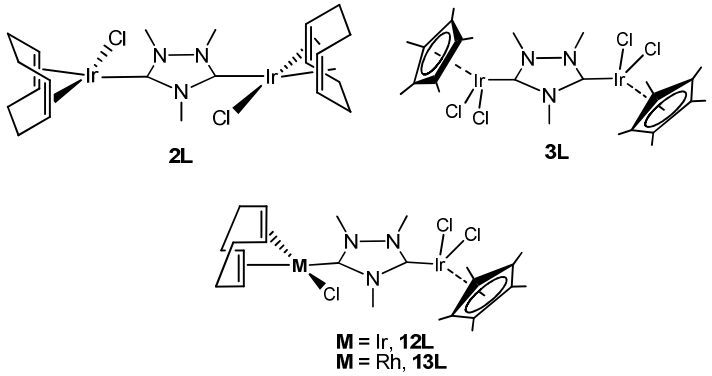

Esquema 5.21

El catalizador de valencia mixta **12L** fue el que proporcionó los mejores resultados catalíticos en términos de selectividad y actividad catalítica. Además, la actividad del catalizador es diferente de la suma de los fragmentos individuales, lo que comportaría una posible cooperación de los dos metales a través del anillo puente triazolil-di-ilideno.

5.3.4 Estudio de procesos catalíticos tipo *tándem* con compuestos heterobimetálicos de Ir^{III}/Pd^{II}: transformación de 4-halobenzofenonas

La coordinación del ligando "L" a dos metales sustancialmente diferentes que puedan ser aplicados a reacciones catalíticas bien diferenciadas, permite ampliar el número de posibles combinaciones catalíticas que conformen el proceso tándem.

La síntesis de complejos heterobimetálicos de Ir/Pd se ha realizado a partir del compuesto **10L** en el que el anillo de triazol actúa como monocarbeno teniendo un CH que puede ser posteriormente activado para generar un segundo carbeno. La reacción de **10L** con diversos precursores de paladio, permite la obtención de tres compuestos heterobimetálicos de Ir/Pd (**Esquema 5.22**).

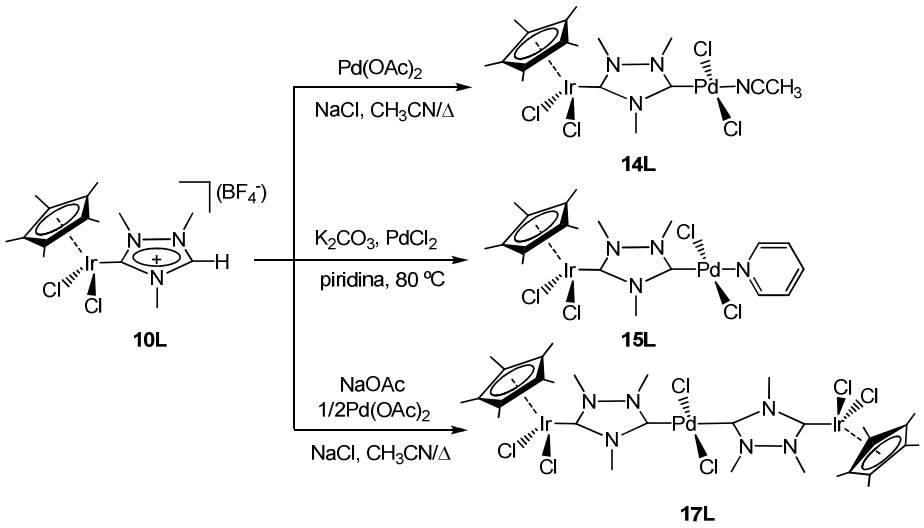

Esquema 5.22

Los compuestos obtenidos han sido caracterizados por las técnicas espectroscópicas habituales, espectrometría de masas y por difracción de Rayos X

La presencia de dos metales diferentes nos ha permitido diseñar procesos tándem que combinan reacciones típicamente catalizadas por Ir y Pd. Para este tipo de catalizador, hemos considerado que las *p*-haloacetofenonas representan sustratos muy adecuados ya que tienen dos grupos funcionales diferentes, activables por paladio (enlace C-halógeno) e iridio (grupo carbonilico). En concreto, se han estudiado tres reacciones tándem: deshalogenación/transferencia de hidrógeno de haloacetofenonas (**Esquema 5.24**), acoplamiento de Suzuki/transferencia de hidrógeno de *p*-bromoacetofenona (**Esquema 5.25**), y acoplamiento de Suzuki/α-alquilación de la *p*-bromoacetofenona (**Esquema 5.25**). Los catalizadores estudiados se muestran en el **Esquema 5.23**.

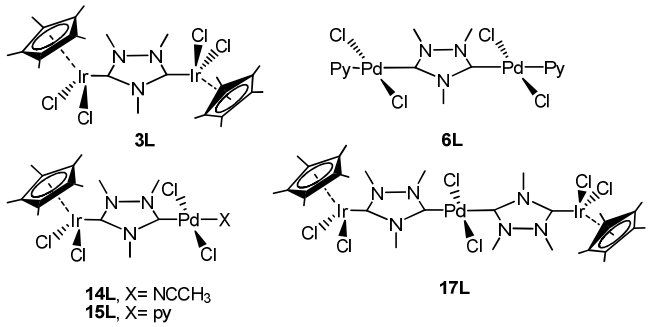

Esquema 5.23

En el **Esquema 5.24**, la reacción de deshalogenación/transferencia de hidrógeno de haloacetofenonas se hace en medio básico en presencia de *i*PrOH que actúa como disolvente y agente reductor. La reacción incluye la abstracción de halógeno, con formación de acetofenona (intermedio **A**), catalizada por el fragmento de paladio y siguiente transferencia de hidrogeno al carbonilo para generar el feniletanol, producto **C**, catalizada por el fragmento de Ir.

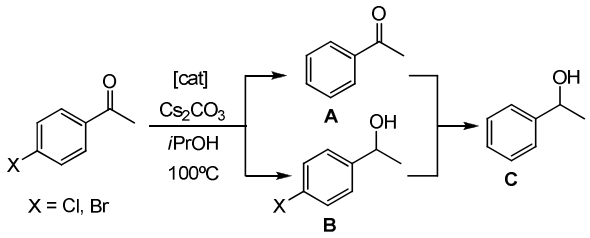

Esquema 5.24

En la reacción con *p*-bromoacetofenona, en *i*PrOH y utilizando Cs_2CO_3 como base, el compuesto **15L** nos proporciona los mejores resultados cataliticos (**Tabla 5.1**, entrada 2), comparando los rendimientos hacia el producto final **C**.

Tabla 5.1. Tándem deshalogenación/transferencia de hidrógeno de *p*-bromoacetofenona.[a]

Entrada	Catalizador	Tiempo (h)	A (%)[b]	B (%)[b]	C (%)[b]
1	**14L**	20	22	0	75
2	**15L**	20	0	0	>99
3	**17L**	20	0	0	95
4	**3L**	20	0	89	0
5	**6L**	20	95	0	0
6	**3L + 6L**[c]	20	72	0	25

[a] Condiciones de reacción: 4-haloacetofenone (0.36 mmol), Cs_2CO_3 (0.43 mmol), anisol como referencia interna (0.36 mmol), catalizador (2 mol%) y 2 mL de 2-propanol. La solución se calienta a 100 ºC en condiciones aeróbicas. [b] Rendimientos determinados por gas-cromatografía. [c] 1 mol % of **3L** + 1 mol % of **6L**.

Los compuestos homobimetálicos de Ir (**3L**) y Pd (**6L**) muestran actividades catalíticas relativas a las reacciones en las que tienen que ser activos, concretamente, el complejo de Ir cataliza la transferencia de hidrogeno reduciendo el grupo carbonilo a alcohol secundario (producto **B**, entrada 4 de la **Tabla 5.1**), mientras que el complejo de Pd favorece el proceso de deshalogenación (producto **A**, entrada 5 de la **Tabla 5.1**). Además, la adicción de las especies homobimetálicas **3L** y **6L** conlleva a la obtención del producto **C** con un rendimiento muchos más inferior en comparación con lo resultados obtenidos con los tres complejos heterobimetálicos (entrada 6 de la **Tabla 5.1**). Este dato sugiere una posible cooperación catalítica entre los dos fragmentos metálicos a través del anillo puente triazolil-di-ilideno.

Con objeto de diseñar un proceso tándem más ambicioso, decidimos sustituir el paso de la deshalogenación, por un acoplamiento de Suzuki, simplemente añadiendo un ácido arilborónico al medio de reacción anterior. Además, si sustituimos el alcohol secundario por un alcohol primario, podemos sustituir la reacción catalizada por Ir^{III} por una α-alquilación de cetonas. El **Esquema 5.25** presenta la reacción de acoplamiento de Suzuki-Miyaura en presencia de diferentes alcoholes primarios y secundarios.

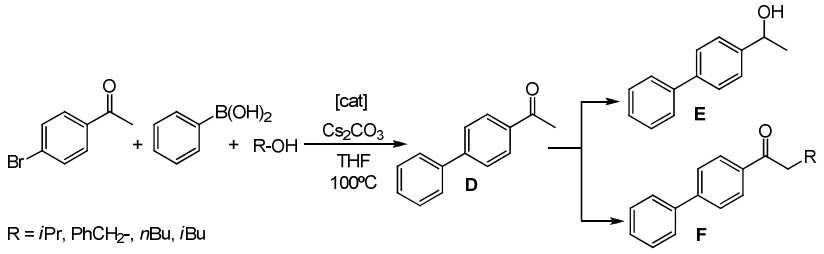

Esquema 5.25

La secuencia catalítica, en este caso, implica la reacción de acoplamiento del ácido fenilboronico a la halocetofenona generando la cetona resultante **D**, catalizada por el fragmento de Pd. Esta cetona en presencia de un alcohol secundario nos facilita la obtención del alcohol **E** mientras que el empleo de un alcohol primario nos proporciona la cetona alquilada en la posición α, **F**. Ambas reacciones han sido catalizadas por el fragmento de Ir. Los resultados más relevantes se resumen en la **Tabla 5.2**

Table 5.2. Acoplamiento de Suzuki de *p*-bromoacetofenona en presencia de alcoholes.[a]

Entry	Catalyst	Time(h)	R-OH	D (%)[b]	E (%)[b]	F (%)[b]
1	**15L**	7	*i*PrOH	2	88	0
2	**15L**	20	$PhCH_2OH$	5	1	80 (72)
3	**15L**	20	*n*BuOH	4	2	92 (86)
4[c]	**3L + 6L**	4	*i*PrOH	55	5	0
5[c]	**3L + 6L**	20	*n*BuOH	21	13	29

[a] Reaction Conditions: 4-bromoacetofenona (0.36 mmol), acido fenilboronico (0.55mmol), Cs_2CO_3 (1.08 mmol), anisol como referencia interna (0.36 mmol), catalizador (2 mol%), 2 mL de R-OH y 2mL de THF. La solución se calienta a 100 ºC en condiciones aeróbicas. [b] Rendimientos determinados por gas-cromatografía (rendimientos aislados). Menos del 8% (respecto a Ph-$B(OH)_2$) de Ph-Ph formado. [c] 1 mol % de **3L** + 1 mol % de **6L**.

La obtención de las cetonas bifenílicas α-alquiladas, no constituye únicamente una reacción modelo de estudio, sino que dada su aplicación como inhibidores no esteroideos de la 5α-reductasa, esta nueva síntesis representa una alternativa sencilla y rápida para obtener especies orgánicas con potenciales aplicaciones farmacéuticas.[31]

El catalizador heterobimetálico **15L** nos proporcionó los mejores resultados catalíticos en términos de selectividad y actividad catalítica (entradas 1, 2 y 3 de la **Tabla 5.2**). Además, la actividad del catalizador es diferente de la suma de los fragmentos individuales (**3L + 6L**, entradas 4 y 5 del la **Tabla 5.2**), lo que de nuevo sugiere una posible cooperación catalítica de los dos metales a través del anillo puente triazolil-di-ilideno.

5.3.5 Estudio de procesos catalíticos tipo *tándem* con compuestos heterobimetálicos de Ir^{III}/Pd^{II}: formación de iminas por reducción de nitro-arenos/acoplamiento con aloholes

Con el objetivo de descubrir nuevas propiedades catalíticas, el complejo **15L** ha sido empleado para la obtención de iminas a través de una reacción entre alcoholes y nitroarenos. Las iminas son intermedios detectados frecuentemente en las reacciones de N-alquilación de aminas con alcoholes a través un proceso tipo *borrowing-hydrogen*,[32, 33] aunque sus preparaciones selectivas han sido descritas en muy pocas ocasiones.

Las iminas destacan por sus diferentes reactividades y por sus aplicaciones a nivel industrial en los procesos de síntesis orgánica.[34] La preparación tradicional de iminas implica la reacción entre cetonas o aldehidos con aminas en presencia de un acido de Lewis como catalizador. Pueden ser también obtenidas por condensación oxidativa de aminas o por simplemente, oxidaciones de aminas.

La secuencia catalítica propuesta implica la reducción del nitroareno a anilina por medio de un alcohol, el cual oxida a aldehído. El acoplamiento entre anilina y aldehído genera selectivamente la imina correspondiente. (**Esquema 5.26**).

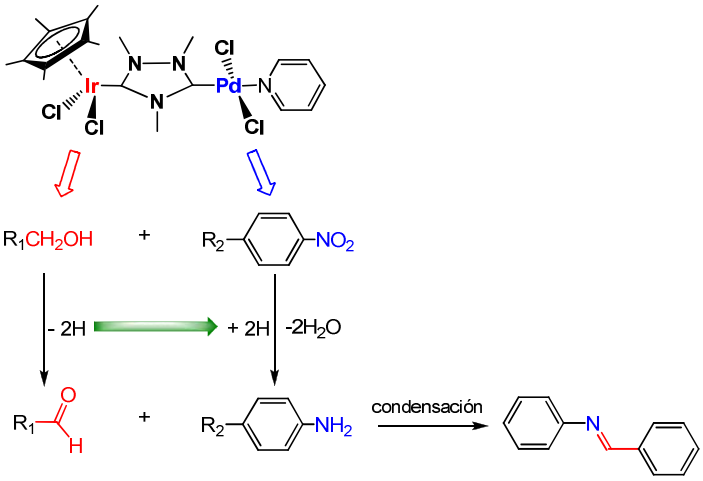

Esquema 5.26

El compuesto heterobimetálico de iridio-paladio representa el mejor candidato para el proceso global. El fragmento de iridio facilitaba la oxidación del alcohol liberando hidrogeno necesario para que el fragmento de paladio produzca la reducción del nitroareno. Los catalizadores estudiados se muestran en el **Esquema 5.27**.

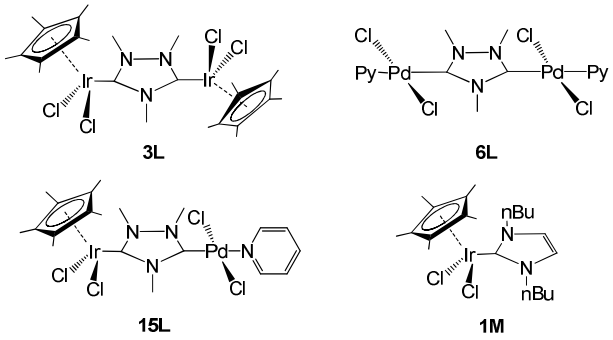

3L **6L**

15L **1M**

Esquema 5.27

El **Esquema 5.28** describe la condensación de diferentes nitroarenos con una serie de alcoholes primarios.

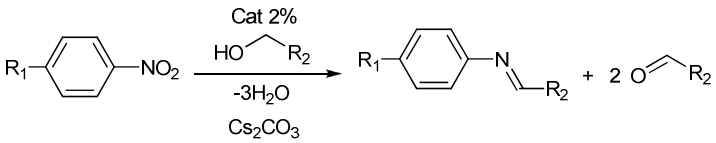

Esquema 5.28

Los resultados catalíticos demuestran que la actividad catalítica del precursor metálico $[Cp^*IrCl_2]_2$ es muy reducida comparándolos con los otros catalizadores, al utilizar una carga de catalizador del 0.2 mol % (confirma este dato). Se necesitan tiempos de reacción largos para alcanzar rendimientos discretos (cerca del 60 %). Sin embargo, es interesante destacar que cuando se utiliza una cantidad de catalizador elevada (2 mol %), los rendimientos son cuantitativos. La suma de los compuestos homodimetalicos de Ir y Pd (**3L** + **6L**) conlleva buenos resultados catalíticos aunque sólo para algunos substratos. El catalizador **15L** es el que proporciona los mejores rendimientos con la mayoría de nitroarenos y benzil alcoholes usados.

Además, la diferente actividad de los catalizadores **15L** y **3L** puede ser ilustrada en la condensación oxidativa entre *p*-bromonitrobenzeno y benzil alcohol, **Esquema 5.29**. Cada catalizador permite la obtención de un producto diferente.

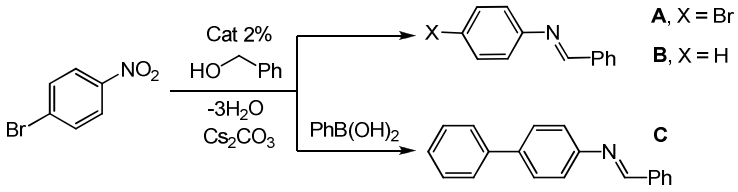

Esquema 5.29

El catalizador **3L**, que sólo contiene Ir, proporciona la formación de la imina **A** mientras que el catalizador **15L** (de Ir/Pd), en las mismas condiciones de reacción, favorece la deshalogenación de la imina **B**, debido precisamente a la presencia del fragmento de Pd.
Añadiendo en el medio de reacción acido fenilboronico, el catalizador **15L** permite también obtener el acoplamiento entre los dos arenos en la clásica reacción de Suzuki-Miyaura hacia la formación de la bisarilimina **C**. Esta nueva reacción comporta la acción individual de los dos fragmentos metálicos en diferentes procesos catalíticos.

En base a los resultados obtenidos, el camino de reacción por el que transcurre esta secuencia catalítica, conlleva dos diferentes mecanismos, dependiendo si se utiliza el catalizador de Ir o el catalizador heterobimetálico de Ir-Pd. En el caso del catalizador de Ir, la reducción del grupo nitro procede con buenos rendimientos a través de un proceso general de *borrowing-hydrogen* (**Esquema 5.30**). Según estudios previos,[35] el paso inicial de la reacción implicaría la oxidación del benzil-alcohol a benzaldehído generando hidrógeno, bien en forma molecular, o como bis-hidruro de Ir. Este hidrógeno generado es responsable de la reducción de nitrobenzeno a anilina. Un equivalente de benzaldehido condensa con la anilina generada para formar la imina. Esta reacción, constituye un nuevo tipo de proceso enmarcado dentro de los conocidos como 'borrowing-hydrogen'.

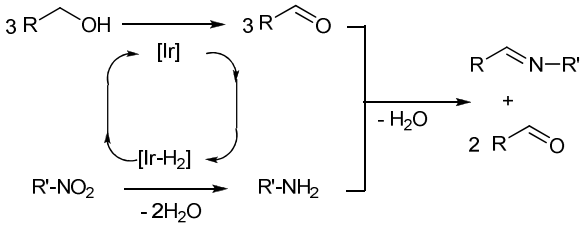

Esquema 5.30

En el caso del catalizador **15L**, la oxidación del benzil-alcohol es facilitada por el fragmento de Ir, generando hidrógeno. En un segundo paso, el fragmento de Pd utiliza el hidrógeno para facilitar la reducción del nitrobenzeno a anilina (**Scheme 5.31**).

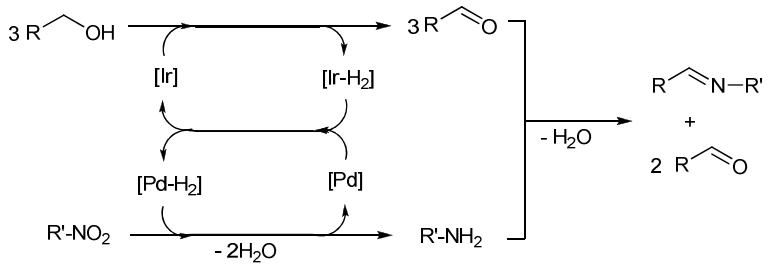

Esquema 5.31

El estudio catalítico realizado representa un nuevo ejemplo de catálisis tándem empleando un catalizador con dos fragmentos metálicos unidos por el ligando *L*. Hemos comentado en el anterior apartado que la conexión de los dos metales a través del ligando *L* puede comportar cooperatividad catalítica de los dos metales. Paralelamente, hay que considerar otras ventajas, como la mejora de la eficiencia atómica alcanzada cuando se utiliza un único catalizador en lugar de dos, además de la evidente reducción de productos indeseados en la síntesis de un solo catalizador.

5.3.6 Estudio de procesos catalíticos tipo *tándem* con compuestos heterobimetálicos de Ir^{III}/Pt^{II} con ligandos triazolil-di-ilideno

La utilización de platino, en su combinación con Ir^{III}, puede proporcionar catalizadores muy interesantes para el diseño de nuevos procesos tándem. Por un procedimiento similar al utilizado en el **Esquema 5.22**, a partir del compuesto **10L**, obtuvimos un compuesto heterobimetálico de Ir^{III}/Pt^{II} (**16L**) (**Esquema 5.32**).

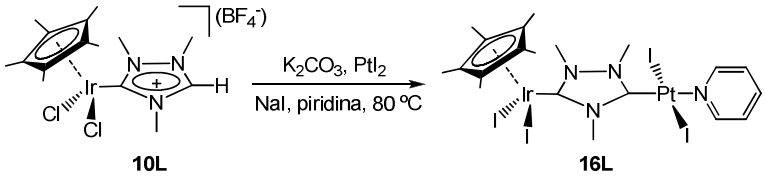

Esquema 5.32

El compuesto obtenido ha sido caracterizado por las técnicas espectroscópicas habituales, espectrometría de masas y por difracción de Rayos X.

Hemos sintetizado este complejo con la intención de estudiar una combinación de reacciones típicamente catalizadas por Ir y por Pt. De este manera hemos combinado la ciclación oxidativa de aminoalcoholes para generar indoles, catalizada por Ir,[26] con una serie de reacciones catalizadas por Pt^{II} a partir de indoles y alquinil alcoholes.[36] El proceso *tándem* resultante incluye tres reacciones consecutivas: 1) ciclación oxidativa de un aminoalcohol para formar indol, 2) hidroalcoxilación intramolecular de un alquinil alcohol para generar un vinil-eter cíclico y 3) adición de indol al vinil-eter cíclico (**Esquema 5.33**).

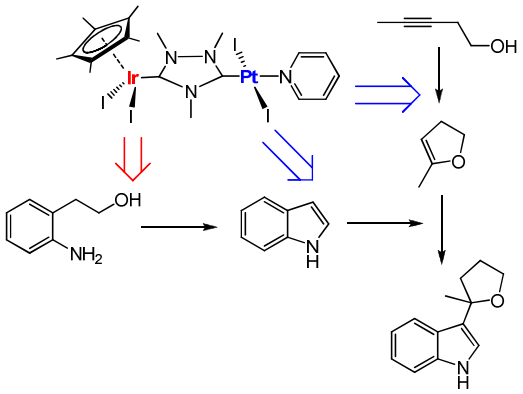

Esquema 5.33

Los catalizadores estudiados se muestran en el **Esquema 5.34**.

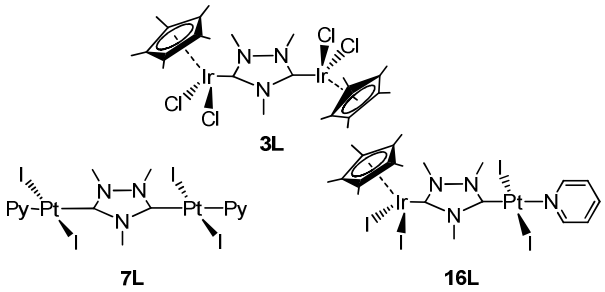

Esquema 5.34

Las reacciones se han efectuado de forma secuencial, añadiendo el correspondiente alquinil alcohol después de que el indol se haya formado, obteniéndose así los indoles funcionalizados (**Esquema 5.35**).

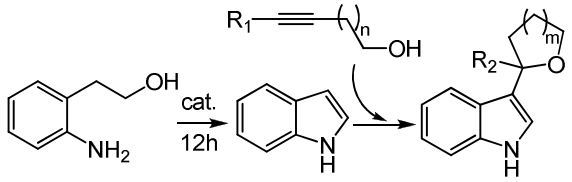

Esquema 5.35

La elección de esta secuencia catalítica implica un estudio detallado de la compatibilidad de nuestro catalizador con los sustratos, intermedios de reacción generados y condiciones de reacción que se producen durante el proceso catalítico.

Los resultados catalíticos, resumidos en la **Tabla 5.3**, demuestran la eficacia del catalizador **16L** para la obtención de indoles funcionalizados con rendimientos entre el 60-81% (entradas 2, 7-11 de la **Tabla 5.3**), empleando varios alquinil alcoholes.

Table 5.3. Tándem ciclación de 2-aminofenetil alcohol y adicción de un alquinil alcohol.[a]

Entrada	Catalizador (carga)[b]	R^1	R^2	n	m	Indol[c,d]	Tiempo (h)[e]	Rendimiento (%)[c]
1	**7L** (2)	Me	Me	1	1	0	15	0
2	**16L** (2)	Me	Me	1	1	77	15	74
3	**3L** (2)	Me	Me	1	1	67	15	56
4	**3L** + **7L** (2)	Me	Me	1	1	51	15	44
5	**3L** + **7L** (2)	H	Me	2	1	ND	15	16
6	**3L** + **7L** (5)	H	Me	2	1	ND	12	35
7	**16L** (2)	H	Me	2	1	ND	15	60
8	**16L** (5)	H	Me	2	1	ND	15	81(77)
9[f]	**16L** (2)	H	Me	3	2	ND	15	15
10[f]	**16L** (5)	H	Me	3	2	ND	12	24
11[f]	**16L** (2)	Pr	Pr	1	1	ND	24	80(74)

[a] Condiciones de reacción: 0.33 mmol 2-aminofenetil alcohol, trifluoro sulfunato de plata (0.03 mmol), anisol como referencia interna (0.25 mmol) en 800 μL de toluene a 110ºC. Después de 12h se añaden 0.38 mmol de alquinil alcohol. [b] Con respecto al metal. [c] Rendimientos determinados por gas-cromatografia. [d] Rendimiento del intermedio de indol antes de añadir el alquinil alcohol. ND = No Determinado [e] Tiempo total, relativo a los dos procesos (el primero es siempre de 12h). [f] Temperatura de reacción: 80 ºC.

El catalizador **7L** no genera producto final, dado su incapacidad en el proceso de ciclación del amino alcohol (entrada 1 de la **Tabla 5.3**). En las mismas condiciones de reacción la suma de los complejos **3L** y **7L** proporciona un rendimiento mucho menor que el producido por el catalizador **16L** (entradas 4-6 de la **Tabla 5.3**). Este resultado apoya la idea de una posible

cooperación catalítica entre ambos centros metálicos. La actividad del catalizador **16L** no se ve modificada por la adición de Hg metálico,[37] sugiriendo que la reacción transcurre según un proceso de catálisis homogénea.

5.3.7 Síntesis y caracterización de catalizadores de Ir^{I} con ligandos alquenil-imidazolil-ilideno.

Los ligandos del tipo N-alquenil-imidazolil-ilideno han sido empleados recientemente en el diseño de nuevos catalizadores de Ir^{I}.[38, 39, 40] En nuestro grupo de investigación hemos utilizado este tipo de ligandos por su capacidad para actuar como *hemiactivables*. Tal y como lo hemos definido, un ligando *hemiactivable* consiste en un ligando inicialmente quelato, que de forma irreversible genera una vacante de coordinación en presencia de uno de los sustratos utilizados en el proceso catalítico (**Esquema 5.36**).

En este sentido, es importante destacar que un ligando hemiactivable es diferente a un ligando hemilábil tradicional, ya que en estos últimos la descoordinación de uno de los brazos del ligando es reversible, a diferencia de lo que ocurre en los ligandos hemiactivables. El concepto *hemiactivable* (“*hemicleaveable”*), ha sido acuñado recientemente en nuestro grupo de investigación.[40, 41]

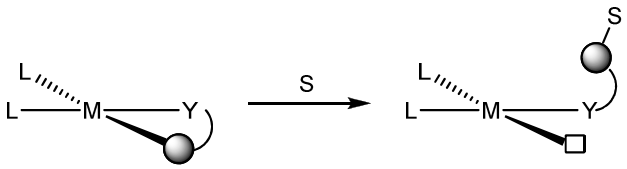

Esquema 5.36

La estabilización de vacantes de coordinación mediante la coordinación-π de olefinas puede ayudar a estabilizar los precatalizadores, a diferencia de lo que ocurre con otros precatalizadores altamente inestables con ligandos muy lábiles. Además, dado que en un ligando *hemiactivable* la generación de la vacante de coordinación no implica la pérdida del ligando de la esfera de coordinación del metal, se evita la generación de residuos innecesarios en el medio.

Se prepararon diferentes sales de imidazolio con el objetivo de modificar las propiedades estéricas y electrónicas. Desde el punto de vista estereoelectrónico, la variación de la distancia entre el anillo NHC y la olefina (variación de n), proporcionará una modificación de la orientación de la olefina con respecto al plano de coordinación del ligando, mientras que los sustituyentes en las posiciones 4 y 5 (H, Cl y Me) modulan las propiedades electrónicas de los compuestos preparados. Las sales han sido posteriormente coordinadas a Ir^{I} por transmetalación con Ag_2O. Dependiendo de la longitud de las cadenas olefínicas se han conseguido diferentes tipos de coordinación: monocoordinado con bis-pentenilos (**2d**), quelato

con bis-propenilo (**1a-c**) y pinza (**2a-c**), a través de abstracción de haluro con sal de plata (**Esquema 5.37**).

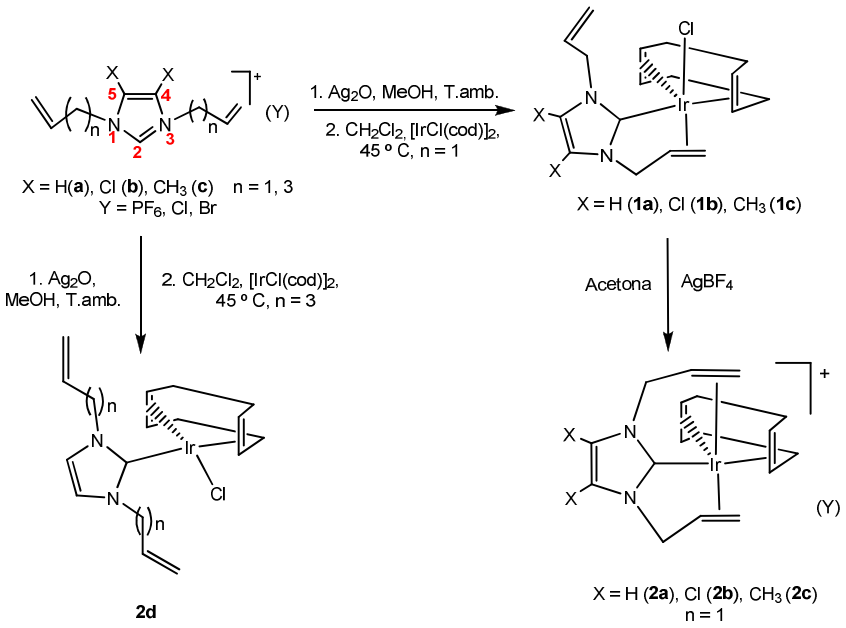

Esquema 5.37

Los compuestos obtenidos han sido caracterizados por las técnicas espectroscópicas habituales. El estudio estructural de los compuestos **2a-c** mediante difracción de Rayos X ha permitido evaluar la influencia de la naturaleza de los sustituyentes en las posiciones 4 y 5 del anillo de azol en los parámetros estructurales de los compuestos.

Los espectros de RMN de ^{1}H de **1a**, **1b** y **1c**, son cualitativamente similares. Estos compuestos generan espectros en los que las señales son muy anchas, lo que indica que se está produciendo un equilibrio dinámico de carácter fluxional que implicaría la coordinación/descoordinación de las olefinas, **Esquema 5.38**.

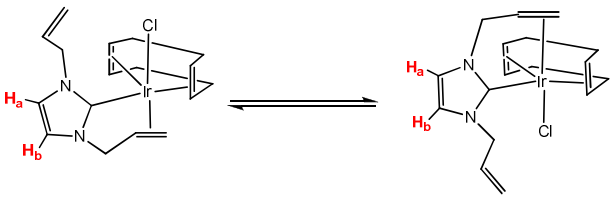

Esquema 5.38

El análisis de anchura de banda y la temperatura de coalescencia de los protones del anillo de imidazol (Ha y Hb en el **Esquema 5.38**), a partir de estudios de VT-RMN, nos han permitido establecer parámetros cinéticos que gobiernan este proceso ($\Delta H^{\neq}$ = 20.9 Kcal/mol; $\Delta S^{\neq}$ = 17.4

cal/molK). Los valores encontrados están en concordancia con estudios experimentales y teóricos de la energía de enlace Ir-olefina.[43, 44] Estos resultados muestran que el proceso fluxional está gobernado por el proceso entálpico correspondiente a la coordinación y descoordinación de la olefina. El valor positivo del factor entrópico nos indica un estado de transición altamente desordenado asociado un proceso de tipo disociativo.

Las propiedades catalíticas de los compuestos obtenidos (**1a-c**, **2a-c** y **2d**) han sido evaluadas en la hidrosililación de alquinos terminales (**Esquema 5.39**).

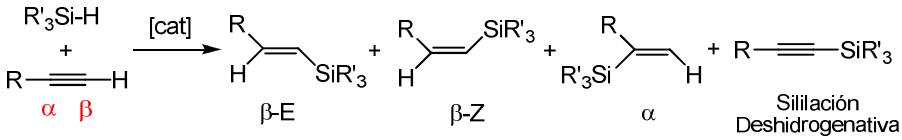

Esquema 5.39

La reacción de hidrosililación se puede describir como la adición de un enlace Si-H a un enlace multiple C-C. La mayoría de los estudios relacionados con la obtención de vinílsilanos, mediante la hidrosililación catalítica de alquinos, se centran en el diseño de catalizadores que permitan la obtención selectiva de los correspondientes alquenilsilanos: el producto ***α***-sililado y los estereoisómeros *β*, ***E*** y ***Z***; tambien se ha observado la obtención de productos de *Sililación deshidrogenativa* (**Esquema 5.39**). Los compuestos empleados en los experimentos catalíticos se muestran en el **Esquema 5.40**. Con el fin de comparar nuestros catalizadores con los sistemas descritos, se obtuvieron los complejos **2e**[42] y **2f**,[39] que habían sido descritos anteriormente.

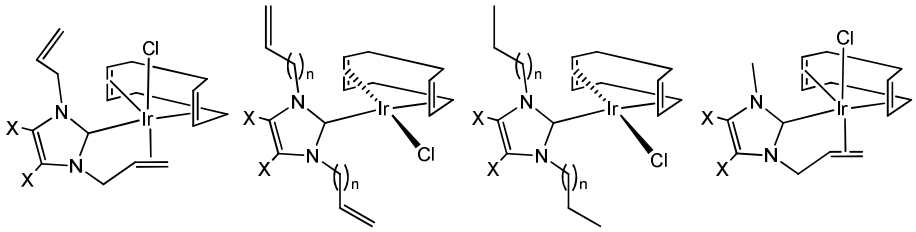

Esquema 5.40

Los compuestos tipo pinza (**2a**, **2b** y **2c**) resultaron inactivos mientras que todos los demás compuestos fueron eficaces en la hidrosililación de alquinos terminales. La introducción de diferentes sustituyentes en las posiciones 4 y 5 del anillo de imidazol en los complejos **1b** y **1c** disminuyen la actividad con respecto al compuesto análogo no substituido, **1a**. Hay que destacar la elevada regioselectividad en la generación del isómero Z, que en algunos casos ha

sido obtenido como único producto. También, tras un primer ciclo catalítico, el catalizador **1a** pudo reutilizarse en dos ciclos catalíticos más sin detectarse pérdida en su actividad. Esto demuestra la alta estabilidad de nuestros compuestos con ligandos de tipo carbeno N-heterocíclico.

5.4 Conclusiones

La presente memoria ha profundizado en el diseño de nuevos catalizadores al utilizar dos nuevos tipos de ligandos diferenciados: triazolil-di-ilideno y bis-alquenil-NHCs. La utilización de estos ligandos persigue el objetivo común de preparar compuestos con ligandos NHC con propiedades fundamentalmente diferentes a los conocidos hasta el momento, y estudiar cuáles son sus repercusiones en catálisis. A continuación se especifican algunas de las conclusiones derivadas del uso de estos ligandos.

a) Triazolil-di-ilideno

El uso del ligando trimetiltriazolil-di-ilideno, ha permitido obtener series de compuestos de tipo homo- y hetero-bimetálicos, estableciéndose criterios claros de coordinación que garantizan que el mismo ligando se puede utilizar de manera amplia en su coordinación a prácticamente cualquier par de fragmentos metálicos. La preparación y la caracterización de los compuestos heterobimetálicos establece un gran avance en el diseño de catalizadores tándem que permitan catalizar secuencias catalíticas formadas por reacciones muy diferentes. En concreto:

- Se ha estudiado la actividad de los compuestos de Ir^{III}/Ir^{I} y Ir^{III}/Rh^{I} en una reacción tándem, consistente en la ciclación oxidativa de un aminoalcohol y la posterior alquilación del indol resultante con un alcohol primario. Esta reacción, genera los correspondientes compuestos indólicos alquilados (bis-indolil-metano y 3-alquil-indole). La reacción es muy selectiva, ya que se ha podido obtener cuantitativamente el compuesto bisindolilmetano o el 3-alquilindol, en función de la cantidad de alcohol añadida. Los resultados obtenidos han permitido proponer un ciclo catalítico para el proceso de la alquilación del indol.

- La obtención de complejos de Ir^{III}/Pd^{II} nos ha permitido diseñar procesos tándem que combinan reacciones típicamente catalizadas por Ir y Pd. Para estos tipos de catalizadores, hemos considerado que las *p*-haloacetofenonas representan sustratos muy adecuados ya que tienen dos grupos funcionales diferentes, activables por paladio (enlace C-halógeno) e iridio (grupo carbonilico). Se han estudiado tres reacciones tándem: deshalogenación/transferencia de hidrógeno de haloacetofenonas, acoplamiento de Suzuki-Miyaura/transferencia de hidrógeno de *p*-bromoacetofenona, y acoplamiento de Suzuki-Miyahura/α-alquilación de *p*-bromoacetofenona. Para este ultimo caso la obtención de cetonas bifenílicas α-alquiladas es de gran interés, dada su aplicación como inhibidores no esteroideos de la 5α-reductasa. Esta nueva síntesis

representa una alternativa sencilla y rápida para obtener especies orgánicas con potenciales aplicaciones farmacéuticas.[31]

- Las propiedades catalíticas del compuesto heterobimetalico de Ir^{III}/Pd^{II} **15L** han sido probadas en la obtención selectiva de iminas a través de una reacción entre alcoholes y nitroarenos. El fragmento de iridio facilita la oxidación del alcohol liberando hidrogeno necesario para que el fragmento de paladio lo utilice en la reducción del nitroareno. Los resultados obtebidos han permitido proponer un ciclo catalítico para el proceso de síntesis de iminas en función del tipo de catalizador empleado.

- La síntesis del complejo heterobimetálico de Ir^{III}/Pt^{II} nos ha permitido estudiar una secuencia catalítica constituida por tres reacciones: 1) ciclación oxidativa de un aminoalcohol para generar indol, 2) hidroalcoxilación intramolecular de un alquinil alcohol para generar un vinil-eter y 3) funcionalización del indol a través de una adición C-H a la parte insaturada del vinil-eter. De este manera hemos combinado la ciclación oxidativa de aminoalcoholes para generar indoles, catalizada por Ir,[26, 27] con una serie de reacciones catalizadas por Pt[36] a partir de indoles y alquinil alcoholes. La reacción estudiada conlleva a la obtención de productos de alto valor añadido en un único paso.

b) Bis-alquenil-NHCs

La utilización de los ligandos de tipo **bis-alquenil-NHC**, ha permitido diseñar de forma sistemática compuestos en los que el ligando actúa como mono-, bi- y tri-dentado. Las condiciones estructurales del ligando y los procedimientos experimentales para obtener uno u otro tipo de coordinación han sido estudiados de forma sistemática.

Los compuestos derivados de la coordinación de los ligandos bis-alquenil-NHC han sido probados como catalizadores en reacciones de hidrosililación de alquinos, observándose que la actividad catalítica depende del grado de coordinación del ligando NHC. De este modo, los complejos monocoordinados y bisquelatos han mostrado las mejores actividades, junto a una elevada selectividad hacia los isomeros *Z*.

Referencias

(1) W. A., Herrmann, *Angew. Chem. Int. Ed*. **2002**, *41*, 1291.

(2) C. M. Crudden, D. P. M.; Allen, Coord. Chem. Rev., **2004**, *248*, 2247; S. P. Nolan, *Eur. J. Inorg. Chem*., **2005**, 1815.

(3) W.A. Herrmann, M. Elison, J. Fisher, C. Kocher, J. R. G. Artus, *Angew. Chem. Int. Ed. Engl*., **1995**, *34*, 2371.

(4) K. Öfele, *J. Organom. Chem*., **1968**, *12*, 42.

(5) H. W. Wanzlick, H. J. Schonher, *Angew. Chem. Int. Ed.*, **1968**, *7*, 141.

(6) A. J. Arduengo, R. L. Harlow, M. Kline, *J. Am. Chem. Soc*., **1991**, *113*, 361.

(7) V. Cesar, S. Bellemin-Laponnaz, L. H. Gade, *Chem. Soc. Rev*., **2004**, 619; W. A. Herrmann, L. J. Goossen, C. Kocher, G. R. J. Artus, *Angew. Chem. Int. Ed. Engl*., **1996**, *35*, 2805.

(8) T. Weskamp, V. P. W. Bohm, W. A. Herrmann, *J. Organom. Chem.*, **2000**, *600*, 12; D. Bourissou, O. Guerret, F. P. Gabbai, G. Bertrand, *Chem. Rev*., **2000**, *100*, 39.

(9) H. M. J.Wang, I. J. B. Lin, *Organometallics*, **1998**, *17*, 972.

(10) A. R. Chianese, X. W. Li, M. C. Janzen, J. W. Faller, R. H. Crabtree, *Organometallics*, **2003**, *22*, 1663; J. A. Mata, A. R. Chianese, J. R.; Miecznikowski, M. Poyatos, E. Peris, J. W. Faller, R. H. Crabtree, *Organometallics*, **2004**, *23*, 1253; I. J. B. Lin, C. S. Vasam, *Comments Inorganic Chem*., **2004**, *25*, 75; E. Mas-Marzá, M. Poyatos, M. Sanaú, E. Peris, *Inorg. Chem*., **2004**, *43*, 2213; J. C. Garrison, W. J. Youngs, *Chem. Rev*., **2005**, *105*, 3978.

(11) D. Enders, K. Breuer, G. Raabe, J. Runsik, J. H. Teles, J. P. Melder, K. Ebel, S. Brode, *Angew.Chem. Int. Ed. Engl.*, **1995**, *34*, 1021; J. H. Teles, J. P. Melder, K. Ebel, R. Schneider, E. Gehrer, W. Harder, S. Brode, D. Enders, K. Breuer, G. Raabe, *Helv. Chim. Acta* **1996**, *79*, 61; O. Guerret, S. Sole, H. Gornitzka, G. Trinquier, G. Bertrand, G. *J. Organom. Chem.*, **2000**, *600*, 112.

(12) J. A Mata, M. Poyatos, E. Peris, *Coord. Chem. Rev*., **2007**, *251*, 841; N. M. Scott, S. P. Nolan, *Eur. J. Inorg. Chem.*, **2005**, 1815; S. Diez-Gonzalez, S. P. Nolan, *Coord. Chem. Rev.* **2007**, *251*, 874.

(13) W. A. Herrmann, *Angew. Chem. Int. Ed.*, **2002**, *41*, 1291; L. H. Gade, S. Bellemin-Laponnaz, *Coord. Chem. Rev.*, **2007**, *251*, 718; V. Cesar, S. Bellemin-Laponnaz, L. H. Gade, *Chem. Soc. Rev.*, **2004**, *33*, 619; M. C. Perry, K. Burgess, *Tetrahedron: Asymmetry* **2003**, *14*, 951.

(14) N. Marion, S. Diez-Gonzalez, S. P. Nolan, *Angew. Chem. Int. Ed.*, **2007**, *46*, 2988; C. Fischer, S. W. Smith, D. A. Powell, G. C. Fu, *J. Am. Chem. Soc.*, **2006**, *128*, 1472; K. M. Hindi, T. J. Siciliano, S. Durmus, M. J. Panzner, D. A. Medvetz, D. V. Reddy, L. A. Hogue, C. E. Hovis, J. K. Hilliard, R. J. Mallet, C. A. Tessier, C. L. Cannon, W. J. Youngs, *J. Med. Chem.*, **2008**, *51*, 1577.

(15) J. C. Wasilke, S. J. Obrey, T. R. Baker, G. C. Bazan, *Chem Rev*., **2005**, *105*, 1001.

(16) L. D. Field, B. A. Messerle, S. L. Wren, *Organometallics*, **2003**, *22*, 4393.

(17) N. Jeong, S. D. Seo, J. Y. Shin, *J. Am. Chem. Soc*., **2000**, *122*, 10220.

(18) E. Mas-Marzá, J. A. Mata, E. Peris, *Angew. Int. Ed.*, **2007**, 46, 3729.

(19) M. Viciano, M. Sanaú, E. Peris, *Organometallics*, **2007**, *26*, 6050.

(20) A. J. Boydston, C. W. Bielawsky, *Dalt. Trans.*, **2006**, 4073; A. J. Boydston, W. A. Kyle, C. W. Bielawsky, *J. Am. Chem. Soc*., **2005**, *127*, 12496; D. M. Khramov, A. J. Boydston, C. W. Bielawsky, *Angew. Chem. Int. Ed.*, **2006**, *45*, 6186.

(21) T. J. Curphey, K. S. Prasad, *J. Org. Chem.*, **1972**, *37(14)*, 2259.

(22) O. Guerret, S. Sole, H. Gornitzka, M. Teichert, G. Bertrand, *J. Am. Chem. Soc.*, **1997**, *119*, 6668.

(23) O. Guerret, S. Sole, H. Gornitzka, G. Trinquier, G. Bertrand, *J. Organom. Chem.*, **2000**, *600*, 112.

(24) B. Sahu, K. Misra, B. K Mohapatra, *Indian J. Chem. Sect A-Inorg. Phys. Theor. Anal. Chem.*, **1982**, *21*, 823.

(25) J. W. Ruan, O. Saidi, J. A. Iggo, J. L. Xiao, *J. Am. Chem. Soc.*, **2008**, *130*, 10510.

(26) K. Fujita, K. Yamamoto, R. Yamaguchi, *Org. Lett.*, **2002**, *4*, 2691.

(27) S. Whitney, R. Grigg, A. Derrick, A. Keep, *Org. Lett*., **2007**, *9*, 3299.

(28) A. B. Zaitsev, S. Gruber, P. S. Pregosin, *Chem. Comm*., **2007**, 4692.

(29) J. S. Yadav, B. V. S. Reddy, S. Aravind, G. Kumar, A. S. Reddy, *Tetrahedron Lett*., **2007**, *48*, 6167.

(30) S. Muthasamy, C. Gunanatan, *Synlett*, **2002**, *11*, 1783.

(31) A. R. McCarthy, R. W. Hartmann, A. D. Abell, *Bioorg. Med. Chem. Lett.* **2007**, *17*, 3603; F. Picard, T. Schulz, W. R. Hartmann, *Bioorg. Med. Chem.*, **2002**, *10*, 437.

(32) G. E. Dobereiner, R. H. Crabtree, *Chem. Rev.* **2010**, *110*, 681-703; G. Guillena, D. J. Ramon, M. Yus, *Chem. Rev.*, **2007**, *110*, 1611-1641.

(33) M. Hamid, P. A. Slatford, J. M. J. Williams, *Adv. Synth. Catal.*, **2007**, *349*, 1555-1575; T. D. Nixon, M. K. Whittlesey, J. M. J. Williams, *Dalton Trans.*, **2009**, 753-762; A. Tillack, D. Hollmann, D. Michalik, M. Beller, *Tetrahedron Lett.*, **2006**, *47*, 8881-8885; K. I. Fujita, Y. Enoki, R. Yamaguchi, *Tetrahedron*, **2008**, *64*, 1943-1954.

(34) J. P. Adams, *J. Chem. Soc., Perkin Trans., 1* **2000**, 125-139; J. Gawronski, N. Wascinska, J. Gajewy, *Chem. Rev.*, **2008**, *108*, 5227-5252.

(35) A. Prades, R. Corberan, M. Poyatos, E. Peris, *Chem.-Eur. J.*, **2008**, *14*, 11474-11479.

(36) S. Bhuvaneswari, M. Jeganmohan, C. H. Cheng, *Chem.-Eur. J.*, **2007**, *13*, 8285-8293.

(37) D. R. Anton, R. H. Crabtree, *Organometallics*, **1983**, *2*, 855-859; P. Foley, R. Dicosimo, G. M. Whitesides, *J. Am. Chem. Soc.*, **1980**, *102*, 6713-6725.

(38) F. E. Hahn, C. Haltgrewe, T. Pape, M. Martin, E. Sola, L. A. Oro, *Organometallics*, **2005**, *24*, 2003.

(39) F. E. Hahn, B. Heidrich, T. Pape, M. Martin, A. Hepp, E. Sola, L. A. Oro, *Inorg. Chim. Acta*, **2006**, *559*, 4840.

(40) A. Zanardi, J. A. Mata, E. Peris, *New J. Chem*., **2008**, *32*, 120.

(41) R. Corberán, M. Sanaú, E. Peris, *Organometallics*, **2007**, *26*, 3492.

(42) A. Chianese, X. W. Li, M. C. Janzen, J. W. C.;Faller, R. H. Crabtree, *Organometallics*, **2003**, 22, 1663.